TECHNISCHE UNIVERSITÄT DRESDEN

Biotechnological production of value-added chemicals from *cis*-aconitate with the help of genetically engineered oleophilic yeasts

DISSERTATION

zur Erlangung des akademischen Grades

Doctor rerum naturalium
(Dr. rer. nat.)

vorgelegt

der Fakultät Biologie
der Technischen Universität Dresden

von

M.Sc. Zsolt Kövesi
geboren am 17.12.1988 in Chemnitz (ehem. Karl-Marx-Stadt)

Gutachter: Prof. Dr. rer. nat. habil. Gerold Barth
               Prof. Dr. rer. nat. habil. Jutta Ludwig-Müller

Eingereicht am Freitag den 13.03.2020

Verteidigt am Freitag den 30.10.2020

Summary

Background: The synthesis of chemicals from fossil fuels is being evaluated increasingly critically, mainly due to its expected exhaustion and negative impact on the environment. An alternative offers 'white biotechnology', especially the fermentation of renewable resources with the help of yeasts. The oleophilic yeast species *Pseudozyma* (*P.*) *tsukubaensis* and *Yarrowia* (*Y.*) *lipolytica* are both natural organic acid producers. Their main products are metabolites of the tricarboxylic acid cycle, namely citrate, *α*-ketoglutarate and malate. In smaller amounts, other compounds like isocitrate (ICA) or itaconate (ITA, solely with *P. tsukubaensis*) are also secreted. The interest for the latter two has been rising steadily during the last decades. However, to this date, there is no established host organism for the ICA production. ITA, on the other hand, is being synthesised with *Aspergillus terreus.* Even with great scientific effort, the ITA productivity of this hyphal fungus appears to reach its limits. Therefore, a different host organism is needed.

Results: In this study, a promising *P. tsukubaensis* strain has been constructed for the production of ITA and a *Y. lipolytica* strain for ICA. First, the genome of the ITA producer *P. tsukubaensis* has been sequenced. As a result, a gene cluster for the synthesis and export of ITA, homologous to that of *Ustilago maydis,* has been identified. By overexpressing four of the five cluster genes, respectively, none to low increases in ITA secretion were observed. The fifth gene is encoding the putative transcription factor Ria1p which probably controls the gene cluster. The overexpression of the gene *PtRIA1* led to a significantly increased ITA production of up to 31.4 g l^{-1} in micro-wells. By optimizing the growth conditions 113.6 g l^{-1} ITA could be produced within 7 d under controlled conditions in a bioreactor without the need of a trigger like phosphate limitation.

For the production of ICA, two putative mitochondrial citric acid transporter proteins were identified in *Y. lipolytica.* One carrier protein is encoded by the novel gene *YlYHM2*, the other one by *YlCTP1.* The mode of function for the two deduced proteins appears to be very distinct from one another. The deletion of *YlCTP1* led to a minor shift in the ICA:CA ratio but the total amount of acids decreased greatly. By deleting *YlYHM2,* the ICA:CA product ratio could be increased from 12 % to 95 % compared to the wild type strain. Within 5 d up to 131.9 g l^{-1} ICA with sunflower oil and 22.0 g l^{-1} with glucose as the sole carbon source could be achieved under controlled production conditions in a bioreactor. Further inhibition of the isocitrate lyase protein with ITA increased the ICA:CA ratio to 98 %.

Conclusion: Within this work, the two yeast strains *P. tsukubaensis* (HR12) and *Y. lipolytica* (Δ*YHM2*) have been created via metabolic engineering. With their help, it is possible to produce the value-added chemicals ITA or ICA on a high scale (> 100 g l^{-1}) from renewable resources like glucose or even vegetable oils.

Zusammenfassung

Hintergrund: Die Synthese von Chemikalien aus fossilen Rohstoffen wird wegen ihrer begrenzten Verfügbarkeit und ihren negativen Auswirkungen auf die Umwelt zunehmend kritisch bewertet. Eine Alternative bietet die „Weiße Biotechnologie", insbesondere die Fermentation nachwachsender Rohstoffe mithilfe von Hefen. Die oleophilen Hefen *Pseudozyma* (*P.*) *tsukubaensis* und *Yarrowia* (*Y.*) *lipolytica* sind natürliche Säureproduzenten. Ihre Hauptprodukte sind Metabolite des Tricarbonsäurezyklus: Citrat (CA), α-Ketoglutarat und Malat. In kleineren Mengen werden auch andere Stoffe wie Isocitrat (ICA) oder Itaconat (ITA, nur von *P. tsukubaensis*) sekretiert. Das Interesse an den beiden Letztgenannten hat in den vergangenen Jahrzehnten stetig zugenommen. Bis heute gibt es allerdings keinen etablierten Wirtsorganismus für die ICA-Produktion. ITA hingegen wird mithilfe von *Aspergillus terreus* synthetisiert. Jedoch stößt die ITA-Produktivität dieses Hyphenpilzes auch mit großem wissenschaftlichem Aufwand an ihre Grenzen. Daher wird ein neuer Wirtsorganismus benötigt.

Ergebnisse: In dieser Studie wurden ein vielversprechender *P. tsukubaensis*-Stamm für die Produktion von ITA und ein *Y. lipolytica*-Stamm für ICA konstruiert. Zunächst wurde das Genom von *P. tsukubaensis* sequenziert. Infolgedessen wurde ein Gencluster für die Synthese und den Export von ITA identifiziert, das homolog zu dem von *Ustilago maydis* ist. Die Überexpression von vier der fünf Clustergene erhöhte die ITA-Sekretion nicht deutlich. Das fünfte Gen kodiert den vermeintlichen Transkriptionsfaktor Ria1p, der vermutlich das Gencluster steuert. Die Überexpression des *PtRIA1* Gens führte zu einer signifikant erhöhten ITA-Produktion von bis zu 31,4 g l^{-1} in Mikrotiterplatten. Durch die Optimierung der Wachstumsbedingungen wurden im Bioreaktor innerhalb von 7 d 113,6 g l^{-1} ITA ohne die Notwendigkeit eines Triggers produziert.

Für die ICA-Produktion wurden zwei mutmaßliche mitochondriale Citrat-Transportproteine in *Y. lipolytica* identifiziert, welche von den Genen *YlCTP1* sowie *YlYHM2* kodiert werden. Die Funktionsweise der beiden Proteine scheint sich stark voneinander zu unterscheiden. Die Deletion von *YlCTP1* führte zu einer leichten Verschiebung des ICA:CA-Verhältnisses, aber die Gesamtmenge beider Säuren nahm stark ab. Durch die Deletion von *YlYHM2* stieg die ICA:CA-Produktrate von 12 % auf 95 % im Vergleich zum Wildtyp. Innerhalb von 5 d wurden bis zu 131,9 g l^{-1} ICA mit Sonnenblumenöl, bzw. 22,0 g l^{-1} ICA mit Glukose als einzige Kohlenstoffquelle in einem Bioreaktor unter kontrollierten Produktionsbedingungen erreicht. Durch die zusätzliche Hemmung des Isocitratlyase-Proteins mit ITA stieg das ICA:CA-Verhältnis bis 98 %.

Fazit: Mittels Metabolic Engineering wurden im Rahmen dieser Arbeit die beiden Hefestämme *P. tsukubaensis* HR12 und *Y. lipolytica* ΔYHM2 erzeugt. Mit ihrer Hilfe ist es möglich, die hochwertigen Chemikalien ITA oder ICA in hohen Mengen (> 100 g l^{-1}) aus nachwachsenden Rohstoffen wie Glukose oder sogar Pflanzenölen herzustellen.

Content

Figures

Tables

Abbreviations

List of genera

A.	*Aspergillus*
C.	*Candida*
E.	*Escherichia*
H.	*Hylotelephium*
P.	*Pseudozyma*
R.	*Rhodotorula*
S.	*Saccharomyces*
U.	*Ustilago*
Y.	*Yarrowia*

List of units

%	percentage
°C	degree Celsius
µl	microlitre
µm	micrometer
a	year
aa	amino acid
bp	base pair
d	day
g	gram
g	gravitational force
h	hour
kb	kilo base
kDa	kilo Dalton
l	litre
M	molar
Mb	Mega base
min	minute
ml	millilitre
mM	millimolar
nt	nucleotides
rpm	revolutions per minute
s	second
t	metric ton
U	enzyme unit
v/v	volume per volume
w/v	weight per volume
w/w	weight per weight

List of genes/proteins

ACO1/2	aconitase gene 1 or 2
ADI1	*cis*-aconitate-Δ-isomerase gene
amp^R	ampicillin resistance gene
AtXYX	respective gene in *A. terreus*
CAD1 (*CADA*)	*cis*-aconitate decarboxylase gene
cbx^R	carboxin resistance gene
CTP1	citrate transport protein gene
CYP3	cytochrome P450 monooxygenase gene
GAPDH	glyceraldehyde 3-phosphate dehydrogenase
GFP	green fluorescent protein
HSP70	heat shock 70 kDa protein
hyg^R	hygromycin resistance gene
ICL1	isocitrate lyase gene
IntB/C	integration platform on chromosome B or C
ITP1	itaconic acid transporter gene
LacZ	β-galactosidase
MTTA/MTT1	mitochondrial tricarboxylate transporter genes
MFSA	itaconic acid transporter gene belonging to the major facilitator superfamily
pXYX	promoter sequence of the respective gene
PtXYX	respective gene in *P. tsukubaensis*
RIA1	regulator of itaconic acid gene
ScXYX	respective gene in *S. cerevisiae*
TAD1	*trans*-aconitate decarboxylase gene
TcR'	partial tetracycline resistance gene
TEF1/TEF	translation elongation factor 1a
UmXYX	respective gene in *U. maydis*
URA3	orotidine-5-phosphate decarboxylase
Xyxp	protein sequence encoded by the respective gene
YHM2	'yeast suppressor of HM mutant' gene (mitochondrial citrate carrier)
YlXYX	respective gene in *Y. lipolytica*

General abbreviations

Δ	deletion	LiAc	lithium acetate
λ	wavelength	M15	*P. tsukubaensis* random mutagenesis ITA overproducing strain
A	adenine		
aa	amino acid		
*α*KG	*α*-ketoglutaric acid	MA	malic acid
ATP	adenosine triphosphate	MCF	mitochondrial carrier family
BLAST	basic local alignment search tool	MEL	mannosylerythritol lipids
C	carbon	MG	minimal medium with glucose
C	cytosine	MCS	multiple cloning site
CA	citric acid	n	number of samples
ca.	Circa	N	nitrogen
CaCO$_3$	calcium carbonate	NAD(P)H	nicotinamide adenine dinucleotide (phosphate)
CAS-nr.	Chemical Abstracts Service-number		
		NCBI	National Centre for Biotechnology Information
CBS	Centraalbureau voor Schimmelcultures (culture collection)		
		NG	N-methyl-N'-nitro-N-nitrosoguanidine
Cd	cadmium		
CoA	coenzyme A	Ni	nickel
CO$_2$	carbon dioxide	o	overexpression
Cr	chromium	ORF	open reading frame
CSL	corn steep liquor	ORI	origin of replication
Cu	cupper	p	probability
DCW	dry cell weight	P	phosphate
dH$_2$O	distilled water	p.a.	per annum
DNA	deoxyribonucleic acid	PCR	polymerase chain reaction
dNTP	deoxynucleotide triphosphate	pH	negative logarithm of the concentration of hydronium ions
DSM	microorganisms belonging to the catalogue of the German Collection of Microorganisms and Cell Cultures		
		pK$_a$	acid dissociation constant
		PPP	pentose phosphate pathway
		qPCR	quantitative real-time PCR
E-value	expected value	RNA	ribonucleic acid
EDTA	ethylenediaminetetraacetic acid	rv	reverse
		SE	steryl ester
e.g.	*exempli gratia* (for example)	sp.	Species
EMP	Embden–Meyerhof–Parnas	T	thymine
et al.	*et alia, et aliae, et alii* (and others)	TAE	Tris-acetic acid-EDTA
		TAG	triacylglycerols
FOA	5-fluoroorotic acid	TCA	tricarboxylic acid
fw	forward	TCDB	transporter classification database
G	guanine		
GC	guanine cytosine	USD	US-Dollar
H$_2$O$_2$	hydrogen peroxide	UV	ultraviolet
H488	*P. tsukubaensis* wild type strain from the Helmholtz Centre for Environmental Research - UFZ	Vis	visible spectrum
		WT	wild type
		YPD	Yeast extract Peptone Dextrose
HR12	*P. tsukubaensis* H488 *PtRIA1* overexpression transformant nr. 12		
IC	ion chromatography		
ICA	isocitric acid		
ITA	itaconic acid		
LB	lysogeny broth		
X			

1. Introduction

1.1. The problem with the conventional synthesis of chemicals

Industrial chemicals and their derivatives are ubiquitous in the industrialized parts of the world. These substances have been a big factor in the advancement of our modern society. Most common examples are fertilizers and plastics. Currently, crude oil, natural gas and coal represent their primary raw material. The demand in fossil fuels rises as the population grows by an additional two billion people until 2050[1]. The International Energy Agency projects a 2.8-fold increase in demand for the sector's 18 most energy intensive chemicals by that time (van der Hoeven et al., 2013; Levi and Cullen, 2018). The oil production remains at an extremely high level, with the USA reaching its historic peak production in 2018[2]. Globally, the combined consumption of coal, gas and crude oil also grows continually (Ritchie and Roser, 2017; Smil, 2016). However, the conventional synthesis of chemicals from fossil-based resources comes with several drawbacks.

First, fossil fuels are a finite resource (Dudley, 2019). An alternative source must be found before fossil fuels are depleted completely. Besides their foreseen limited abundance in the future, the use of fossil-based chemicals is accompanied by extensive environmental issues. For one, locally active pollutants such as sulphur dioxide, nitrogen oxide, black carbon, polycyclic aromatic hydrocarbons, mercury, and volatile chemicals that form ground level ozone (O_3) are emitted into the environment. All are associated with adverse effects on the ecosphere (OECD, 2016; Perera, 2018). In addition to that, fossil fuels represent a key source of carbon dioxide (CO_2) in the atmosphere (IPCC, 2006). It is expected that the chemical sector alone is responsible for approximately 7 % of the total anthropogenic global greenhouse gas emissions, and 5.5 % when only counting CO_2 emissions (van der Hoeven et al., 2013; Levi and Cullen, 2018). This makes them one of the main drivers of climate change.

One possible alternative to this problem is offered by the production of value-added chemicals through biological means. This field of application is also called white biotechnology. The most succinct benefit of the biotechnological synthesis of chemicals is the fact that it offers the possibility to utilize biomass as educts which represent a sustainable resource and does not liberate fossilized carbon (El-Imam and Du, 2014).

---

[1] United Nations, DESA/Population Division, World Population Prospect, World: Total Population graph. Retrieved August 10th, 2019, from https://population.un.org/wpp/Graphs/Probabilistic/POP/TOT/900
[2] U.S. Energy Information Administration: US Field Production of Crude Oil. Retrieved August 10th, 2019, from https://www.eia.gov/dnav/pet/hist/LeafHandler.ashx?n=pet&s=mcrfpus1&f=a

1.2. White biotechnology

Industrial or white biotechnology refers to the use of natural processes catalysed by enzymes or whole cells for industrial manufacturing. In that, it is distinct from red biotechnology where pharmaceuticals (e.g. insulin) are produced, green biotechnology that focuses on agricultural processes or blue biotechnology which exploits aquatic organisms. According to the OECD and the German Federal Ministry of Education and Research, white biotechnology has two main goals (Van Beuzekom and Arundel, 2006):

1. Replacing finite fossil fuels with similar substances from renewable raw materials, i.e. biomass;
2. the replacement of conventional, industrial production by biological-based systems.[3]

By replacing fossil fuels with bio-based resources, multiple negative impacts can be circumvented. For one, biomass as a resource is inexhaustible, renewable and the necessary plants can grow almost everywhere around the globe. Especially, lignocellulosic and starch-rich wastes and by-products are promising candidates because they are omnipresent, extremely cheap, and their use does not compete with food production. The use of biomass for the biological production of chemicals can spur economic growth in most regions and diminish the dependency on oil producing countries. Furthermore, global CO_2 emissions can be reduced by utilizing bio-based resources. Due to the fact that the carbon cycle is almost balanced between photosynthetic CO_2 fixation by plants and the CO_2 emission from combustion, their usage can be virtually carbon emission neutral (Rabl et al., 2007). Figure 1 illustrates the basic approach followed in white biotechnological processes.
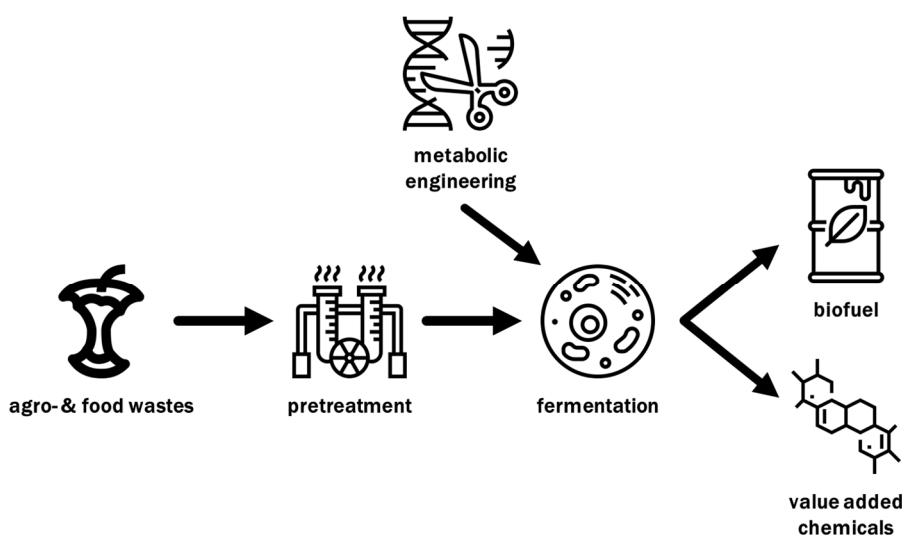
Figure 1 Biotechnological production of value-added chemicals and biofuel from organic waste products with the help of genetically engineered microorganisms. Images used from www.flaticon.com

---

[3] BMBF, Weiße Biotechnologie, Chancen für eine biobasierte Wirtschaft. Retrieved August 10th, 2019 from https://www.bmbf.de/upload_filestore/pub/Weisse_Biotechnologie.pdf

In a broader sense, biotechnology was conducted unwittingly for millennia already. Earliest examples are the alcoholic fermentation of grains and fruits with the help of yeasts and the production of acetic acid with the help of various microorganisms. This process of 'ancient biotechnology' can be dated back for at least 10000 years (Budak et al., 2014; Liu et al., 2018).

From 1800 to the middle of the 20th century, the second phase or classical biotechnology prevailed. During that time period, ground-breaking discoveries were made in the general field of biology, which were essential for later scientific achievements. For example, the characterization of inheritance by Gregor Mendel and the first description of evolutionary processes by Charles Darwin. The era of the classical biotechnology came to an end with the discovery of the first antibiotic – penicillin – by Alexander Fleming in 1928 (Verma et al., 2011).

Modern white biotechnology was gaining momentum in the second half of the 20th century. Its beginning can be attributed to the mass production of penicillin via deep-tank fermentation during the 1940s (Ligon, 2004; Verma et al., 2011). As early as 1988, the first rationally designed enzyme used in detergents to break down fat was introduced (Frazzetto, 2003). More recently, *Escherichia* (*E.*) *coli* cells were genetically modified to produce a precursor for biodegradable plastics (Liu et al., 2007). Currently, large scientific efforts are spent to make the biotechnological production of biofuels viable. Especially oleaginous yeasts receive significant attention due to their ability to efficiently accumulate extremely high amounts of lipids inside their cells. Those lipids can be easily converted into oleochemicals by *trans*-esterification (Sitepu et al., 2014).

Also, another group of high value bio-based chemicals, namely organic acids, have come into the focus of the scientific community. Organic acids are low molecular-weight natural intermediates in the metabolic pathways of all living organisms, among which the tricarboxylic acid (TCA) cycle is the most crucial. Several different organic acids represent excellent value-added chemicals because they have multiple functional groups that possess the potential to be transformed into new families of useful molecules e.g. carboxyl, sulfonic, alcohol, and thiol groups. The U.S. Department of Energy compiled a list of the twelve most promising sugar-based building blocks. Six out of those twelve candidates are organic acids (see table 1), including Itaconic acid (Werpy et al., 2004).

Table 1 U.S. Department of Energy's top twelve value added chemicals from biomass (Werpy et al., 2004)

building blocks			
1.	1,4-diacids (succinic, fumaric and malic acid)	7.	itaconic acid
2.	2,5-furan dicarboxylic acid	8.	levulinic acid
3.	3-hydroxy propionic acid	9.	3-hydroxybutyrolactone
4.	aspartic acid	10.	glycerol
5.	glucaric acid	11.	sorbitol
6.	glutamic acid	12.	xylitol/arabinitol

1.3. Itaconic acid

Itaconic acid (ITA; also known as methylene succinic acid; CAS-nr.: 97-65-4) is an organic, monounsaturated C-5 dicarboxylic acid with the following molecular formula: $C_5H_6O_4$. Its structure is illustrated in figure 2. ITA was first described in 1837 as a thermal decomposition product of citric acid (CA) by Baup. Three years later, in 1840 Crasso described ITA as a thermal decomposition product of aconitic acid and coined the term "itaconic acid" as an anagram (Luskin, 1974). It crystallizes in rhombic double pyramids (Willke and Vorlop, 2001). At room temperature, it is a white, crystalline and hygroscopic powder with a molar mass of 130.1 g mol^{-1} and a density of 1.632 g ml^{-1}. It's melting and boiling points are 168 °C and 268 °C, respectively. ITA has three different protonation states (H_2ITA, $HITA^-$ and ITA^{2-}) with pK_a1 = 3.84, pK_a2 = 5.55 being its two dissociation constants at room temperature (De Robertis et al., 1990; Magalhães et al., 2017; Patty, 1963). In a strong alkaline environment and at temperatures of ≥ 170 °C ITA can be converted into one of two isomers, citraconic or mesaconic acid (Sakai, 1976).
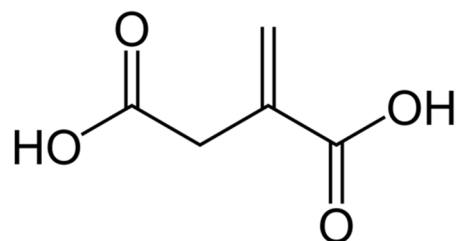
Figure 2 Chemical structure of itaconic acid.

Almost 100 years after its characterization, the first microbial synthesis of ITA was observed on acidic medium with the filamentous fungus *Aspergillus* (*A.*) *itaconicus,* which was isolated from dried salted plums (Kinoshita, 1932). In 1939 during screening processes, *A. terreus* was found to be a superior ITA producing microorganism by Calam. Only three years later, Charles Pfizer co-patented an industrial ITA production process of submerged *A. terreus* cultures (Kane et al., 1945). Shortly after, the first large-scale fermentation processes were established (Nelson et al., 1952; Pfeifer et al., 1952). The first industrial production plant, for example, was built 1955 in Brooklyn, NY, USA also by Pfizer (Kuenz and Krull, 2018). During the 1960s, the biotechnological production of ITA with the help of *A. terreus* was largely established. These practices are still applied today but the industry is looking for ways to improve processes in order to increase yields and reduce costs (Klement and Büchs, 2013; Okabe et al., 2009).

In the past, several alternative methods for ITA synthesis have been proposed (Berg and Hetzel, 1978; Blatt, 1943; Carlsson et al., 1994; Chiusoli, 1962; Luskin, 1974; Pichler et al., 1967; Shekhawat et al., 2006; Tate, 1981). However, none of them has been successfully adapted due to their economic non-profitability. For ITA, the petrochemical synthesis approaches still do not compete with biotechnological production (Willke and Vorlop, 2001).

1.3.1. Applications for ITA

ITA possesses an interesting chemical structure in that it is composed of two carboxylic acid functionalities and an α,β-unsaturated exo-double bond. These properties make ITA universally applicable and allow for the synthesis of polyesters, that are currently not achievable with standard building blocks derived from petrochemicals (Geilen et al., 2010; Medway and Sperry, 2014; Robert and Friebel, 2016). The threefold functional structure makes a variety of reactions and applications possible. Viable reactions are the formation of salts with metals, esterification with alcohols, anhydride formation, addition reactions and polymerization. Thus, ITA can potentially replace the structurally similar building block chemicals methacrylic acid and acrylic acid (Kuenz and Krull, 2018; Magalhães et al., 2017).

Its current use is focused on the application as an intermediate in the preparation of complex organic compounds, mostly as a monomer or co-monomer for the synthesis of various polymers. ITA itself or its derivatives are used to form elastomers, superabsorbent polymers, synthetic latex (e.g. styrene-butadiene-itaconic acid latex) and unsaturated polyester resins. These products can be employed as chemical fibres, coatings, corrosion inhibitors, dental materials, detergents, drug-delivery systems, paints, lacquer, plasticizers, or (thermo-)plastics. In summary, ITA is applied among others in the construction, hygiene, medical and paper industry (Delidovich et al., 2016; Klement and Büchs, 2013; Kuenz and Krull, 2018; Kumar et al., 2017; Magalhães et al., 2017; Okabe et al., 2009; Robert and Friebel, 2016; Saha et al., 2017; Willke and Vorlop, 2001).

Besides its potential use as an alternative for (meth-)acrylic acids, several other fields of application are investigated at the moment: ITA based polyesters have been used as precursors for bio-erodible vaccine-loaded hydrogel microspheres (Singh et al., 1991). The group around Barrett (2010) developed several bio-based polyesters derived from ITA. The resulting materials can be applied in drug delivery systems, tissue engineering and other biomedical applications (Barrett et al., 2010b, 2010a). It has also a high potential to serve as an alternative cross-linking group for radiation curing binders for coatings and printing inks (Dai et al., 2015). Some derivatives such as 2-methyl1,4-butanediol and 3-methyl tetrahydrofuran have potential as biofuels (Geilen et al., 2010). Another promising field is its use for the synthesis of shape memory polymers (Guo et al., 2011).

Between 2009 and 2015, estimates for the annual production ranged from 41000 t to over 80000 t. The market was projected to grow to 197000-408000 t p.a. until 2020 with a market value of 315-567 million USD. The production is limited on the Asian region with no larger facilities in the EU or the USA. The world market for ITA is currently estimated between 75-126 million USD with one-kilogram costing between 1.8-2.0 USD depending on the supplier and quality. (Okabe et al., 2009; Transparency Market Research, 2015; WEASTRA, 2013). By effectively displacing methacrylic acid or acrylic acid with ITA as a starting substance for the production of polyacrylic acids, its value

could rise significantly because this particular market is worth over eleven billion USD (El-Imam and Du, 2014; Karaffa and Kubicek, 2019; Saha et al., 2019).

1.3.2. Biosynthesis of ITA

Despite its biotechnological production that has been ongoing for decades now, the underlying biosynthesis pathway of ITA has remained unclear for a long time.

The first revelatory advancements were made by Bentley and Thiessen (1957b, 1957a). Via 1-^{14}C-marked glucose, they could prove that the sugar is metabolized through glycolysis and the subsequent TCA cycle. Furthermore, they could demonstrate that ITA is a direct product from *cis*-aconitate. Because of this and the fact that *cis*-aconitate is a central metabolite in the TCA cycle (Krebs and Johnson, 1937), Bentley and Thiessen proposed that the synthesis of ITA, therefore, must be linked to the TCA cycle. At that time they hypothesized that *cis*-aconitate would be directly decarboxylated into ITA (Bentley and Thiessen, 1957c).

Considering the transformation of *cis*-aconitate, Shimi and Nour El Dein (1962) proposed a stepwise condensation of three acetyl-CoA molecules into propane-1,2,3-tricarboxylic which is oxidized into *cis*-aconitate and is ultimately decarboxylated into ITA. In 1996, Bressler and Braun presented one alternative route, where *cis*-aconitate is decarboxylated into citraconic acid. This intermediate would then be isomerized into ITA.

Other research groups discarded the idea of *cis*-aconitate being the precursor of ITA all together: Jakubowska et al. (1974) and Nowakowska-Waszczuk (1973) proposed the idea that citramalic acid would be synthesised from acetyl-CoA and pyruvic acid. Afterwards, dehydration of citramalic acid into ITA would occur.

In 1995, the group around Bonnarme investigated the metabolites of *A. terreus* with C^{13} and C^{14}-marked substrates and the help of nuclear magnetic resonance spectroscopy. This way, they could confirm the biosynthesis pathway proposed earlier by Bentley and Thiessen (1957c) which is the generally accepted route today (see figure 3). The identification of the *AtCAD1* gene and the characterization of its deduced protein Cad1p further substantiated this pathway (Bentley and Thiessen, 1957c; Dwiarti et al., 2002; Kanamasa et al., 2008). Since then, other key proteins in the ITA biosynthesis of *A. terreus* have been identified, mainly the mitochondrial *cis*-aconitate shuttling transporter MttAp and the cell wall located ITA exporter MfsAp which belongs to the Major Facilitator Superfamily (MFS). Interestingly, the responsible genes *AtCAD1, AtMTTA* and *AtMFSA* are structured in a gene cluster. This gene cluster is potentially regulated by a zinc finger transcription factor, whose gene is also located inside the cluster (Li et al., 2011).

Recently, the group around Geiser (2016a, 2016b) investigated the synthesis route of ITA in the parasitic corn smut fungus *Ustilago* (*U.*) *maydis*. A similar gene cluster to that of *A. terreus* was found. However, instead of a gene encoding a *cis*-aconitate decarboxylase two genes with

divergent functions were inferred. This pathogenic fungus which forms galls on corn species, syntheses ITA from *cis*-aconitate via the unusual intermediate *trans*-aconitate. Figure 3 shows that first, *cis*-aconitate is shuttled to the cytosol with the help of Mtt1p where it is isomerized to *trans*-aconitate by **a**conitate-**Δ**-**i**somerase 1 (Adi1p). This intermediate is then decarboxylated into ITA by the ***t**rans*-**a**conitate **d**ecarboxylase (Tad1p). Ultimately, the resulting ITA is transported into the surrounding medium by the **i**taconate **t**ransporting **p**rotein (Itp1p). The gene cluster is controlled by the fifth member of the cluster namely **r**egulator for **i**taconic **a**cid (Ria1p).

By using these pathways, both *A. terreus* and *U. maydis* can form 1 mol ITA from 1 mol glucose in theory. That would correspond to a theoretical ITA yield of 0.72 g g^{-1} glucose (Saha, 2017).
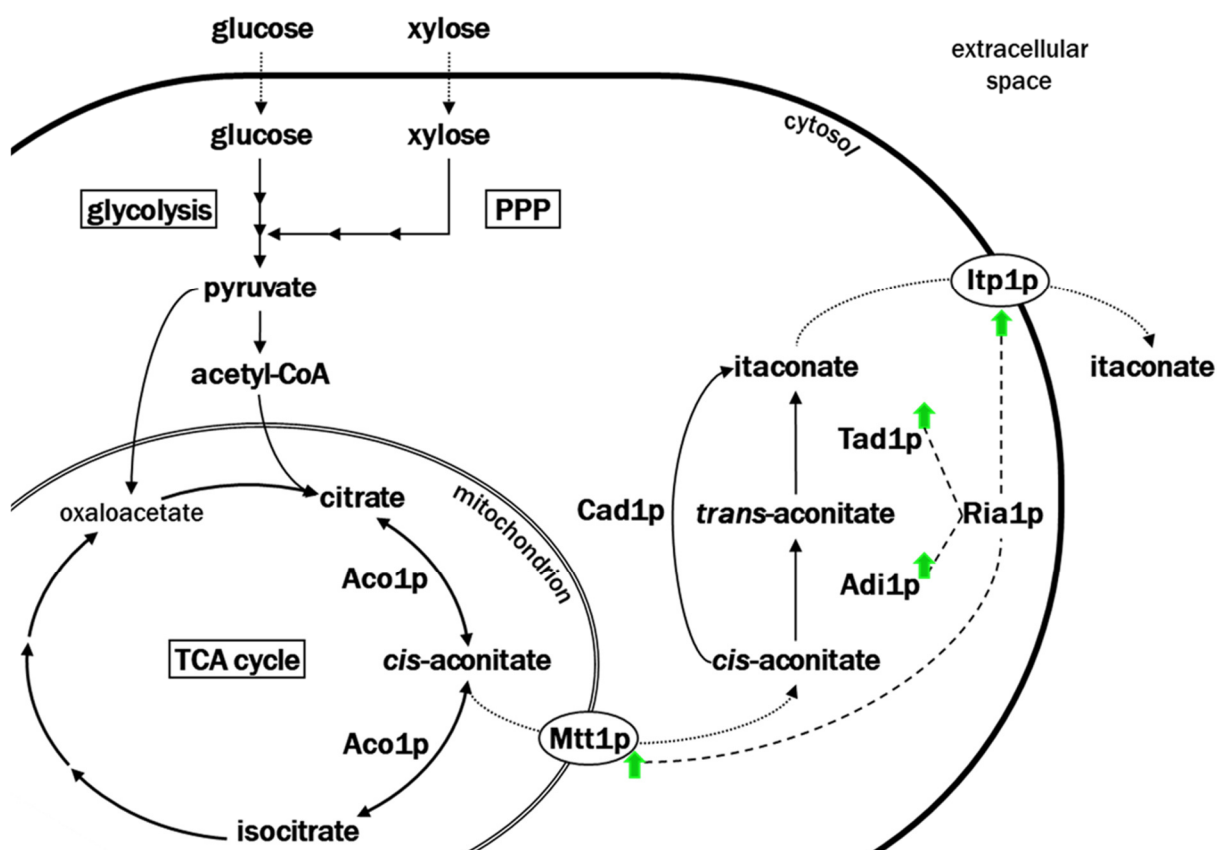
Figure 3 Schematic overview of the itaconic acid (ITA) pathway in the known ITA producing microorganisms *U. maydis* and *A. terreus* (modified according to Geiser et al. (2016b) and Kuenz and Krull (2018)).

Carbon sources e.g. glucose or xylose are taken up by the fungi and metabolized into pyruvate via glycolysis and the pentose phosphate pathway (PPP). The resulting intermediates pyruvate and acetyl-CoA fuel the tricarboxylate acid (TCA) cycle inside the mitochondria. In the course of the TCA cycle, citrate is synthesised which is then isomerized into isocitrate by an aconitase (Aco1p). During the isomerization reaction, the intermediate *cis*-aconitate is formed. The *cis*-aconitate is transported into the cytosol by a mitochondrial tricarboxylate carrier (Mtt1p or MttAp) where it is isomerized into *trans*-aconitate by an aconitate-Δ-isomerase (Adi1p). *trans*-Aconitate is then decarboxylated into ITA by *trans*-aconitate decarboxylase (Tad1p). In the hyphal fungus *A. terreus*, *cis*-aconitate is directly decarboxylated into ITA by a *cis*-aconitate decarboxylase (Cad1p). The finished acid ITA is secreted into the surrounding medium with the help of a carrier protein belonging to the major facilitator superfamily (Itp1p in *U. maydis*; MfsAp in *A. terreus*). In *U. maydis*, the genes coding for Adi1p, Itp1p, Mtt1p and Tad1p are organized in a cluster together with the *RIA1* gene whose gene product regulates the transcription of the complete gene cluster (green arrows represent the transcriptional upregulation of the ITA cluster genes by Ria1p).

Despite *A. terreus* being a good ITA producing organisms with reported concentration of 130-160 g l^{-1} (Hevekerl et al., 2014a; Karaffa et al., 2015; Krull et al., 2017), the production cost of ITA and polyitaconic acid has to be reduced in order to replace petrochemical-based polyacrylic acid (Durant, 2009). Even after substantial efforts to enhance the productivity of *A. terreus* wild type (WT) and even genetically engineered strains, this cost-effectiveness could not be reached yet (for an overview of recent advancements in the biotechnological production of ITA see Bafana and Pandey, 2018; El-Imam and Du, 2014; Karaffa and Kubicek, 2019; Klement and Büchs, 2013; Kuenz and Krull, 2018; Teleky and Vodnar, 2019; Zhao et al., 2018).

The issue of high production costs is further compounded by several other factors. One is that several *A. terreus* strains have been reported to produce mycotoxins like citrinin and citreoviridin and can also cause opportunistic infections in plants, animals and humans (Edite Bezerra da Rocha et al., 2014). This led several countries e.g. Germany, Holland, UK and the USA to classify *A. terreus* as a biosafety level 2 organism which comes along with bureaucratic hurdles and technical safety measures (Hoog, 1996).

As a potential alternative, the closely related fungus and exceptionally good CA producer *A. niger* is receiving increasing attention (Hossain et al., 2016; Show et al., 2015; Steiger et al., 2016). However, the general use of filamentous fungi comes with multiple disadvantages: the handling of spores is laborious, the filaments of the fungi are sensitive to hydro-mechanical stress and impurities in the medium like manganese ions. In addition to that, *Aspergillus* spp. easily form cell pellets in submerged cultivations due to their hyphal growth. This leads to elevated viscosity and interruption of oxygen supply especially in the centre of the pellets which can ultimately decrease ITA yields (Bafana and Pandey, 2018; Karaffa et al., 2015; Klement et al., 2012; Kuenz and Krull, 2018; Kuenz et al., 2012).

To combat these issues, researchers are focusing on finding alternative single-cell ITA production hosts. Currently known ITA producing organisms are *U. zeae* (Haskins et al., 1955), *Candida* sp. (Tabuchi et al., 1981), *Pseudozyma* (*P.*) *antarctica* (Levinson et al., 2006), *P. tsukubaensis* (Bodinus, 2011), *Rhodotorula* sp. (Kawamura et al., 1981), *Helicobasidium* sp. (Sayama et al., 1994), and even mammalian cells (Strelko et al., 2011).

Compared to filamentous fungi, yeasts like *Pseudozyma* spp. are more advantageous in several aspects: they can be easily genetically engineered. The single cells are presumably metabolically more active than mycelia in submerged cultures and have, thus, higher fermentation rates. Moreover, they have short duplication times, large substrate specificity with elevated resistance to high substrate concentrations and tolerance to metal ions and they can be easily cultivated in large bioreactors (Adrio, 2017; Bellou et al., 2014; Cavallo et al., 2017).

1.4. Isocitric acid

Isocitric acid (ICA; also known as 1-hydroxypropane-1,2,3-tricarboxylic acid; CAS-nr.: 6061-97-8) with the molecular formula $C_6H_8O_4$ belongs to the class of tricarboxylic acids due to its three carboxyl functional groups. It is also a hydroxycarboxylic acid since it has a hydroxyl group at the C2-position (see figure 4). At room temperature, ICA is a crystalline solid with a molecular weight of 191.12 g mol^{-1} and a melting point of 162-165 °C [4].
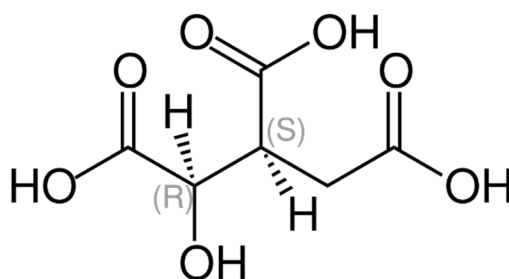
Figure 4 Chemical structure of D-*threo*-isoctric acid (2R,3S-isocitric acid).

ICA is a key metabolite of the TCA cycle. It has four isomers: D-*erythro*-, L-*erythro*-, D-*threo*- and L-*threo*-isocitric acid. However, in living organisms, only D-*threo*-ICA is formed from *cis*-aconitate with the help of an aconitase (see figure 3 above) (Martius and Knoop, 1937).

Earliest used natural sources for ICA are plants, primarily belonging to the *Crassulaceae* family (Pucher et al., 1948; Soderstrom, 1962; Vickery, 1969). One well-known representative is *Hylotelephium spectabile* (formerly *Sedum spectabile*). This plant accumulates high concentrations of organic acids e.g. ICA in its leaves (Tolbert and Zill, 1954). *H. spectabile* served as an ICA source for the D-*threo*-isocitric acid potassium salt sold by Sigma-Aldrich[5]. Also, several fruits, for example, strawberries, raspberries, blackberries and blackcurrant have been shown to contain a significant amount of ICA (Fan-Chiang and Wrolstad, 2010; Stój and Targoñski, 2006).

1.4.1. Production & Application of ICA

The potential applications of ICA have been limited for a long time. This is mostly due to the difficulties in obtaining adequate amounts of this compound. Chemical synthesis yields a racemic mixture containing all its four stereoisomers of which only D-*threo*-ICA is biologically active. The other three isomers are non-natural inhibitors of some enzyme systems and thus are unwanted. By chemical methods, these isomers cannot be separated adequately (Finogenova et al., 2005; Laptev et al., 2016).

The isolation of D-*threo*-ICA from plant leaves or fruits and its separation from the other organic acids proved to be a complicated and expensive technological process. This is because of the low

---

[4] PubChem, Isocitric acid (compound). Retrieved September 1st, 2019, from
https://pubchem.ncbi.nlm.nih.gov/compound/1198
[5] Sigma-Aldrich, products, *threo*-D$_s$(+)Isocitric acid potassium salt. Retrieved September 1st, 2019, from
https://www.sigmaaldrich.com/catalog/product/sigma/i1627?lang=de&region=DE

concentrations of ICA in the plant material and the large quantities of raw material needed. Dried leaves from the *Crassulaceae* family contain solely up to 15 % ICA (w/w) and fruit juices have ICA concentrations well below 1 g l^{-1} (Soderstrom, 1962; Stój and Targoñski, 2006).

In the 1960s, Russian and Japanese researchers demonstrated for the first time, that several yeast species, *Candida* (*C*.) *brumptii*, *C. guilliermondii* and *Yarrowia lipolytica* (formerly *C. lipolytica*), are able to secrete a mixture of CA and ICA into the medium (Abe and Tabuchi, 1968; Finogenova et al., 2005). Despite these early results, it took until 2008 for a first biotechnological process to obtain large quantities of the biologically active D-*threo*-ICA from yeast fermentation broth (Heretsch et al., 2008). ICA has been the only intermediate of the TCA cycle that has **not** been prepared in multigram amounts until then. Since that time, several works have been published that focus on the development of feasible methods to retrieve ICA from yeast culture broth. However, with the lack of a viable production host organisms, these studies focus on the separation and isolation of ICA from culture media that contain a mixture of ICA and at least one other organic like CA (Aurich et al., 2017; Bullin et al., 2019).

With ICA being available in multigram scale, the interest for it in the fields of pharmacology, medicine and the chemical, food or cosmetics industries grew steadily (Aurich et al., 2012; Heretsch et al., 2008; Kamzolova et al., 2008). ICA can be used to buffer Ca^{2+} activity at physiological concentrations and serve as an anticoagulant (Rånby et al., 1999). ICA is already being used as a chiral building block for the synthesis of pharmaceuticals: Moore et al. (2017) obtained ICA from the fermentation broth of *Y. lipolytica* and described its usage as a key intermediate (furofuranol) in the synthesis of Darunavir, an antiretroviral medication. Furofuranol can be utilized to produce other HIV-protease inhibitors as well e.g. brecanavir, GS-9005, and SPI-256 (Aurich et al., 2017; Khmelnitsky et al., 2011).

Due to its unique ability to unblock the succinate dehydrogenase (Kondrashova et al., 2013), ICA potentially promotes the utilization of oxygen inside the cell. This antihypoxic activity can contribute to an enhanced physical performance, which makes it a viable candidate as a dietary supplement for performance sports (Kamzolova et al., 2018; Rivera-Angulo and Peña-Ortega, 2014). Recent studies carried out by Morgunov et al. (2018, 2019) suggest that ICA can serve as an antioxidant agent and protect against cell damages caused by reactive oxygen species and some heavy metal salts. Furthermore, in the food industry ICA can also be used as a marker to detect food adulteration mainly in fruit juices due to the general use of its isomer CA as an adulterant (Saavedra et al., 2000).

1.5. Oleaginous yeasts

Species are considered oleaginous yeasts if they are able to produce and accumulate more than 20 % of their dry cell weight (DCW) in the form of lipids e.g. triacylglycerols (TAG) and steryl esters (SE) (Ratledge, 2004). First reports of yeast that can accumulate high levels of intracellular lipids were made as early as 1899 by Lindner when he described *Metschnikowia pulcherrima* (formerly *Torula pulcherrima,* Woodbine, 1959). Other examples include *Cryptococcus albidus, Cryptococcus curvatus, Lipomyces starkeyi, Rhodosporidium toruloides, Rhodotorula glutinis,* and *Trichosporon pullulans.* Some of those species can accumulate more than 65 % of their biomass as lipids (Adrio, 2017; Beopoulos et al., 2009).

The unconventional yeast *Y. lipolytica* is one of the most well-studied members of oleaginous yeasts (Adrio, 2017; Barth and Gaillardin, 1996). Naturally, its lipid content can reach 40 % of its DCW (Nicaud, 2012). However, there are reports of engineered so-called "obese" strains that accumulate up to 75-90 % lipids (Blazeck et al., 2014; Dulermo and Nicaud, 2011).

Recently, it was discovered that *P. tsukubaensis* is also able to accumulate at least 32 % (DCW) intracellular lipids. Furthermore, its fatty acid composition is highly similar to that of palm oil (Kunthiphun et al., 2018).

What makes oleaginous yeasts especially interesting to the biotechnological industry, is not only the ability to synthesise exceedingly high amounts of fatty acids and oil but their reaction to very high carbon (C) source concentrations in the medium: If oleaginous yeasts are cultivated with an excess in C and a limited amount of an essential nutrient e.g. nitrogen (N) or phosphate (P), they experience a C-overflow which is diverted by overproducing CA. The N exhaustion leads to an inhibition of isocitrate dehydrogenase in the TCA cycle due to the accumulation of adenosine monophosphate. Thus, CA accumulates inside the mitochondria and is then transported into the cytosol where it can be used for the synthesis of fatty acids or it is secreted into the surrounding medium (Adrio, 2017; Barth and Gaillardin, 1996; Ratledge, 2004; Tehlivets et al., 2007). This CA overflow, by uncoupling of the electron transport and TCA cycle from ATP synthesis, is a feature of oleaginous yeasts that makes them a perfect platform for the overproduction of organic acid and fatty acid-derived oleochemicals.

1.5.1. Pseudozyma tsukubaensis

Pseudozyma spp. are generally thought to be the asexual yeasts derived from smut fungi that are no longer pathogenic to plants. It is still unclear whether these species kept the pathogenicity against plants but do not activate it or if they completely lost this ability and only live as yeasts

(Kitamoto, 2019; Kruse et al., 2017). However, the German Central Committee on Biological Safety ruled that *P. tsukubaensis* does not pose a risk for plants or humans[6].

The definite phylogenetic classification of the genus is still being debated by researchers. The genus *Pseudozyma* was first described in 1985 by Bandoni. Later, Boekhout (1995) proposed seven species to be members of the genus *Pseudozyma*. These seven microorganisms have previously been assigned erroneously to other genera like *Candida*, *Cryptococcus*, *Sporobolomyces*, *Stephanoascus*, *Sterigmatomyces*, *Trichosporon* and *Vanrija*. One of the seven members is *P. tsukubaensis*. This yeast was first isolated by Onishi from a plant leaf at the Japanese mountain 'Tsukuba' in 1972. He had previously classified it as an ascomycetous yeast belonging to the *Candida* genus.

P. tsukubaensis are mostly present as single cells. The cells are ellipsoidal in shape with an average size of 5-15 x 3-4 µm and usually contain two to four lipid bodies (see figure 5). During mitosis, cell buds can occur polar, sessile or on short denticles. Depending on the environmental conditions, *P. tsukubaensis* also forms hyphae which measure ca. 10-80 µm in length and 1-3 µm in width. Sporulation can be induced. In that case cylindrical to fusiform blastoconidia are formed on sterigmata (Boekhout, 2011).
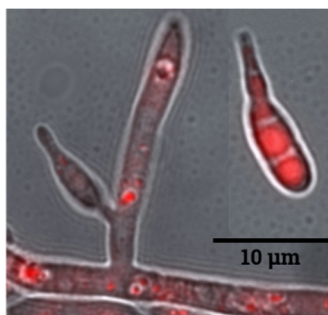
Figure 5 *P. tsukubaensis* budding single cell and hyphal aggregate with visualized lipid bodies
(brightfield and a fluorescence overlay, 1000 x magnification. Lipid bodies stained with the fluorescent dye Nile-red).

In 2000, based on the nuclear large-subunit-rDNA sequences, Begerow et al. suggested the genus *Pseudozyma* to be a cohesive genus within the Ustilaginomycetes. More specifically, he proposed that the species of *Pseudozyma* represent anamorphs of the smut causing pathogens belonging to the Ustilaginales and that *P. tsukubaensis* is probably synonymous with *U. spermophora*.

Later, Wang et al. (2015) advised taxonomic revisions in the subphylum Ustilaginomycotina after conducting phylogenetic analyses based on seven genes. As a result, the authors suggested disbanding the genus *Pseudozyma* because it is a polyphyletic anamorphic genus with species occurring in various clusters together. The investigated *Pseudozyma* species were located in various clades together with the teleomorphic species of *Ustilago*, *Sporisorium* and

---

[6] Statement by the German Central Committee on Biological Safety (ZKBS) on the risk assessment of *Pseudozyma tsukubaensis* as a donor or recipient organism in genetic engineering work (Az.: 6790-05-03-47, December 2009)

Moesziomyces. Most of these *Pseudozyma* species were transferred to other genera. However, *P. tsukubaensis* along with *P. alboarmeniaca, P. thailandica, P. hubeiensis* and *P. pruni* could not be classified unequivocally because of the taxonomic confusion between the teleomorphic genera. Therefore, these species should be taxonomically revised together with their closely related teleomorphic species. Until the affected species are assigned to their proper genus, the authors suggest to temporarily keep the genus name *Pseudozyma*.

Based on the available data, *P. tsukubaensis'* taxonomic classification can solely be resolved to the level of its family, the *Ustilaginaceae.* The phylogenetic relationship between the members of the temporary genus *Pseudozyma* is illustrated in figure 6.
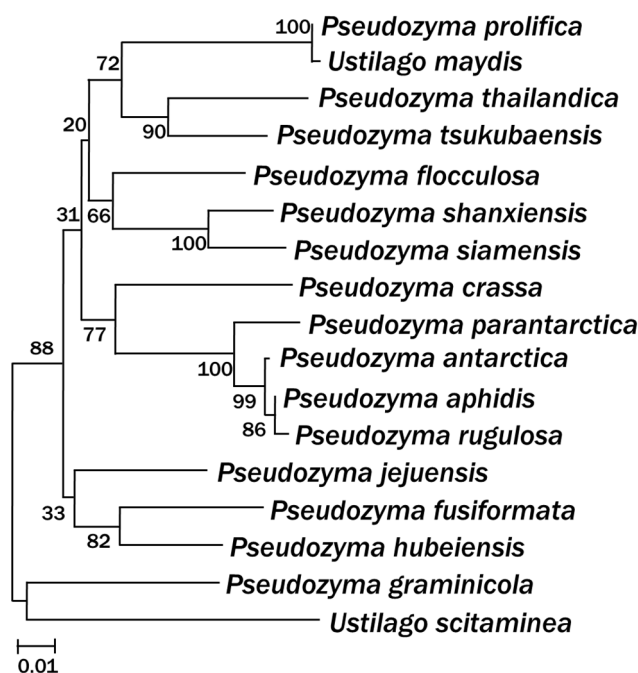
Figure 6 Phylogenetic relationship between *Pseudozyma* species based on internal transcribed spacer sequences of rRNA genes in the chromosome (adapted from Kitamoto, 2019)

1.5.1.1. Biotechnological usage of *P. tsukubaensis*

Yeasts belonging to the temporary genus *Pseudozyma* can utilize natural oils and fats by secreting triglyceride-degrading lipases (Kitamoto, 2019). Furthermore, *P. tsukubaensis* is able to assimilate a variety of C sources, amongst others, sugars (e.g. glucose, lactose, cellobiose, starch, xylose, arabinose), sugar alcohols (e.g. glycerol, erythritol), organic acids (e.g. CA, glucuronic-, lactic-, succinic acid), ethanol and *myo*-inositol (Boekhout, 2011). Its broad substrate specificity, the single-celled growth and the secretion of different products have drawn attention to *P. tsukubaensis* and related *Pseudozyma* spp.

One generic form of application is the use as a biocontrol agent. This potential is constantly increasing, as pesticides in the form of agrochemicals are progressively abandoned. Several *Pseudozyma* yeasts are reportedly effective against powdery mildew causing fungi e.g. *Blumeria*

graminis, the necrotizing fungus *Botrytis cinerea* and even against phytopathogenic bacteria and viruses (Bélanger and Labbé, 2002; Buxdorf et al., 2013; Lee et al., 2017; Yoshida et al., 2015). The antifungal properties of *P. flocculosa* can partially be traced back to the unusual cellobiose lipid flocculosin and the structural similar ustilagic acid (Cheng et al., 2003; Hewald et al., 2005; Kulakovskaya et al., 2005). The two glycolipids are also investigated for their potential use against human pathogens (Mimee et al., 2005; Rodrigues et al., 2006). Additionally, *P. tsukubaensis* is known to excrete the fungicidal killer toxin mycocin (Golubev et al., 2006).

For several decades now, the usage of *Pseudozyma* species for the biotechnological production of several different proteins, especially enzymes, have been investigated. *P. tsukubaensis* secretes a distinct glucoamylase that displays its highest activity at a low pH (De Mot et al., 1985). This yeast species has also been described to express other promising proteins such as a glycogen degrading *α*-glucosidase and a rennet protease (Fungaro et al., 1994; Kinsella et al., 1991).

P. antarctica came into the focus in the late 1980s for its ability to secrete lipases when large-scale screenings were conducted by Novo Nordisk. More specifically, the identified enzymes lipase A & lipase B exhibit a low thermal profile. However, it was demonstrated that the two enzymes are stable at temperatures up to 96 °C and that they exhibit a high degree of substrate specificity. Nowadays, these lipases are already mass-produced for various industries like paper/pulp and textile manufacturing (Kitamoto, 2019; Nielsen et al., 1999). *P. antarctica, P. aphidis* and *P. rugulosa* have been shown to express esterases that are able to break down biodegradable plastics such as polybutylene succinate (Kitamoto et al., 2011; Shinozaki et al., 2013).

Another class of substances that are commonly secreted by *Pseudozyma* species are mannosylerythritol lipids (MELs) which are so-called biosurfactants. These substances have an excellent interfacial activity, are biodegradable, biocompatible and can be produced in an environmentally friendly way through fermentation. Moreover, MELs are self-assembling, can be used as gene delivery carriers, they possess a high affinity to immunoglobulins, exhibit anti-tumour, anti-bacterial, and anti-oxidative activities, and can even repair damaged human skin and hair (Im et al., 2003; Kitamoto et al., 1993, 2002, 2009; Morita et al., 2010a; Saika et al., 2018a; Takahashi et al., 2012; Yamamoto et al., 2012; Zhao et al., 2001).

MELs consist of mannose and erythritol as hydrophilic moieties, fatty acids and acetyl groups as hydrophobic moieties. These molecules are categorized into the four types MEL-A, -B, -C and -D based on the degree of the acetylation (Saika et al., 2018a). The various classes of MELs are not produced by every *Pseudozyma* species equally. *P. antarctica, P. aphidis, P. parantarctica* and *P. rugulosa* synthesise a mixture of MEL-A, -B, -C and -D with concentrations reaching up to 165 g l^{-1} (Kitamoto, 2019; Saika et al., 2018a). *P. crassa* secretes diastereomer types of MEL-A, -B, and-C (Morita et al., 2015). The four following yeasts produce predominantly MEL-C:

P. graminicola, P. hubeiensis, P. shanxiensis and *P. siamensis* (Fukuoka et al., 2007; Konishi et al., 2008; Morita et al., 2008a, 2008b; Saika et al., 2018a).

P. tsukubaensis holds a special position. It produces exclusively a special diastereomer type of MEL-B (Fukuoka et al., 2008). Morita et al. (2010b) isolated the MEL-B overproducing *P. tsukubaensis* strain 1E5 from *Perilla frutescens* leaves. This strain can produce up to 73 g l^{-1} MEL-B with a yield of 43.5 % (g g^{-1} olive oil). The ability to overproduce the MEL-B diastereomer has already been commercialized for a cosmetic ceramide-like moisturizing agent under the brand name SurfMellow® by the Japanese Toyobo company[7] (Morita et al., 2015). Like other MEL producing *Ustilaginaceae*, *P. tsukubaensis* also possesses a gene cluster for the synthesis of MELs that consists of five genes. One gene, encoding an erythritol/mannose transferase (*PtMET1*), differs substantially from homologous counterparts in related species. The deduced protein of *PtMET1* is the reason, why this yeast produces MEL-B (Saika et al., 2016). By deleting one of the cluster genes *PtMAT1* or *PtMAC2* the yeast produces MEL-D or a novel monoacetylated MEL instead of MEL-B (Saika et al., 2018b, 2018c). Therefore, *P. tsukubaensis* holds the potential to synthesise tailor-made biosurfactants that can later be used in various industries including cosmetics, pharmaceuticals, agriculture, food, and environmental fields (Saika et al., 2018a).

P. tsukubaensis can also be applied for the microbial production of erythritol. The sugar alcohol is an important additive in the food industry as a noncaloric and non-cariogenic sweetening agent (Moon et al., 2010). The isolated *P. tsukubaensis* strain KN75 produces up to 245 g l^{-1} erythritol with a productivity of 2.86 g l^{-1} h^{-1} and a yield of 61 % (w/w) from glucose. The erythritol production on plant scale (50000 l) has already been achieved (Jeya et al., 2009).

Recently, also the synthesis of the non-digestible prebiotic galactooligosaccharides (73 g l^{-1}, yield 18 % (w/w)) from cassava wastewater and lactose was demonstrated (Cavalcante Fai et al., 2015).

Another promising application for *P. tsukubaensis* involves the production of organic acids such as ITA from simple sugars. First studies with mutagenized and genetically modified *P. tsukubaensis* strains proved its applicability. The UV-mutagenesis strain M15 (DSM 21214) produced already 2.3-times more ITA than the wild type H488 (CBS 422.96). By additionally overexpressing the *cis*-aconitate decarboxylase gene *AtCAD1* from *A. terreus*, it was possible to produce up to 60.6 g l^{-1} ITA in a 3.6 l-bioreactor. Later, yields of more than 75 g l^{-1} ITA were achieved with glucose as C source (Aurich et al., 2009; Bodinus, 2011; Specht et al., 2014). Only one other *Pseudozyma* species, namely *P. antarctica*, has been demonstrated to, similarly, secrete substantial concentrations of ITA. However, the resulting ITA yield has been much lower with an end concentration of only 30 g l^{-1} (Levinson et al., 2006).

---

[7] TOYOBO, SurfMellow® (*Pseudozyma tsukubaensis*). Retrieved September 15th, 2019, from
https://www.toyobo-global.com/seihin/cosme/surfmellow.htm

1.5.2. Yarrowia lipolytica

The ascomycetous yeast *Y. lipolytica* is an oleaginous species that has first been isolated in the year 1928 by Harrison as *Mycotorula lipolytica* and in the same year by Nannizzi as *Monilia cornealis.* In 1972, Yarrow reclassified the yeast to the novel genus *Saccharomycopsis.* Its current generic name was proposed by Walt and Arx (1980) in honour of Yarrow's work. Until then, it was assigned to the genera of *Azymoprocandida, Candida, Endomycopsis, Torula* and *Torulopsis* (Barth and Gaillardin, 1996, 1997; Kurtzman et al., 2011; Nicaud, 2012).

Y. lipolytica's taxonomic name already implies its lipolytic capabilities but it exerts pronounced proteolytic activities as well (Groenewald et al., 2014). Hence, the yeast is able to assimilate unusual hydrophobic substrates containing *n*-alkanes, 1-alkenes, fats, fatty acids, oils and paraffin. Its substrate range for C also includes simple alcohols, acetate, glycerol and simple sugars (mono- and disaccharides). Naturally, it can be isolated from a variety of ecosystems for example marine waters, mycorrhizae, oil-polluted environments, sewages and soils. Additionally, the oleaginous yeast is often found on different food products that are rich in fats and proteins like cheese, kefir, shoyu, yoghurts, sausages and even shrimp salad (Barth and Gaillardin, 1996, 1997; Gardini et al., 2001; Groenewald et al., 2014; Guerzoni et al., 1993; Madzak, 2018; Spencer et al., 2002; Vasdinyei and Deák, 2003).

Y. lipolytica is an obligate aerobic yeast and is considered apathogenic. Hence, it has been classified as Generally Regarded As Safe (GRAS) by the US American Food and Drug Administration (Groenewald et al., 2014). Much like its diverse colony morphologies ranging from heavily convoluted and matt to smooth and glistening, it exhibits different growth forms depending on its genetic background and environmental conditions. Generally, isolates are present as single haploid yeasts cells but, it can also form pseudo-hyphae and true mycelium with septate hyphae. Single cells are spheroidal, ellipsoidal with typical dimensions of 3-5 x 3-15 µm or elongated when forming (pseudo-)hyphae (Barth and Gaillardin, 1996, 1997; Bellou et al., 2014; Kurtzman et al., 2011; Nicaud, 2012).
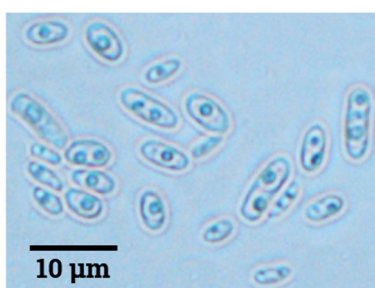
Figure 7 Single *Y. lipolytica* cells with one to three lipid bodies.
(phase contrast microscopy, 400 x magnification)

Furthermore, this yeast belongs to heterothallic fungi with the two mating types MATA and MATB. Haploid cells can reproduce sexually by conjugating with cells from the complementary

mating type to form a diploid zygote. Both haploid and diploid cells are vegetatively stable. Under certain circumstances the diploid zygote can form one or multiple asci with one to four spores (Barth and Gaillardin, 1997; Barth and Weber, 1985). Currently numerous *Y. lipolytica* strains are used for research without consensus on the reference strain. However, the applied working strains can mostly be traced back to the three main inbred lines H222 (German), W29 (French) and CBS6124-2 (US America) (Barth and Gaillardin, 1996; Nicaud, 2012).

1.5.2.1. Applications of *Y. lipolytica*

Because of its unique abilities and peculiar phenotypes compared to the conventional yeast *Saccharomyces* (*S.*) *cerevisiae, Y. lipolytica* has been used since the 1960s as a model organism to study various biological mechanisms. These are, inter alia, dimorphic growth and the formation of hyphae, production of single-cell proteins & oils; the utilization of hydrophobic substrates; lipid homeostasis; lipid body & peroxisome biogenesis; intron & alternative splicing; and the formation of the mitochondrial complex (Harzevili, 2014; Nicaud, 2012).

Besides being a model organism, the oleaginous yeast can be applied for environmental purposes. Difficult to treat agro-industrial waste products e.g. olive mill waste are treated and upgraded with it (Azbar et al., 2004; Darvishi, 2012). Its ability to degrade hydrocarbons enable it to bioremediate oil-polluted environments. Moreover, it can aid environmental detoxification attempts by the bioaccumulation of heavy metals e.g. Cd, Cr, Cu & Ni or by the biotransformation of trinitrotoluene (Bankar et al., 2009a, 2009b; Harzevili, 2014; Smets et al., 2007).

The British Petroleum company pioneered its industrial use in the 1950s for the production of high-quality single-cell proteins from low-cost substrates like ethanol, methanol and petroleum fractions for livestock feed (Groenewald et al., 2014). Further advancements, mostly by the industrial heavy weights DuPont, Pfizer, Codexis and Microbia, led to many successes in the production of lipases and lipids, including fish oil substitutes. Various other extracellular enzymes are secreted at a high level by *Y. lipolytica* ranging from alkaline or acid proteases, phosphatases, RNase to inulinase (Harzevili, 2014; Markham and Alper, 2018). Upon the increase in available molecular biology tools, a plethora of value-added chemicals could also be produced with the help of this yeast. According to Markham and Alper (2018), the substances that are possible to synthesise can be assigned to four groups:

- oleochemicals: e.g. arachidonic acid (Damude et al., 2015); eicosapentaenoic acid (Damude et al., 2007); fatty alkenes and alcohols (Xu et al., 2016)
- fine chemicals and pharmaceuticals: L-dopa (Ali et al., 2007); dicarboxylic acids and lactones (Barth, 2013; Gatter et al., 2014); erythrulose (Carly et al., 2018); L-hydroxybutyric acid (Kyong and Shin, 2000); mevalonate derivatives (Cao et al., 2017; Zhang et al., 2017) and triacetic acid lactone (Markham et al., 2018)

- nutraceuticals and feed stock: carotenoids (Kildegaard et al., 2017; Larroude et al., 2018; Matthäus et al., 2014); sugar alcohols e.g. erythritol, mannitol, arabitol (Tomaszewska et al., 2012); single cell protein (Groenewald et al., 2014) and terpenes (van Dyk et al., 1998; Ferrara et al., 2014)

- organic acids with TCA cycle intermediates being the most prominent targets: e.g. CA & ICA (Förster et al., 2007a; Holz et al., 2009), α-ketoglutaric acid (Otto et al., 2012), pyruvic acid (Morgunov et al., 2004), succinic acid (Kamzolova et al., 2012) but also non-native organic acids like ITA (Blazeck et al., 2015).

Since *Y. lipolytica* is such an effective acid secreting organism, the interest for the production of CA with its help started already 40 years ago (Stottmeister et al., 1982). Nowadays, CA concentrations of 160-175 g l^{-1} are easily achieved (Kamzolova et al., 2011; Rywińska and Rymowicz, 2010). Because it produces CA in a similar magnitude as the most common CA-production host *A. niger*, its potentially is already explored on an industrial scale (Sauer et al., 2008).

Naturally, the CA secretion is accompanied by ICA. The proportion of ICA varies between 8-50 % depending on the strain, C source and culture conditions (Barth and Gaillardin, 1996; Mauersberger et al., 2003; Stottmeister et al., 1982). Not only do contaminations of ICA negatively affect the crystallization of CA during the purification processes but it also displays inferior buffer capacity and chelating abilities compared to CA. Thus, ICA was considered an unwanted by-product in the microbial synthesis of CA (Barth and Gaillardin, 1997; Mattey, 1992; Stottmeister et al., 1982).

Akiyama et al. (1973) was one of the first groups to try to circumvent this negative aspect by selecting mutant strains that exhibit a more beneficial CA:ICA ratio compared to the wild type strains. Via random mutagenesis, several other strains have been obtained that secrete CA with only insignificant amounts of ICA. The most notable strains N15, AWG7 and NG40/UV7 reach final CA concentrations up to 150 g l^{-1} with CA:ICA ratios between 25:1-30:1 on sunflower oil or glycerol (Kamzolova et al., 2008; Morgunov et al., 2013; Rywińska and Rymowicz, 2010).

Förster et al. (2007a, 2007b) carried out targeted genetic modification to rationally construct CA over-producing *Y. lipolytica* strains. By doing so, the multicopy overexpression of the *YlICL1* gene coding for an isocitrate lyase resulted in a strain that was able to secrete up to 140 g l^{-1} CA with only 4-6 % ICA on sugars and hydrophobic substrates.

However, after it was possible to obtain larger quantities of it, the interest for ICA grew rapidly circa ten years ago (Heretsch et al., 2008). Thus, initial attempts were made to increase the proportion of ICA in the secretion profile. Holz et al. (2009) carried out early metabolic engineering experiments by overexpressing the aconitase encoding gene *YlACO1*. The constructed *Y. lipolytica* strain produced up to 71 % ICA on sunflower oil compared to 35-49 % with the wild

type. Later, the group around Kamzolova et al. (2015, 2016, 2018) undertook great efforts to maximize the ICA yield by selecting for overproducing *Y. lipolytica* strains. As a result, the selected mutant strain UV/NG (mutagenized by UV-irradiation and N-methyl-N'-nitro-N-nitrosoguanidine) was able to secrete 88.7 g l^{-1} ICA with an ICA:CA ratio of 6:1 on rapeseed oil with the addition of ITA as an inhibitory agent.

1.5.2.1. Mitochondrial citrate transporters in yeast

Until recently, the strategies to modify the ratio between CA and ICA had focused on the engineering of the main TCA cycle enzymes e.g. aconitase, isocitrate lyase, citrate synthase or malate synthase. Another possibility to influence the ICA:CA ratio could be achieved by modulating the transport of these organic acids at the interface between the mitochondrion and the cytosol. Mitochondrial solute carriers are members of the mitochondrial carrier family (MCF). These carrier proteins are located in the inner membranes of mitochondria and are responsible for transport of various metabolites including ions, nucleotides, amino acids, organic acids and other native compounds between the mitochondrial and cytosolic matrices, which are essential for numerous biological processes. Antiport (obligatory counter-exchange of one solute for another) is the preferential mode of transportation for these carrier proteins (Palmieri, 2004, 2013; Palmieri and Pierri, 2010; Palmieri et al., 2000). The MCF contains 50 identified members in humans and 35 in *S. cerevisiae*.

For the transport of tricarboxylates like CA, ICA and malic acid (MA) into the cytosol, CTP has been described as the main mitochondrial carrier protein in mammals. In *S. cerevisiae*, several transporters are believed to be able to transport CA at least to a certain degree (Iacobazzi et al., 1997; Palmieri, 2013). Although ScCtp1p showed a high transporting activity for CA and to a lesser degree ICA, its deletion led to no phenotype on various C sources. This indicates that *ScCTP1* is not an essential gene under the tested conditions (Kaplan et al., 1995, 1996).

First Mayor et al. (1997) suggested that *YM9408.03* (*ScYHM2*) codes for a mitochondrial transport protein that displays substrate specificity for CA, α-ketoglutaric acid (αKG, synonymic: 2-oxoglutaric acid) and succinic acid. Shortly thereafter Cho et al. (1998) named the gene encoding the same protein *ScYHM2* and identified it in *S. cerevisiae* as a member of the MCF. The group also postulated that the protein is involved in the maintenance of mitochondrial genome stability. Later, it was demonstrated by Castegna et al. (2010) that ScYhm2p and not ScCtp1p is, in fact, the main carrier protein in yeasts for CA transport in exchange for αKG. However, a clear biochemical characterization of Yhm2p is still needed (Palmieri and Monné, 2016). Recently, Scarcia et al. (2017) reported that ScYhm2p plays an important role in nitrogen fixation and lysine biosynthesis by exporting αKG and 2-oxodiapate, respectively, into the cytosol. Moreover, the group around Scarcia questioned ScYhm2p's role in mtDNA stability that was postulated by Cho et al. (1998).

1.6. Scope

The non-conventional yeast species *P. tsukubaensis* and *Y. lipolytica* are naturally able to synthesize the industrially valuable organic acids ITA and ICA from the common precursor *cis*-aconitate, respectively. The overall goal of this thesis is to utilize this natural asset and create acid overproducing production strains by the means of metabolic engineering.

The biotechnological production of ITA with the hyphal fungus *A. terreus* is an established but still not economically viable process for it to compete with synthetically produced alternatives. *P. tsukubaensis* as a single-celled microorganism comes with characteristics that make it possible to overcome the drawbacks of the fermentation with fungi from the genus *Aspergillus* e.g. shear stress and sensitivities towards impurities in the medium.

Here, the first objective is to understand the underlying ITA biosynthesis pathway in the not well understood yeast *P. tsukubaensis*. This insight is to be attained with the help of recently gained information on the ITA biosynthesis in *A. terreus* and *U. maydis* and with molecular biological tools like whole genome sequencing and quantitative real-time PCR. Subsequently, by utilizing this knowledge, production strains are to be generated by modifying specific genetic targets in the H488 wild type strain or Bodinus' mutagenized ITA overproducing strain M15.

In addition to that, a full synthetic defined minimal medium should be established for the cultivation of *P. tsukubaensis* to ensure consistent growth and high fermentation rates. The establishment of such a medium without complex components also allows for the investigation of environmental triggers for the natural ITA synthesis e.g. nutrient depletion.

In the last stage, the metabolically engineered production strain should be transferred to a fermenter where its ITA synthesis behaviour is further investigated. By modifying particular cultivation parameters, further increases in ITA productivity ought to be achieved.

As a second goal, a host organism for the microbial production of ICA from *cis*-aconitate must be developed from *Y. lipolytica* because to this date there are no high-yielding production strains described in the literature. Therefore, the well-characterized oleophilic model organism must be metabolically engineered to secrete high concentrations of ICA with less to no amounts of the by-product CA. In order to achieve this, potential mitochondrial citrate transporters are targeted. Appropriate genes coding for citrate carriers must be identified and respective deletion strains generated afterwards. The resulting strains should be characterized in their ICA/CA production behaviour. Potentially, further genetic modifications should be carried out to distinctly enhance the ICA secretion. After such a strain has been created, its cultivation is scaled up to large-volume bioreactor to gain more insight into its production behaviour.

2. Materials and Methods

2.1. Equipment

Autoclaves

Hot-air sterilizer SFE 500	Memmert GmbH
MicroJet Microwave autoclave	SERVA Electrophoresis GmbH
Steam sterilizer HiClave HV-85 L	HMC Europe GmbH
Steam sterilizer Varioklav 500 E	H+P Labortechnik AG
Table-top autoclave 2540 EL	Systec GmbH
Table-top autoclave DE-45	Systec GmbH

Balances

KERN 770-13	Kern & Sohn GmbH
Talent TE1502S	Sartorius AG
Talent TE214S	Sartorius AG

Centrifuges

Biofuge Fresco	Heraeus Instruments GmbH
Sigma 1-15K	Sigma Laborzentrifugen GmbH
Sigma 3K30	Sigma Laborzentrifugen GmbH
Sigma 3-18K	Sigma Laborzentrifugen GmbH

Fermentation equipment

Two-vessel fermentation system Multifors (2 X 1 l)	Infors AG
pH sensors	Mettler-Toledo GmbH
pO_2 sensors	Mettler-Toledo GmbH

Gel electrophoresis equipment

Electrophoresis power supply EPS 200	PEQLAB Biotechnologie GmbH
Electrophoresis power supply PowerPac 300	Bio-Rad Laboratories GmbH
Gel electrophoresis chambers	PEQLAB Biotechnologie GmbH

IC equipment

Ion chromatograph IC-2100	Thermo Fisher Scientific Inc.
Autosampler AS50	Thermo Fisher Scientific Inc.
Column IonPac AS27 (2 X 250 mm)	Thermo Fisher Scientific Inc.
Guard column IonPac AG27 (2 X 50 mm)	Thermo Fisher Scientific Inc.
Suppressor ASRS 300	Thermo Fisher Scientific Inc.

Incubators and shakers

Cooled incubator BK 800	Heraeus Instruments GmbH
Incubator BE500	Memmert GmbH
Incubator shaker Multitron	Infors AG
Incubator shaker Novotron AK82	Infors AG

Microscope and filters

AxioCam 702 mono microscope camera	Carl Zeiss Microimaging GmbH
Axio Observer 7 inverted fluorescence micr.	Carl Zeiss Microimaging GmbH
Digital camera U-TV1X	Olympus Europa Holding GmbH
Filter U-M41007A (ex 545/30 nm, em 610/75 nm)	Olympus Europa Holding GmbH
Fluorescence microscope Provis AX70	Olympus Europa Holding GmbH

PCR cyclers

CFX96 cycler	Bio-Rad Laboratories GmbH
Mastercycler ep gradient S	Eppendorf AG
Primus 25	MWG Biotech AG
Primus 96 Plus	MWG Biotech AG
T1-Thermocycler	Biometra GmbH

UV-Vis spectrophotometers

Cary 60 UV-Vis	Agilent Technologies Inc.
Double beam spectrophotometer Helios Alpha	Thermo Fisher Scientific Inc.
Infinite 200 microplate reader	Tecan Trading AG
Nano Drop ND 1000	Thermo Fisher Scientific Inc.
Single beam spectrophotometer Ultrospec 2000	Pharmacia Biotech AG
Synergy 2 microplate reader	BioTek Instruments Inc.
Synergy HTX microplate reader	BioTek Instruments Inc.

Other equipment

Block thermostat BT 100	Kleinfeld Labortechnik GmbH
Cell disruptor FastPrep FP120A-230	Thermo Fisher Scientific Inc.
DNA Speed Vac DNA 110	Savant Instruments Pvt Ltd.
Drying cabinet S1 6200	Heraeus Instruments GmbH
Electroporator MicroPulser	Bio-Rad Laboratories GmbH
Magnetic stirrer IKAMAG RH	IKA-Werke GmbH & Co. KG
Microwave R-937	Sharp Electronics GmbH
pH meter HI 83141	Hanna Instruments GmbH
Pipettes	Eppendorf AG
Rotary Evaporator Laborota 4000	Heidolph Instruments GmbH
Safety cabinet HeraSafe HS12	Heraeus Instruments GmbH
Thermomixer comfort 1.5 ml	Eppendorf AG
Ultrapure water system Milli-Q Reference	Merck KGaA
UV transilluminator with dark hood DH-30/32	Biostep GmbH
Vibration mill MM200	Retsch GmbH
Vortexer Minishaker MS2	IKA Works Inc.
Vortexer REAX 2000	Heidolph Instruments GmbH
Water bath with circulation thermostat MP-5	JULABO Labortechnik GmbH
Water bath GFL-1008	Ges. f. Labortechnik GmbH

2.2.   Chemicals, biochemicals and nucleic acids

Relevant chemicals

All used chemicals have been obtained commercially.

1 kb DNA ladder	Thermo Fisher Scientific Inc.
λ-DNA	Thermo Fisher Scientific Inc.
Agar	AppliChem GmbH
Agarose	Biozym Scientific GmbH
Ampicillin	Carl Roth GmbH & Co. KG
ATP	Thermo Fisher Scientific Inc.
Bradford reagent	Bio-Rad Laboratories GmbH
Bovine serum albumin	Carl Roth GmbH & Co. KG
Carboxin	Sigma-Aldrich Co. LLC.
cis-Aconitic acid ≥ 98 %	Sigma-Aldrich Co. LLC.
Citric acid monohydrate	AppliChem GmbH

Diisopropyl ether	Merck KGaA
D,L-Na-Isocitrate	Sigma-Aldrich Co. LLC.
dNTPs	Thermo Fisher Scientific Inc.
Ethidium bromide	Carl Roth GmbH & Co. KG
FOA	Thermo Fisher Scientific Inc.
Glass beads (diameter: 0.75-1 mm)	Carl Roth GmbH & Co. KG
D-Glucose	Carl Roth GmbH & Co. KG
Herring sperm DNA	Roche Dtl. Holding GmbH
n-Hexadecane ($\geq$ 99 %)	Merck KGaA
HPLC grade water	Carl Roth GmbH & Co. KG
Hydrogen peroxide	Carl Roth GmbH & Co. KG
Hygromycin B	Carl Roth GmbH & Co. KG
Itaconic acid $\geq$ 99 %	Sigma-Aldrich Co. LLC.
Iron sulphate Fe(II)SO$_4$ x 7 H$_2$O	Merck KGaA
α-Ketoglutaric acid sodium salt $\geq$ 98 %	Sigma-Aldrich Co. LLC.
PEG4.000	Merck KGaA
Phytosphingosine hydrochloride	Sigma-Aldrich Co. LLC.
Magnesium sulphate	Grüssing GmbH
D-Malate	Carl Roth GmbH & Co. KG
Nile red (Nile blue oxazone)	Sigma-Aldrich Co. LLC.
ONPG	Carl Roth GmbH & Co. KG
Oxaloacetate	Sigma-Aldrich Co. LLC.
D-Sorbitol	Carl Roth GmbH & Co. KG
Sucrose	Carl Roth GmbH & Co. KG
Sunflower seed oil 100 %, cold-pressed	Ölmühle Fandler
Thiamine pyrophosphate	Sigma-Aldrich Co. LLC.
TMCS	Macherey-Nagel GmbH & Co. KG
Tween 80	Carl Roth GmbH & Co. KG
Uracil	Sigma-Aldrich Co. LLC.

Enzymes

DNA ligase T4	Thermo Fisher Scientific Inc.
DNase I – RNase free	EUR$_X$ Sp. z o.o.
DreamTaq DNA polymerase	Thermo Fisher Scientific Inc.
FastAP thermosensitive alkaline phosphatase	Thermo Fisher Scientific Inc.
Glucanex®	Sigma-Aldrich Co. LLC.
Phusion DNA polymerase	Thermo Fisher Scientific Inc.
Restriction enzymes	Thermo Fisher Scientific Inc.
RNase A	Thermo Fisher Scientific Inc.

Kit systems

Glucose and Sucrose colorimetric Assay Kit	Sigma-Aldrich Co. LLC.
Glucose UV test	R-Biopharm AG
Invitek Invisorb Spin DNA Extraction Kit	Stratec Molecular GmbH
Invitek Invisorb Spin Plasmid Mini Two	Stratec Molecular GmbH
Invitek MSB Spin PCRapace	Stratec Molecular GmbH
Maxima SYBR Green/ROX qPCR Master Mix	Thermo Fisher Scientific Inc.
NucleoSpin RNA Clean-up XS	Macherey-Nagel GmbH & Co. KG
RevertAid First Strand cDNA Synthesis Kit	Thermo Fisher Scientific Inc.

Test strips

Glucose test strip BIOPHAN G	Kallies Feinchemie AG
pH test strip pH-Fix 2.0-9.0	Macherey-Nagel GmbH & Co. KG
pH test strip pH 0-6.0 Acilt	Merck KGaA

2.2.1. Oligonucleotides (PCR primers)

The oligonucleotides listed below in table 2 & table 3 were used as primers for polymerase chain reactions (PCR) and purchased from Eurofins MWG GmbH.

Table 2 Primers used in this study for genetic modifications of *Y.* lipolytica.
Non-complementary sequences are written in small letters and introduced restriction sites (RS) are underlined. * Primer pTef_SpeI_fw3 was also used for the overexpression of *YHM2*.

Primers used for *Yarrowia lipolytica*		
Name	**Sequence (5' → 3')**	**RS**
Primers for the overexpression of *YlACO1*		
pTef_SpeI_fw3 *	CTACGCTTGTTCAGACTTTG	-
pTef_ol_*ACO1*_rv	gaaactcgagaagccagcatTTTGAATGATTCTTATACTC	-
*ACO1*_ol_pTef_fw	gagtataagaatcattcaaaATGCTGGCTTCTCGAGTTTC	-
*ACO1*_rv_SphI	atatag<u>catgc</u>TTATTTCTTGGAGGCAGCCATC	SphI
*AscI*_CI_rv_out	AGAGACCTCCCACAAAG	-
Primers for the deletion of *YlCTP1*		
p*CTP1*_fw	TTTCCTTGATGGCGTACTCC	-
p*CTP1*_rv_BglII	atata<u>agatct</u>TGTCAATGTGTCTGTGTCTG	BglII
t*CTP1*_fw_BglII	atata<u>agatct</u>ACGTTTATACATAATGACTA	BglII
t*CTP1*_rv_KpnI	atata<u>ggtacc</u>GCTGGAAACACCGGTTCTGG	KpnI
p*CTP1*-DK-Ampl_fw	TTGGCCACTCCATCCCAGTC	-
Primers for the deletion of *YlYHM2*		
p*YHM2*_fw	AGTGGTGCCGATACGATTAC	-
p*YHM2*_rv_BamHI	<u>ggatcc</u>GTCGGAGGAGAGGGAAATGG	BamHI
t*YHM2*_fw_BamHI	<u>ggatcc</u>TCCGTGATTCCCCTTAGAC	BamHI
t*YHM2*_rw_BglII	<u>agatct</u>GGCTCTGGTGTTTGTTTC	BglII
Primers for the overexpression of *YlYHM2*		
pTef_*YHM2*_ol_fw	ttctgagtataagaatcattcaaaATGGGTGCTGCTAACCTC	-
pTef_*YHM2*_ol_rv	gaggttagcagcacccatTTTGAATGATTCTTATACTCAGAA	-
*YHM2*_rv_MluI	atata<u>acgcgt</u>TAGTGCTTACCAACAGGTCG	MluI
IntB_out_rv	TCCTTGGCTAGACGAATG	-

Table 3 Primers used in this study for the genetic modifications of *P. tsukubaensis*.
Non-complementary sequences are written in small letters and introduced restriction sites (RS) are underlined. * Primer pActin_KpnI_fw was also used for the overexpression of *ADI1, AtCAD1, ITP1, MTT1, RIA1* & *TAD1*.

Primers used for *Pseudozyma tsukubaensis*		
Name	**Sequence (5' → 3')**	**RS**
Primers for the overexpression of *LacZ*		
pActin_KpnI_fw *	atata<u>ggtacc</u>GGCCCGTTCAACACAATGCG	KpnI
pActin_o*LacZ*_rv	acgaccatcgtgccggccatGTTGAAAGTAAGTGGTGGGG	-
*LacZ*_oActin_fw	ccccaccacttactttcaacATGGCCGGCACGATGGTCGT	-
*LacZ*_PstI_rv	atata<u>ctgcag</u>TTAACCGGTTTTTGACACCAG	PstI
pGAPDH_KpnI_fw	atata<u>ggtacc</u>ATCCTTCGGACGGCGACATC	KpnI
pGAPDH_o*LacZ*_rv	acgaccatcgtgccggccatTGTGAATAATTTTTGGGATG	-

Primers for the overexpression of *LacZ*		
*LacZ*_oGAPDH_fw	catcccaaaaattattcaca ATGGCCGGCACGATGGTCGT	-
pHSP70_KpnI_fw	atata<u>ggtacc</u>ACGCAGCAACCGAGTGTCAG	KpnI
pHSP70_o*LacZ*_rv	acgaccatcgtgccggccatGATGAATGATGTGAACCTTT	-
*LacZ*_oHSP70_fw	aaaggttcacatcattcatcATGGCCGGCACGATGGTCGT	-
pTef_KpnI_fw	atata<u>ggtacc</u>GTCCGTTGCCGCAGTCGCTC	KpnI
pTef_o*LacZ*_rv	acgaccatcgtgccggccatTTTGGATGATGTTTTTGATG	-
*LacZ*_oTef_fw	catcaaaaacatcatccaaaATGGCCGGCACGATGGTCGT	-
Primers for the overexpression of *PtACO1*		
pActin_BsrGI_fw	atatat<u>gtaca</u>GGCCCGTTCAACACAATGCG	BsrGI
pActin_o*ACO1*_rv-long	gagtgcgcgaaggggaagcatGTTGAAAGTAAGTGGTGGGGG	-
*ACO1*_oActin_fw-long	cccccaccacttactttcaacATGCTTCCCCTTCGCGCACTC	-
*ACO1*_Ex_rv	gcgaaagaggtcggttgaggCGGGATCGAACGACCTTGAG	-
*ACO1*_Ex_fw	ctcaaggtcgttcgatcccgCCTCAACCGACCTCTTTCGC	-
*ACO1*_NsiI_rv	atata<u>atgcat</u>TTAGGCGGACTTGGCGGCAG	NsiI
Primers for the overexpression of *PtACO2*		
pActin_Pfl23II_fw	atata<u>cgtacg</u>GGCCCGTTCAACACAATGCG	Pfl23II
pActin_o*ACO2*_rv	agcgagcgaggcaatcatGTTGAAAGTAAGTGGTG	-
*ACO2*_oActin_fw	caccacttactttcaacATGATTGCCTCGCTCGCT	-
*ACO2*_NsiI_rv	atata<u>atgcat</u>TCAAATCTGACTAGGCTCAA	NsiI
Primers for the overexpression of *PtADI1*		
pActin_o*ADI1*_rv	cccgcaagaggattcgacatGTTGAAAGTAAGTGGTGGGG	-
*ADI1*_oActin_fw	ccccaccacttactttcaacATGTCGAATCCTCTTGCGGG	-
*ADI1*_NsiI_rv	atata<u>atgcat</u>TCATAGGGCTGTGGAATGCG	NsiI
Primers for the overexpression of *AtCAD1*		
pActin_o*CAD1*_rv	tccgcagattgcttggtcatGTTGAAAGTAAGTGGTGGGG	-
*CAD1*_oActin_fw	ccccaccacttactttcaacATGACCAAGCAATCTGCGGA	-
*CAD1*_NsiI_rv	atata<u>atgcat</u>TTATACCAGTGGCGATTTCA	NsiI
Primers for the overexpression of *PtITP1*		
pActin_o*ITP1*_rv	acaggtgtctgtggaagcatGTTGAAAGTAAGTGGTGGGG	-
*ITP1*_oActin_fw	ccccaccacttactttcaacATGCTTCCACAGACACCTGT	-
*ITP1*_NsiI_rv	atata<u>atgcat</u>TCAAGAGTGCTTGCGAGCTG	NsiI
Primers for the overexpression of *PtMTT1*		
pActin_o*MTT1*_rv	ttgcgttgaacggacggcatGTTGAAAGTAAGTGGTGGGG	-
*MTT1*_oActin_fw	ccccaccacttactttcaacATGCCGTCCGTTCAACGCAA	-
*MTT1*_SdaI_rv	atata<u>cctgcagg</u>TCAAAACTCGGGACCGGCGA	SdaI
Primers for the overexpression of *PtRIA1*		
pActin_o*RIA1*_rv	ttgctgttcgagaggctcatGTTGAAAGTAAGTGGTGGGG	-
*RIA1*_oActin_fw	ccccaccacttactttcaacATGAGCCTCTCGAACAGCAA	-
*RIA1*_NsiI_rv	atata<u>atgcat</u>TCATCGGTGCCGTCTCCTGG	NsiI
Primers for the overexpression of *PtTAD1*		
pActin_o*TAD1*_rv	gcgttgagagaaggtgccatGTTGAAAGTAAGTGGTGGGG	-
*TAD1*_oActin_fw	ccccaccacttactttcaacATGGCACCTTCTCTCAACGC	-
*TAD1*_NsiI_tv	atata<u>atgcat</u>TCACGTGGAAGGAGGTAGCA	NsiI
Primers for real-time PCR		
ADI1_I	GCGGACACTGCCTTGCTATC	-
ADI_II	TGGAACCTGGTCCGATGAGAG	-
EF1_I	CTCCTCGACGCCATTGACG	-
EF1_II	ACGGGCACAGTTCCGATACC	-
ITP1_I	AAGGCCTCTCGCCGGTCATC	-

25

Primers for real-time PCR		
ITP1_II	CTGCGGCTTGAACCATACGC	-
MTT1_I	AGGGCATAGCAGCTCTGTGG	-
MTT1_II	GGACCGGCGAGAAGCCAAAC	-
RIA1_I	TGGCTGCTGAGAGGAAGGAC	-
RIA1_II	GCAGCTTAGCCAGCCCAAAC	-
TAD1_I	CATCTCAAACCGTGGCTCATCG	-
TAD1_II	ATCCAACAGCGCAGCAGTTC	-
UBC6_I	CCGATTCGGCAAGCAAGACAG	-
UBC6_II	GACTTCTCAAGCCCTGCGATG	-

2.2.2. Plasmids

Starting vectors used for the construction of plasmids are shown in table 4. The resulting plasmids are described in table 5. Their mode of construction is elaborated in the results section. To conserve them for the future, the plasmids were transformed into *E. coli* Dh10b. The illustrated maps for all used plasmids can be found in the respective results section.

Table 4 Overview of the starting plasmids.

amp^R − ampicillin resistance gene of *E. coli*, *ORI* − origin of replication, MCS − multiple cloning site, p*XXX/XXX*t − promoter/terminator region of the respective gene, TcR' − partial tetracycline resistance gene of *E. coli*, *URA3* − *URA3* gene of *Y. lipolytica* with promoter and terminator region, *eco47IR* − gene for the restriction enzyme *Eco*47IR, *hyg*^{R} − hygromycin B resistance gene, sGFP − synthetic *GFP* gene of *Aequorea victoria*, *TKL1'* − partial *TKL1* gene of *Y. lipolytica*, *cbx*^{R} − carboxin resistance gene.

Plasmid	Genetic markers	Description	Reference
pIntC-ACS1	*amp*^{R}, *ORI*, p*TEF1*, *ACS1*, *ICL1*t, *TcR'*, *URA3*, INTC	Single-copy overexpression plasmid for the *ACS1* gene in *Y. lipolytica*. Integrates into non-coding region on chromosome C.	Gatter et al. (2016)
pIntB-CrtI	*amp*^{R}, *ORI*, p*TEF1*, *CrtI*, *ICL1*t, *TcR'*, *URA3*, INTF	Single-copy overexpression plasmid for the codon optimized *CrtI* gene in *Y. lipolytica*. Integrates into non-coding region on chromosome B.	Matthäus et al. (2014)
pJET1.2	*amp*^{R}, *ORI*, *eco47IR*	Base plasmid used for the construction of the deletion plasmid for *YHM2* in *Y. lipolytica*.	Thermo Fisher Scientific Inc.
pPTT	*amp*^{R}, *hyg*^{R}, sGFP	Used as base plasmid for the overexpression of itaconic acid cluster genes and the *AtCAD1* gene in *P. tsukubaensis*.	Bodinus (2011)
pPTT.Cbx	*amp*^{R}, *cbx*^{R}, sGFP	Used as base plasmid for additional overexpression of the aconitase genes *PtACO1*, *PtACO2* and the *AtCAD1* gene in *P. tsukubaensis*.	Limmer (2008)
pUCBM21	*amp*^{R}, *ORI*, MCS, *E. coli LacZ*	Base plasmid used for the construction of deletion plasmids.	Roche Dtl. Holding GmbH
pUC-Lys2-DK2	*amp*^{R}, *ORI*, p*LYS2*, *LYS2*t, *TKL1'*, *TcR'*, *URA3*	The plasmid served as source for the URA Blaster (*TcR'-URA3-TcR'* cassette).	S. Leubner, C. Otto (unpublished)
pUmPYC.Cbx	*amp*^{R}, *cbx*^{R}, *UmPYC1*	Plasmid for the expression of the *U. maydis PYC1* gene. Used for the overexpression of *PtACO1* & *PtACO2* in *P. tsukubaensis*.	Bodinus (2011)

Table 5 Overview of the constructed plasmids.

amp[R] – ampicillin resistance gene of *E. coli, ORI* – origin of replication, MCS – multiple cloning site, p*XXX/XXX*t – promoter/terminator region of the respective gene, TcR' – partial tetracycline resistance gene of *E. coli, URA3* – *URA3* gene of *Y. lipolytica* with promoter and terminator region, *eco47IR'* – gene fragments of the restriction enzyme *Eco*47IR, *hyg*[R] – hygromycin B resistance gene, *cbx*[R] – carboxin resistance gene, s*PtACO1* – native *ACO1* gene of *P. tsukubaensis* without the naturally occurring intron.

Plasmid	Genetic markers	Description	Reference
Plasmids used for *Y. lipolytica*			
pIntC-*ACO1*	*amp*[R], *ORI,* p*TEF1, YlACO1, ICL1*t, *TcR', URA3,* INTC	Single-copy overexpression plasmid for the *YlACO1* gene in *Y. lipolytica.* Integrates into non-coding region on chromosome C.	This work
pIntB-*YHM2*	*amp*[R], *ORI,* p*TEF1, YHM2, ICL1*t, *TcR', URA3,* INTF	Single-copy overexpression plasmid for the *YlYHM2* gene in *Y. lipolytica.* Integrates into non-coding region on chromosome B.	This work
pJET-DK-*YHM2*	*amp*[R], *ORI, eco47IR',* p*YHM2, YHM2*t, *TcR', URA3,*	Deletion plasmid for the *YlYHM2* gene of *Y. lipolytica.*	Gatter, 2015
pUC-DK-*CTP1*	*amp*[R], *ORI,* p*CTP1, CTP1*t, *TcR', URA3*	Deletion plasmid for the *YlCTP1* gene of *Y. lipolytica.*	This work
Plasmids used for *P. tsukubaensis*			
pPTT.Cbx-pActin-*ACO1*-Ex	*amp*[R], *cbx*[R], pActin, s*PtACO1*	Plasmid for the additional overexpression of the *PtACO1* gene (without intron) under the control of the native Actin promoter in *P. tsukubaensis*.	This work
pPTT.Cbx-pActin-*ACO2*	*amp*[R], *cbx*[R], pActin, *PtACO2*	Plasmid for the additional overexpression of the *PtACO2* gene under the control of the native Actin promoter in *P. tsukubaensis*.	This work
pPTT.Cbx-pActin-*AtCAD1*	*amp*[R], *cbx*[R], pActin, *AtCAD1*	Plasmid for the additional overexpression of the *AtCAD1* gene under the control of the native Actin promoter in *P. tsukubaensis*.	This work
pPTT-pActin-*ADI1*	*amp*[R], *hyg*[R], pActin, *ADI1*	Overexpression plasmid for the native *PtADI1* gene under the control of the native Actin promoter in *P. tsukubaensis*.	This work
pPTT-pActin-*AtCAD1*	*amp*[R], *hyg*[R], pActin, *AtCAD1*	Overexpression plasmid for the *AtCAD1* gene under the control of the native Actin promoter in *P. tsukubaensis*.	This work
pPTT-pActin-*ITP1*	*amp*[R], *hyg*[R], pActin, *ITP1*	Overexpression plasmid for the native *PtITP1* gene under the control of the native Actin promoter in *P. tsukubaensis*.	This work
pPTT-pActin-*LacZ*	*amp*[R], *hyg*[R], pActin, *LacZ*	Overexpression plasmid for the *LacZ* reporter gene under the control of the native Actin promoter in *P. tsukubaensis*.	This work
pPTT-pActin-*MTT1*	*amp*[R], *hyg*[R], pActin, *MTT1*	Overexpression plasmid for the native *PtMTT1* gene under the control of the native Actin promoter in *P. tsukubaensis*.	This work

Plasmids used for *P. tsukubaensis*			
pPTT-pActin-*RIA1*	*amp*[R], *hyg*[R], pActin, *RIA1*	Overexpression plasmid for the native *PtRIA1* gene under the control of the native Actin promoter in *P. tsukubaensis*.	This work
pPTT-pActin-*TAD1*	*amp*[R], *hyg*[R], pActin, *TAD1*	Overexpression plasmid for the native *PtTAD1* gene under the control of the native Actin promoter in *P. tsukubaensis*.	This work
pPTT-pGAPDH-*LacZ*	*amp*[R], *hyg*[R], pGAPDH, *LacZ*	Overexpression plasmid for the *LacZ* reporter gene under the control of the native Glyceraldehyde 3-phosphate dehydrogenase (GAPDH) promoter in *P. tsukubaensis*.	This work
pPTT-pHSP70-*LacZ*	*amp*[R], *hyg*[R], pHSP70, *LacZ*	Overexpression plasmid for the *LacZ* reporter gene under the control of the native heat shock protein, HSP70, promoter in *P. tsukubaensis*.	This work
pPTT-pTef-*LacZ*	*amp*[R], *hyg*[R], pTef, *LacZ*	Overexpression plasmid for the *LacZ* reporter gene under the control of the native translation elongation factor 1 (*Tef*) promoter in *P. tsukubaensis*.	This work

2.3. Microorganisms

All the microorganisms used and constructed in this study are part of the strain collection of the Institute of microbiology of the TU Dresden. The strains were cryopreserved in 25 % (v/v) glycerol at -80 °C. For a summary of the strains see table 6.

Table 6 Overview of the used and constructed microorganisms in this study.

E. coli strain	Genotype	Reference
DH10b	F⁻ mcrA Δ(*mrr-hsd*RMS-*mcr*BC) Φ80d*lacZ*ΔM15 Δ*lac*X74 *end*A1 *rec*A1 *deo*R Δ(*ara,leu*)7697 *ara*D139 *gal*U *gal*K *nup*G *rps*L λ⁻ Sm^R	Invitrogen, Karlsruhe
***P. tsukubaensis* strain**	**Description**	**Reference**
CBS422.96 (H488)	Wild type. H488 is the denomination for the wild type given at the strain collection of the Helmholtz Centre for Environmental Research UFZ Leipzig.	Kawamura et al. (1983)
H488 M15 (= CBS21214)	Mutant strain of strain 488 obtained by random UV-radiation mutagenesis.	Bodinus (2011)
H488 M15-CAD5	Strain H488-M15 transformed with the plasmid pAtCAD1, a plasmid containing the *A. terreus CAD1* gene controlled by the *U. maydis HSP70* promoter.	Bodinus (2011)
H488 HA	Strain H488 transformed with the plasmid pPTT-pActin-*ADI1*.	This work
H488 HC	Strain H488 transformed with the plasmid pPTT-pActin-*AtCAD1*.	This work
H488 HI	Strain H488 transformed with the plasmid pPTT-pActin-*ITP1*.	This work
H488 HM	Strain H488 transformed with the plasmid pPTT-pActin-*MTT1*.	This work
H488 HM14	Clone 14 of the transformants of strain H488 transformed with the plasmid pPTT-pActin-*MTT1*.	This work

H488 HoMoC	Strain H488 HM14 transformed with the plasmid pPTT-pActin-*AtCAD1*.	This work
H488 HR	Strain H488 transformed with the plasmid pPTT-pActin-*RIA1*.	This work
H488 HR12	Clone twelve of the transformants of strain H488 transformed with the plasmid pPTT-pActin-*RIA1*.	This work
H488 HR12 A1	Strain H488 HR12 transformed with the plasmid pPTT.Cbx-pActin-*ACO1*-Ex.	This work
H488 HR12 A2	Strain H488 HR12 transformed with the plasmid pPTT.Cbx-pActin-*ACO2*.	This work
H488 HT	Strain H488 transformed with the plasmid pPTT-pActin-*TAD1*.	This work
H488 MA	Strain H488 -M15 transformed with the plasmid pPTT-pActin-*ADI1*.	This work
H488 MC	Strain H488-M15 transformed with the plasmid pPTT-pActin-*AtCAD1*.	This work
H488 MI	Strain H488-M15 transformed with the plasmid pPTT-pActin-*ITP1*.	This work
H488 MM	Strain H488-M15 transformed with the plasmid pPTT-pActin-*MTT1*.	This work
H488 MM11	Clone eleven of the transformants of strain H488-M15 transformed with the plasmid pPTT-pActin-*MTT1*.	This work
H488 MoMoC	Strain H488 MM11 transformed with the plasmid pPTT-pActin-*AtCAD1*.	This work
H488 MR	Strain H488-M15 transformed with the plasmid pPTT-pActin-*RIA1*.	This work
H488 MR2	Clone two of the transformants of strain H488 transformed with the plasmid pPTT-pActin-*RIA1*.	This work
H488 MT	Strain H488-M15 transformed with the plasmid pPTT-pActin-*TAD1*.	This work
***Y. lipolytica* strain**	**Genotype**	**Reference**
H222	*MATA* wild type	Barth and Gaillardin (1996)
H222-SW2-1	*MATA* ura3-302 SUC2 ku70Δ-*1572*	Kretzschmar et al. (2013)
H222Δ*CTP1*	*MATA* ura3-302 SUC2 ku70Δ-*1572* Δ*ctp1::URA3*	This work
H222Δ*YHM2*	*MATA* ura3-302 SUC2 ku70Δ-*1572* Δ*yhm2::URA3*	This work
H222Δ*YHM2* ura⁻	*MATA* ura3-302 SUC2 ku70Δ-*1572* Δ*yhm2*	This work
H222Δ*YHM2*Δ*CTP1*	*MATA* ura3-302 SUC2 ku70Δ-*1572* Δ*yhm2* Δ*ctp1::URA3*	This work
H222Δ*YHM2*o*ACO1*	*MATA* ura3-302 SUC2 ku70Δ-*1572* Δ*yhm2 IntC-pTef-ACO1-URA3*	This work
H222o*ACO1*	*MATA* ura3-302 SUC2 ku70Δ-*1572 IntC-pTef-ACO1-URA3*	This work
H222o*YHM2*	*MATA* ura3-302 SUC2 ku70Δ-*1572 IntB-pTef-YHM2-URA3*	This work

2.4. Cultivation

For the preparation of solid agar plates, 2 % (w/v) agar was added to the liquid medium. All media were autoclaved for 20 min at 121 °C, if not stated otherwise.

2.4.1. Media and cultivation of *E. coli*

E. coli was cultivated in lysogeny broth (LB) medium according to Sambrook et al. (1989). Plasmid carrying, ampicillin resistant *E. coli* transformants were cultivated in 100 µg ml^{-1} ampicillin (stock solution: 10 mg ml^{-1}) containing LB$_{amp}$ medium. Cells were grown overnight at 37 °C either on solid LB$_{amp}$ agar plates or in 3 ml liquid LB$_{amp}$ cultures in a shaking incubator at 220 rpm for plasmid preparation.

LB medium

Tryptone	10 g l^{-1}
Yeast extract	5 g l^{-1}
NaCl	5 g l^{-1}

2.4.2.   Media for yeasts

The yeasts *Y. lipolytica* and *P. tsukubaensis* were cultivated in YPD (Yeast extract Peptone Dextrose) medium according to Barth and Gaillardin (1996). Before the transformation of *Y. lipolytica* pre-cultivation was performed in YPD pH 4.0. For the selection of plasmid containing *P. tsukubaensis* strains Hygromycin B with a concentration of 100 µg ml^{-1} or carboxin with a concentration of 50 µg ml^{-1} was added.

YPD medium		YPD medium pH 4.0
Yeast extract	10 g l^{-1}	10 g l^{-1}
Peptone from casein	20 g l^{-1}	10 g l^{-1}
Dextrose	20 g l^{-1}	10 g l^{-1}
pH	5.5-6.0	50 mM citric acid/sodium citrate, pH 4.0

Minimal medium with glucose, MG medium, (modified according to Bodinus, 2011; Kawamura et al., 1981, 1982; Mauersberger et al., 2001) was used for growth tests and characterisation of organic acid production behaviour for both *P. tsukubaensis* and *Y. lipolytica.*

MG medium	*Y. lipolytica*	*P. tsukubaensis* – MG	*P. tsukubaensis* – MG-IA
<u>Carbon source</u>			
	20 g l^{-1} D-glucose	50 g l^{-1} D-glucose	X g l^{-1} D-glucose
<u>Iron</u>			
	6 mg l^{-1} FeCl$_3$ x 6 H$_2$O (stock solution in EtOH)	"	"
<u>Mineral salts</u>			
	3 g l^{-1} (NH$_4$)$_2$SO$_4$	3 g l^{-1} (NH$_4$)$_2$SO$_4$	X g l^{-1} NaNO$_3$ → NH$_4$Cl
	1 g l^{-1} KH$_2$PO$_4$	1 g l^{-1} KH$_2$PO$_4$	X g l^{-1} KH$_2$PO$_4$
	0.16 g l^{-1} K$_2$HPO$_4$ x 3 H$_2$O	0.16 g l^{-1} K$_2$HPO$_4$ x 3 H$_2$O	X g l^{-1} K$_2$HPO$_4$ x 3 H$_2$O
	0.7 g l^{-1} MgSO$_4$ x 7 H$_2$O	"	"
	0.5 g l^{-1} NaCl	"	"
	0.4 g l^{-1} Ca(NO$_3$)$_2$ x 4 H$_2$O	"	0.4 g l^{-1} CaCl$_2$ x 2 H$_2$O
	-	-	0.5 g l^{-1} K$_2$SO$_4$
<u>Trace elements</u>			
	0.5 µg l^{-1} H$_3$BO$_3$	"	"
	0.04 µg l^{-1} CuSO$_4$ x 5 H$_2$O	"	"
	0.1 µg l^{-1} KI	"	"
	0.4 µg l^{-1} MnSO$_4$ x 4 H$_2$O	"	"
	0.2 µg l^{-1} Na$_2$MoO$_4$ x 2 H$_2$O	"	"
	0.4 µg l^{-1} ZnSO$_4$ x 7 H$_2$O	"	"
<u>Vitamin</u>			
	0.3 mg l^{-1} thiamine hydrochloride	-	0.4 mg l^{-1} thiamine hydrochloride
<u>pH stabilization</u>			
	-	3.3 g l^{-1} CaCO$_3$ (insoluble)	"

For certain experiments the carbon, nitrogen and/or phosphorus sources were modified (for MG-IA medium X represents the varying concentration). The specific media compositions for these cases are described in the respective results section.

For *Y. lipolytica* the MG medium was also used as a selective medium for uracil prototrophic transformants. For the cultivation of uracil auxotrophic *Y. lipolytica* strains, 20 mg l^{-1} uracil was added to the MG medium (MG$_{Ura}$). Uracil auxotrophy was regained by 5-fluoroorotic acid (FOA) selection.

2.4.3. Cultivation of yeasts

The yeast cells were streaked from a -80 °C cryo-conserve (emers) onto agar plates containing complete medium YPD or medium for selection (YPD-Hyg, YPD-Cbx for *P. tsukubaensis*; MG for *Y. lipolytica*) and grown for 2-3 d. Growth temperature for *P. tsukubaensis* was 30 °C and 28 °C for *Y. lipolytica*.

Screening of constructed yeast strains for organic acid production was carried out in a culture volume of 3 ml in 12-well plates (Sarstedt). The well plates were sealed with semipermeable adhesive membranes. The yeast cells were either grown in MG (*Y. lipolytica*) or MG-IA (*P. tsukubaensis*) medium with approximately 5 g l^{-1} CaCO$_3$ as buffering agent.

For larger volume cultivations, the yeast cells were pre-cultivated overnight in 10 ml YPD medium. The cells were harvested by centrifugation (3.500 rpm, 5 min) and washed with dH$_2$O. Subsequently, 50 ml of minimal medium in 500 ml-baffled flasks were inoculated with the cells needed for a starting OD$_{600}$ = 1.0 and cultivated for several days at 28 °C/30 °C and 220 rpm. The pH was either adjusted daily with the titration of 10 M NaOH and 3 M HCl or kept constant at pH 5.5-6.0 with the initial addition of 3.3 g l^{-1} CaCO$_3$ (specified in the respective results section).

Large volume fed-batch cultivation was carried out in a 600 ml-bioreactor. Either 50 ml MG medium (*Y. lipolytica*) or 50 ml YPD medium (*P. tsukubaensis*) were inoculated with cells from agar plates and incubated in a 500 ml-baffled shaking flask at 28 °C/30 °C and 220 rpm for at least 24 h until a cell density of OD$_{600}$ = 25-35 was reached. The amount of cells mass needed to obtain a starting OD$_{600}$ = 1.0 in the fermenter was harvested by centrifugation at 3.500 rpm for 5 min and resuspended in 3 ml sterile H$_2$O. Start of fermentation was the point of inoculation. Cells were cultivated under the following conditions if not stated otherwise:

Table 7 Growth conditions for large volume cultivations of *P. tsukubaensis* and *Y. lipolytica* in a 600 ml-bioreactor (Multifors, INFORS HT).

	P. tsukubaensis	*Y. lipolytica*
Medium	MG-IA (see results section)	MG + 15 % (w/v) glucose or 10 % (v/v) sunflower oil
Temperature	30 °C	28 °C
O$_2$ saturation	55 %	
Aeration	airflow: 1 l min^{-1} normal air & stirring: $\geq$ 400 rpm	
pH	pH 4.0 or 5.5 (adjusted by continuous titration of 1 M HCl and 2.5-5.0 M NaOH)	pH 5.5 (adjusted by continuous titration of 3 M H$_2$SO$_4$ and 10 M NaOH)

2.4.4. Sampling

Sampling of cultures was carried out every 24 h by directly removing 200-1.000 µl of culture broth in case of culture experiments in well-plates and shaking flasks. Bioreactor cultures were sampled every 24 h by removing 20 ml of culture broth through two three-way valves (to maintain sterility). The first 5 ml of broth were discarded (to avoid potentially accumulated dead cells in the sampling tube). The remaining 15 ml of culture broth were collected into a previously weighted 15 ml-falcon tube.

2.4.4.1. Determination of cell density (OD$_{600}$) and dry cell weight (DCW)

Optical density at a wavelength of λ = 600 nm was measured to track cell growth. The cells were pelleted by centrifugation for 5 min at 3.500 rpm, RT. The pellet was washed with 1 x mineral salt solution. If the cells were grown with CaCO$_3$ as a solid buffer, the pellet was washed with 1 M HCl instead of the salt solution to completely dissolve the remaining calcium carbonate. After the washing step, the cells were resuspended and diluted with 1 x mineral salt solution (for the composition see mineral salts section for the *Y. lipolytica*-MG medium). Measuring was carried out in 1.5 ml disposable cuvettes (layer thickness: 10 mm) with a single beam photometer (Ultrospec 2000, Pharmacia Biotech).

Dry-cell weight (DCW) was only determined for cell cultures grown in the bioreactor. 10 ml of the culture broth was pelleted (10 min at 3.500 rpm, RT) in the previously weighed 15 ml-falcon tube. The pellet was washed with 10 ml dH$_2$O and pelleted again (10 min at 3.500 rpm, RT). The supernatant was removed. The pellet was then dried for 12 h at 100 °C and weighed to ultimately determine the DCW.

In the case of cultivation with hydrophobic substrates, the residual amounts of oil had to be removed. Therefore, the cell pellets were first resuspended in 10 % Tween 80 shaken vigorously for 5 min and centrifuged (5 min at 3.500 rpm, RT). This was followed by another washing step with 10 % Tween 80 and the washing step described above.

2.4.4.2. Microscopy

The cells were centrifuged and resuspended in 100 µl fixation solution (4.5 % (v/v) formaldehyde in PBS, PBS according to Sambrook et al. (1989)). Visualization was done via light and phase-contrast microscopy at 400 X magnification.

Fluorescence microscopy was done by staining the cells with 10 µl nile red solution (1 g l^{-1} nile red in acetone). The cells were later visualized at 1.000 X magnification with a U-M41007A filter (525-560 nm). Additional cell images were obtained with the Axio Observer 7 inverted fluorescence microscope using the Pln Apo 100 X/1.4 oil objective (excitation: 511 nm). Data was obtained and analysed using the Zen 2.3 Pro software (Carl Zeiss).

PBS

NaCl	8.0 g l^{-1}
KCl	0.2 g l^{-1}
Na$_2$HPO$_4$ x 2 H$_2$O	1.78 g l^{-1}
KH$_2$PO$_4$	0.27 g l^{-1}

2.5.   Genetic engineering methods

2.5.1.   Polymerase chain reaction (PCR)

The proteins Phusion and Dream *Taq* served as polymerases for the performed polymerase chain reactions.

The Phusion polymerase possesses a proof-reading function and thus drastically reduces the risk of incorporating a wrong nucleotide into the polynucleotide chain. It is therefore used for preparative PCR purposes. When the Phusion polymerase was used for overlap PCR, a second DNA template in an equimolar amount was added to the PCR mixture. The PCR products were either directly purified with the help of a PCR purification kit or separated with agarose gel electrophoresis and subsequently extracted from the gel.

Dream *Taq* is not equipped with a proof-reading capability. For that reason, Dream *Taq* was only used for analytical applications e.g. screening of *E. coli* transformants (colony PCR) and analysis of genomic yeast DNA. For colony PCR, a single *E. coli* colony was picked with a sterile toothpick, transferred to 10 µl of the PCR mixture and afterwards streaked on solid LB$_{amp}$ medium. When analysing the genomic yeast DNA, 10 ng of the DNA was added to a 10 µl PCR mixture. After amplification, 1 µl of each reaction was checked with agarose gel electrophoresis for the presence of a DNA product with the desired size.

For typical PCR mixtures see table 8 and for the respective temperature programs see table 9.

Table 8 Composition of PCR mixtures for analytical and preparative reactions.

Component	Volume - Dream*Taq*	Volume - Phusion
Buffer	1 µl 10 X green Dream*Taq*	10 µl 5 X Phusion Buffer
MgCl$_2$ (50 mM)	0.25 µl	0.5 µl
Forward primer (10 µM)	0.25 µl	0.5 µl
Reverse primer (10 µM)	0.25 µl	0.5µl
dNTPs (10 mM each)	0.3 µl	1 µl
Polymerase	0.1 µl Dream*Taq* (2.5 U µl^{-1})	0.5 µl Phusion (2.5 U µl^{-1})
Template 1	10 ng	50 ng
[Template 2]	-	equimolar to template 1
RNase A (10 g l^{-1})	0.1 µl	-
HPLC water	ad 10 µl	ad 50 µl

Table 9 Typical temperature program for the analytical and preparative PCR.
T_m − annealing temperature of the primer with the lower annealing temperature.

Reaction	Dream*Taq*			Phusion		
	Temperature	Time	Cycles	Temperature	Time	Cycles
Initial denaturation	95 °C	5 min	1	98 °C	30 s	1
Denaturation	95 °C	30 sec	30	98 °C	10 s	25
Annealing	T_m − 3 °C	30 sec		T_m	30 s	
Extension	72 °C	1 min per 1 kb		72 °C	30 s per 1 kb	
Final extension	72 °C	5 min	1	72 °C	10 min	1

2.5.1.1. Quantitative Real-time PCR (qPCR)

The *P. tsukubaensis* strains H488 (wild type) and HR12 were cultivated in itaconic acid production medium (MG-IA) until an OD$_{600}$ = 2-3 was reached. The total RNA of these cultures was isolated by Sina Science Services GmbH (Berlin, DE). Remaining DNA was eliminated with the help of DNase I for 15 min at 37 °C (for the composition of the reaction mixture see table 10). The RNA was afterward purified using the NucleoSpin RNA Clean-up XS kit. Synthesis of cDNA was done using the RevertAid First Strand cDNA Synthesis Kit according to the manufacturer's protocol. For the qPCR the Maxima SYBR Green mastermix was utilized. The composition of the qPCR reaction and the temperature program are summarized in table 11 & table 12.

Table 10 Composition for DNA elimination with DNase I

Component	DNase I
RNA	30 − 40 µl
10 X DNase I buffer	5 µl
Ribolock Ribonuclease Inhibitor	1 µl
DNase I	0.5 µl
dH$_2$O RNase free	ad 50 µl

Table 11 Composition of the reaction mixture used for qPCR.

Component	DNase I
SYBR Green Mastermix	5 µl
Primermix (2.5 pmol µl^{-1} each)	1.2 µl
cDNA (or RNA, H$_2$O as control)	1 µl
dH$_2$O	2.8 µl

Table 12 Temperature program used for qPCR

Reaction	qPCR		
	Temperature	Time	Cycles
Initial denaturation	95 °C	8 min	1
Denaturation	95 °C	15 sec	40
Annealing	58 °C	30 sec	
Extension	72 °C	10 sec	
Final extension	72 °C	2 min	1
Melting point analysis	60 °C to 95 °C	Increment 0.5 °C every 4 sec	

2.5.2. Agarose gel electrophoresis

With the help of agarose gel electrophoresis DNA fragments have been separated based on their molecular weight. To prepare a 0.8 % agarose gel, 8 g l^{-1} agarose was solved in 1 X TAE buffer with 0.2 mg l^{-1} ethidium bromide. The DNA samples were mixed with 1/5 volume of loading dye. The DNA-ladder (1 kb-ladder) and the DNA samples were separated in 1 X TAE buffer at 10 V cm$^{2\ -1}$. The ethidium bromide forms a complex with the nucleic acid. This complex was visualized with a UV-transilluminator at a wavelength of 312 nm.

50 X TAE-buffer (autoclaved)

Tris	242 g l^{-1}
Glacial acetic acid	57.1 ml l^{-1}
EDTA 0.5 M (pH 8.0)	100 ml l^{-1}
dH$_2$O	ad 1 l

Ethidium bromide stock solution   10 mg ml^{-1}

6 X loading dye

Glycerol	30 % (v/v)
Bromophenol blue	0.05 % (w/v)

2.5.2.1. Isolation of DNA from agarose gels

Separated DNA fragments were excised from the gel with a sterile scalpel under an UV-transilluminator. The DNA was extracted from the gel block using the Invisorb spin DNA Extraction Kit according to the manufacturer's protocol. The DNA was eluted with 20 µl HPLC-H$_2$O.

2.5.3. Restriction digestion of DNA fragments

Vector DNA and DNA fragments were cut enzymatically with the aid of restriction enzymes. The DNA samples ($\leq 2\,\mu g$) were mixed with the restriction enzyme and the corresponding buffer (according to the manufacturer's protocol). In the case of double digestion with two enzymes, both buffers were applied. The concentrations of the enzymes and buffers were then halved. If a simultaneous restriction was not possible, the DNA was digested one after another and purified in between. The restriction reactions were incubated for 3 h or overnight at 37 °C.

2.5.4. Purification of DNA fragments

DNA fragments ($> 100\,bp$) resulting from restriction digestion, PCR or from agarose gels (occasional additional purification) were purified from the reaction mixture components or other impurities. This was done with the help of the MSB Spin PCRapace kit. All steps of the manufacturer's protocol, but the elution, were followed. The elution was carried out with 55 °C HPLC-H_2O.

2.5.5. Determination of DNA concentration

DNA concentrations of purified fragments were determined spectrophotometrically (Nano Drop ND 1000). For each sample the absorption (wavelength $\lambda = 260\,nm$) of 1 µl DNA was measured against 1 µl of HPLC water (eluent) with the help of a UV-Vis spectrophotometer.

2.5.6. Dephosphorylation of vectors

In some cases, the vectors were digested with a single enzyme or with two enzymes creating compatible sticky ends. In order to prevent recircularization of linearized vectors when ligation with an insert took place, the phosphate group at the 5'-end of the vector had to be removed. This was achieved by adding one unit of FastAP thermosensitive alkaline phosphatase and the corresponding phosphatase buffer to the linearized vector. The reaction was incubated for 30 min at 37 °C. The reaction was stopped for 15 min at 65 °C.

2.5.7. Ligation of DNA fragments

Ligation of DNA fragments was done with the help of the enzyme T4 DNA ligase. For a typical ligation, the insert was added in a molar ratio of 5:1 to the vector. The necessary DNA mass of the insert was calculated with the following equation:

$$\text{insert DNA mass [ng]} = \frac{5 \text{ x vector mass [ng] x insert length [bp]}}{\text{vector length [bp]}}$$

The ligation reaction (for composition see table 13) was incubated at 22 °C for 3-4 h. As a negative control, HPLC-H_2O was used instead of the insert.

Table 13 Composition of the ligation reaction with the T4 DNA ligase.

Component	Ligation
Vector DNA (dephosphorylated)	75 ng
Insert DNA	5:1 molar ratio
T4 DNA ligase	1 U
ATP	5 mM
HPLC-H_2O	ad 20 µl

2.5.8. Transformation of *E. coli*

Electrocompetent *E. coli* DH10b cells were prepared according to Dower et al. (1988).

Before transformation into *E. coli*, dialysis of the plasmid was carried out. This was done by applying 5 µl of the ligated plasmid solution onto a nitrocellulose membrane (pore diameter: 0.025 µm, Millipore). Desalination happened against ultrapure water for 15 min. In the meantime, the *E. coli* cells were slowly unfrozen on ice. The plasmid solution was mixed with the cells and added into a pre-chilled electroporation cuvette (0.2 cm). After incubating on ice for 5 min, the cells were electroporated with an electrical pulse of 2.5 kV. Immediately after, the *E. coli* cells were mixed with 1 ml preheated SOC medium (37 °C) and incubated for one hour. 200 µl of this cell suspension was plated onto LB_{amp} and incubated overnight at 37 °C.

SOC medium (sterile filtered)

Peptone from casein	20 g l^{-1}
Yeast extract	5 g l^{-1}
NaCl	10 mM
$MgCl_2$	10 mM
KCl	2.5 mM
Glucose	20 mM

2.5.9. Isolation of plasmid DNA from *E. coli*

Plasmid DNA from *E. coli* was isolated with the aid of the Invisorb Spin Plasmid Mini Two kit according to the manufacturer's protocol. Elution of the plasmid DNA was done with 50 µl 55 °C HPLC-H_2O.

2.5.10. Integrative transformation of *Y. lipolytica*

Integration of heterologous DNA into the genomic DNA of *Y. lipolytica* was carried out according to a modified version of the lithium acetate method described by Barth and Gaillardin (1996).

The uracil auxotrophic recipient *Y. lipolytica* strain was pre-cultivated overnight in YPD pH 4.0 at 28 °C and 220 rpm. The cells were harvested by centrifugation (3.500 rpm, 5 min, 28 °C) when the culture reached a cell density of 9×10^7 cells ml^{-1} – 1.2×10^8 cells ml^{-1}. After removing the supernatant, the cell pellet was washed two times with TE buffer (pH 8.0). This cell pellet was then resuspended in 0.1 M LiAc buffer (pH 6.0), adjusted to a cell count of 5×10^7 cells ml^{-1} and incubated

for 1 h with slight shaking (100 rpm, 28 °C). The competent *Y. lipolytica* cells were then centrifuged and resuspended in 1:10 volume of LiAc buffer and stored at 4 °C.

Y. lipolytica yeast cells were transformed with linearized DNA molecules. For the overexpression of a gene 1 µg if the whole linearized plasmid was transformed. For the deletion of a gene, 250 ng of only the respective deletion cassette (consisting of the promoter region (approximately 1 kb), the URA Blaster (TcR', *YlURA3*, TcR') and the terminator region (approximately 1 kb)) was transformed. Initially, 5 µl of the DNA was denatured at 95 °C for 5 min.

Deletion of the ORFs was confirmed by PCR, using the forward primer of the respective promoter sequence and the reverse primer of the terminator.

Homologous integration of the overexpression plasmid was confirmed by PCR using the primers AscI_CI_rv_out & ACO1_rv_SphI; IntB_out_rv & YHM2_rv_MluI.

The actual transformation was carried out by gently mixing 100 µl of competent *Y. lipolytica* cells with 5 µl of the DNA (dH$_2$O was used as negative control) and 5 µl carrier DNA (denatured). After incubating the cells for 15 min at 28 °C, 700 µl of PEG4000 (40 % (w/v) polyethylene glycol 4000 in 0.1 M LiAc buffer, pH 6.0, sterile filtered) was added. Another 60 min incubation at 100 rpm and 28 °C followed. The cells were treated with a 39 °C heat shock for 10 min. Afterwards, two times 600µl LiAc buffer were added and the cells were harvested by centrifugation (5 min, 3.500 rpm, RT). 750 µl of the supernatant was discarded. With the remaining supernatant, the yeast cells were gently streaked onto selective plates with glucose and incubated for several days at 28 °C.

TE buffer pH 8.0

Tris/HCl pH 8.0	10 mM
EDTA pH 8.0	1 mM

LiAc buffer

Lithium acetate	0.1 M
Acetic acid	volume needed to adjust to a final pH 6.0

Carrier DNA

Herring sperm DNA	10 g l^{-1} (fragmented with ultrasound, size approximately 500 bp)
Tris pH 8.0	50 mM
EDTA pH 8.0	5 mM

2.5.10.1. Marker rescue (5-FOA selection)

The uracil auxotrophy for strain H222Δ*YHM2* was regained according to Boeke et al. (1987) by plating the cells of an overnight culture (10^4-10^6 cells) on solid minimal medium containing 2 % (w/v) glucose, 20 mg l^{-1} uracil and 1 g l^{-1} FOA (SL: 100 g l^{-1} in DMSO). The cells were incubated at 28 °C for multiple days.

2.5.11. Transformation of *P. tsukubaensis*

Transformation of whole circular plasmid DNA was carried out according to Gillissen et al. (1992) & Schulz et al. (1990) modified by Bodinus (2011).

For the transformation of *P. tsukubaensis* only freshly prepared protoplasts were used. To obtain protoplasts, *P. tsukubaensis* cells were grown overnight in 3 ml YM medium at 30 °C and 220 rpm. On the next day, 1 ml of the culture was transferred to 50 ml YEPSlight medium and grown for at least 3 h at 30 °C and 220 rpm until an OD_{600} = 0.5 was reached. The cells were harvested by centrifugation (5 min at 3.500 g, RT). The cell pellet was washed with 20 ml SCS, pelleted again and resuspended in 2 ml Glucanex (6 % (w/v) in SCS, sterile filtered). For the enzymatic lysis of the cell wall, the cells were incubated in a 50 ml-falcon tube at RT and soft shaking for 30-45 min until approximately 50 % of the cells were present in the form of protoplasts. Harvesting the protoplasts was done by centrifugation (10 min, 2.500 rpm, 4 °C). The pellet was consecutively washed in 20 ml SCS-, 10 ml SCS- and 20 STC-buffer (ice-cold SCS & STC). After the last washing step, the cells were resuspended in 0.5 ml STC (ice-cold) and ultimately aliquoted into 1.5 ml-reaction tubes with a final volume of 80 µl per tube.

The protoplasts were gently mixed with up to 15 µg circular plasmid DNA (max volume: 10 µl) and incubated on ice for 10 min. As a control 10 µl of dH_2O was used instead of DNA. The cells were overlaid with 500 µl PEG4000 (40 % (w/v) polyethylene glycol 4000 in STC, sterile filtered) and incubated on ice for 15 min. In the meantime, the selective agar plates were prepared: Reg-medium was liquefied and cooled down to approximately 50 °C and mixed with the doubled concentration of Hygromycin B (200 µg ml^{-1}) or Carboxin (100 µg ml^{-1}). 10 ml of Reg-Hyg/ Reg-Cbx was used as a base-agar and overlaid with the same amount of Reg-medium (no marker) as a top-agar. The protoplasts were gently plated and incubated at 30 °C for 3-15 d. Colonies obtained after transformation were streaked onto selective plates for purification. Single colonies were then screened phenotypically for itaconic acid production. Genomic DNA was isolated from suitable candidates. The genomic DNA was used as template for PCR to check for integration of the respective overexpression plasmid.

YEPSlight			**SCS buffer**	
Yeast extract	10 g l^{-1}		Sorbitol	1 M
Peptone from casein	4 g l^{-1}		Sodium citrate	20 mM pH 5.8
Sucrose	4g l^{-1}			

Reg medium			**STC buffer**	
Peptone	20 g l^{-1}		Sorbitol	1 M
Sucrose	20 g l^{-1}		Tris/HCl	10 mM pH 7.5
Sorbitol	1 M		$CaCl_2$	0.1 M
Agar	20 g l^{-1}			

2.5.12. Isolation of genomic yeast DNA

For the isolation of genomic DNA, the yeast cells were grown overnight in 10 ml YPD full medium at 28 °C and 220 rpm. A volume of 2 ml of the cells was harvested by centrifugation (5 min, 13.000 rpm, 4 °C). The cell pellet was resuspended in 500 µl lysis buffer. 400 µl of glass beads (0.75-1 mm) were added and cell lysis was performed with the help of a vibration mill (FastPrep FP120A-230) for two times 30 s at 5.5 m s^{-1}. The supernatant was collected, mixed with 275 µl 7 M ammonium acetate pH 7.0 and incubated at 65 °C for 5 min. Another incubation on ice for 5 min followed. Then the samples were mixed with 500 µl chloroform and centrifuged. The upper phase was collected, precipitated with 1 ml isopropanol and centrifuged (15 min, 13.000 rpm, RT). The DNA pellet was washed two times with 200 µl ice-cold 70 % (v/v) ethanol, dried and eluted in 50 µl HPLC-H_2O at 37 °C overnight. RNA was eliminated by adding 0.2 g l^{-1} RNase A.

Lysis buffer

Tris pH 8.0	100 mM
EDTA	50 mM
SDS	1 % (w/v) in H_2O

2.5.13. DNA sequencing

De novo sequencing of genomic DNA and RNA of *P. tsukubaensis* strains, the assembly of the reads into contigs and the preliminary annotation was carried out by IIT Biotech GmbH in Bielefeld.

Sequencing of plasmid DNA for the verification of the validity of the respective sequence was done by Eurofins Genomics GmbH. For the sequencing service, 15 µl of plasmid DNA with a concentration of 50-100 ng µl^{-1} was mixed with 2 µl 10 pmol µl^{-1} primer.

2.6. Biochemical methods

2.6.1. Determination of promoter activity – β-galactosidase assay

In order to quantify the activity of the different promoters in *P. tsukubaensis*, their sequence was fused to the *E. coli* reporter gene *LacZ*. The respective constructs were transformed into strain H488 and M15. Cultivation of the resulting transformants was carried out in 2.5 ml YPD or MG-IA (minimal medium with glucose for itaconic acid production with 2 g l^{-1} N source and 0.1 g l^{-1} P source) in 12-well plates sealed with a semipermeable membrane. Duration of cultivation at 30 °C and 220 rpm was 2 d for YPD and 4 d for MG-IT.

After cultivation, the *β*-galactosidase activity of each transformant was determined according to Smale (2010). Thus, the cells were harvested by centrifugation (5 min, 3.500 rpm, RT), washed with PBS and after another centrifugation step (1 min, 8.000 rpm, RT) resuspended in 1 ml PBS. The washing step was repeated once again, and the cell pellet was resuspended in 2 ml 0.25 M Tris/HCl pH 8.0. For cell lysis, the suspension was frozen in an ethanol/dry ice bath and thawed at 37 °C. This was repeated three times. Cell debris was sedimented by centrifugation (5 min, 13.000 rpm,

4 °C). The supernatant or raw protein extract was kept on ice and used for the β-galactosidase activity assay. For the quantification of β-galactosidase activity, a reaction mixture with the following composition was mixed in a disposable 1.5 ml cuvette (layer thickness: 10 mm) and incubated at 37 °C until the reaction changed its colour to faint yellow:

β-galactosidase reaction mixture   **Mg^{2+} buffer**

raw protein extract	30 µl	β-mercaptoethanol	4.9 M
Mg^{2+} buffer	3 µl	$MgCl_2$	0.1 M
ONPG (4 mg ml^{-1})	66 µl		
0.1 M KPP buffer pH 7.5	201 µl		

The incubation period was recorded and the amount of o-nitrophenyl-β-D-galactopyranoside (ONPG) converted into galactose and o-nitrophenol (ε = 4500 $M^{-1}\,cm^{-1}$) was then measured spectrophotometrically at a wavelength of λ = 420 nm.

PBS

NaCl	137 mM
KCl	2.7 mM
Na_2HPO_4	10 mM
KH_2PO_4	1.8 mM

2.6.2. Aconitase (YlACO1p) enzyme assay

For the determination of aconitase activity in the yeast *Y. lipolytica*, cells were precultured overnight in 50 ml YPD medium at 28 °C and 220 rpm. On the following day, the cells were harvested (5 min, 3.500 rpm, RT) and washed with a 1 x mineral salt solution. A 500 ml-shaking flask with 50 ml minimal medium with glucose was then inoculated with an initial OD_{600} = 2.0. The yeast culture was grown for 16 h at 28 °C and 220 rpm. After the 16 h incubation, the cells were harvested by centrifugation (5 min, 5.000 rpm, 4 °C). Subsequently, the cell pellet was washed with aconitase lysis buffer and centrifuged again. The cell pellet was then resuspended in 1 ml aconitase lysis buffer. 500 µl glass beads (0.75-1 mm) were added and mechanical cell lysis was carried out two times for 30 s at 5.5 m s^{-1} with the aid of a vibration mill. Cell debris was separated by centrifugation (5 min, 13.000 rpm, 4 °C). The supernatant or raw protein extract was kept on ice and used for the aconitase activity assay.

The spectrophotometric assay, according to Anfinsen (1955), was carried out using cell-free supernatant fractions for the determination of aconitase enzyme activity. During the assay, the change in absorbance at a wavelength of λ = 240 nm was measured for 4 min. This change in absorbance is due to the conversion of isocitrate into *cis*-aconitate (ε = 4.88 $mM^{-1}\,cm^{-1}$) catalysed by aconitase. Measurements were performed with a total volume of 1 ml in 1.5 ml disposable cuvettes (layer thickness: 10 mm). For the reaction mixture 50 mM KPP pH 7.4, 10 mM D,L-isocitrate and the raw protein extract was used. If needed, the raw protein extract was diluted using KPP.

Aconitase lysis buffer

Tris/HCl pH 7.0	100 mM
MgCl$_2$	5 mM

In order to calculate the final enzyme activity, the Beer-Lambert law was applied as follows:

$$\text{enzyme activity [U/mg]} = \frac{\Delta OD}{\varepsilon \text{ x protein [mg/ml]x } \Delta t} \text{ x dilution factor}$$

where, ΔOD is the change in absorbance at a specific wavelength over time Δt (for the β-galactosidase assay only the final absorbance was considered)

ε is the wavelength-dependent molar absorptivity coefficient [mM^{-1} cm^{-1}].

2.6.3.   Determination of total protein amount

Total protein amounts of the protein raw extracts for the β-galactosidase and aconitase assays were determined spectrophotometrically according to Bradford (1976). For one reaction, 160 µl of the raw protein extract were mixed with 40 µl of Bradford reagent (Bio-Rad). Measurements were carried out in 96-well plates at a wavelength of λ = 595 nm. Ultrapure water served as a negative control. The standard curve was obtained with different concentrations of bovine serum albumin (BSA).

2.6.4.   Determination of glucose and sucrose concentrations

Glucose concentration in the culture medium was determined by performing an enzyme assay with the help the enzyme assay kit Glucose UV test. It was executed according to the manufacturer's protocol.

Sucrose concentrations in the culture medium were determined with the aid of the glucose and sucrose assay kit. The manufacturer's protocol for the colorimetric assay was followed.

2.6.5.   Quantification of organic acids

One millilitre of culture broth was collected and centrifuged (18000 rpm, 4 °C, 15 min). The cell-free supernatant was collected and diluted with Milli-Q H$_2$O (1:100-1:1000). Those samples were analysed with the ion chromatograph IC-2100 equipped with the autosampler AS50, the suppressor ASRS 300, the column IonPac AS27 (2 x 250 mm) and the pre-column IonPac AG27 (2 x 50 mm). The chromatograms were analysed with the software Chromeleon 6.81 (ThermoFisher Scientific). If the cells were cultivated with sunflower seed oil, the samples were degreased previously by adding 500 µl n-hexane to the sample, vigorous mixing for 5 min and centrifugation (13.000 rpm, 5 min, 4 °C). The aqueous phase was collected, 500 µl n-hexane was added, mixed again and centrifuged. The aqueous phase was collected and diluted with Milli-Q H$_2$O for ion chromatography.

For parameters used for chromatography see table 14.

Table 14 Parameters used for separation and quantification of relevant organic acids and anions with the ion chromatography system Dionex IC-2100

anion-exchange column	IonPac AS27 (2 x 50 mm) + guard column AS27 (2 x 50 mm)			
flow rate	0.38 ml min⁻¹			
injection volume	10 µl			
eluent	KOH			
gradient	0 – 3 min	5 mM isocratic		
	3 – 5 min	16 mM linear		
	5 – 34 min	45 mM linear		
	34 – 43 min	45 mM isocratic		
	43.1 – 45 min	5 mM isocratic		
retention times	malate	16.3 min	nitrate	10.9 min
	itaconate	17.3 min	sulphate	15.3 min
	α-ketoglutarate	19.4 min	phosphate	25.9 min
	citrate	32.1 min	isocitrate	34.0 min

3. Results

3.1. Itaconic acid production with the yeast *Pseudozyma tsukubaensis*

3.1.1. Minimal medium for growth and ITA production

The initial ITA production medium according to Kawamura et al. (1981, 1982) consisted of 100 g l^{-1} glucose, 1.5 g l^{-1} NaNO$_3$, 0.5 g l^{-1} KH$_2$PO$_4$, 0.1 g l^{-1} MgSO$_4$ and 0.2 % corn steep liquor (CSL). During his work, Bodinus (2011) altered the composition of this medium but CSL remained an integral part of it. The viscous CSL is a by-product arising from corn wet milling that is rich in vitamins, amino acids, minerals and trace elements. For an optimized and highly standardized production process of fermentation products, such a complex ingredient is undesired, since it has a variable composition due to differences in the processing of the corn starch and due to the variability in the chemical makeup of the corn itself. Hence, the use of CSL can lead to increased variability in growth behaviour or organic acid production.

At the beginning of this study, it was important to find a substitute for CSL in the minimal medium. Supplementation of the medium with different vitamins was tested. The micronutrients were selected because they are generally known to be necessary for the growth of microorganisms. Table 15 shows the supplements which enabled growth of *P. tsukubaensis* H488 wild type cells in liquid cultures with minimal medium + glucose (MG). As a reference, yeast extract-peptone-dextrose (YPD) medium was used. YPD medium also has complex components which provide every essential nutrient. Thus, the yeast cells grew rapidly when cultivated in YPD.

Table 15 Growth behaviour of *P. tsukubaensis* wild type strain H488 in liquid minimal medium with 5 % (w/v) glucose (MG) and different vitamins.
The yeast cells were either pre-cultivated with YPD or MG medium (3 g l^{-1} (NH$_4$)$_2$SO$_4$, 1 g l^{-1} KH$_2$PO$_4$, for composition see section 2.4.2). The main cultures were inoculated with a starting OD$_{600}$ = 1. The yeast cells were incubated for 2 d while shaking (220 rpm) at 30 °C. In two cases, the minimal medium was supplemented on the first day of growth either with YPD or the vitamin solution. The vitamin solution consists of the listed vitamins at the respective concentration. * (✔) - marks slow initial growth.

Medium	pre-culture	Supplementation at 1ˢᵗ d	Growth
MG	MG	-	-
MG	YPD	-	(✔)*
YPD	YPD	-	✔
MG + YPD	MG	+ 10 % (v/v) YPD	✔
MG + Vit	MG	vitamin solution	✔
MG + 0.2 mg l^{-1} 4-aminobenzoic acid	MG	-	-
MG + 0.2 mg l^{-1} biotin	MG	-	-
MG + 0.4 mg l^{-1} calcium pantothenate	MG	-	-
MG + 0.2 mg l^{-1} folic acid	MG	-	-
MG + 2.0 mg l^{-1} inositol	MG	-	✔
MG + 0.4 mg l^{-1} niacin	MG	-	-
MG + 0.4 mg l^{-1} pyridoxin hydrochloride	MG	-	-
MG + 0.2 mg l^{-1} riboflavin	MG	-	-
MG + 0.4 mg l^{-1} thiamine hydrochloride	MG	-	✔

As expected, the yeast cells did not grow when both pre- and main cultivation were carried out in plain MG medium. However, when the MG medium was directly inoculated with *P. tsukubaensis* cells from YPD (without transferring any YPD medium) a slow growth was observable. This was an indicator that the cells potentially store or at least bind the necessary nutrients needed for cell growth. Even these small amounts seemed to be enough to maintain a low level of cell proliferation for the observed 48 h of cultivation.

In the case, where the pre- and main cultures were set-up in non-supplemented MG medium, the yeast cells remained dormant. Despite no cell multiplication being detectable after 24 h incubation, growth could be induced by adding liquid YPD or the composite vitamin solution. This showed that the vitamin solution was enough to substitute for CSL. During the next step, only one out of the nine supplements was added to the MG medium. That way, it was demonstrated that inositol and thiamine, each individually, enabled growth of *P. tsukubaensis* in minimal medium. This was a surprising result because the two molecules are structurally very distinct from another and don't share a common metabolic pathway. In later experiments, thiamine hydrochloride was chosen to substitute for CSL.

3.1.1.1. Relationship of organic acid production to phosphate and nitrogen concentrations

For *A. terreus* it is believed that a limitation of an essential element other than the C source is needed to induce ITA production. Commonly, P limitation is used to trigger ITA synthesis in this filamentous fungus. (Klement and Büchs, 2013; Welter, 2000). For *U. maydis* and *P. antarctica* it was demonstrated that a limitation in N is beneficial for the ITA production (Klement et al., 2012; Levinson et al., 2006).

As mentioned above, a basic composition for a minimal medium for the growth of *P. tsukubaensis* H488 had been found, but it was now crucial to develop it further regarding its N and P content, to ensure high ITA production with *P. tsukubaensis*. Therefore, the role of the ratio between the available N and P source in the minimal medium was investigated. To elaborate, which N:P ratio leads to a substantial organic acid production, a preliminary test was performed with strain H488 in which four different N:P ratios were tested [in g l^{-1}]: 10:0.4, 3:1, 2.5:0.1, 0.75:0.25

Since the *P. tsukubaensis* wild type produces very low levels of ITA, the production of MA was used as the acid production benchmark during preliminary tests.
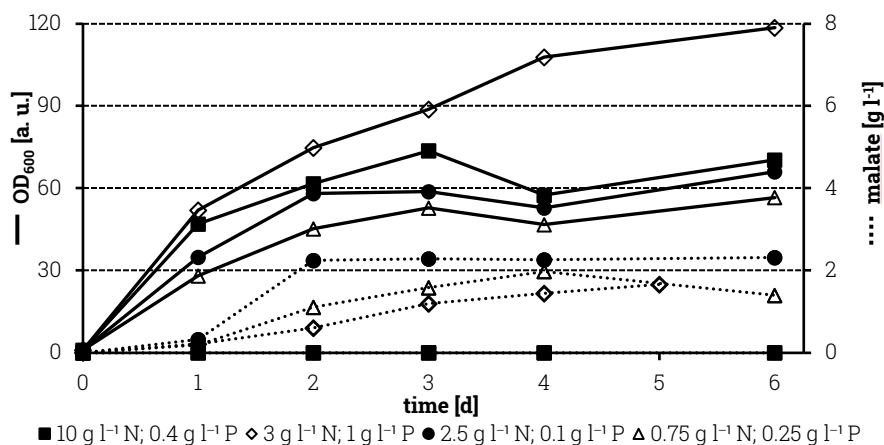
Figure 8 Malic acid (MA) production behaviour of *P. tsukubaensis* H488 wild type strain in minimal medium with glucose when cultivated with different nitrogen (N) and phosphate (P) concentrations.
The yeast cells have been grown for up to 6 d in modified minimal medium (MG) with 5 % (w/v) glucose, and different concentrations of $(NH_4)_2SO_4$, and KH_2PO_4 in 500 ml-baffled flasks at 30 °C and 220 rpm. The medium was kept at a neutral pH with the addition of 3.3 g l^{-1} $CaCO_3$.

Figure 8 shows that a high N:P ratio (2.5:0.1) was advantageous for the production of MA. With this medium, a rapid increase in MA concentration was detected. After 48 h, 2.2 g l^{-1} MA were measured in the culture's supernatant. Afterwards, the concentration did not increase further. With the same N:P ratio but with higher initial concentrations (10:0.4) almost no organic acid was synthesised.

A high N:P ratio but with low initial concentrations (0.75:0.25) also led to the secretion of organic acid but the synthesis rate was considerably slower. After 4 d of cultivation, 2.0 g l^{-1} MA have been detected in the medium. Although the yeast grew much more rapidly with 3 g l^{-1} N and 1 g l^{-1} P, the synthesis rate for MA was even slower when larger amounts of substrates were present initially. In this case, after 5 d of cultivation, only 1.4 g l^{-1} MA were detected in the medium.

Based on this data, further cultivations were carried out with initial maximum N concentrations of 5 g l^{-1} and 0.1 or 2.0 g l^{-1} P. Also, the N source, previously $(NH_4)_2SO_4$, was exchanged for $NaNO_3$, because the sulphate anions were interfering during the analytics of ITA quantification. This medium was named MG-IA (for composition see 2.4.2).

With the aid of the adjusted medium composition, not solely MA but also the production of ITA was induced in strain H488. The production behaviour for both organic acids appeared to be correlated. Highest concentrations for MA (6.8 g l^{-1} at 5th d) and ITA (1.8 g l^{-1} at 4th d) were reached with 5 g l^{-1} N source and 0.1 g l^{-1} P source. With the same amount of P but less N (N:P = 2:0.1) slightly lower organic acid levels were achieved (see figure 9).

By substantially limiting the initial N amounts, the acid production rate was drastically lowered. The organic acid synthesis was brought to baseline levels with 2.0 g l^{-1} P source and limited N supply. This drastic reduction is not solely due to the decrease in cell mass. When both compounds were limited, comparable low cell densities have been observed but the secretion of

MA (1.0 g l^{-1} at 4th d) and ITA (0.8 g l^{-1} at 4th d) into the medium were higher. Providing initially 2.0 g l^{-1} of N & P sources, led to the highest cell density. This fact did not reflect on the resulting concentrations of the secreted organic acids. Less ITA was secreted than with an N:P ratio of 5:0.1 or 2:0.1 besides the higher cell density.
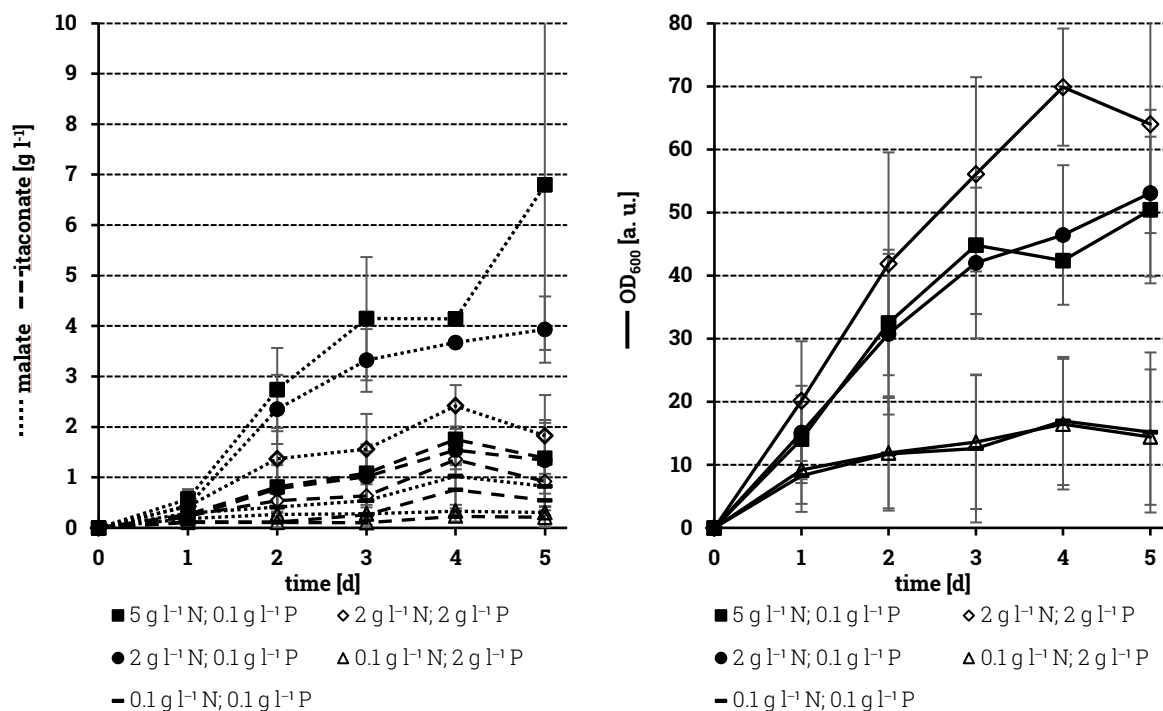
Figure 9 Organic acid production behaviour of *P. tsukubaensis* H488 wild type strain in minimal medium with glucose when cultivated with different nitrogen (N) and phosphate (P) concentrations.
The yeast cells have been grown for up to 5 d in modified minimal medium (MG-IA) with 5 % (w/v) glucose, and different concentrations of NaNO$_3$, and KH$_2$PO$_4$ in 500 ml-baffled flasks at 30 °C and 220 rpm. The medium was kept at a neutral pH with 3.3 g l^{-1} CaCO$_3$. Shown are the mean values for three separate cultivations.

Bodinus (2011) established the high ITA producing *P. tsukubaensis* strain M15-CAD. The strain was derived from the wild type H488 by UV-mutagenesis and additional overexpression of the *A. terreus AtCAD1* gene. This strain was also tested in MG-IA medium with N:P ratios that deemed optimal for strain H488. Figure 10 shows that the proportions of ITA to MA are reversed with this strain compared to the wild type. It secretes mainly ITA. For all three tested media, high concentrations of ITA and relatively low concentrations of MA were secreted. The final concentrations for MA were relatively similar, ranging from 1.2 to 1.7 g l^{-1}, for all three media compositions. The highest ITA yield of 16.2 g l^{-1} ITA at the end of the cultivation period, was achieved with 2 g l^{-1} N and 0.1 g l^{-1} P. With the same amount of P and higher concentrations of N source much less ITA was produced (8.9 g l^{-1} at 5th d). By increasing N and P concentrations to 5 g l^{-1} and 1 g l^{-1}, respectively, the yeast cells grew to a high cell density. Contrary to strain H488, strain M15-CAD maintained a high productivity of ITA (13.6 g l^{-1} at 5th d) even during increased cell growth.
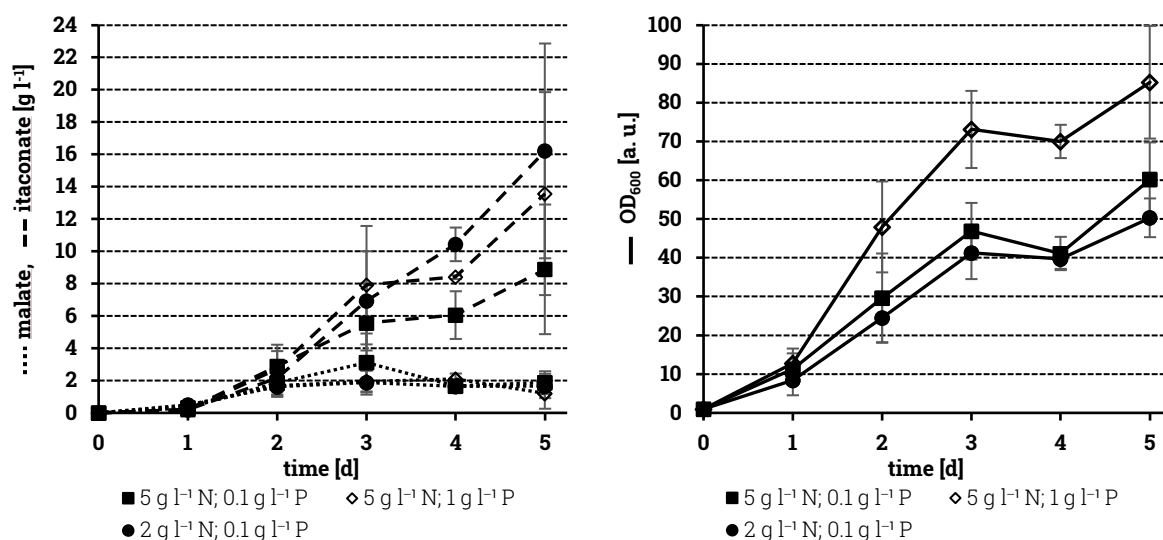
Figure 10 Organic acid production behaviour of the ITA overproducing strain *P. tsukubaensis* M15-CAD (Bodinus, 2011) in minimal medium with glucose when cultivated with different nitrogen (N) and phosphate (P) concentrations.
The yeast cells have been grown for up to 5 d in modified minimal medium (MG-IA) with 5 % (w/v) glucose, and different concentrations of $NaNO_3$, and KH_2PO_4 in 500 ml-baffled flasks at 30 °C and 220 rpm. The medium was kept at a neutral pH with 3.3 g l^{-1} $CaCO_3$. Shown are the mean values for three separate cultivations.

These findings suggest that not the sheer N:P ratio but also the amount of available nitrogen and phosphate at the beginning of cultivation played a role in the induction of organic acid synthesis. A high N:P ratio with low initial P concentrations appeared to be most beneficial for the initiation of organic acid synthesis in *P. tsukubaensis* while high initial P concentrations accelerated cell growth without necessarily enhancing the synthesis of organic acids. This observation was taken into account for subsequent cultivation experiments. For the preparation of the ITA production minimal medium (MG-IA) during subsequent experiments, N:P ratios of 4:1 to 20:1 were applied (the specific N and P concentrations are listed for each respective cultivation).

3.1.2. Identification of genes involved in ITA production

At the beginning of this work, there was no available information about the genetic makeup of *P. tsukubaensis*. In order to gain more insight, the whole genome of the wild type strain H488 had to be sequenced. In the beginning, a *shotgun* and a *mate-pair* library were constructed. The libraries were then paired end sequenced. The resulting non-contiguous reads of genomic sequences were first assembled into contigs and finally into 38 scaffolds. De novo sequencing of genomic DNA and RNA of *P. tsukubaensis*, the assembly of the reads into contigs, and the preliminary annotation was carried out by IIT Biotech GmbH in Bielefeld.

In total, the entire genome was 20.28 Mb large and exhibited a guanine-cytosine (GC) content of 53.6 %. In the genomic sequence, 7017 proposed genes were identified. Although, the number of proteins these open reading frames (ORF) encode is still unclear.

U. maydis 521 is a closely related ITA producing fungus. Compared to *U. maydis,* the genome of *P. tsukubaensis* is slightly larger in size and contains more ORFs (see table 16).

Table 16 Comparison of genome size, GC-content, number of chromosomes, genes and proteins between *P. tsukubaensis* **and other yeast species (as reported on** NCBI genome**).**

Species	Chromosomes	Size [Mb]	GC [%]	Genes	Proteins
Pseudozyma tsukubaensis H488	? (38 scaffolds)	20.28	53.6	7017	?
Ustilago maydis 521	23	19.64	54.0	6910	6783
Ustilago hordei Uh4857-4	23	20.7	51.2	7230	7111
Sporisorium reilianum SRZ2	23	18.50	59.5	6811	6682
Yarrowia lipolytica CLIB122	6	20.22	49.0	7144	6472
Saccharomyces cerevisiae S288C	16	11.88	38.3	6445	6002

By mapping the scaffolds to the reference genome of *U. maydis* with the comparative genome assembly tool *r2cat* (Husemann and Stoye, 2010), their close relationship was confirmed. Furthermore, the created synteny plot showed that the chromosomal makeup appears to be largely similar to that of *U. maydis*. All of the 23 chromosomes could be matched to one or more scaffolds. It is possible that chromosome 5 and 20 represent a single chromosome in *P. tsukubaensis* H488 since scaffolds number 4 and 9 are both partially mapped to those chromosomes. A partial reciprocal translocation is also a plausible explanation for the co-mapping of scaffold number 4 and 9 to chromosomes 5 and 20. Scaffolds 31,32,34,35 and 37 could not be mapped against the reference genome. These scaffolds are all less than 10 kb in size and possibly represent distinct genetic information deviating from *U. maydis* 521.

U. maydis chromo-some	*P. tsukuba-ensis* scaffold
1	1+27+25
2	2+12'+30
3	3
4	7
5	9'+'4+36
6	5
7	6
8	14+'10
9	24+10'
10	13
11	11
12	26+8
13	17+38
14	15
15	29+'12
16	19
17	18
18	20
19	16
20	4'+'9
21	21
22	22
23	23+33
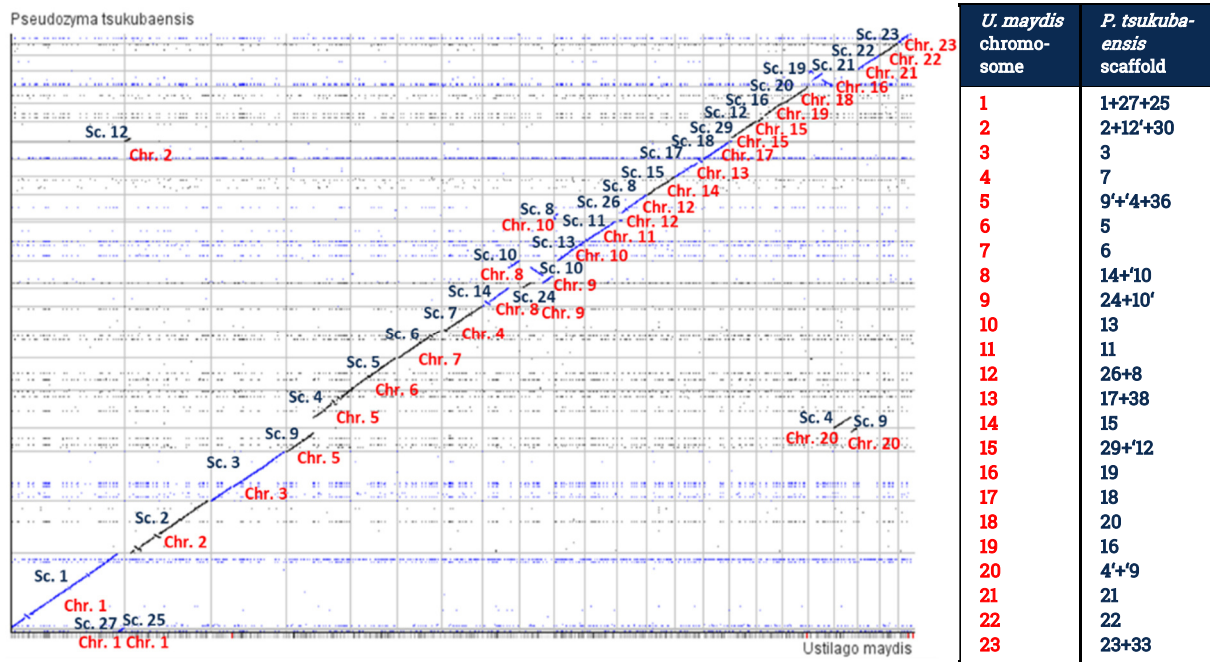
Figure 11 Synteny plot created by *r2cat*. **The scaffolds of** *P. tsukubaensis* **H488 are mapped onto the reference sequence of** *U. maydis* **521.**
The table shows the scaffolds or parts of scaffolds (marked with ') that constitute for the corresponding chromosome in *U. maydis*.

After establishing the global genomic similarity between *P. tsukubaensis* and *U. maydis*, genes potentially involved in the production of ITA were investigated. In other fungi e.g. *A. terreus* and *U. maydis,* the genes needed for the production of secondary metabolites like ITA are organized in clusters (Geiser et al., 2016a; Keller, 2015; Li et al., 2011). To identify suitable candidates, the genome of *P. tsukubaensis* was searched for related genes. With the help of the NCBI BLASTP algorithm, the putative translational products of the *P. tsukubaensis* H488 genome were searched for amino acid sequences of ITA biosynthesis proteins of the known producers *U. maydis* and *A. terreus*. By doing so, it was possible to identify five genes in direct proximity to each other on scaffold 19. Table 17 and figure 12 show that all five genes share high sequence identities to the ITA cluster genes of *U. maydis*. The genes potentially code for all proteins needed for ITA production. In detail: Mtt1p represents a mitochondrial tricarboxylate transporter which channels *cis*-aconitate out of the mitochondrion. The aconitate-Δ-isomerase (Adi1p) converts *cis*-aconitate into *trans*-aconitate which is metabolized into ITA by the *trans*-aconitate decarboxylase (Tad1p). ITA is then exported into the surroundings by the itaconate transport protein (Itp1p). All those cluster genes are described to be regulated by the regulator protein for itaconic acid (Ria1p) whose gene also lies inside the ITA cluster of *U. maydis* and *P. tsukubaensis*. The similar gene *ATEG_09969* can also be found in the ITA gene cluster of *A. terreus*.

Table 17 List of *P. tsukubaensis* genes with high similarity to ITA cluster genes from *U. maydis* 521 and *A. terreus* NIH2624.

The protein sequences resulting from ITA cluster genes from *U. maydis* and *A. terreus* were used as query in BLASTP (NCBI) against the translational products of the whole *P. tsukubaensis* genome. Shown are the homologous gene products with amino acid (aa) identity [query coverage] and the Expected value. Also given are the respective lengths of the deduced protein sequences (number of aa) and the predicted molecular weight (MW). Molecular weights were estimated with the ProtParam tool (https://web.expasy.org/protparam/).

P. tsukubaensis gene	deduced protein	*U. maydis* gene	identity E-value	*A. terreus* gene	deduced protein	identity E-value
PtADI1	478 aa	*UmADI1 (UMAG_11778)*	72 % [88 %]	*PRPF (ATEG_07328)*	395 aa	32 % [81 %]
PSEUDOG_6268	51.0 kDa	gene ID: 23567624	0.0	gene ID: 4319292	41.1 kDa	$4 \times e^{-49}$
PtITP1	532 aa	*UmITP1 (UMAG_11777)*	83 % [91 %]	*AtMFSA (ATEG_09972)*	403 aa	22 % [75 %]
PSEUDOG_6270	57.7 kDa	gene ID: 23567623	0.0	gene ID: 4319518	43.5 kDa	$2 \times e^{-14}$
PtMTT1	191 aa	*UmMTT1 (UMAG_05079)*	77 % [99 %]	*AtMTTA (ATEG_09970)*	301 aa	33 % [96 %]
PSEUDOG_6267	20.6 kDa	gene ID: 23565067	$5 \times e^{-105}$	gene ID: 4319645	32.1 kDa	$4 \times e^{-24}$
PtRIA1	393 aa	*UmRIA1 (UMAG_05080)*	43 % [95 %]	*Regulator (ATEG_09969)*	751 aa	32 % [17 %]
PSEUDOG_6266	43.4 kDa	gene ID: 23565068	$1 \times e^{-63}$	gene ID: 4319644	84.9 kDa	0.043
PtTAD1	485 aa	*UmTAD1 (UMAG_05076)*	85 % [100 %]	*AtCADA (ATEG_09971)*	490 aa	41 % [19 %]
PSEUDOG_6271	52.9 kDa	gene ID: 23565066	0.0	gene ID: 4319646	53.0 kDa	0.12

Figure 12 Comparison of the putative ITA cluster in _P. tsukubaensis_ H488 to the itaconic acid clusters of _U. maydis_ 521 and _A. terreus_ NIH2624.
Genes responsible for ITA production have been identified on protein level by NCBI protein BLAST. _P. tsukubaensis_ possesses five homologous genes out of seven _U. maydis_-ITA cluster genes. Both _U. maydis_ and _P. tsukubaensis_ have genes that code for a _trans_-aconitate decarboxylase (_tad1_), a Major Facilitator Superfamily extracellular itaconate transport protein (_itp1_), an aconitate-Δ-isomerase (_adi1_), a mitochondrial tricarboxylate transporter (_mtt1_) and a regulator for itaconic acid (_ria1_). _U. maydis_ additionally contains a Cytochrome P$_{450}$ monooxygenase (_cyp3_) and a gene that codes for an unknown protein (_rdo1_). The structure of the ITA cluster in _A. terreus_ is simpler: Genes present in the cluster encode a Cytochrome P$_{450}$ monooxygenase (_P$_{450}$_), a Major Facilitator Superfamily transporter (_mfsA_), a _cis_-aconitate decarboxylase (_cadA_, synonymic _cad1_), a mitochondrial tricarboxylate transporter (_mttA_) and a transcriptional regulator for ITA (_regulator_). Numbers in the lines indicate amino acid identity in percentage obtained by NCBI BLASTP.

Deviating from the _U. maydis_ ITA cluster, there appeared to be an additional gene, _PSEUDOG_6269_, in _P. tsukubaensis_. This ORF is only 297 base pair long and is located between _PtITP1_ and _PtADI1_. The putative function of the deduced 99 aa long gene product is still unknown. Additionally, no homologous genes could be found for _cyp3_ or _rdo1_ in the genome of _P. tsukubaensis_ H488. The translational products of _cyp3_ (codes for a cytochrome P$_{450}$ monooxygenase) and _rdo1_ (unknown gene product) are thought to convert ITA into 2-hydroxyparaconate and then metabolize it further into the acid itatartarate (Geiser et al., 2016a, 2016b).

In _A. terreus_ NIH2624, the ITA cluster has a similar composition. It consists of a cytochrome P$_{450}$ monooxygenase (P$_{450}$), two carrier proteins: one for the export of _cis_-aconitate out of the mitochondrion (MttAp) and another for the export of ITA (MfsAp), a regulator protein for ITA production and a _cis_-aconitate decarboxylase (CadAp, synonymic Cad1p), which alone converts _cis_-aconitate directly into ITA. The carrier proteins Itp1p and Mtt1p, and the regulator Ria1p from _P. tsukubaensis_ share some sequence identity with the homologous proteins MfsAp, MttAp and Regulator, respectively. Although the protein Cad1p catalyses for the direct decarboxylation of _cis_-aconitate instead of _trans_-aconitate, parts of the protein were 41 % identical to the Tad1p protein in _P. tsukubaensis_ which is responsible for the decarboxylation of _trans_-aconitate. Additionally, the fungus _A. terreus_ carries a gene whose translational product resembled the sequence of PtAdi1p. This protein, encoded by _ATEG_07328_, is potentially a PrpF protein and maybe catalyses the conversion of _trans_-aconitate into _cis_-aconitate.

It stands to reason, that for all the mentioned ITA producing microorganisms the main precursor is *cis*-aconitate. In the tricarboxylic acid cycle, *cis*-aconitate is formed by the dehydration of CA. This step is catalysed by the enzyme aconitase that also catalyses the isomerization of CA by rotating *cis*-aconitate and rehydrating it in the 'isocitrate mode'. In order to increase the intramitochondrial *cis*-aconitate concentration and thus increase ITA production, the overexpression of the native aconitase from *P. tsukubaensis* was pursued. To that intent, first the protein sequences of *P. tsukubaensis* were used as subjects in a BLASTP search for putative aconitase enzymes using the sequence of the aconitase of *U. maydis* as a query. Table 18 shows the similarities between the translational products of the identified putative aconitase genes *PSEUDOG_3035* and *PSEUDOG_2814,* and their homologous counterparts in *U. maydis* and other microorganisms.

Table 18 List of *P. tsukubaensis* genes with high similarity to aconitase encoding genes from *U. maydis* 521 and other microorganisms.

The protein sequences encoded by aconitase genes from *U. maydis* were BLASTed against the translational products of the whole *P. tsukubaensis* genome. The identified targets were additionally analysed against the whole NCBI non-redundant database. Shown are the homologous gene products with aa identity, query coverage (values in brackets) and the Expected value. Also given are the respective lengths of the deduced protein sequences (number of aa) and the predicted molecular weight (MW). Molecular weights were estimated with the ProtParam tool (https://web.expasy.org/protparam/). Put. – putative.

P. tsukubaensis gene	deduced protein	homologous gene	deduced protein	identity E-value
PtACO1 *PSEUDOG_3035*	796 aa 85.7 kDa	*U. maydis* putative *ACO1* *UMAG_02899* gene ID: 23563532	796 aa 86.1 kDa	95 % [100 %] 0.0
		Moesziomyces antarcticus aconitase *PAN0_010c4087* gene ID: 26304836	796 aa 85.9 kDa	97 % [100 %] 0.0
PtACO2 *PSEUDOG_2814*	1050 aa 112.1 kDa	*U. maydis* putative aconitase *UMAG_11923* gene ID: 23567732	1048 aa 112.3 kDa	93 % [99 %] 0.0
		Kalmanozyma brasiliensis aconitase *PSEUBRA_SCAF5g02353* gene ID: 27421334	1035 aa 111.0 kDa	93 % [99 %] 0.0

3.1.3. Identification of suitable promoters for overexpression studies

In order to ensure a constitutive and high expression rate for the genes potentially involved in ITA production in *P. tsukubaensis*, a suitable promoter sequence had to be identified. A promoter sequence is considered strong if it shows a high affinity for the RNA polymerase. A high affinity is given when the consensus sequence of the promoter matches the consensus sequence recognized by the RNA polymerase. Genes that are expressed constitutively and at high levels, like housekeeping genes, are such appropriate targets to search for such strong promoters. In general, the upstream regions of housekeeping genes contain promoters that enable a consistent and high transcriptional rate. Typical proteins that perform housekeeping functions are Actin1, Elongation factor 1-alpha (TEF1p), Glyceraldehyde-3-phosphate-dehydrogenase (GAPDHp) and the HSP70 chaperone.

By conducting a protein BLAST search against the proteins of *P. tsukubaensis*, four candidate genes were identified which are homologous to the above-mentioned housekeeping genes. Table 19 shows the investigated genes from *P. tsukubaensis* H488 which are homologous to housekeeping genes from other organisms.

The translational product from *PSEUDOG_6713* is highly similar to the Actin1 protein from *U. maydis* 521. The deduced proteins from *PSEUDOG_4929* and *PSEUDOG_930* share high sequence similarities with the HSP70 chaperone and the TEF1 protein (both from *Kalmanozyma brasiliensis*), respectively. PtGAPDHp (encoded by *PSEUDOG_2568*) was matched to GAPDH (*PANT_12c00136*) from *Moesziomyces antarcticus* with a sequence similarity of 99 %. We additionally identified the putative gene in *P. tsukubaensis* that codes for a protein similar to the ubiquitin-conjugating enzyme UBC6-E2 from *Melanopsichium pennsylvanicum* (*PtUBC6* was not considered for promoter activity studies but was used together with *PtTEF1* as reference genes for qPCR described in section 3.1.6).

Table 19 List of *P. tsukubaensis* genes with high similarity to housekeeping genes from *U. maydis* 521 and other microorganisms.

The protein sequences resulting from housekeeping genes from *U. maydis* were analysed with BLASTP against the translational products of the whole *P. tsukubaensis* genome. The identified targets were additionally compared to the whole NCBI non-redundant database. Shown are the homologous gene products with aa acid identity, [query coverage] and the Expected value. Also given are the respective lengths of the deduced protein sequences (number of aa) and the predicted molecular weight (MW). Molecular weights were estimated with the ProtParam tool (https://web.expasy.org/protparam/). Put. - putative

P. tsukubaensis gene	deduced protein	homologous gene	deduced protein	identity E-value
PtActin1 *PSEUDOG_6713*	375 aa 41.8 kDa	*U. maydis* put. Actin1 *UMAG_11232* gene ID: 23567141	375 aa 41.8 kDa	100 % [100 %], 0.0
		Sporisorium reilianum probable Actin *sr11345* ID: FQ311444.1	375 aa 41.8 kDa	99 % [100 %], 0.0
PtGAPDH *PSEUDOG_2568*	342 aa 36.4 kDa	*U. maydis* UmGAPDH *UMAG_ 02491* gene ID: 23563225	342 aa 36.3 kDa	97 % [100 %], 0.0
		Moesziomyces antarcticus GAPDH *PANT_12c00136* gene ID: DF196778.1	337 aa 35.9 kDa	98 % [98 %], 0.0
PtHSP70 *PSEUDOG_4929*	645 aa 70.3 kDa	*U. maydis* HSP70 ATPase *UMAG_03791* gene ID: 23564150	645 aa 70.3 kDa	99 % [100 %], 0.0
		Kalmanozyma brasiliensis HSP70/HSC70 *PSEUBRA_SCAF19g03268* gene ID: 27418201	646 aa 70.4 kDa	99 % [100 %], 0.0
PtTEF1 *PSEUDOG_930*	457 aa 49.8 kDa	*U. maydis* put. Elongation factor 1-α *UMAG_ 00924* gene ID: 23562087	459 aa 50.0 kDa	96 % [99 %], 0.0
		Kalmanozyma brasiliensis Elongation factor 1-α *PSEUBRA_SCAF1g00572* gene ID: 27418763	457 aa 49.6 kDa	98 % [100 %], 0.0
PtUBC6 *PSEUDOG_4405*	293 aa 31.3 kDa	*U. maydis* put. E2 ubiquitin-conjugating enzyme *UMAG_ 11635* gene ID: 23567494	274 aa 29.9 kDa	76 % [100 %], 1 x e^{-142}
		Melanopsichium pennsylvanicum probable UBC6-E2 *BN887_05967* gene ID: HG529627.1	281 aa 30.5 kDa	80 % [100 %], 4 x e^{-154}

3.1.4. Development of overexpression plasmids

For the construction of plasmids for the purpose of promoter activity studies, the reporter gene *LacZ* from *E. coli* was fused with one of the upstream regions of the four previously identified housekeeping genes *Actin1*, *GAPDH*, *HSP70* and *TEF1*. This was achieved by amplifying approximately 1000 bb long sequences of the respective upstream region while extending the 5'-end with a KpnI-restriction enzyme recognition site and the 3'-end with the first 20 bp of the *LacZ* ORF. The *LacZ* gene was amplified while complementing the 5'-end with the respective 3'-sequence (20 bp) of the promoter and the other end with a PstI-restriction enzyme recognition site. The two fragments were purified and fused together by overlap extension PCR. The resulting fragments were purified, then subjected to restriction by PstI and KpnI and finally ligated each into the linearized pPTT plasmid, thus creating the pPTT-pActin-*LacZ*, pPTT-pGAPDH-*LacZ*, pPTT-pHSP70-*LacZ* and pPTT-pTef-*LacZ* plasmids.

3.1.4.1. Determination of a strong, native promoter in *P. tsukubaensis*

For the promoter testing, the *LacZ* reporter gene was under the control of the respective putative promoter containing upstream region. The constructed reporter plasmids were individually transformed into the *P. tsukubaensis* wild type strain H488 and the ITA producing UV-mutagenesis strain M15. As a reference, the plasmid pPTT-pUmHSP70-*LacZ* was also transformed. In this plasmid the *LacZ* gene was placed under the control of the HSP70 promoter from *U. maydis*. All of the resulting transformants were grown in YPD and MG-IA media and tested for β-galactosidase activity.

From figure 13 it is evident that β-galactosidase activity was observed for all tested promoters and both media. The variability in enzyme activities between the transformants even with the same specific promoter were, however, quite large for every condition. Some transformants showed a low enzyme activity while other transformants with the same vector displayed a significantly higher β-galactosidase activity. With the HSP70 promoter from *U. maydis* an already high induction could be achieved in strain H488 which was even greater than with the native HSP70 promoter in YPD medium. When cultivated in minimal medium the activities for both were relatively equal.
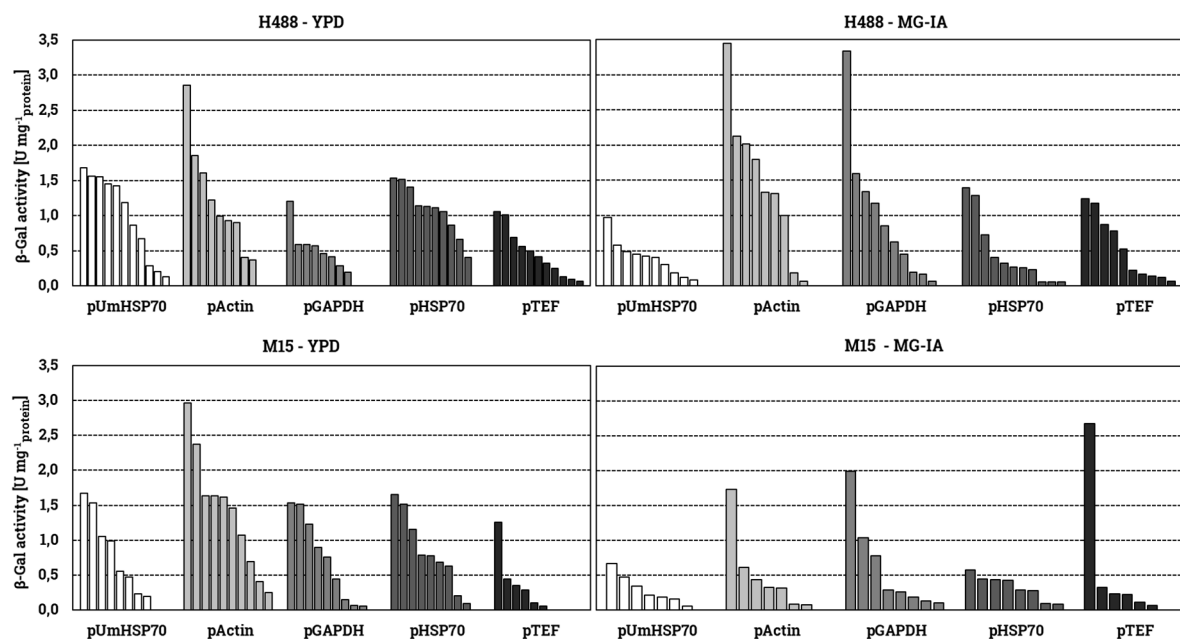
Figure 13 β-Galactosidase activities [U mg$^{-1}_{protein}$] in various generated *P. tsukubaensis* H448 (wild type) and M15 (UV-mutant) *LacZ*-overexpression transformants, in which the reporter gene was placed under the control of the HSP70 promoter from *U. maydis* or the native promoters pActin, pGAPDH, pHSP70, pTEF.
The yeast cells were grown either in YPD full medium or minimal medium with glucose for ITA production (MG-IA, 2 g l^{-1} NaNO$_3$, 0.1 g l^{-1} KH$_2$PO$_4$). The cultivation was carried out in a volume of 2.5 ml in 12-well plates for 2 d (YPD) or 4 d (MG-IA) at 30 °C and 220 rpm. As buffering agent, a spatulas tip of CaCO$_3$ per well was added.

The detected β-galactosidase activity with the TEF promoter of yeasts grown in minimal medium was also very low. In general, the promoter activity of TEF proved to be one of the modest.

When the *LacZ* gene was under the control of the GAPDH promoter region, the results for the enzyme activities were diverse. In minimal medium, a quite high induction was achieved but the β-galactosidase activity was medium to low in YPD medium compared to the other promoter sequences.

On average, the highest activity was reached when the *LacZ* transcription was initiated by pActin. This is true for all conditions, except for strain M15 when cultivated in MG-IA medium. However, a decrease in enzyme activity in strain M15 was an overall phenomenon in the minimal medium, for every tested promoter. Such a decline in β-galactosidase activity is striking. Although, the transformants with the wild type background also showed differences between the two media, the effect was not that pronounced.

In conclusion, β-galactosidase was highest when *LacZ* was under the control of the Actin promoter. Therefore, this upstream region was chosen as the promoter for all subsequent overexpression studies.

3.1.4.2. ITA overproduction plasmids

Plasmids for the overexpression of genes potentially needed for or aiding ITA production were constructed by amplifying approximately 1000 bp of the upstream region of the *Actin1* gene (*PSEUDOG_6713*). At the 5'-end, a recognition site for a restriction enzyme (KpnI, BsrGI or Pfl23II) was introduced and at the 3'-end the first 20-22 bp of the respective gene. The native ITA cluster genes from *P. tsukubaensis* and the *AtCAD1* gene from *A. terreus* were amplified while extending the 5'-end with the last 20-22 bp of the promoter sequence and at the 3'-end with a restriction enzyme recognition site. The two fragments were purified and fused together by overlap extension-PCR. The resulting fragments were purified, then subjected to restriction and finally ligated each into the linearized pPTT plasmid, thus creating the pPTT-pActin-*ADI1*, pPTT-pActin-*ITP1*, pPTT-pActin-*MTT1*, pPTT-pActin-*RIA1*, pPTT-pActin-*TAD1* and pPTT-pActin-*AtCAD1* plasmids.

In order to create plasmids for the additional overexpression of the *PtACO1*, *PtACO2* and *AtCAD1* genes into *P. tsukubaensis* with the background of an already existing overexpression, the construction was executed similarly to the above described method. Deviating from that, the resulting pActin-gene fusion products were ligated into the pPTT.Cbx-plasmid. According to this, the following plasmids were created: pPTT.Cbx-pActin-*ACO1*-Ex, pPTT.Cbx-pActin-*ACO2*, pPTT.Cbx-pActin-*AtCAD1* (Note: The ORF of the native *PtACO1* gene contains an intron. The gene was amplified without this intron by amplifying solely the exons first, fusing these PCR-products together during an overlap-PCR and then fusing the pActin promoter to it in the course of a second overlap-PCR).

The correctness of the plasmids was confirmed by colony-PCR using the oligonucleotide pXXXX_KpnI_fw (XXXX represents the respective promoter) as the forward primer and the reverse primer for the respective gene. Additional confirmation was carried out by control digestion and/or plasmid sequencing.

An overview of the size of the inserts and the linearized vector backbones after restriction with the appropriate enzymes can be found in table 20. The utilized vector backbones and a schematic of the created overexpression plasmids are illustrated in figure 14.

Table 20 List of all promoter-gene fusion and vector backbones used for the overexpression of the relevant genes.

Gene	Promoter-gene fragment (size)	Vector fragment (size)
PtADI1 *PSEUDOG_6268*	(KpnI)-pActin-*PtADI1*-(NsiI) (2686 bp)	(KpnI)-pPTT-(NsiI) (6801 bp)
PtITP1 *PSEUDOG_6270*	(KpnI)-pActin-*PtITP1*-(NsiI) (2955 bp)	(KpnI)-pPTT-(NsiI) (6801 bp)
PtMTT1 *PSEUDOG_6267*	(KpnI)-pActin-*PtADI1*-(SdaI) (2217 bp)	(KpnI)-pPTT-(NsiI) (6801 bp)
PtRIA1 *PSEUDOG_6266*	(KpnI)-pActin-*PtRIA1*-(NsiI) (2366 bp)	(KpnI)-pPTT-(NsiI) (6801 bp)

Gene	Promoter-gene fragment (size)	Vector fragment (size)
PtTAD1 *PSEUDOG_6271*	(KpnI)-pActin-*PtTAD1*-(NsiI) (2558 bp)	(KpnI)-pPTT-(NsiI) (6801 bp)
AtCAD1 *ATEG_09971*	(KpnI)-pActin-*AtCAD1*-(NsiI) (2629 bp)	(KpnI)-pPTT-(NsiI) (6801 bp)
		(KpnI)-pPTT.Cbx-(NsiI) (5916 bp)
PtACO1' (without exon) *PSEUDOG_3035*	(BsrGI)-pActin-*PtACO1'*-(NsiI) (3495 bp)	(Pfl23II)-pPTT.Cbx-(NsiI) (5905 bp)
PtACO2 *PSEUDOG_2814*	(Pfl23II)-pActin-*PtACO2*-(NsiI) (4257 bp)	(Pfl23II)-pPTT.Cbx-(NsiI) (5905 bp)
LacZ *EG10527*	(KpnI)-pActin-*LacZ*-(PstI) (4174 bp)	(KpnI)-pPTT-(NsiI) (6801 bp)
	(KpnI)-pGAPDH-*LacZ*-(PstI) (4091 bp)	(KpnI)-pPTT-(NsiI) (6801 bp)
	(KpnI)-pHSP70-*LacZ*-(PstI) (4118 bp)	(KpnI)-pPTT-(NsiI) (6801 bp)
	(KpnI)-pTef-*LacZ*-(PstI) (4094 bp)	(KpnI)-pPTT-(NsiI) (6801 bp)
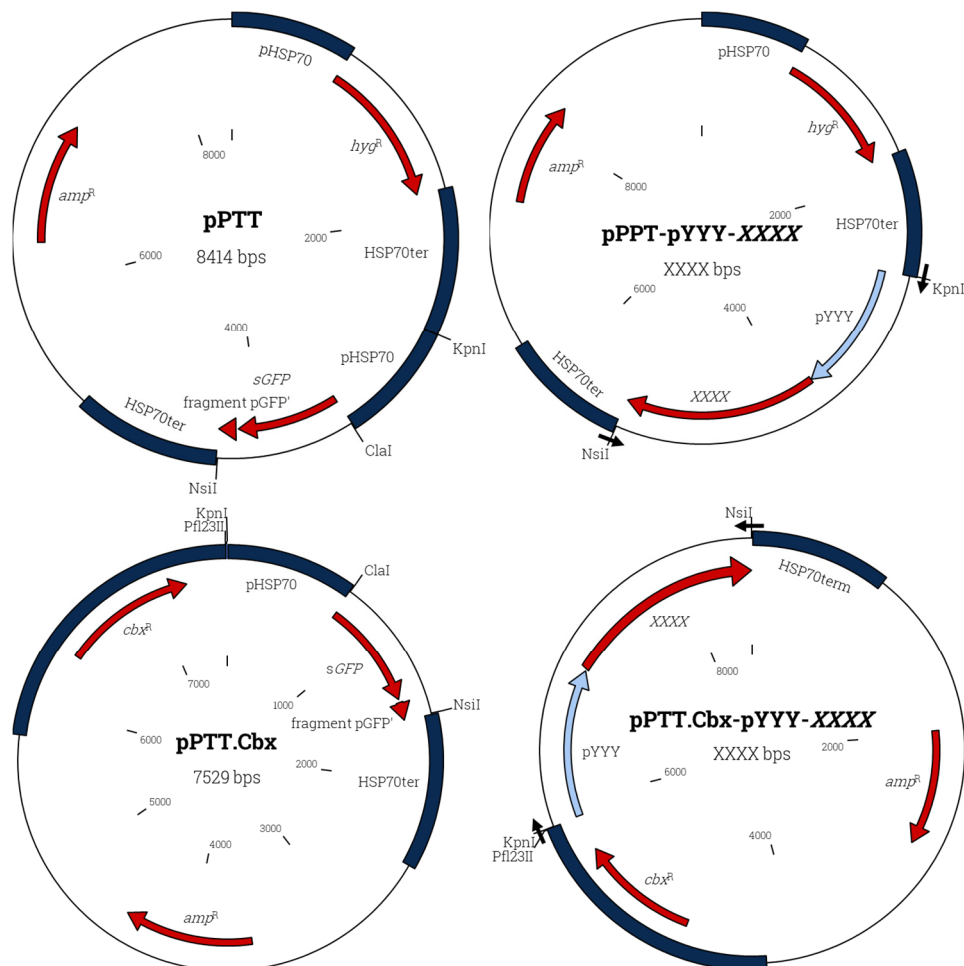
Figure 14 General maps of the original vectors and the resulting overexpression derivatives used in this study.
The plasmids pPTT and pPTT.Cbx are transformation vectors for cloning purposes. The heterologous genes were originally placed under the control of the HSP70 promoter and terminator from *U. maydis* (dark blue boxes). They both contain the ampicillin resistance gene (*amp*[R]) for the selection in *E. coli* and either a hygromycin B resistance cassette (*hyg*[R]) or a carboxin-resistance cassette (*cbx*[R]) for the selection of *P. tsukubaensis* transformants. The resulting overexpression plasmids contain the respective gene (*XXXX*) under the control of one of the four identified promoter sequences (pYYY). Small black arrows on top of the vectors show the primer sites used for colony PCR (for specific primers see table 3).

3.1.5. Screening of overexpression transformants

Previously identified genes which are potentially involved in the ITA pathway in *P. tsukubaensis,* were overexpressed under the control of the native Actin promoter. Those were: *PtADI1*, *PtITP1*, *PtMTT1*, *PtRIA1*, *PtTAD1* and *AtCAD1*. The overexpression in the yeast was accomplished by introducing the whole circular plasmid via PEG-mediated protoplast transformation according to Bodinus (2011); Gillissen et al. (1992); Schulz et al. (1990). The transformants were then selected on hygromycin B containing medium. Subsequently, screening for organic acid production in 3 ml liquid MG-IA cultures was carried out.

First, the effect of additional copies of the *PtMTT1* gene was examined. This gene encodes a putative mitochondrial tricarboxylate carrier protein. It is believed that the gene product Mtt1p transports *cis*-aconitate out of the mitochondrion into the cytosol, where its conversion takes place. By introducing the pActin-*MTT1* overexpression plasmid into the wild type strain H488, a minor increase in ITA production was observed for the majority of transformants. On average 0.2 g l^{-1} ITA were secreted compared to 0.1 g l^{-1} with the wild type. Interestingly, also the amount of MA increased from 2.61 g l^{-1} to 3.43 g l^{-1}.

The overexpression of *PtMTT1* in the M15 strain had a more nuanced effect. The parental strain M15 secreted 2.2 g l^{-1} ITA and 5.0 g l^{-1} MA into the medium. That accounts for an ITA:MA ratio of 30 %. Compared to that, some transformants stopped ITA synthesis altogether (see figure 15). Most transformants produced considerably less amounts of organic acids than the parental strain M15. Four transformants – MM5, MM7, MM8, and MM11 – showed an increase in the proportion of ITA from 30 % to 42 %, 38 %, 38 % and 43 %, respectively. This was interpreted as a sign that an increased *cis*-aconitate transport could facilitate the synthesis of ITA. Although, only few of the M15-transformants tested positive for enhanced ITA production, the MA secretion increased on average to 6.3 g l^{-1} compared to the parent strain (0.1 g l^{-1} ITA).

Figure 15 Screening of *P. tsukubaensis* overexpression transformants for the mitochondrial tricarboxylate transporter Mtt1p.
P. tsukubaensis H488 (WT) and M15 (UV-mutagenized strain for enhanced ITA production established by Bodinus, (2011)) strains were transformed with the pPTT-pActin-*MTT1* plasmid. The resulting transformants and the reference strains (n = 6 for H488 & M15, n = 2 for M15-CAD) were incubated for 10 d in 3 ml well cultures with minimal medium for itaconic acid production (MG-IA) with 15 % (w/v) glucose, 1 g l^{-1} NaNO$_3$, 0.1 g l^{-1} KH$_2$PO$_4$. As buffering agent, a spatulas tip of CaCO$_3$ per well was applied. The cultivation was carried out at 30 °C and 220 rpm.

In general, the overexpression of *PtMTT1* had a positive effect for the synthesis of ITA but also MA. This was true for almost all tested clones with the wild type background. With M15 as the parental strain, the responses varied greatly. The reasons for that observation are still unclear.

In the cytosol, *cis*-aconitate is then isomerised by the protein aconitate-Δ-isomerase into *trans*-aconitate. The intermediate *trans*-aconitate is then decarboxylated into ITA. This reaction is catalysed by the enzyme *trans*-aconitate decarboxylase. The two enzymes are encoded by the genes *PtADI1* and *PtTAD1*, respectively. By overexpressing the two genes separately in the wild type, only three transformants for *PtADI1* and four transformants for *PtTAD1* showed any ITA secretion (see figure 16 & figure 17). During reference cultivation, the wild type strain did not produce any ITA.

The random UV-mutagenized strain M15 produced 8.9 g l^{-1} MA and 2.4 g l^{-1} ITA during reference cultivations. The majority of generated transformants with the M15 background did not produce detectable concentrations of ITA. Collectively five of all transformants secreted diminishable ITA amounts, well below 0.2 g l^{-1}. Consequently, neither the overexpression of *PtADI1*, nor *PtTAD1* had a significantly positive effect on the ITA production behaviour.
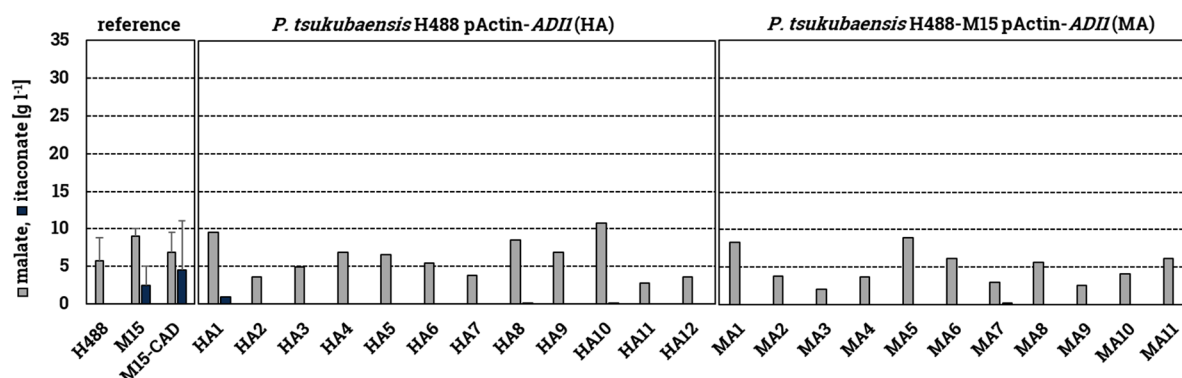
Figure 16 Screening of *P. tsukubaensis* overexpression transformants for the aconitate-Δ-isomerase Adi1p.
P. tsukubaensis H488 (WT) and M15 (UV-mutagenized strain for enhanced ITA production, Bodinus, (2011)) strains were transformed with the pPTT-pActin-*ADII* plasmid. The resulting transformants and the reference strains (n = 4 for H488 & M15, n = 2 for M15-CAD) were incubated for 10 d in 3 ml-well cultures with minimal medium for itaconic acid production (MG-IA) with 15 % (w/v) glucose, 1 g l^{-1} NaNO$_3$, 0.1 g l^{-1} KH$_2$PO$_4$. As buffering agent, a spatulas tip of CaCO$_3$ per well was applied. The cultivation was carried out at 30 °C and 220 rpm.
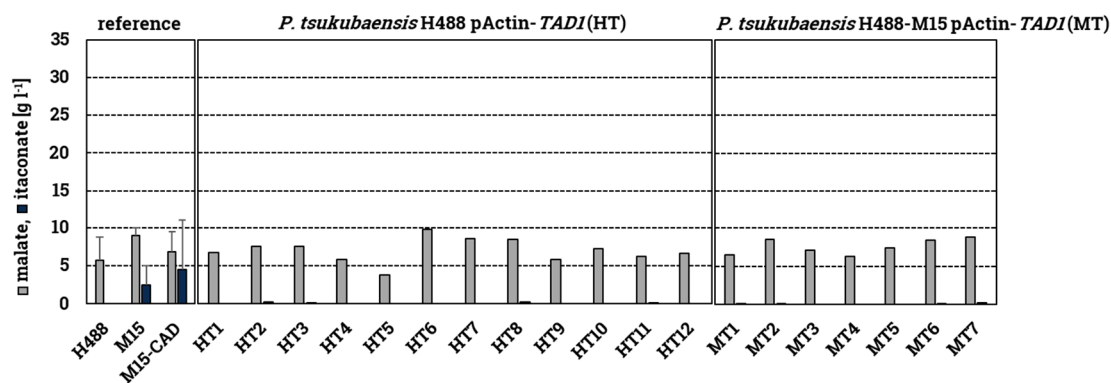
Figure 17 Screening of *P. tsukubaensis* overexpression transformants for the *trans*-aconitate decarboxylase Tad1p.
P. tsukubaensis H488 (WT) and M15 (UV-mutagenized strain for enhanced ITA production, Bodinus, (2011)) strains were transformed with the pPTT-pActin-*TAD1* plasmid. The resulting transformants and the reference strains (n = 4 for H488 & M15, n = 2 for M15-CAD) were incubated for 10 d in 3 ml-well cultures with minimal medium for itaconic acid production (MG-IA) with 15 % (w/v) glucose, 1 g l^{-1} NaNO$_3$, 0.1 g l^{-1} KH$_2$PO$_4$. As buffering agent, a spatulas tip of CaCO$_3$ per well was applied. The cultivation was carried out at 30 °C and 220 rpm.

The so generated ITA is then exported out of the cell into the surrounding medium with the help of the itaconic acid transporter, whose protein is encoded by *PtITP1*. Overexpression of *PtITP1* had little to no effect on the *P. tsukubaensis* wild type strain H488. Six transformants exhibited a marginal ITA increase in the ITA:MA ratio from 3 % (wild type) to 8-13 % (see figure 18). The *PtITP1*-overexpression led to a decrease in ITA production for most of the M15 transformants. However, the transformants MI8, MI9 and MI11 showed a substantial increase in the amount of ITA. With a shift in the ITA:MA ratio from 30 % (M15 strain) to 59 %, 59 % and 52 %, respectively, the main product became ITA. These results indicate that the overexpression of *PtITP1* alone does not lead to enhanced ITA synthesis. When other factors are also in effect, e.g. unknown changes in the genome of strain M15, additional Itp1p activity could help bypass a potential bottleneck and thus ultimately elevate ITA secretion.
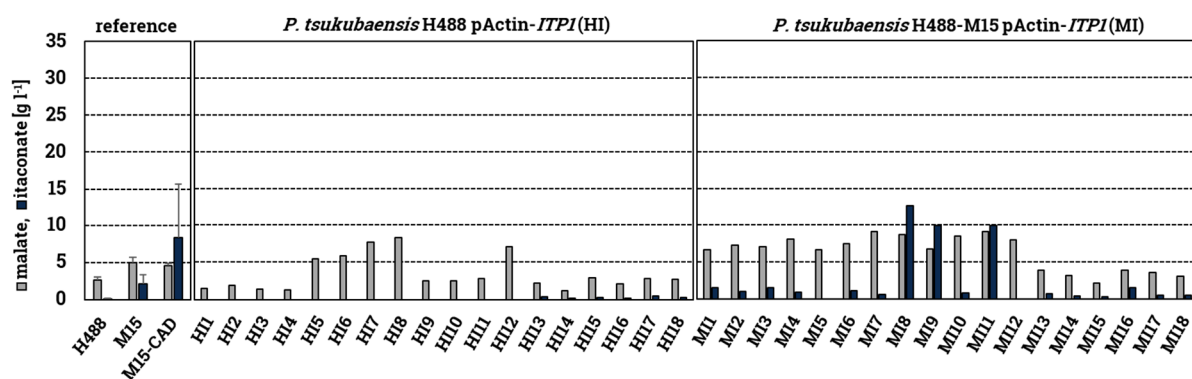
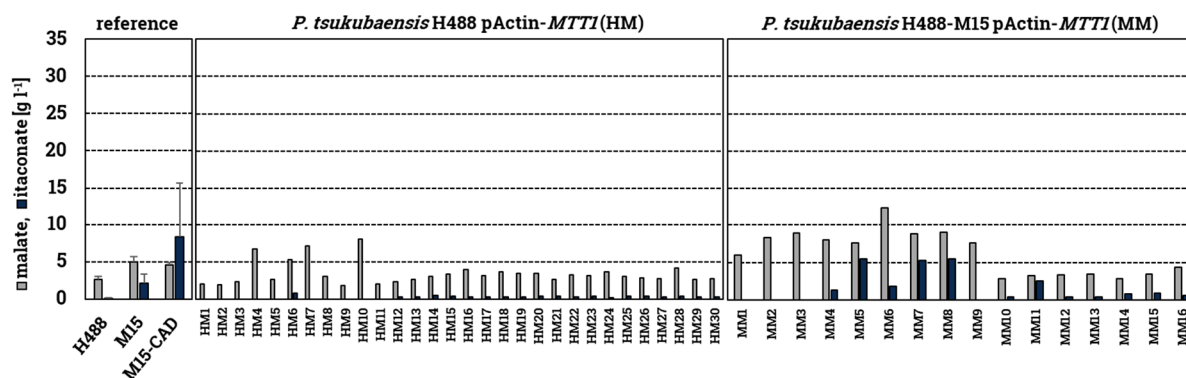**Figure 18 Screening of *P. tsukubaensis* overexpression transformants for the itaconate transport protein Itp1p.**
P. tsukubaensis H488 (WT) and M15 (UV-mutagenized strain for enhanced ITA production, Bodinus, (2011)) strains were transformed with the pPTT-pActin-*ITP1* plasmid. The resulting transformants and the reference strains (n = 6 for H488 & M15, n = 2 for M15-CAD) were incubated for 10 d in 3 ml-well cultures with minimal medium for itaconic acid production (MG-IA) with 15 % (w/v) glucose, 1 g l^{-1} NaNO$_3$, 0.1 g l^{-1} KH$_2$PO$_4$. As buffering agent, a spatulas tip of CaCO$_3$ per well was applied. The cultivation was carried out at 30 °C and 220 rpm.

The four above mentioned genes and *PtRIA1* are organized in a cluster. The whole cluster is believed to be regulated by Ria1p. ITA production was strongly affected by overexpressing this potential transcription factor. Figure 19 shows that for 13 out of 21 tested transformants drastic increases in the amount of ITA were observed, when compared to the parental wild type strain. Similar results were achieved with *PtRIA1*-overexpression in the M15 strain. During the reference cultivation, the parental strain secreted 21 % ITA (ITA:MA). This ITA:MA ratio increased for the 13 transformants up to 98 %. Overall highest productivities achieved clones 'HR12' and 'MR2' with 31.4 g l^{-1}; 33.4 g l^{-1} ITA and only 0.7 g l^{-1}, 1.1 g l^{-1} MA (ITA:MA ratio: 98 %, 97 %), respectively.
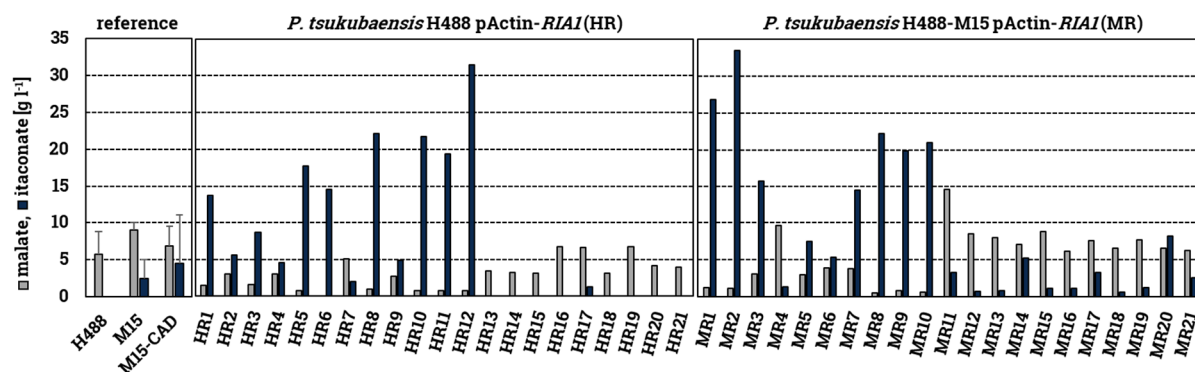
Figure 19 Screening of *P. tsukubaensis* overexpression transformants for the regulator protein of itaconic acid biosynthesis Ria1p.
P. tsukubaensis H488 (WT) and M15 (UV-mutagenized strain for enhanced ITA production, Bodinus, (2011)) strains were transformed with the pPTT-pActin-*RIA1* plasmid. The resulting transformants and the reference strains (n = 6 for H488 & M15, n = 2 for M15-CAD) were incubated for 10 d in 3 ml-well cultures with minimal medium for itaconic acid production (MG-IA, with 15 % (w/v) glucose, 1 g l^{-1} NaNO$_3$, 0.1 g l^{-1} KH$_2$PO$_4$). As buffering agent, a spatulas tip of CaCO$_3$ per well was applied. The cultivation was carried out at 30 °C and 220 rpm.

Regarding the screening process of the constructed overexpression transformants, it is obvious that the protein Ria1p plays an integral part in the metabolic pathway of ITA in *P. tsukubaensis*. Not only was the product ratio shifted drastically in favour of ITA, the total amount of secreted acids was also considerably increased.

The three-best performing transformants for each initial strain were then cultivated in larger culture volumes to confirm their acid production capabilities. After 4 d of cultivation, two transformants, HR12 and MR2, showed similar elevated production rates as in the previous screening. MR2 secreted 12.8 g l^{-1} ITA with a product ratio of 75 % (ITA:MA). During the same period, 19.3 g l^{-1} ITA and 0.6 g l^{-1} MA were synthesised by transformant HR12 (see figure 19 and figure 20). This corresponds to a product ratio of 97 %. This ITA:MA ratio is completely in accordance with the results obtained during the small volume screening. It is not only remarkable, that HR12 produced the highest concentration of ITA with only diminishable amounts of MA. It also did so with a significantly lower cell density than all other *RIA1*-overexpression transformants. The reason for the decrease in biomass could be a result of the heightened organic acid secretion itself as cell growth is potentially slowed down as a consequence of the steady accumulation of the weak organic acid in the medium.

P. tsukubaensis H488 pActin-RIA1 (HR) P. tsukubaensis H488 pActin-RIA1 (HR)
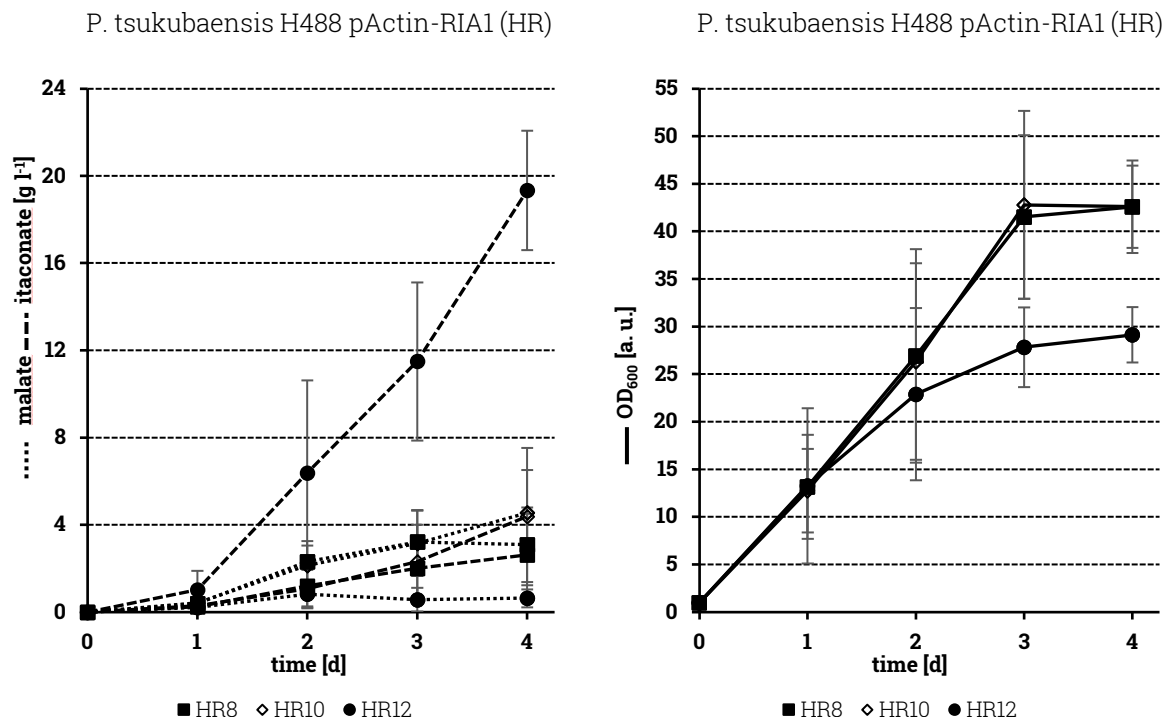
Figure 20 Screening of the three highest ITA producing *P. tsukubaensis* H488 overexpression transformants for the regulator protein of itaconic acid biosynthesis Ria1p.
The previously identified ITA producing transformants HR8, HR10 and HR12 were incubated for 4 d in 50 ml well cultures with minimal medium for itaconic acid production (MG-IA, with 15 % (w/v) glucose, 2 g l^{-1} NaNO$_3$, 0.1 g l^{-1} KH$_2$PO$_4$). The cultivation was carried out in 500 ml baffled flasks at 30 °C and 220 rpm. The medium was kept at a neutral pH with 3.3 g l^{-1} CaCO$_3$. Shown are the mean values and error bars for standard deviation (n = 3).

P. tsukubaensis H488-M15 pActin-RIA1 (MR) P. tsukubaensis H488-M15 pActin-RIA1 (MR)
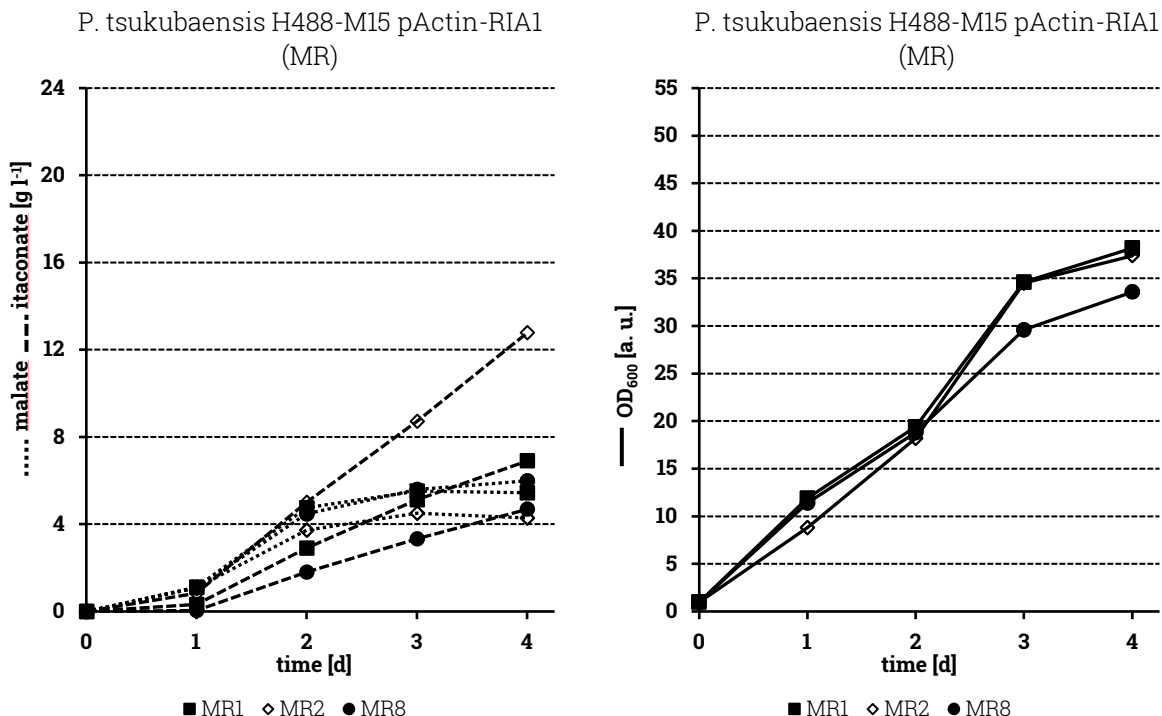
Figure 21 Screening of the three highest ITA producing *P. tsukubaensis* M15 overexpression transformants for the regulator protein of itaconic acid biosynthesis Ria1p.
The previously identified ITA producing transformants MR1, MR2 and MR8 were incubated for 4 d in 50 ml-well cultures with minimal medium for itaconic acid production (MG-IA, with 15 % (w/v) glucose, 2 g l^{-1} NaNO$_3$, 0.1 g l^{-1} KH$_2$PO$_4$). The medium was kept at a neutral pH with 3.3 g l^{-1} CaCO$_3$. The cultivation was carried out in 500 ml-baffled flasks at 30 °C and 220 rpm.

With ITA:MA ratios ranging from 44 % to 56 %, the remaining four transformants (HR8, HR10, MR1 & MR8) still produced proportionately more than it would have been expected for their parental strains. This is especially true for transformants HR8 and HR10. The two transformants secreted 2.6 g l^{-1} and 4.4 g l^{-1} ITA, respectively. Figure 9 shows that their initial strain, H488, produced mainly 2.4 g l^{-1} MA with only 1.4 g l^{-1} ITA (ITA:MA: 37 %) under the same conditions. It is still unclear, why those four transformants performed considerably different than in 3 ml-cultures. One simple explanation would be differences of the physical aspects between the two cultivation methods. Especially aeration is greatly reduced in wells compared to baffled shaking flasks. However, differences in the regulation of the ITA cluster could also play a role.

Based on this data, transformant HR12 represents an improved ITA synthesising yeast strain. Because of its stable and exceedingly high productivity rate, HR12 was chosen as a suitable candidate for subsequent analyses.

In the fungus *A. terreus, cis*-aconitate is directly converted into ITA. The isomerization step of *cis*-aconitate into *trans*-aconitate is omitted. The direct decarboxylation step of *cis*-aconitate is catalysed by the gene product of *AtCAD1*. This reaction appears to be more resourceful in the ITA metabolism, since it is a single step reaction by only one enzyme. This is why, *AtCAD1* overexpressing *P. tsukubaensis* strains have been constructed. Figure 22 shows the ITA production behaviour of the screened transformants.

With the *P. tsukubaensis* M15 background no significant increase in ITA production was achieved (see figure 22). The parental strain secreted 2.9 g l^{-1} ITA with a ratio of 40 %. Only transformants MC11 (46 %) and MC12 (48 %) secreted proportionately more ITA but the overall acid production was greatly reduced. The *AtCAD1*-overexpression in the wild type strain, however, led to noticeable rises in the ITA:MA ratios. For 14 out of the 18 tested transformants, the ITA:MA ratio surpassed the values obtained with the parental strain H488 (7 %). Transformants HC16 and HC17 even synthesised ITA as their main product (HC16: 2.2 g l^{-1} ITA, 1.1 g l^{-1} MA; HC17: 2.6 g l^{-1} ITA, 1.2 g l^{-1} MA). According to this data, it appeared that it depended on the genetic make-up of the *P. tsukubaensis* strain whether the introduction of this heterologous gene is beneficial or not. It is possible that in strain M15 the activity of *PtADI1* and *PtTAD1* is already elevated and therefore the AtCad1p protein would compete with PtAdi1p and PtTad1p for the precursors of ITA e.g. *cis*-aconitate. This was certainly not the case in the wild type, since it naturally produces marginal amounts of ITA.

Figure 22 Screening of *P. tsukubaensis* overexpression transformants for the *trans*-aconitate decarboxylase from *A. terreus*, Cad1p.

P. tsukubaensis H488 (WT) and M15 (UV-mutagenesis strain for enhanced ITA production, Bodinus, (2011)) strains were transformed with the pPTT-pActin-*AtCAD1* plasmid. The resulting transformants and the reference strains (n = 6 for H488 & M15) were incubated for 10 d in 3 ml well cultures with minimal medium for itaconic acid production (MG-IA, with 15 % (w/v) glucose, 1 g l^{-1} NaNO$_3$, 0.1 g l^{-1} KH$_2$PO$_4$). As buffering agent, a spatula's tip of CaCO$_3$ per well was applied. The cultivation was carried out at 30 °C and 220 rpm.

3.1.5.1. Screening of co-overexpression transformants

Results from the above-mentioned screening for *PtMTT1*-overexpression transformants gave rise to the question whether the export of *cis*-aconitate represents a bottleneck during the synthesis of ITA. To further investigate that hypothesis, the clones HM14 and MM11 were selected because these two transformants showed the largest increase in ITA production. An additional overexpression plasmid for *AtCAD1* was then introduced into HM14 and MM11. This way, it was ensured that not only the transport **or** the conversion of *cis*-aconitate was enhanced. Thus, another complete metabolic pathway for the synthesis of ITA was recreated in the yeast *P. tsukubaensis*.

Although, the productivity rates were low for the resulting transformants HoMoC and MoMoC, a more apparent effect of the two overexpressions was discernible. Figure 23 illustrates that by co-overexpressing *PtMTT1* and *AtCAD1*, essentially all of the transformants showed an increase in the detected ITA compared to the strains with only the overexpressed mitochondrial carrier (see figure 23). The parental strains, HM14 and MM11 displayed an ITA:MA ratio of 28 % and 54 %, respectively. Transformants with the H488 background produced 30-66 % ITA (ITA:MA) and even 53-75 % with the M15 background. This also represented a proportionately higher ITA production than the transformants with only the overexpressed *AtCAD1* gene. It is therefore evident that an elevated mitochondrial tricarboxylate transporter activity is needed for enhanced ITA synthesis. Identifying the export of *cis*-aconitate into cytosol as a bottleneck, is an important finding.
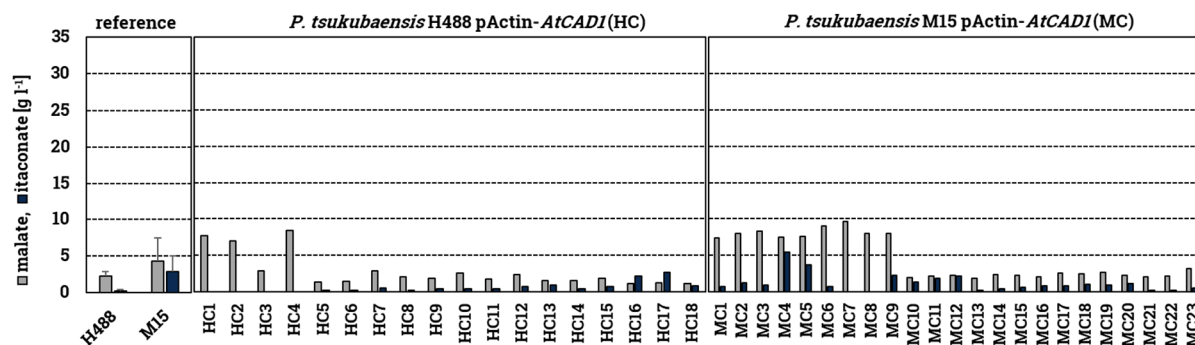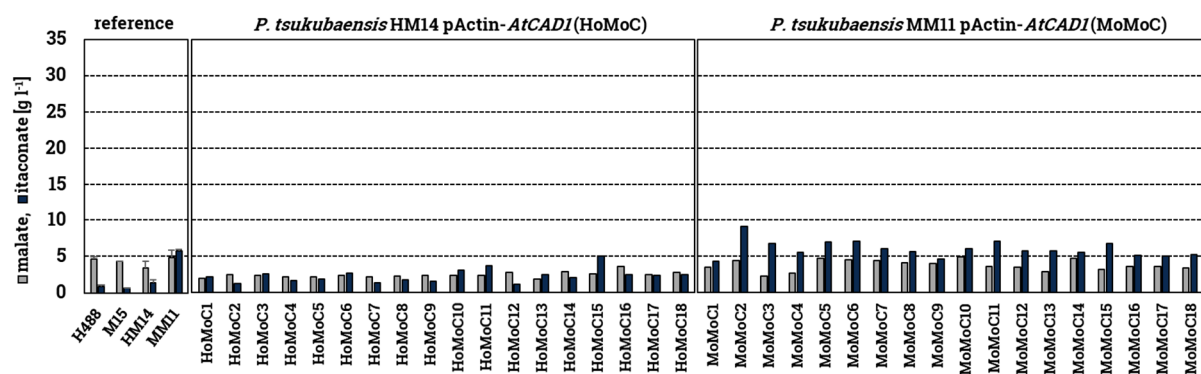
Figure 23 Screening of *P. tsukubaensis* overexpression transformants (HoMoC and MoMoC) for the *trans*-aconitate decarboxylase from *A. terreus*, Cad1p.

P. tsukubaensis PtMTT1-overexpression strains HM14 (background: H488 (WT)) and MM1 (background: M15, Bodinus, (2011)) strains were transformed with the pPTT.Cbx-pActin-*AtCAD1* plasmid. The resulting transformants and the reference strains (n = 2 for H488, M15, HM14 & MM11) were incubated for 10 d in 3 ml well cultures with minimal medium for itaconic acid production (MG-IA, with 15 % (w/v) glucose, 1 g l^{-1} NaNO$_3$, 0.1 g l^{-1} KH$_2$PO$_4$). As buffering agent, a spatula's tip of CaCO$_3$ per well was applied. The cultivation was carried out at 30 °C and 220 rpm.

Another topic of interest was, if the enhanced capabilities of strain *P. tsukubaensis* HR12 for its ITA production could be increased any further. The main precursor of ITA is *cis*-aconitate. This main intermediate of the TCA is formed by the dehydration of CA or ICA. The reaction is catalysed by an aconitase or more specifically an aconitate hydratase. Previously, the two genes *PSEUDOG_3035* and *PSEUDOG_2814* were identified in *P. tsukubaensis* H488 to putatively code for aconitase enzymes. The genes were thus named *PtACO1* and *PtACO2*, respectively. Accordingly, overexpression plasmids for the two genes under the control of the strong Actin promoter were constructed and introduced into the ITA overproducing strain HR12.
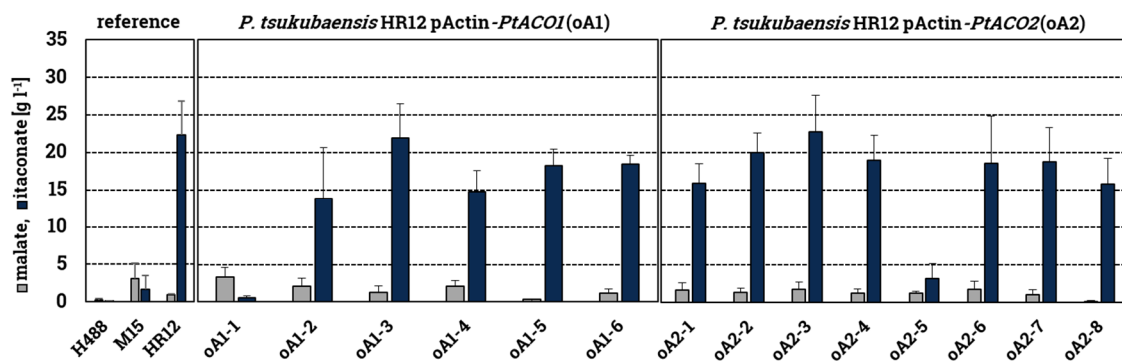
Figure 24 Screening of *P. tsukubaensis* overexpression transformants (oA1 and oA2) for the native aconitase enzymes, PtAco1p and PtAco2p.

P. tsukubaensis PtRIA1-overexpression strain HR12 (background: H488 (WT)) was transformed with either the pPTT.Cbx-pActin-*PtACO1*-Ex (does not contain the naturally occurring intron) or with the pPTT.Cbx-pActin-*PtACO2* plasmid. The resulting transformants, oA1, oA2 and the reference strains were incubated for 10 d in 3 ml-well cultures with minimal medium for itaconic acid production (MG-IA, with 15 % (w/v) glucose, 1 g l^{-1} NaNO$_3$, 0.1 g l^{-1} KH$_2$PO$_4$). The cultivation was carried out at 30 °C and 220 rpm. As buffering agent, a spatula's tip of CaCO$_3$ per well was applied. Shown are the averages and error bars for standard deviation (n = 4).

Figure 24 shows that the resulting transformants did not show an increase in ITA production compared to strain HR12. Transformants oA1-5 and oA2-8 exhibited a minor rise in the ITA:MA ratio. However, this was accompanied by a decline in the final ITA concentration. The reference

strain HR12 produced 22.3 g l^{-1} ITA (ITA:MA: 96 %) after 10 d of cultivation, while oA1-5 and oA2-8 secreted 18.3 g l^{-1} ITA (ITA:MA: 98 %) and 15.8 g l^{-1} ITA (ITA:MA: 99 %), respectively.

Consequently, it can be assumed that the conversion of CA to *cis*-aconitate by an aconitase does not represent a rate-limiting step in the synthesis of ITA in this overproducing strain HR12. Furthermore, the elevated levels of MA are potentially due to the elevated aconitase activity and the resulting increased ICA concentrations inside the mitochondrion. The Aco1p/Aco2p enzyme may compete with the Mtt1p transporter for *cis*-aconitate. After *cis*-aconitate is converted to ICA, it is further metabolized into MA in the course of the TCA cycle. Ultimately, this is unfavourable to produce ITA because it lowers the productivity and final yield.

3.1.6. Characterization of strain HR12

During the screening process of different overexpression transformants, *P. tsukubaensis* strain HR12 proved to be the most reliable and active ITA producer. Since the integration most probably took place because of heterologous recombination events between the genomic DNA and the vector DNA, the locus of integration for the overexpression plasmid cannot be determined beforehand. To gain more insight, into how the introduction of the whole pPTT-pActin-*RIA1* plasmid led to the changes in the phenotype, the genomic DNA of strain HR12 was sequenced.

In doing so, the sequencing showed that the regulator gene for ITA, *PtRIA1* under the control of the strong constitutive pActin promoter was integrated two times in tandem orientation with parts of the vector backbone (see figure 25). The first copy consists of 82.2 % of the overexpression plasmid (1627-9167 bp) and the second 85.1 % (1-7804 bp). Integration of the two vector fragments occurred on strain H488's scaffold 9 in the ORF of *PSEUDOG_4086* while deleting an approximately 34 kb long sequence. Thus, the ORF of *PSEUDOG_4086* was disrupted and nine other ORFs, *PSEUDOG_4087-PSEUDOG_4095*, were deleted.
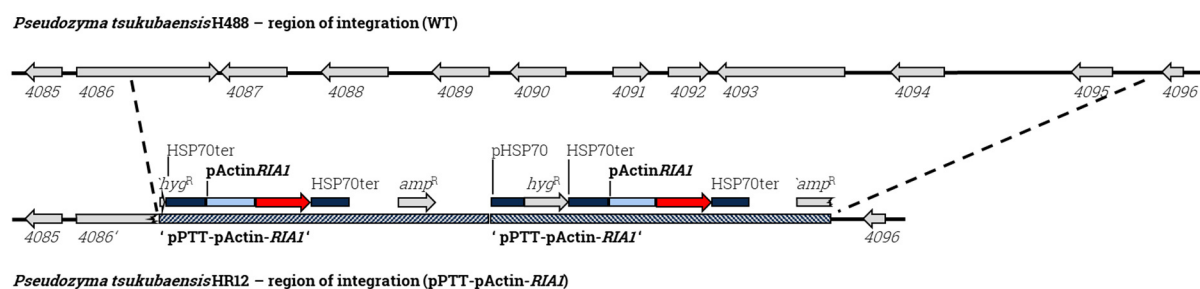
Figure 25 Comparison between the genomic locus where the integration of the plasmid pPTT-pActin-*RIA1* in strain HR12 took place and the corresponding region in *P. tsukubaensis* H488.
Large parts of the plasmid integrated two times in tandem orientation between gene *PSEUDOG_4086* and *PSEUDOG_4096*. *PSEUDOG_4086* got partially disrupted (tattered box). The genes PSEUDOG_4087-4095 were completely deleted. The dashed lines represent the region of the integration. Grey arrows mark ORFs. Dark blue boxes represent the HSP70 promoter and terminator sequences from *U. maydis* that were used for the construction of the plasmid. The native Actin promoter is marked by a light blue box and the *PtRIA1* gene by a red arrow.

The translational products of the affected genes were subsequently analysed using BLASTP and the NCBI non redundant database. The identified homologous proteins of *U. maydis* 521 and other organisms are summarized in table 21. Four targets are still uncharacterized or hypothetical proteins with no known functions (encoded by *PSEUDOG_4088, 4090, 4094* and *4095*). However, six proteins could be classified as a potential acetyl-CoA-synthetase, alcohol dehydrogenase, aldo/keto reductase, 2-deoxy-D-gluconate 3-dehydrogenase, adenylate kinase, and a potassium channel, respectively.

Considering the current knowledge, the identified genes play no direct role in the biosynthesis of ITA. It is unclear, whether their deletion had an (immediate) effect on certain metabolic pathways or underlying regulatory mechanisms that could have resulted in the rerouting of intermediates towards ITA.

Table 21 List of *P. tsukubaensis* genes deleted by the overexpression of *PtRIA1* and their homologs in *U. maydis* 521 and other microorganisms.

The deduced protein sequences resulting from genes *PSEUDOG_4086-4095* were analysed by BLASTP against the whole nonredundant NCBI database. Shown are the homologous gene products with aa identity, query coverage (values in brackets) and the Expected value. Also given are the respective lengths of the deduced protein sequences (number of aa) and the predicted molecular weight (MW). Molecular weights were estimated with the ProtParam tool (https://web.expasy.org/protparam/). Put. - putative

P. tsukubaensis gene	deduced protein	homologous gene	deduced protein	identity E-value
PSEUDOG_4086	767 aa 85.0 kDa	*U. maydis* hypothetical protein *UMAG_02235* gene ID: 23563034	602 aa 66.9 kDa	85 % [78 %] 0.0
		Moesziomyces antarcticus putative acetyl-CoA synthetase *PAN0_008d3441* gene ID: 26304376	602 aa 66.5 kDa	86 % [78 %] 0.0
PSEUDOG_4087	510 aa 54.7 kDa	*U. maydis* put. alcohol dehydrogenase *UMAG_10077* gene ID: 23566151	510 aa 54.8 kDa	90 % [99 %] 0.0
		Pseudozyma hubeiensis SY62 alcohol dehydrogenase *PHSY_002011* gene ID: 24107306	743 aa 81.1 kDa	91 % [99 %] 0.0
PSEUDOG_4088	513 aa 54.3 kDa	*U. maydis* hypothetical protein *UMAG_12316* gene ID: 23568061	503 aa 53.2 kDa	78 % [84 %] 0.0
		Moesziomyces antarcticus conserved hypothetical protein *PAN0_008c3437* gene ID: 26304231	497 aa 52.9 kDa	74 % [98 %] 0.0
PSEUDOG_4089	283 aa 31.7 kDa	*U. maydis* hypothetical protein *UMAG_02151* gene ID: 23562965	286 aa 32.0 kDa	81 % [99 %] $2 \times e^{-173}$
		Moesziomyces antarcticus aldo/keto reductase *PAN0_008c3436* gene ID: 26304230	284 aa 31.5 kDa	87 % [98 %] 0.0
PSEUDOG_4090	428 aa 44.9 kDa	*U. maydis* hypothetical protein *UMAG_02238* gene ID: 23563037	399 aa 42.3 kDa	48 % [84 %] $5 \times e^{-97}$
		Sporisorium reilianum SRZ2 conserved hypothetical protein *sr13433* ID: FQ311470.1	408 aa 41.8 kDa	50 % [89 %] $4 \times e^{-117}$
PSEUDOG_4091	280 aa 29.2 kDa	*U. maydis* put. 2-deoxy-D-gluconate 3-dehydrogenase *UMAG_05923* gene ID: 23565673	278 aa 29.1 kDa	89 % [99 %] 0.0

		Moesziomyces antarcticus NAD(P)-binding protein *PAN0_008d3433* gene ID: 26304374	280 aa 29.3 kDa	89 % [99 %]
				0.0
PSEUDOG_4092	247 aa 27.6 kDa	*U. maydis* putative adenylate kinase *UMAG_05924* gene ID: 23565674	288 aa 31.8 kDa	75 % [98 %]
				8 x e^{-131}
		Moesziomyces antarcticus adenylate kinase *PAN0_008d3432* gene ID: 26304373	288 aa 31.9 kDa	82 % [99 %]
				3 x e^{-152}
PSEUDOG_4093	975 aa 107.0 kDa	*U. maydis* hypothetical protein *UMAG_05925* gene ID: 23565675	928 aa 101.3 kDa	65 % [94 %]
				0.0
		Moesziomyces antarcticus voltage-gated potassium channel *PAN0_008c3431* gene ID: 26304227	1302 aa 143.2 kDa	65 % [93 %]
				0.0.
PSEUDOG_4094	411 aa 46.3 kDa	*U. maydis* hypothetical protein *UMAG_05926* gene ID: 23565676	332 aa 38.2 kDa	35 % [56 %]
				4 x e^{-26}
		Ustilago bromivora uncharacterized protein *UBRO_20380* ID: LT558125.1	947 aa 103.4 kDa	30 % [57 %]
				9 x e^{-27}
PSEUDOG_4095	313 aa 35.2 kDa	*U. maydis* hypothetical protein *UMAG_05928* gene ID: 23565678	381 aa 42.4 kDa	31 % [74 %]
				2 x e^{-18}
		Sporisorium reilianum SRZ2 conserved hypothetical *Ustilaginaceae*-specific prot. *sr16552* ID: FQ311470.1	335 aa 37.5 kDa	31 % [75 %]
				4 x e^{-27}

3.1.6.1. Regulation of the ITA cluster in strain HR12

Given that an increased ITA production was observed in *P. tsukubaensis* HR12, it was expected that at least some of the genes of the ITA-cluster would be upregulated. After the extent of the integration event on the DNA level was compiled, it was then important to understand how this affected the regulation of the gene cluster because alone, the introduction of additional copies of the regulator gene RIA1 under the control of the constitutive and strong Actin promoter did not necessarily imply an increased transcription of all genes involved in the synthesis of ITA. To gain this knowledge, quantitative real-time PCR (qPCR) was conducted. The results of the qPCR provided the evidence that, in fact, all of the five ITA cluster genes are highly upregulated in strain HR12 compared to the wild type H488 (see figure 26).

The overexpressed *PtRIA1* gene itself displayed a 473-fold increase in the transcription rate in strain HR12 compared to H488. This was followed by a 4766-fold higher transcription rate of gene *PtMTT1* than in the wild type. The expression of the genes encoding the two metabolic enzymes Adi1p and Tad1p both experienced an approximate 2700-fold upregulation. Compared to the other cluster genes, the expression of *PtITP1* was elevated 65-fold. That upregulation appears to be much lower, but it should be noted that the transcription rate for *PtITP1* was already relatively elevated in strain H488 (*PtITP1* showed a 4 to 69-fold higher transcription rate than the other cluster genes in strain H488 – data not shown).
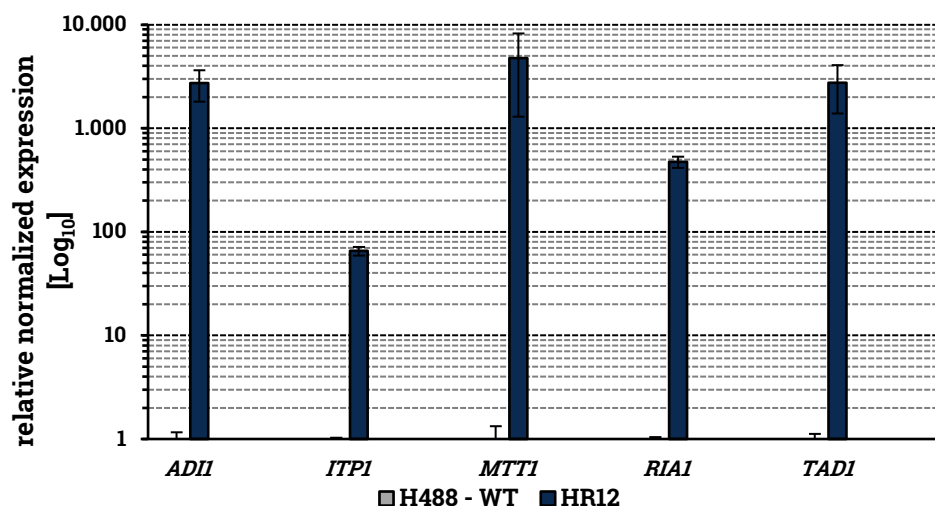
Figure 26 Result of quantitative real-time PCR for the relative transcription rate of the itaconic acid cluster genes in *P. tsukubaensis* HR12 compared to the wild type, H488.
The cells were grown in minimal medium with 15 % (w/v) glucose for itaconic acid production (MG-IA) until an OD_{600} of 2 to 3 was reached. The elongation factor-1 (*PtEF1*) and the ubiquitin-conjugating enzyme (*PtUBC6*) were used as reference genes. Expression levels in HR12 were normalized for H488 expression levels. n = 2, error bars show standard deviation

3.1.6.2. Relationship between nitrogen, phosphate and the production of ITA

P. tsukubaensis strains H488 and M15 produced considerable amounts of MA and ITA only under certain substrate-limited conditions. As was shown in section 3.1.1.1, it was important to supply an excess in C source but also limit the N and/or P sources. Both strains displayed a clear pattern, in which the synthesis of ITA was significantly induced when the initial amount of P was very limited and the ratio of N to P was high.

The overproducing *P. tsukubaensis* strain HR12 exhibited an upregulation in the transcription rate of the genes responsible for ITA production. Still, it was not clear, whether there was a remaining control mechanism regulated by the available N and P concentrations in the medium. Therefore, the wild type strain H488 and the production strain HR12 were cultivated in 3 ml well cultures with minimal medium and combinations of different N and P concentrations (the applied concentrations are summarized in table 22). As expected, both strains multiplied according to the available substrate levels. Because P was chosen as the limiting nutrient, lowest cell densities (OD_{600} = 10-13) were reached with 0.01 g l^{-1} P (see figure 27 A). An initial concentration of at least 0.15 g l^{-1} P was enough to reach maximum cell densities of approximately OD_{600} = 35.

Table 22 Concentrations of phosphate and nitrogen source used for 3 ml well cultures of *P. tsukubaensis* H488 and HR12.

MG-IA medium with 15 % (w/v) glucose	
Phosphate [g l^{-1}]	0.01; 0.05; 0.1; 0.15; 0.25; 0.5
Nitrogen [g l^{-1}]	2; 3; 4; 5

The production rate of organic acids for strain H488 was heavily influenced by the available P concentration. Synthesis of MA was immediately induced when P was limited and dropped off if a surplus (> 0.15 g l^{-1} P) was present. The regulation of ITA synthesis in the wild type was more nuanced. For very low P concentrations, the ITA amount was merely above the detection limit. With increasing levels of P, the concentrations of ITA also rose until an optimum of 1 g l^{-1} ITA was reached (P = 0.15 g l^{-1}). After that, ITA production declined heavily with further increasing P concentrations.

P. tsukubaensis strain HR12 showed an induction of MA-synthesis at very low P levels as well. With 0.01 g l^{-1} available P source, an average of 1.0 g l^{-1} MA was secreted into the medium. This value decreased under 0.5 g l^{-1} ITA if higher amounts of P were supplied.

Interestingly, the ITA production was not influenced by P and N concentrations in this strain. Figure 27 B shows that the production of ITA followed the pattern of growth for this strain (note the differing scale of the Z-axis for ITA concentration compared to strain H488). Low densities of cells secreted only 5 g l^{-1} ITA on average. High cell densities amounted for up to 25.7 g l^{-1} ITA in the medium.

A
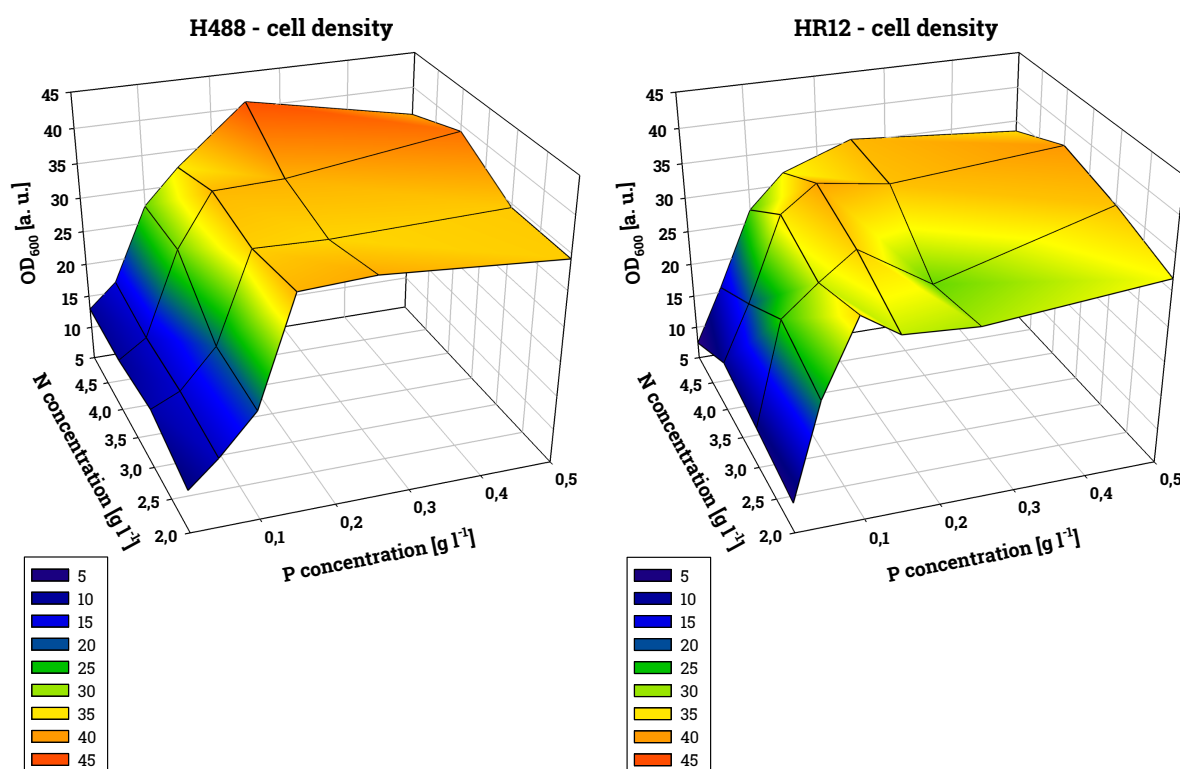
B
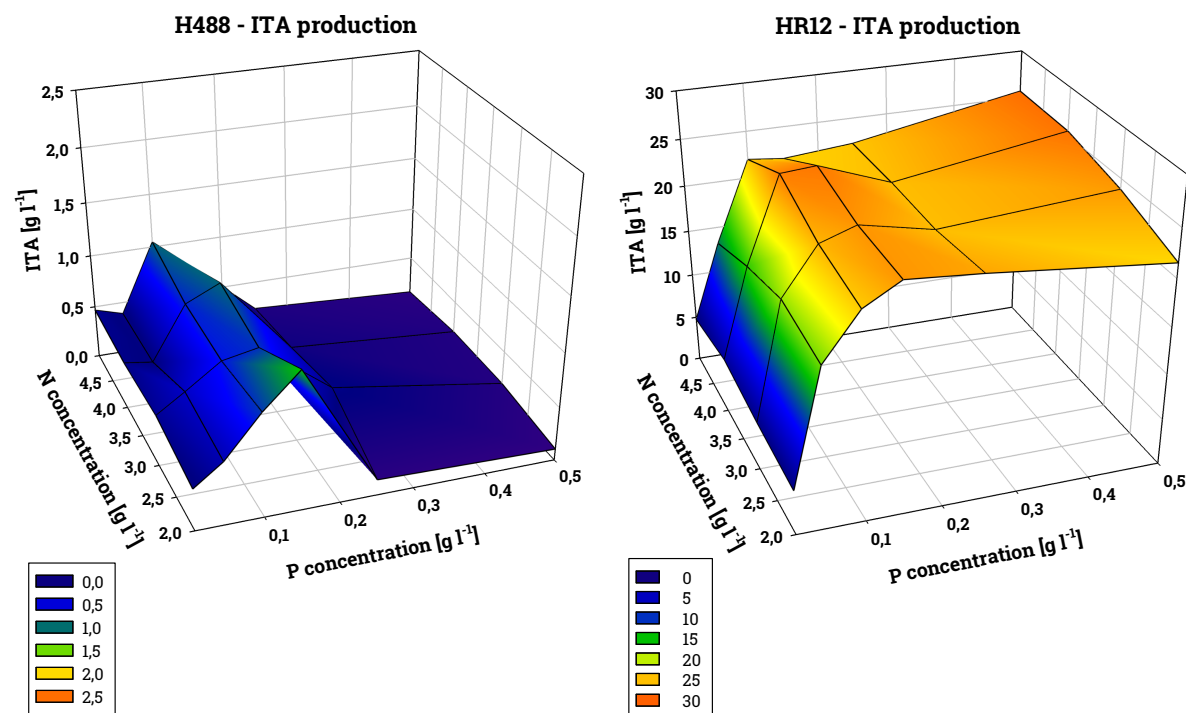
C
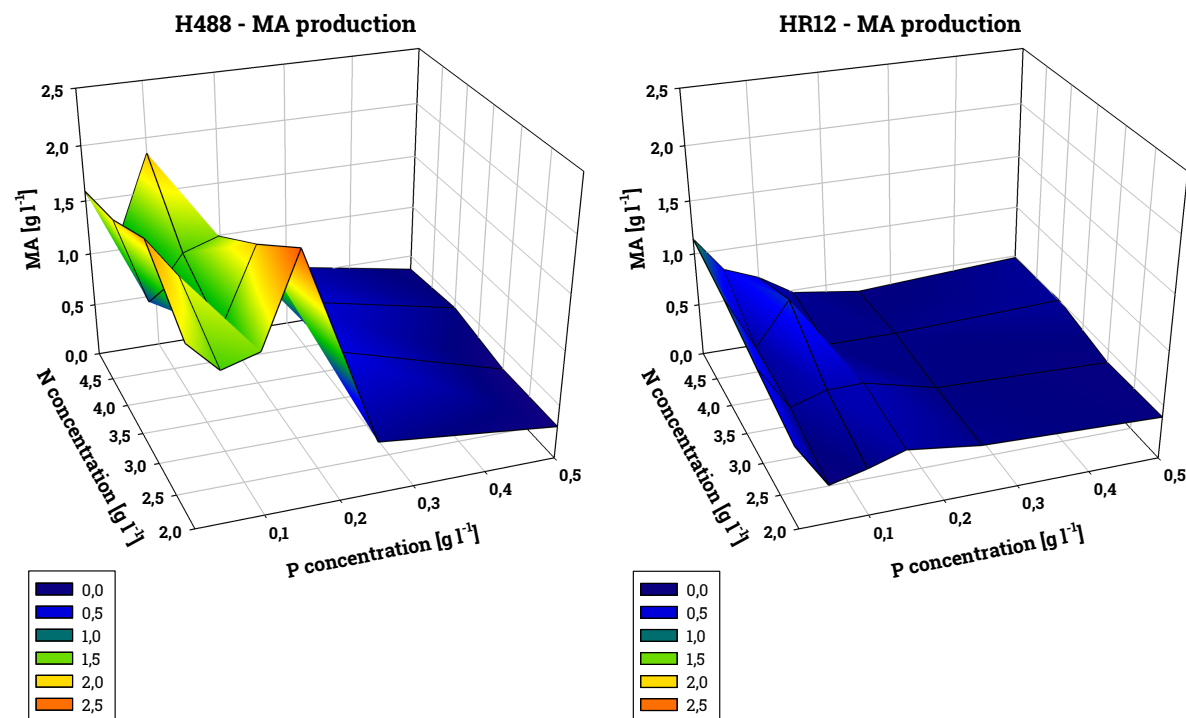
Figure 27 Phosphate and nitrogen dependency for the production of ITA in *P. tsukubaensis* strains H488 (WT) and HR12.

The yeast cells were pre-cultivated in 50 ml liquid cultures with MG-IA medium (15 % (w/v) glucose, 1 g l^{-1} NH$_4$Cl, 0.1 g l^{-1} KH$_2$PO$_4$) for 2 d at 30 °C and 220 rpm. The main cultures were grown in 3 ml wells. Cells of the pre-cultivation were harvested by centrifugation (5 min, 3500 rpm) and washed with sterile water. The wells were inoculated with the cell mass needed for a starting OD$_{600}$ = 1. The medium for the main cultures consisted of minimal medium for ITA production (MG-IA) with 15 % (w/v) glucose and combinations of different N and P concentrations (NH$_4$Cl: 2, 3, 4, 5 g l^{-1}; KH$_2$PO$_4$: 0.01, 0.05, 0.1, 0.15 0.25, 0.5 g l^{-1}). As the buffering agent, a spatulas tip of CaCO$_3$ per well was used. The cells were incubated for 3 d at 30 °C and 220 rpm. A – cell density (OD$_{600}$ at λ = 600 nm) for each N P concentration. B - Concentration of ITA [g l^{-1}] that was measured in the supernatant (note the differing scales of the Z-axis for ITA concentration for the two strains). C – Concentration of detected MA [g l^{-1}]. Values represent the average for three separate cultivations.

3.1.6.3. Alternative substrates for strain HR12

Despite the tremendous upregulation of the complete ITA cluster and the consequential enhanced ITA production, the genomic rearrangement was assessed critically. A significant segment of the genomic DNA, consisting of numerous ORFs, was disrupted. This fact can lead to serious changes in the yeast's phenotype. Such changes can have wide ranging and complex consequences that are difficult to predict.

Acetate is a natural substrate of *P. tsukubaensis*. In order to metabolize acetic acid, the yeast must first activate it by coenzyme A ligation. This ATP-dependent reaction is catalysed by acetyl-CoA synthetase. Similarly, for the utilization of ethanol and other alcohols, it is essential to oxidize these compounds to their corresponding aldehyde. For this NADH generating reaction, alcohol dehydrogenases are essential.

Hence, the deletions of the genes responsible for the putative acetyl-CoA synthetase (*PSEUDOG_4086*) and alcohol dehydrogenase (*PSEUDOG_4087*) in the HR12 strain were deemed critical. These two enzymes could play central roles in the metabolism of different substrates. The lack of these two genes but of the other eight too, could therefore drastically alter the range in possible substrates. This could ultimately have an impact on the applicability of this ITA overproducing strain, since the utilization of alternative substrates to simple sugars (e.g. glucose) are an important factor in the selection of new host organisms. This is because the biotechnological use of mono- and disaccharides competes with the food industry. The selected C sources can often be found as by-products of industrial processes and are from an industrial perspective low-priced. Thus, they represent promising educts for an economically and ecologically viable process.

The *P. tsukubaensis* strain HR12 was hence cultivated on medium containing only acetate or ethanol as the sole C source, to test for changes in the substrate range of this strain. From figure 28 it is apparent, that no impairment in the utilization of any C source was observed. The yeast strain HR12, just like the wild type H488, is able to grow on all substrates tested. Thus, the degradation pathways for ethanol and acetate appeared to be functional in the engineered strain.
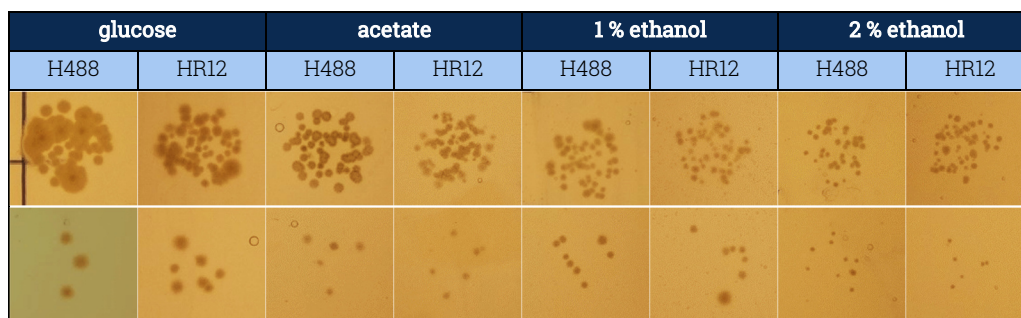
Figure 28 Growth behaviour of *P. tsukubaensis* HR12 and wild type strain H488 on different carbon sources.
Drops of liquid overnight culture with a cell count of 10 or 100 were dripped onto agar plates with minimal medium and either 2 % (w/v) glucose, 30 mM sodium acetate, 1 % (v/v) ethanol or 2 % (v/v) ethanol as the sole carbon source. The plates were incubated for 2 d at 30 °C.

By searching the protein library of *P. tsukubaensis* H488, three proteins were found which could compensate for the loss of function of *PSEUDOG_4086* and *PSEUDOG_4087*: the gene product of *PSEUDO_3222* potentially represents another acetyl-CoA synthetase and, *PSEUDOG_1552* and *PSEUDOG_1699* putatively encode proteins that function as alcohol dehydrogenases. Hence, the activity of these proteins appeared to be sufficient to convert acetate and ethanol and thus supply the metabolic pathways to the utilization of these C sources.

It was nonetheless still unclear whether *P. tsukubaensis* HR12 was still able to grow and produce ITA on C sources other than glucose. The yeast HR12 was therefore grown in liquid minimal medium with D-sucrose, glycerol or D-xylose as the only C source.

Figure 29 illustrates that all of the tested substrates were being used by the yeast HR12 for growth and for the production of ITA. The highest cell densities were reached with glycerol (OD_{600} = 45.6) and glucose as a C source (OD_{600} = 44.8). Despite resulting in the lowest cell density, *P. tsukubaensis* HR12 produced the highest amounts of ITA with sucrose as C source. After 5 d of cultivation, an end-point concentration of 27.9 g l^{-1} ITA was measured. Glucose was equally fast converted into ITA but reached a lower end-concentration of 24.1 g l^{-1}. Potentially because more of the C was used for cell growth or storage in form of lipid bodies or mannosylerythritol lipids (common storage compounds of the genus *Pseudozyma*) than for organic acid production. For xylose and glycerol, the growth and productivity rates were slower compared to glucose. However, at the end of the cultivation, similar concentrations of ITA were reached (24.5 g l^{-1}) with glycerol as with glucose, indicating a slower utilization or an initial metabolic adjustment to glycerol. Growth on xylose was a bit delayed like in the case of glycerol. For xylose, the ITA production was also the overall lowest with 16.9 g l^{-1} after 5 d. The results however are non-significant due to the large standard deviations.

The detected MA concentrations were low for every tested C source. With glucose and sucrose 0.8-0.9 g l^{-1} MA were produced. Interestingly, for xylose and glycerol, even lower concentrations of just 0.2 g l^{-1} MA were detected in the supernatant. The reason for the reduced by-product formation may be a generally slower organic acid synthesis. Glycolysis is generally activated by glucose. Xylose and glycerol must be metabolized over several steps before their intermediates (fructose-1,6-bisphosphate and/or glyceralderhyde-3-phosphate) can enter the last reaction steps of the glycolysis. During these preceding steps, no glucose is formed directly, which potentially leads to an overall lower glycolysis rate.
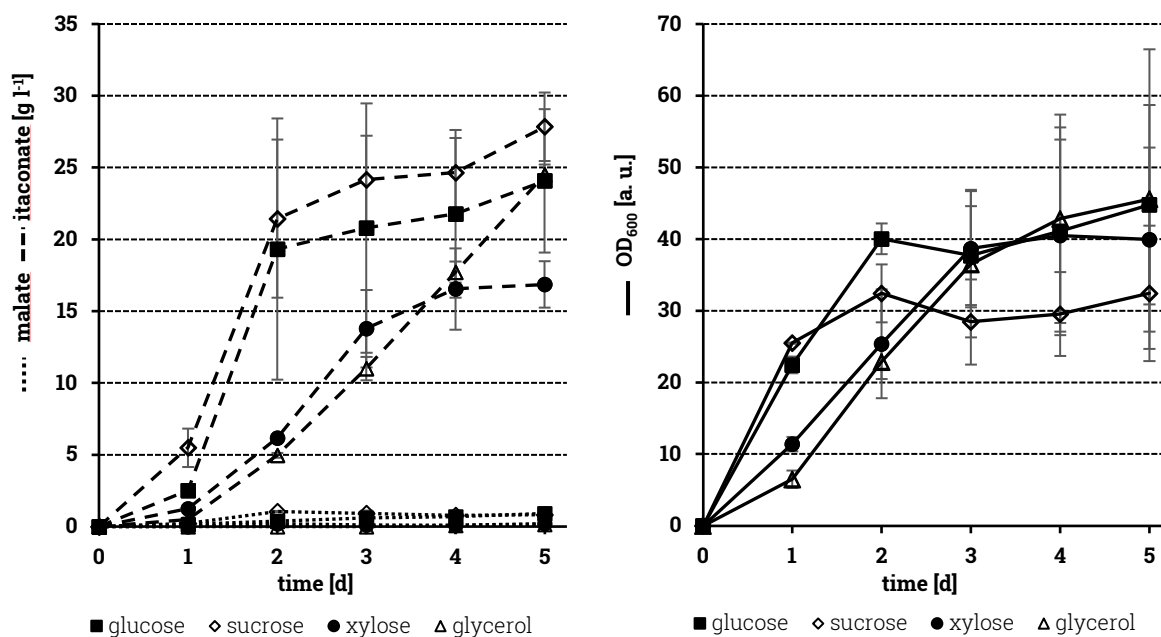
Figure 29 Growth and organic acid (MA and ITA) production behaviour of *P. tsukubaensis* strain HR12 on different carbon sources.
The yeast was pre-cultivated for 2 d in 50 ml YPD full medium at 30 °C and 220 rpm. The main cultures of 50 ml minimal medium for itaconic acid production (NaNO$_3$: 4 g l^{-1}, KH$_2$PO$_4$: 1 g l^{-1}) were inoculated with the cell mass needed for a starting OD$_{600}$ = 1. As C sources, 10 % (w/v) of either D-sucrose, D-xylose, glycerol or glucose (reference) were used. To maintain a neutral pH, 3.3 g l^{-1} CaCO$_3$ was applied. The yeast cells were incubated for 5 d at 30 °C and 220 rpm. Shown are the mean values for two separate cultivations.

3.1.6.4. Production behaviour of *P. tsukubaensis* strains in a 600 ml-bioreactor

The ability of *P. tsukubaensis* for organic acid production has been determined in small to medium volume cultures of 3 and 50 ml. This approach was sufficient to gain first insights into the potential quantities that could be realized with the respective yeast strain. The main disadvantage for basic laboratory scale cultivations was the variability in culture conditions because it was not possible to keep certain factors like pH, oxygen saturation or the temperature at a constant level throughout the complete cultivation duration. Therefore, the two most promising *P. tsukubaensis* strains, M15-CAD and HR12, were chosen and their culture volume scaled up to 600 ml in a bioreactor. In doing so, it was possible to maintain crucial cultivation factors at a constant level, such as oxygen saturation, temperature, and pH for the whole duration of fermentation. Besides simply increasing the culture volume, we were also able to investigate the responses to certain changes in the medium composition or culture conditions more closely.

In 2011, Bodinus established this high achieving ITA producing strain M15-CAD. Here, the cultivation of the yeast strain M15-CAD was carried out in an initial volume of 600 ml in total at a constant temperature of 30 °C. The pH of the medium was maintained at 5.5 or 7.0 and the oxygen saturation at 55 % or 90 %. First, the minimal medium compositions which led to considerable ITA synthesis in the shaking flasks were applied. More specifically, minimal medium with glucose was tested with the three following N:P ratios: 2:0.1; 5:0.1; 4:1.

In tendency, the yeast *P. tsukubaensis* M15-CAD followed a similar pattern to the shaking flask cultures. Highest activity in ITA synthesis was achieved while limiting both the N and P source (N:P = 2:0.1). After 6 d of cultivation, 32.1 g l^{-1} ITA and 0.8 g l^{-1} MA were detected in the culture broth (see figure 30 A). This constituted for a productivity rate of 5.4 g l^{-1}d^{-1} for ITA. The results represented a substantial rise in productivity compared to the shaking flasks where only 3.2 g l^{-1} of ITA were secreted per day. In the course of the fermentation process, 25 % of the glucose was converted into ITA and 11 % into dry cell weight (DCW).

When higher amounts of N source (N:P = 5:0.1) were supplied, the ITA synthesis rate dropped immensely to 1.9 g l^{-1}d^{-1}. The end-concentration amounted to 11.6 g l^{-1} ITA and 0.5 g l^{-1} MA after a period of 6 d. With the identical medium composition, a very similar productivity rate of 1.8 g l^{-1}d^{-1} ITA was observed compared to the shaking flask culture. From figure 30 B it is evident that the biomass almost tripled in comparison to the previous fermentation. Instead of acid production, a large proportion of the consumed glucose (18 %) was allocated for cell growth.

The N:P ratio of 4:1 deemed also favourable for cell growth in the bioreactor (see figure 30 C). During the first 4 d of cultivation up to 31.3 g l^{-1} biomass was generated. Afterwards, the glucose was consumed completely and the DCW declined towards the end of fermentation. The resulting ITA concentrations remained relatively low (14.0 g l^{-1}, 1.4 g l^{-1} MA).

From here, it can be concluded that in order for strain M15-CAD to reliably secrete high amounts of ITA, the P concentration had to be very low and the overall cell growth had to be limited. It seems therefore plausible, that for this yeast strain a very restricted N and P supply is beneficial.

Furthermore, the effects of a more alkaline pH and an elevated oxygen saturation were tested with the ITA production medium MG-IA 2:0.1. By increasing the oxygen saturation to 90 % no further improvements in the ITA production behaviour were accomplished. With an ITA end-concentration of 22.8 g l^{-1} and 1.4 g l^{-1} MA after 6 d (see figure 30 E), the productivity rate moderately declined to 3.8 g l^{-1}d^{-1} ITA compared to the fermentation with 55 % oxygen in the medium.

Figure 30 D shows that a neutral pH 7 resulted in a significant decrease in total acid synthesis. Merely 0.8 g l^{-1} ITA per day were secreted into the surrounding medium. Additionally, the main product changed from ITA to MA. After 6 d 8.3 g l^{-1} MA, whereas 4.6 g l^{-1} ITA were detected. As a result, the ITA specific yield was diminished. On average, solely 0.03 g ITA were synthesised for every 1 g glucose that was consumed.

Figure 30 Bioreactor cultivation of *P. tsukubaensis* M15-CAD in minimal medium with glucose for itaconic acid production (MG-IA).
The yeast cells were cultivated in minimal medium with 15 % (w/v) glucose with different ratios of N to P sources. Incubation was carried out for 6 d at 30 °C. **A** - MG-IA with a N:P ratio of 2:0.1; pH 5.5 and pO_2 = 55 %. **B** - MG-IA with a N:P ratio of 5:0.1; pH 5.5 and pO_2 = 55 %. **C** - MG-IA with a N:P ratio of 4:1; pH 5.5 and pO_2 = 55 %. **D** - MG-IA with a N:P ratio of 2:0.1; pH 7.0 and pO_2 = 55 %. **E** - MG-IA with a N:P ratio of 2:0.1; pH 5.5 and pO_2 = 90 %. The table beneath depicts the main characteristics for every single fermentation. Shown are the end-concentrations of ITA, the resulting productivity rates and the specific yields for ITA and DCW (g g^{-1} consumed glucose [%]).

MG-IA N:P-ratio	pH	pO$_2$ [%]	ITA$_{max}$ [g l^{-1}]	Productivity [g l^{-1} d^{-1}]	Yield ITA [%]	Yield DCW [%]
MG-IA 2:0.1	5.5	55	32.1	5.4	25	11
MG-IA 5:0.1	5.5	55	11.6	1.9	7	21
MG-IA 4:1.0	5.5	55	14.0	2.3	7	11
MG-IA 2:0.1	7.0	55	4.6	0.8	3	14
MG-IA 2:0.1	5.5	90	22.8	3.8	9	5

During the next step, the strain *P. tsukubaensis* HR12 was investigated for its ITA secretion capabilities in the bioreactor. First, the MG-IA medium compositions were applied which deemed most promising according to the previous fermentations with the help of strain M15-CAD. Therefore, batch cultivations were carried out with 2 g l^{-1} N and 0.1 g l^{-1} P source or with 4 g l^{-1} N and 1 g l^{-1} P, respectively. Figure 31 A illustrates that strain HR12 maintained its high productivity also in large culture volumes. After 5 d of cultivation, approximately half of the C source was consumed. In the course of this time, 58.3 g l^{-1} ITA were rapidly generated. The biomass increased until the 3rd day where a maximum of 32.7 g l^{-1} DCW was built up. Afterwards, the DCW subsided remarkably. The glucose consumption was not affected by this. This is an indicator that cells were still vital. An explanation for the reduction in DCW is, that simply an increasing portion of cells accumulated in the headspace of the bioreactor and formed a biofilm there due to the heavy aeration.

The yeast behaved very similarly when higher concentrations of N and P (4:1) were applied. The main difference was, that the cell mass did not decrease after the 3rd day but maintained stable around 35 g l^{-1} DCW (see figure 31 B). This heightened amount of cell mass ensured a more constant acid production. The ITA concentration rose linearly with a productivity rate of 12.9 g l^{-1}d^{-1} until an end-concentration of 64.3 g l^{-1} was obtained.

The utilization of the C source was also investigated. Hence, the fermentation with the MG-IA 4:1 medium was recreated (see figure 31 C). The sole difference to the previous cultivation was that the initial glucose concentration was reduced to 7.5 % (w/v). The glucose concentration was then monitored at least daily. If needed, the C source was resupplied to approximately 7.5 %. By doing so, the growth of strain HR12 could be prolonged. The biomass increased consistently until the 5th day. Afterwards, it decreased slightly. In the beginning, the amount of ITA in the medium followed a linear increase. The productivity slowed down after the 4th day. At the 5th day mark, ITA concentrations of 62.7 g l^{-1} were detected. This result is very much akin to the results of the previous fermentation. Conversely, the C source was converted more efficiently during the same time period. On average 35 % of the glucose was metabolized into ITA. Because of the slowed down productivity, the yield dropped marginally to 33 %. Therefore, the more stable and predictable growth behaviour led to the adoption of the fed-batch fermentation process. All of the following fermentations were carried out with a starting concentration of 7.5 % (w/v) glucose and re-supplying the C source daily.

Further increasing the initial N source to 8 g l^{-1} led to very promising results. With more available resources for cell multiplication, the growth of the yeast cells was accelerated drastically. Up to 50 g l^{-1} DCW was generated. The ITA production reflected this rise in cell mass. Over 113 g l^{-1} ITA were secreted into the medium during the 7 d of fermentation, which corresponds to a

productivity rate of 16.2 g l^{-1}d^{-1} (see figure 31 D). According to this data, it stands to reason that for this strain two factors are crucial for the heightened production of ITA. First, the transcription rate of the ITA gene cluster is coupled to the growth rate due to the actin promoter. Faster growth means higher transcription. Second, the sheer number of active cells: The conversion rate of glucose to ITA rose with an increased biomass.
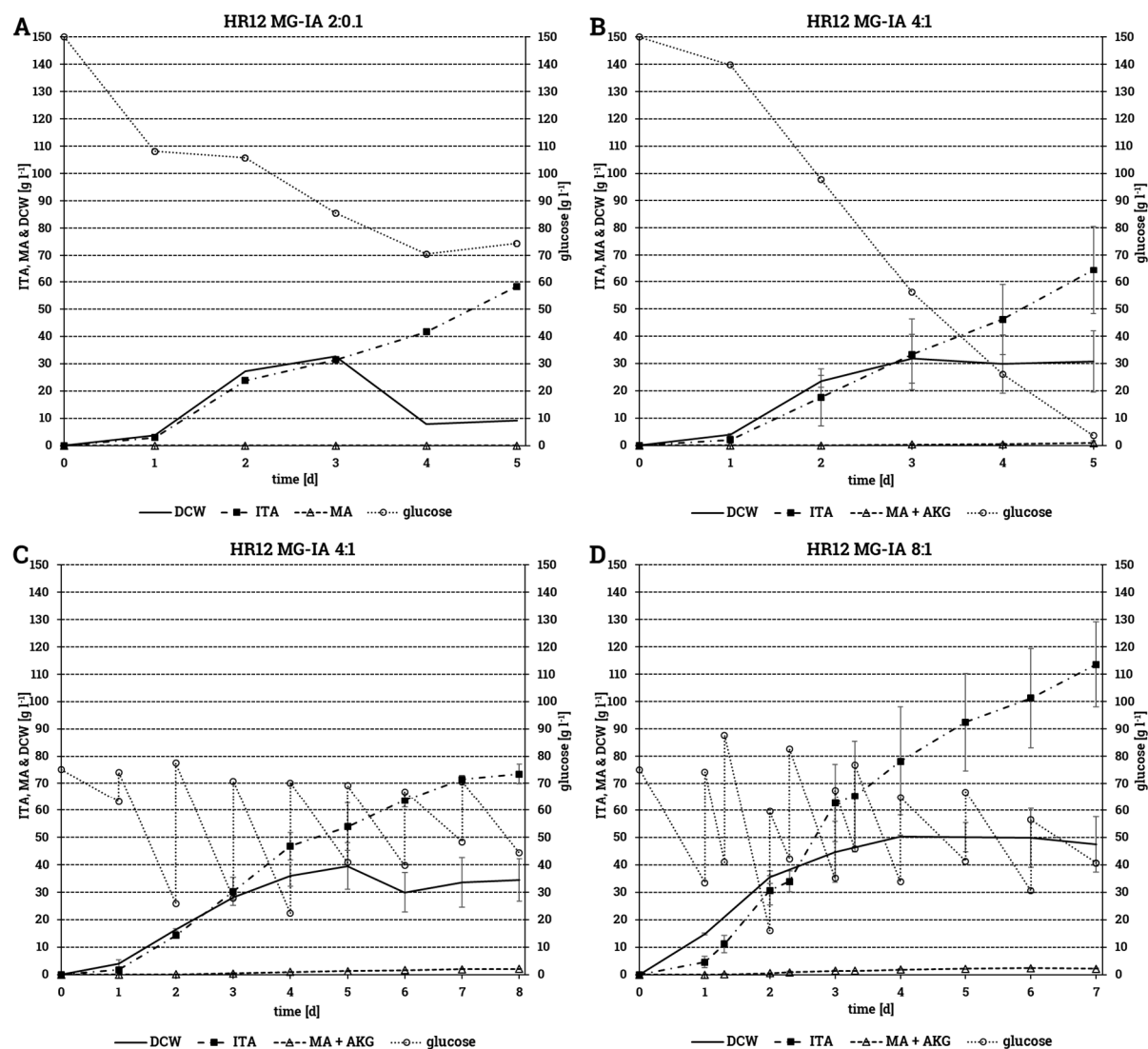
MG-IA N:P-ratio	Duration [d]	Glucose supply	ITA$_{max}$ [g l^{-1}]	Productivity [g l^{-1} d^{-1}]	Yield ITA [%]	Yield DCW [%]
MG-IA 2:0.1	5	Batch	58.3	11.7	43	7
MG-IA 4:1	5	Batch	64.3	12.9	31	14
MG-IA 4:1	8	Fed-batch	73.4	9.2	33	13
MG-IA 8:1	7	Fed-batch	113.6	16.2	42	16

Figure 31 Bioreactor cultivation of *P. tsukubaensis* HR12 in minimal medium with glucose for itaconic acid production (MG-IA).
The yeast cells were cultivated in minimal medium with 15 % or 7.5 % (w/v) glucose with different ratios of N to P sources. Incubation was carried out for 5-8 d at 30 °C, pH 5.5 and 55 % oxygen saturation. **A** − Batch cultivation in MG-IA medium with a N:P ratio of 2:0.1; 15 % (w/v) initial glucose. **B** − Batch cultivation in MG-IA medium with a N:P ratio of 4:1; 15 % (w/v) initial glucose. **C** − Fed-batch cultivation in MG-IA medium with a N:P ratio of 4:1; 7.5 % (w/v) initial glucose and fed daily. **D** − Fed-batch cultivation in MG-IA medium with a N:P ratio of 8:1; 7.5 % (w/v) initial glucose and fed daily. Data points represent the mean value of two independent fermentations (except for A) with error bars for standard deviation. The table beneath depicts the main characteristics for every single fermentation. Shown are the end-concentrations of ITA, the resulting productivity rates and the specific yields for ITA and DCW (g g^{-1} consumed glucose [%]).

It should be noted that in respect of other organic acids, MA and very low levels of αKG (near the limit of detection) were the exclusive side-products for every fermentation at the neutral pH. Accumulatively, these two acids represented approximately 2 % of the total acid content. By observing the morphology of the yeast cells microscopically, other side-products such as storage substances in the form of lipids could not be ruled out. In oleophilic yeasts these lipids are commonly stored as triglycerides inside so-called lipid droplets or lipid bodies. From figure 32 it is evident, that at the beginning of fermentation young *P. tsukubaensis* cells exhibited a minimum of two small lipid droplets located symmetrically near the two poles of the cell. In the course of the fermentation, large amounts of hydrophobic products were accumulated inside the cells. Thus, the lipid droplets grew in size until they virtually filled out the complete cell. The accumulation of storage fats led to the unwanted effect that the yeast cells floated towards the end of cultivation. This is because the lipid bodies accounted for a considerable part of the cell and the density of the lipids is less than that of water. The floating led to the undesired phenomenon that large parts of the cells adhered to the headspace of the bioreactor and were no longer in contact with the liquid medium beneath.
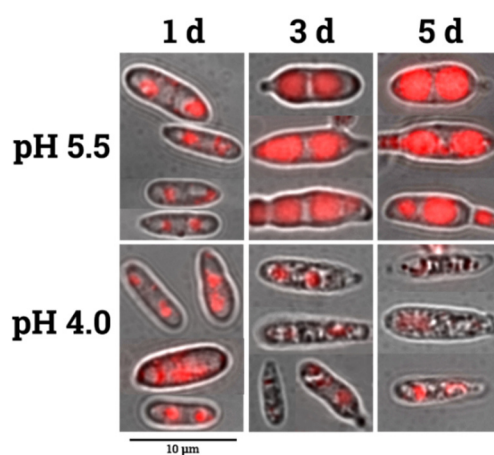
Figure 32 Lipid accumulation of *P. tsukubaensis* HR12 during fermentation in minimal medium with glucose (MG-IA 8:1) and neutral pH vs. acidic pH.
Overlay images of brightfield and fluorescence photographs at 1000 x magnification. The hydrophobic substance containing cell organelles (lipid bodies) appear red due to the staining with the fluorescent dye Nile-red. A – Lipid bodies containing yeast cells at the 1st, 3rd and 5th day of cultivations at pH of 5.5. The lipid bodies' size increases throughout the fermentation. B - Yeast cells at the 1st, 3rd and 5th day of cultivations at pH of 4.0. Lipid accumulation is largely restricted in the acidic environment

For acids, the solubility increases with rising pH values. Earlier, the fermentation of *P. tsukubaensis* M15-CAD proved that elevating the pH from 5.5 to 7.0 is counterproductive for synthesis of ITA (see figure 30). It was unclear, whether a more acidic pH has a substantial impact on the ITA production behaviour. Therefore, the cultivation with the previously recorded highest ITA productivity rate was carried out again. The yeast cells were incubated in MG-IA 8:1 minimal medium with an initial glucose concentration of 7.5 % (w/v) at a pH 5.5 for 24 h. Deviating from the earlier fermentation, the pH was decreased to 4.0 after 24 h. This approach ensured the generation

of enough biomass before the change to an acidic milieu. In doing so, an immediate arrest in cell growth after lowering the pH was observed (see figure 33 A). At the point of induction, DCW of approximately 20 g l^{-1} had been formed. This level was maintained throughout the whole fermentation. Despite the reduced cell mass, the ITA acid production was not hampered substantially. Until the 4th day, continuously high concentrations of ITA were secreted. Afterwards, the production slowed down marginally. The final concentration came to 71.8 g l^{-1} ITA.

Since the uninterrupted generation of biomass was not necessary under this condition, another fermentation was carried out with 4 g l^{-1} N available in the medium. Nevertheless, a certain quantity of cells was needed to ensure a high production rate. Thus, the pH was reduced only 48 h after inoculation. This way, biomass of nearly 30 g l^{-1} DCW was present when the pH change took place (see figure 33 B). Although, the biomass dropped to approximately 20 g l^{-1} DCW soon after reducing the pH, the remaining cells were vital enough to sustain a linearly increasing ITA synthesis for the whole duration of fermentation. With a productivity rate of 11.6 g l^{-1}d^{-1}, a total of 81.5 g l^{-1} ITA was formed after the 7 d of cultivation.

Conspicuously, the *P. tsukubaensis* cells did not float during fermentation at lower pH values. They remained inside the fermentation broth and could be easily sedimented by centrifugation. By examining the cells microscopically, it was apparent that an accumulation of lipids had not taken place. Figure 32 shows that the size of lipid droplets inside the cells did not extend in the course of cultivation but remained small. This is potentially why the highest ITA specific yield was achieved. Cell growth and the production of storage substances were both limited while the ITA cluster genes were overexpressed. Thus, most of the available C source was allocated to the synthesis of ITA.

Another advantageous aspect of this fermentation process were the remarkably low levels of other side-products as well. At the end of cultivations with a pH of 4.0, the combined concentrations of MA and *α*KG amounted for just 0.4 % of the total organic acids detected in the supernatant (data not shown).

During subsequent cultivation experiments, two other factors were investigated in combination with the decreased pH. Increased oxygen saturation is described to be beneficial for enhanced ITA production (Molnár et al., 2018). Even though no improvement was detected for strain M15-CAD, fermentations of strain HR12 were carried out with an increased oxygen saturation of 70 %. By doing so, the yeast strain behaved very similar to fermentation B. Figure 33 C shows that the productivity rate and the final ITA concentration were very much comparable to fermentation B. However, the elevated ITA synthesis rate was accompanied by a heightened glucose consumption. Both, the ITA and the DCW specific yield were low, with 28 % and 7 %, respectively. The additional increase of the culture temperature to 32 °C in combination with pH 4 had an even

more negative effect. The productivity rate suffered vastly. On average, 9.6 g l^{-1} ITA were formed per day. The glucose consumption was also intensified. Merely 26 % of the C source was directed into the synthesis of ITA and 8 % into biomass. A possible explanation for that occurrence is an accelerated aerobic respiration rate for both cases of increased aeration and temperature. This occurrence could stem from an increased activity in the glycolysis pathway and subsequently the tricarboxylic acid cycle. As a result, large proportions of the C source would solely be converted into CO_2. Additional off-gas analysis would be needed to confirm this hypothesis.

Further decreasing the pH to 3.5 had a detrimental effect on the yeast's performance. For this particular fermentation, the pH was lowered in two increments: first after 24 h from 5.5 to 4.0 and after an additional 24 h further to 3.5. This condition led to the lowest observed productivity rate. Daily, on average 7.0 g l^{-1} ITA were secreted. Especially, after the 4th day the ITA synthesis did slow down considerably to 3.5 g l^{-1}d^{-1}. By observing the glucose consumption data more closely, it appears that the metabolic rate was heavily restricted. In the course of the last 3 d of cultivation, only 16.7 g l^{-1} of glucose were metabolized.

The chemical compound calcium carbonate ($CaCO_3$) is a naturally occurring buffer agent. It reacts with acids by forming the corresponding acid calcium salt and releasing carbonic acid which rapidly disintegrates into H_2O and CO_2. At neutral pH values, this crystalline substance is insoluble. If dissociated acids are present in the medium only the $CaCO_3$ amount needed to regain a neutral pH will dissolve. At high concentrations the Ca^+ and ITA^{2-} ions should precipitate as calcium itaconate. Easily removable calcium itaconate crystals would represent an interesting way to harvest the product with minimum effort in an industrial fermentation process. Figure 33 F illustrates the effect of using this buffering agent during fermentation of *P. tsukubaensis* strain HR12. For the cultivation, no active pH control was used. Instead, 5 g $CaCO_3$ was supplied daily, after the ITA reached considerable amounts in the medium. The first application happened 72 h after inoculation. In doing so, the pH remained constant at approximately pH 5.0. By ensuring a relatively neutral pH, high quantities of ITA were secreted. After 7 d, 69.4 g l^{-1} ITA were measured directly in the supernatant. In addition to that, calcium itaconate occurred in the form of an insoluble salt. Accounting for that product, in total 89.7 g l^{-1} ITA were synthesised with a productivity rate of 12.8 g l^{-1}d^{-1}. The difference in the two concentrations amounts to a total mass of 10.5 g or 0.08 mol ITA. Since 1 mol of $CaCO_3$ is able to neutralize 1 mol ITA, approximately 40 % of the total buffer (0.2 mol) was depleted in the formation of calcium itaconate. In contrast to the high ITA production rate, also large quantities of DCW were generated, especially towards the end of the fermentation process. This fact was reflected in the relatively low ITA specific yield. 33 % of the consumed glucose was spent for the formation of ITA and 15 % for biomass.

Figure 33 Effect of lowered pH on the ITA productivity of *P. tsukubaensis* HR12 in a bioreactor with minimal medium with glucose (MG-IA).

Fed-batch cultivations of the yeast cells in minimal medium with 7.5 % (w/v) glucose with different ratios of N to P sources. The cultures were incubated for 7 d and fed daily to maintain approximately 7.5 % glucose. Initial pH was set to 5.5. Black arrows mark the time point when the pH was lowered to 4.0 **A** - MG-IA with a N:P ratio of 8:1, pH was lowered to 4.0 at 1st day, pO_2 = 55 %, 30 °C. **B** - MG-IA with a N:P ratio of 4:1; * pH was lowered to 4.0 at the 2nd day, pO_2 = 55 %, 30 °C. **C** - MG-IA with a N:P ratio of 5:1, pH was lowered to 4.0 at 1st day, pO_2 = 70 %, 30 °C. **D** - MG-IA with a N:P ratio of 4:1, pH was lowered to 4.0 at 1st day, pO_2 = 55 %, 32 °C. **E** - MG-IA with a N:P ratio of 4:1; pH was lowered to 4.0 at 1st day and then to 3.5 at 2nd day (second black arrow), pO_2 = 55 %, 30 °C. **F** - MG-IA with a N:P ratio of 5:1; no active pH control. The medium was supplied four times with 5 g $CaCO_3$ each time (grey arrows), pO_2 = 55 %, 30 °C. Data points represent the mean value of two independent fermentations (except for C, D & F) with error bars for standard deviation. The table beneath depicts the main characteristics for every single fermentation. Shown are the end-concentrations of ITA, the resulting productivity rates and the specific yields for ITA and DCW (g g^{-1} consumed glucose [%]).

In industrial settings, numerous fermentation processes are carried out over a long period of time. For certain cases continuous fermentation methods are applied, where culture broth is removed at a constant rate and substrate is supplied at an equivalent rate. In other cases, semi-continuous fermentation methods are followed. By doing so, a large part of the culture volume is removed and replaced with fresh medium. Before such a biotechnological process can be established, it must be proven that the whole cell catalyst provides a stable conversion rate for the substrate throughout the whole fermentation period. Therefore, a semi-continuous fermentation in minimal medium with glucose was performed for 14 d with *P. tsukubaensis* HR12. The results are summarized in figure 34. For the process, a low pH of 4.0 was chosen since it ensured a moderate growth rate and thus an enough cell vitality until the medium was refreshed. In addition, the floating of the cells and the forming of a biofilm inside the bioreactor was prevented with this approach also. The culture conditions at the beginning were analogous to the previous fermentation with the medium MG-IA 8:1 at pH 4.0 (see figure 33 A). However, the productivity rate was slightly accelerated compared to the analogous cultivation. At the seven-day mark, 84.4 g l^{-1} ITA were detected in the supernatant which corresponds to an average production rate of 12.1 g l^{-1} ITA per day. At that time, one half of the culture broth was removed and replenished with the same volume of fresh MG-IA 6:1 medium. The following ITA synthesis was not negatively affected by this and remained consistently high. After another 7 d of cultivation, a final ITA concentration of 112.1 g l^{-1} was measured. By accounting for the significant quantities of ITA that were removed at 7 d, the theoretical end-concentration amounted to 160 g l^{-1} ITA. The ITA specific yield was also in accordance with earlier experiments. In total, 35 % of the consumed glucose was utilized for the synthesis of ITA.

During experiments in shaking flasks, it was already established that other C sources than glucose could be metabolized. Figure 34 B illustrates, that an upscaling of the cultivation with sucrose as the sole C source was also successful. In the course of fermentation at pH 4.0, on average 7 % of sucrose was converted into dry biomass. With respect to glucose, this value is comparatively low. The trials in baffled shaking flasks also led to decreased cell densities when grown with the non-reducing sugar. However, in the bioreactor less ITA was formed in relations to glucose. Merely 63.5 g l^{-1} ITA were secreted compared to 71.8 g l^{-1} or 81.5 g l^{-1} ITA with glucose under similar conditions (see figure 33). This was not the case in shaking flasks. From figure 34 B it is noticeable that the productivity rate is very high until the 3rd d but levels out thereafter. This decline led to the overall inferior ITA production. The reasons for that occurrence are still unclear.

Mx-IA N:P-ratio	Duration	Notes	ITA_max [g l⁻¹]	Productivity [g l⁻¹ d⁻¹]	Yield ITA [%]	Yield DCW [%]
MG-IA 6:1	14	semi-continuous	112.1 (160.4)	8.0 (11.5)	23 (35)	7 (10)
MS-IA 5:1	7	sucrose	63.5	9.0	24	7
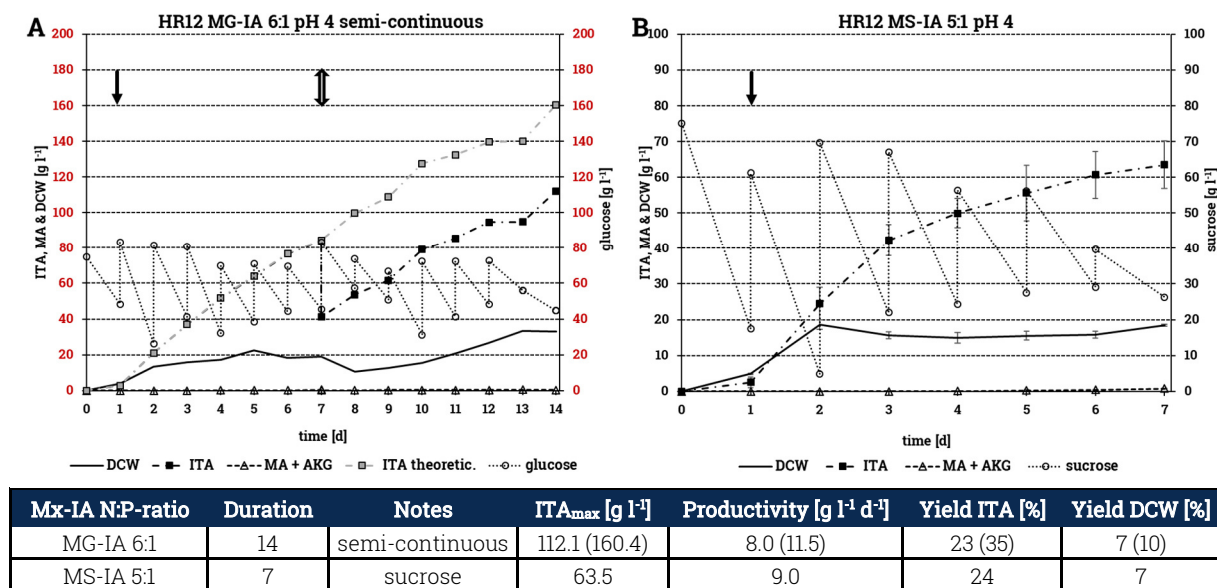
Figure 34 Semi-continuous cultivation of *P. tsukubaensis* HR12 in minimal medium with glucose (MG-IA) and fed-batch cultivation with minimal medium with sucrose (MS-IA).
The yeast cells were cultivated in minimal medium with 7.5 % (w/v) glucose or sucrose with a N:P ratio of either 6:1 or 5:1, respectively. The yeast cells were fed daily. Incubation was at 30 °C and 55 % oxygen saturation. The pH was initially adjusted to 5.5 and was lowered to 4.0 after 24 h incubation. **A** - MG-IA with a N:P ratio of 6:1. After 7 d of incubation ½ of the culture broth was removed and replenished with fresh medium (marked with double-headed arrow). **B** – Fermentation with sucrose as C-source and a N:P ratio of 5:1. Data points represent the mean value of two independent fermentations (**except A**) with error bars for standard deviation. The table depicts the main characteristics for every particular fermentation. Shown are the end-concentrations of ITA, the resulting productivity rates and the specific yields for ITA and DCW (g g⁻¹ consumed glucose [%]). Values in brackets represent the respective data after adjusting for the losses that resulted by removing ½ of the culture.

Concluding from all cultivations, it appears, that *P. tsukubaensis* strain HR12 represents a very versatile ITA acid producing organism. The yeast can synthesise and secrete remarkably high concentrations of this organic acid. Elevated acid production is sustained reliably under various conditions, for different substrates and even for a prolonged time. In addition, the formation of ITA is accompanied by only small amounts of MA and αKG as potentially interfering side-products. According to the accumulated fermentation data, it appears natural that high cell densities account for a severely enhanced ITA production with *P. tsukubaensis* strain HR12. After just 7 d, a maximum of 113.6 g l⁻¹ ITA could be generated by dry biomass of approximately 50 g l⁻¹. Decreasing the pH during cultivation can be considered stressful to the yeast cells. Additional parameter changes during cultivations in an acidic environment e.g. temperature increases should be carried out carefully. Since these factors could serve as extra stressors. At pH levels below 4.0 a normal cell vitality can no longer be guaranteed. Although lower final concentrations of ITA were achieved at pH 4.0 compared to neutral conditions, it could still represent a beneficial factor considering certain aspects. These included marginal concentrations of the side-products MA and αKG but also potentially lipids. In addition, the lack of hydrophobic storage fats leads to more effortless handling because the cells do not float.

3.2. Isocitric acid production with the yeast *Yarrowia lipolytica*

3.2.1. Identification of mitochondrial citrate transporters

In mammalian mitochondria, CA is transported by the protein CIC (synonymic: CTP, tricarboxylate carrier). The protein is encoded by *SLC25A1* in humans (Palmieri 2013). For yeasts, such as *S. cerevisiae* two proteins are known to transport tricarboxylates, Ctp1p and Yhm2p (Castegna et al., 2010; Kaplan et al., 1996). To this date, tricarboxylate carriers in the yeast *Y. lipolytica* have not been characterized. In order to investigate the function of possible CA carriers, the respective candidate genes had to be identified first.

Therefore, the protein sequences of the known CA carriers from *S. cerevisiae* and *C. albicans* were compared to the protein library of *Y. lipolytica* CLIB122 (E150) using the BLASTP algorithm. It has been found that the *Y. lipolytica* gene products of *YALI0F26323g* shared high sequence similarity with the two gene products *ScCTP1* and *CaCTP1* (see table 23). Gene *YALI0B10736g* had previously been identified by Gatter (2015) as the homolog of *ScYHM2* and named *YlYHM2* or *YHM2*, accordingly.

Table 23 *Y. lipolytic* CLIB122 (E150) genes with high similarity to mitochondrial carrier genes from *S. cerevisiae* S288C and *C. albicans* SC5314.
The deduced protein sequences of the genes *CTP1* and *YHM2* were analysed by BLASTP against the translational products of the whole *Y. lipolytica* genome. Shown are the homologous gene products with amino acid identity, query coverage (values in brackets) and the Expected value. Also given are the respective lengths of the deduced protein sequences (number of aa) and the predicted molecular weight (MW). Molecular weights were estimated with the ProtParam tool (https://web.expasy.org/protparam/).

Y. lipolytica gene	deduced protein	homologous gene	deduced protein	identity E-value
YlCTP1 *YALI0F26323g* gene ID: 2908112	292 aa 31.7 kDa	*S. cerevisiae* S288C *ScCTP1* gene ID: 852594	299 aa 32.2 kDa	67 % [99 %] $5 \times e^{-144}$
		C. albicans SC5314 *CaCTP1* gene ID: 3635141	294 aa 31.4 kDa	70 % [99 %] $8 \times e^{-154}$
YlYHM2 *YALI0B10736g* gene ID. 2907495	311 aa 33.8 kDa	*S. cerevisiae* S288C *ScYHM2* gene ID: 855282	314 aa 34.2 kDa	77 % [96 %] $3 \times e^{-169}$
		C. albicans SC5314 *CaYHM2* gene ID: 3647137	301 aa 32.9 kDa	80 % [95 %] $4 \times e^{-163}$

The *Y. lipolytica* gene *YALI0F26323g* is located on chromosome F. The 935 bp long ORF consists of two exons which are separated by a short intron (at position 24-81 bp). The gene encoding the putative Yhm2p homolog is located on chromosome B. This gene (*YALI0B10736g*) has a considerably larger ORF (1561 bp) and harbours two introns. Intron 1 stretches from position 93-421 bp and intron 2 from position 459-747 bp.

The deduced protein sequences of *YALI0F26323g* and *YALI0B10736g* are 292 aa and 311 aa in length, respectively. Both proteins could be classified as mitochondrial carrier proteins by examining their aa sequences with the protein homology search algorithm HMMER (Finn et al.,

2015). In doing so, the conserved protein domain for the mitochondrial carrier family (MCF) was detected (identifiers: Pfam - PF00153; PROSITE - PS50920). This domain is found three times in tandem orientation in the protein sequence of the members of the MCF. The tandemly repeated homologous domains are each about 100 aa long and contain the signature motif PX[D/E]XX[K/R]X[K/R]-X$_{20-30}$-[D/E]GXXXX[W/Y/F][K/R]G (Nury et al., 2006; Palmieri, 1994; Saraste and Walker, 1982). This was also the case for the investigated proteins YALI0F26323p and YALI0B10736p. The three MCF domain repeats were discovered for YALI0B10736p at the following positions: 14-103 aa (E-value: $5.2 \times e^{-07}$), 105-203 aa (E-value: $2.4 \times e^{-06}$) and 208-303 aa (E-value: $5.2 \times e^{-13}$) and for YALI0F26323p at positions: 7-100 aa (E-value: $1.01 \times e^{-14}$), 102-197 aa (E-value: $2.15 \times e^{-16}$) and 204-292 aa (E-value: $5.10 \times e^{-25}$).

According to the deduced protein sequence, YALI0F26323p could be identified as a mitochondrial carrier protein, which belongs to the mitochondrial carrier family or more specifically to the family 2.A.29 according to the transporter classification database (TCDB). Because of the identification as a mitochondrial carrier and the great sequence identity to the homologous counterpart in *S. cerevisiae* and *C. albicans*, *YALI0F26323g* was named *YlCTP1*, hereafter.

3.2.2. Genetic engineering of *Y. lipolytica*

In this study, one key aspect was the enhanced production of ICA with the help of a genetically engineered *Y. lipolytica* strain. Because the functions of the two identified genes were still unknown in this yeast, respective deletion strains had to be constructed. A positive effect of enhanced *YlACO1* activity on the ICA production was already published by Holz et al. (2009). Therefore, also overexpression strains had to be constructed. The following section focuses on the design and realization of the deletion and overexpression strains.

3.2.2.1. Deletion of *YlCTP1* and *YlYHM2*

In contrast to *P. tsukubaensis*, more advanced genetic tools were available for the genetic modification of *Y. lipolytica*. Decades worth of previous work on the genetic mechanisms for the yeast *Y. lipolytica* made it possible to directly target and delete single specific genes. Homologous recombination has been proven to be a reliable and productive method for the purpose of gene disruption. In doing so, the ORF of the gene is exchanged for a marker by homologous recombination events at the promoter and terminator regions. Usually, the target sequences in *Y. lipolytica* are approximately 1000 bp long directly upstream and downstream of the targeted ORF.

Here, the genes *YlCTP1* and *YlYHM2* were disrupted using the URA blaster system. This system consisted of the complete native *YlURA3* gene, including promoter and terminator sequences. The *YlURA3* gene served as the selection marker for uracil prototrophic transformants. In addition, *YlURA3* was flanked by two homologous TcR' sites that share the same orientation.

These TcR' sites are necessary for the recovery of the uracil auxotrophy by excising the marker gene and one of the TcR' sites (loop-out). Leaving only one TcR' site behind in the genome (scar).

Ultimately, the deletion cassette was made up of the promoter sequence of the gene to be deleted, the URA blaster, and the terminator sequence (see figure 35).
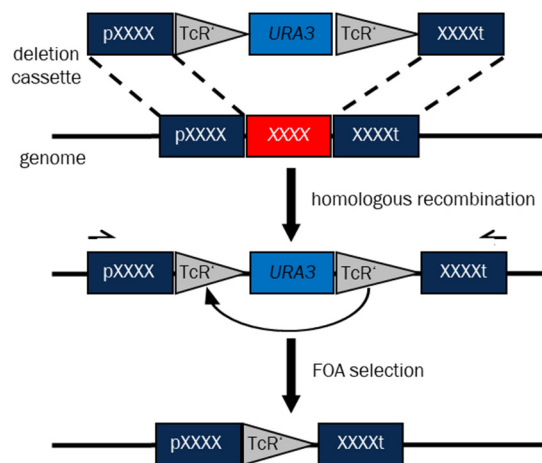
Figure 35 Schematic overview of the molecular mechanism for the disruption of a target gene in *Y. lipolytica*.
A deletion cassette in the form of a linear DNA fragment is provided to competent *Y. lipolytica* cells. Homologous recombination events take place between the deletion cassette and the genome, because of the sequence homology at the promoter and terminator regions. The deletion cassette consists of the upstream region of the to be deleted gene (pXXXX), the URA blaster and the downstream region of the gene (XXXXt). The pXXXX & XXXXt regions are approximately 1000 bp long. This leads to the exchange of the ORF (*XXXX*) for the URA blaster. The uracil auxotrophy can be regained by FOA selection. The *URA3* gene and one of the TcR' sites are excised from the genome, due to cyclic recombination events between the two TcR' sites. This leaves only one TcR' site behind as a scar. Black arrows represent the primer sites used for PCR to confirm the deletion of the respective ORF (modified according to Gatter, 2015).

3.2.2.1.1. Construction of deletion plasmids

The deletion cassettes that were applied during the transformation of the yeast were designed and amplified with the help of *E. coli* plasmids.

The plasmid for the deletion of *YlYHM2*, pJET-DK-*YHM2*, was designed by Gatter (2015).

The plasmid for the deletion of *YlCTP1* (see figure 36) was constructed by amplifying approximately 1000 bp long sequences from the 5'-upstream and the 3'-downstream regions of the *YlCTP1* ORF. The 1194 bp long promoter fragment was amplified using the primers p*CTP1*_fw and p*CTP1*_rv_BglII. The 3'-end of the promoter fragment was complemented with a BglII restriction enzyme recognition site. The resulting purified fragment was then digested with HindIII (at a naturally occurring recognition site) and BglII. For the terminator region, the primers t*CTP1*_fw_BglII and t*CTP1*_rv_KpnI were used. Both ends of this fragment were complemented with a recognition sequence for either the BglII or KpnI restriction enzyme. These two recognition sites were subsequently utilized to cut the 1081 bp long PCR-product. Both fragments were ligated into a HindIII & KpnI-linearized pUCBM21 plasmid. The derived pUC-IP-*CTP1* plasmid was then linearized using BglII. Afterwards, the pUC-DK-*CTP1* plasmid was completed by ligating the URA

blaster (BglII & BamHI-digested) into it. Prior to the transformation, the deletion cassette was amplified with the help of PCR using the primers p*CTP1*-DK-Ampl_fw and t*CTP1*_rv_KpnI.

Solely the deletion cassette was provided as a linear DNA fragment to the uracil auxotrophic yeast *Y. lipolytica* H222 SW2-1 (Δ*YHM2*) ura⁻ during transformation.
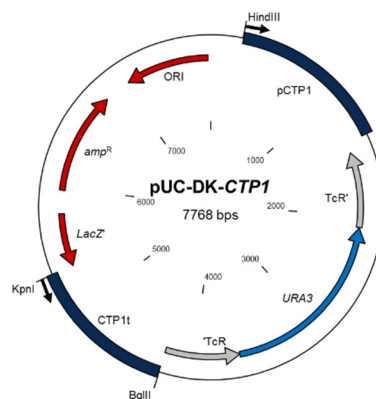
Figure 36 Map of the *YlCTP1* deletion plasmid.
The plasmid contains the ampicillin resistance gene (*amp*ᴿ) for the selection of *E. coli* clones and an origin of replication (ORI). The URA blaster marker system for the selection of uracil prototrophic *Y. lipolytica* transformants is present. The URA blaster is made-up of the *YlURA3* gene flanked by two TcR' fragments. The complete URA blaster is flanked by the upstream and downstream regions of *YlCTP1* (pCTP1; CTP1t). Small black arrows mark the primer binding sites for pCTP1-DK-Ampl_fw and tCTP1_rv_KpnI that were used to amplify the deletion cassette before the transformation of the yeast.

Table 24 List of all cut components that were used for the construction of the deletion plasmid pUC-DK-*CTP1*.

component	fragment (size)
CTP1 promoter fragment	(HindIII)-p*CTP1*-(BglII) (1161 bp)
CTP1 terminator fragment	(BglII)-*CTP1*t-(KpnI) (1069 bp)
vector fragment	(HindIII)-pUCBM21-(KpnI) (2670 bp)
marker system	(BglII)-URA blaster-(BamHI) (2868 bp)

3.2.2.2. Overexpression of *YlACO1* and *YlYHM2*

For the purpose of overexpression, the chosen genes were upregulated with the strong and constitutive promoter of the translation elongation factor 1-α (*YlTEF1*) gene (pTef). The pTef-target gene construct represented the key part of the overexpression plasmids. The transcription termination of the genes *YlACO1* and *YlYHM2* was additionally controlled by the terminator sequence of the *Y. lipolytica* isocitrate lyase gene (Icl1t). Furthermore, both overexpression plasmids contained the complete URA blaster. Another integral component were the target sequences needed for directed integration into the genome. This directed integration was guaranteed by the used plasmids. These included sequences that are homologous to non-coding sequences either from the yeast's chromosome B (IntB) or chromosome C (IntC). Therefore, homologous recombination events took place during the transformation process between the genomic DNA and the linearized vector. Consequently, the whole overexpression plasmid integrated into the target sequence on chromosome B or C (so-called loop-in, see figure 37).
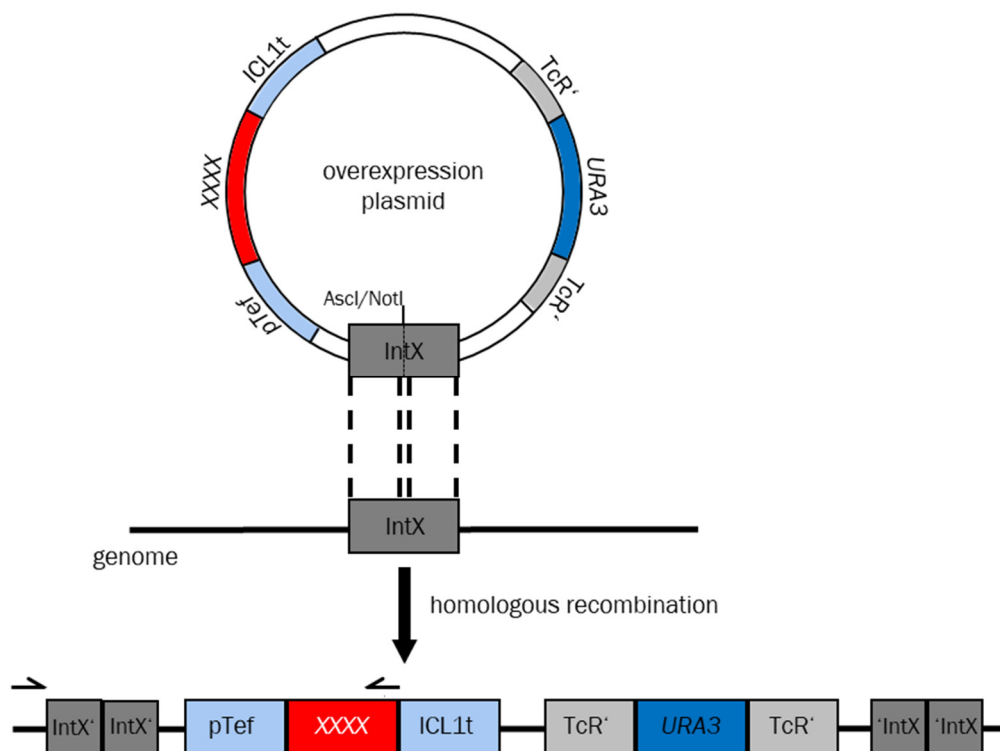
Figure 37 Schematic overview of the mechanism for the overexpression of *YlACO1* and *YlYHM2* in the yeast *Y. lipolytica*.
Integration into the genome of *Y. lipolytica* was made possible by the homologous regions IntB or IntC (represented by **IntX**), which are homologous to non-coding sequences on chromosome B or C (**IntX**). Because of homologous recombination events the complete linear plasmid is integrated into the chromosome. The overexpression plasmid contains the URA blaster (*URA3* gene flanked by two TcR' sites) for the selection of uracil prototrophic transformants. The target gene is upregulated by the strong, constitutive *TEF1* promoter (pTef) and its transcription termination is controlled by the terminator sequence of the *YlICL1* gene (ICL1t). Prior to transformation, linearization of the plasmid is done (AscI or NotI). Linearization increases integration efficiency and ensures integration at a specific known site. Black arrows mark the primer binding sites used for PCR to confirm the integration of the upregulated gene (modified according to Gatter, 2015).

3.2.2.2.1.   Construction of overexpression plasmids

First step of plasmid construction was the generation of the pTef-ORF fusion product. For that reason, overlap extension PCRs were carried out to merge the 3'-terminal region of the *TEF1*-promoter to the respective ORF. The 3'-terminal region of pTef was amplified with a 3'-overhang which was complementary to the first 20 bp of the *YlYHM2* or *YlACO1*-ORF, respectively (primers for the 3'-Tef fragments: pTef_SpeI_fw3, pTef_ol_ACO1_rv / pTef_ol_YHM2_rv). The ORFs themselves were amplified by extending the 3'-end with a restriction enzyme recognition site for either SphI (*YlACO1*) or MluI (*YlYHM2*). The 5'-end was extended with a 20 bp overhang which was complementary to the pTef'-fragment. The following primer combinations were used for the PCR of the ORFs: ACO1_ol_pTef_fw & ACO1_rv_SphI, pTef_YHM2_ol_fw & YHM2_rv_MluI.

During a second amplification reaction, only the outer primers were used. In this way, the pTef'-fragment was fused to the respective ORF. Both overlap-PCR products were digested using BcuI and SphI (for *YlACO1*) or MluI (for *YlYHM2*). Overexpression plasmid pIntB-*YHM2* was completed by inserting the pTef'-*YHM2* fragment into a similarly cut pIntB-CrtI vector. Plasmid pIntC-*ACS1* was digested with BcuI and SphI and ligated with the cut *YlACO1* overlap-PCR product. Thus, the

overexpression plasmid pIntC-*ACO1* was created (for a general overview of the overexpression plasmids see figure 38). Prior to transformation into *Y. lipolytica*, linearization of the overexpression vectors was achieved by using the following enzymes. AscI (pIntC-*ACO1*) and NotI (pIntB-*YHM2*).
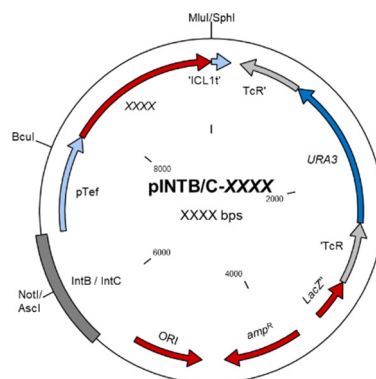
Figure 38 General map of the overexpression plasmids used for the overexpression of *YlACO1* and *YlYHM2*. The resulting plasmids pIntB-*YHM2* and pIntC-*ACO1* both contained the ampicillin resistance gene (*amp*R) for the selection of *E. coli* clones and an origin of replication (ORI). The URA blaster marker system for the selection of uracil prototrophic *Y. lipolytica* transformants was present. The URA blaster was made up of the *YlURA3* gene flanked by two TcR' fragments. The overexpression plasmids contained the respective gene (*XXXX*) under the control of the strong and constitutive TEF1 promoter (pTef). Transcription termination was regulated by the terminator sequence of the *YlICL1* gene ('ICL1t). Integration of the whole plasmid into the yeast's genome was made possible by the integration platform IntB (*YlYHM2*) or IntC (*YlACO1*).

Table 25 List of all cut pTef'-gene fusion fragments and cut vector backbone fragments for the overexpression of *YlACO1* and *YlYHM2*.

Gene	Promoter-gene fragment (size)	Vector fragment (size)
YlACO1 *YALI0D09361g*	(BcuI)-pTef'-*YlACO1*-(SphI) (2906 bp)	(SphI)-pINTC-(BcuI) (8083 bp)
YlYHM2 *YALI0B10736g*	(BcuI)-pTef'-*YlYHM2*-(MluI) (1768 bp)	(MluI)-pINTB-(BcuI) (7550 bp)

3.2.3. Growth behaviour of the constructed *Y. lipolytica* strains

In total, six differing *Y. lipolytica* strains were generated with the above-described methods. Two strains had one of the potential CA carriers deleted: H222 SW2-1 Δ*YHM2*, H222 SW2-1 Δ*CTP1* and one had them both deleted: H222 SW2-1 Δ*YHM2*Δ*CTP1*. One strain was overexpressing the tricarboxylate carrier: o*YHM2*. The single copy integration of the deregulated *YlACO1* gene (coding for aconitase) was also investigated with the wild type and Δ*YHM2* background: o*ACO1* and Δ*YHM2*o*ACO1*. Aconitase was chosen as an additional target because this is a key enzyme in the TCA cycle and responsible for the isomerisation of CA into ICA.

Growth behaviour on minimal medium with various C sources was investigated for all the genetically modified *Y. lipolytica* strains and the wild type H222. Glucose was chosen as the reference C source. This fermentable simple sugar is generally metabolized in the course of

glycolysis and subsequently the tricarboxylate cycle. Thus, a prevalent impairment in the TCA would have been made visible on glucose.

This was not the case for any of the strains. As figure 39 shows, all the investigated strains grew in a near identical manner.CA is described to be the main substrate for the carrier proteins Yhm2p and Ctp1p. The metabolization of CA mainly takes place inside the mitochondria in the course of the TCA cycle. In theory, an effect should be discernible if CA cannot be shuttled into the cellular compartment of its degradation. Therefore, the growth on this tricarboxylate and its precursor (oxaloacetate) as well its successor (αKG) molecules in the TCA were tested. None of the genetic modifications, not even the combined deletion of the CA carriers led to any visible growth deficits. Cultivation on the non-fermentable monocarboxylate, acetate also did not lead to any changes in the phenotype.

Overall, no major growth defects were detected for any C source. According to these results, the main metabolic pathways were not considerably impacted by any of the genetic modifications. However, compensation mechanisms cannot be ruled out yet. This stands to reason especially for strain $\Delta YHM2\Delta CTP1$ when cultivated on the CA containing medium. Other pathways were maybe amplified to channel metabolites into the mitochondria. Alternatively, other transport proteins were potentially upregulated. These potentially functionally redundant transporters could then transport the tricarboxylates into the mitochondria.

Additionally, the effect of hydrogen peroxide was examined. In the yeast *S. cerevisiae*, it was reported that Yhm2p exerts an antioxidative role by shuttling metabolites that are needed for the generation of NADP(H) in the cytosol (Castegna et al., 2010). Thus, the antioxidative capabilities of the engineered strains were investigated on minimal medium with glucose in the presence of 1.25 mM H_2O_2. Under this circumstance, the deletion of *YlYHM2* had a similar consequence than it had on *S. cerevisiae*. Strain $\Delta YHM2$ was evidently impaired in its growth. Therefore, Yhm2p is most probably an important factor in the NAD(H)/NADP(H) homeostasis in *Y. lipolytica* as well.

Deletion of *YlCTP1*, on the other hand, did not cause the same phenotype. This indicates, that Ctp1p is not involved in the formation of NADP(H) in *Y. lipolytica*. The overexpression of *YlACO1* (o*ACO1*) led to similar deleterious effects in the presence of the oxidant. Meaning, that the enhanced aconitase activity negatively affected the formation of NADP(H) in the presence of the oxidant. Interestingly, the combination of the *YlYHM2*-deletion and the *YlACO1*-overexpression alleviated this phenotype for strain $\Delta YHM2$o*ACO1* in the presence of hydrogen peroxide. Possibly, the *YlACO1* overexpression leads to an increased CA conversion into ICA inside the mitochondria, which is then exported into the cytosol, where it is metabolized into αKG while simultaneously synthesizing NADP(H).

Strain	Glucose	Glucose + H₂O₂	Citrate	Oxaloacetate	α-Ketoglutarate	Acetate
H222						
oACO1						
Δ YHM2						
Δ YHM2 oACO1						
ΔCTP1						
ΔCTP1Δ YHM2						
o YHM2						
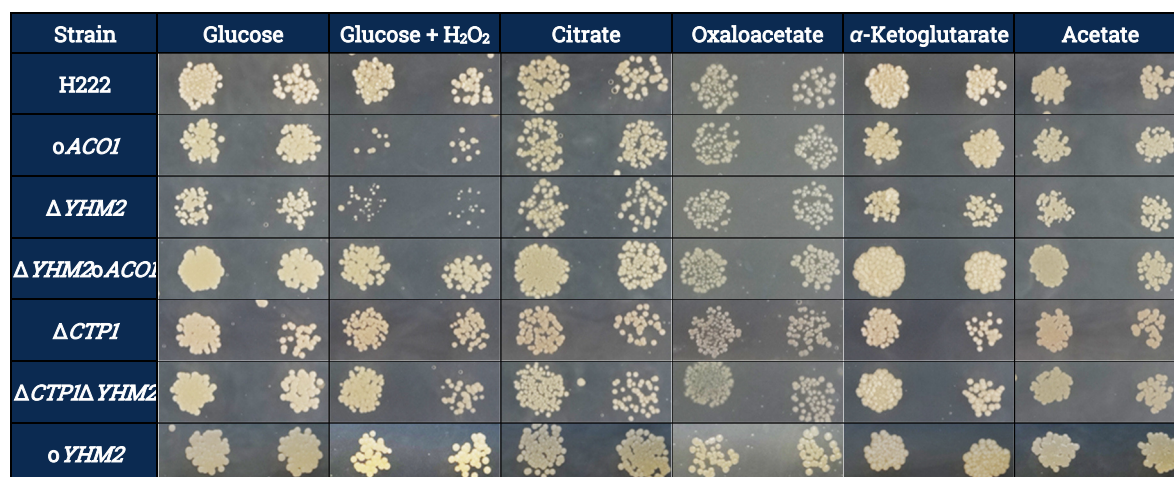
Figure 39 Growth behaviour of the constructed *Y. lipolytica* strains on minimal medium with various carbon sources.
The genetically altered strains and the wild type strain (H222) were cultivated either with 1 % (w/v) citrate, oxaloacetate, α-ketoglutarate, acetate, glucose or glucose + 1.25 mM H_2O_2 supplemented minimal medium. o*ACO1*/o *YHM2* – single-copy overexpression of *ACO1*/ *YHM2* under control of the *TEF1* promoter integrated into a non-coding region on chromosome C or B, respectively; *ΔYHM2*/*ΔCTP1* – disrupted for the respective carrier protein (with the help of the URA blaster system); *ΔYHM2*/*ΔCTP1* – both genes that encode tricarboxylate carriers were deleted; *ΔYHM2*o*ACO1* – single-copy overexpression of *ACO1* under control of *TEF1* promoter into the strain *ΔYHM2*. Ten-fold serial dilutions of 10^2 cells (pre-cultivated overnight in liquid YPD full medium at 28 °C and 220 rpm) were dripped onto solid minimal medium and cultivated for 48 h at 28 °C.

3.2.4. Aconitase activity of the constructed *Y. lipolytica* strains

The enzyme aconitase plays an integral part in the TCA. It converts CA into ICA via *cis*-aconitate as an intermediate. In 2009, Holz et al. introduced multiple copies of the native *YlACO1* gene under the control of the native promoter into the oleaginous yeast *Y. lipolytica*. The following enhanced aconitase activity caused an increase in the isomerisation rate of CA into ICA. Therefore, the ICA:CA ratio shifted into the favour of ICA on fermentable, non-fermentable and hydrophobic substrates.

In this study, *YlACO1* was overexpressed in single copy under the control of the strong constitutive *TEF1* promoter, because multicopy overexpression transformants targeting the rDNA often exhibit a delayed growth phenotype (personal observation). Since, another strategy was followed in this work to overexpress *YlACO1* compared to Holz et al. (2009), it was detrimental to ensure, in fact, enhanced aconitase activity. Thus, the enzymatic activity of aconitase was determined not just for the overexpression strains (o*ACO1* & Δ *YHM2*o*ACO1*) but for all constructed strains. This approach also had another advantage: it allowed further insight on the protein level into the consequences the genetic modifications had on one main step of the TCA. More specifically, this way it was possible to test, whether the deletions of the transporter(s) influenced the isomerisation step of CA inside the mitochondrion catalysed by aconitase. The yeast cells needed for the enzyme assay were all cultivated for 16 h in minimal medium under conditions for unrestricted growth (no N exhaustion) and with 5 %(w/v) glucose as C-source.

The results, represented in figure 40, show that the *YlACO1* overexpression was successful. Both strains exhibited a drastic increase in aconitase activity. The integration of the *YlACO1* gene

under the control of the *TEF1* promoter led to a 3.2-fold increase in the *YlYHM2*-deleted strain Δ*YHM2*o*ACO1* compared to H222. For strain o*ACO1,* the effect was even stronger (3.7-fold).

Overexpression of *YlYHM2* had no significant effect on the aconitase activity in comparison to the wild type strain. Conversely, all strains with disrupted tricarboxylate carriers had in common, that the observed aconitase activity was heavily reduced. Strain Δ*YHM2* was affected the most. It showed only 36 % of the wild type's ICA conversion rate. For strains Δ*CTP1* and Δ*YHM2*Δ*CTP1*, the reduction was less severe, but the activity levels were still significantly lower than in the wild type. The changes in the conversion rate of ICA were 0.4-fold lower after the deletion of *YlCTP1* and 0.3-fold lower with both deleted citrate transporters. This outcome gave ground to infer, that the lack in CA export out of the mitochondrion led to compensatory mechanisms in the metabolism of the yeast. At least parts of the TCA were downregulated in response to the deletion of *YlCTP1* and/or *YlYHM2*. The downregulation could help prevent the cell from toxic impacts by too high intramitochondrial CA levels.
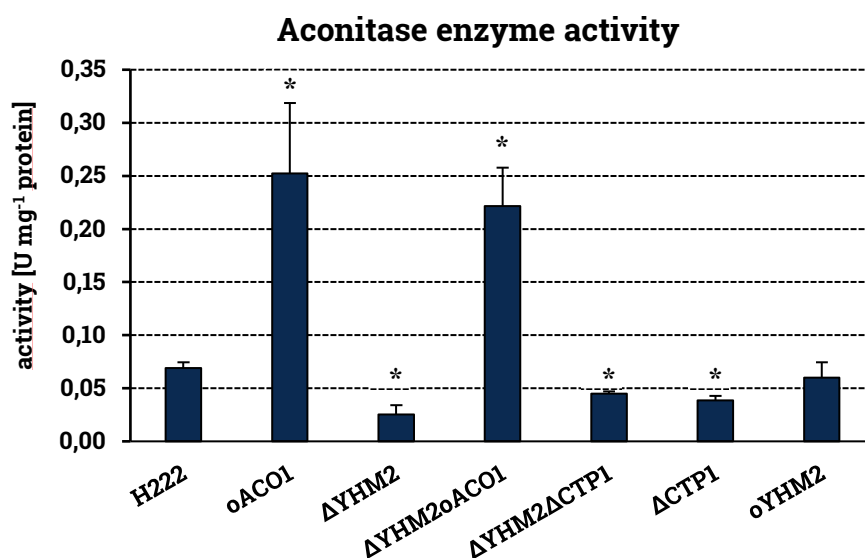
Figure 40 Enzyme assay for the activity of aconitase (Aco1p) in genetically modified *Y. lipolytica* strains.
The conversion of isocitrate to *cis*-aconitate was measured photometrically for 4 min at a wavelength of $\lambda = 240$ nm. The reaction was catalysed by the aconitase containing raw protein extract. The yeast cells were pre-cultivated overnight in YPD medium. The main cultures were incubated for 16 h in minimal medium with 50 g l^{-1} glucose. H222 – wild type, o*ACO1* – single copy overexpression of *YlACO1*, Δ*YHM2* – disruption of the gene coding for the citrate transporter *YlYHM2*, Δ*YHM2*o*ACO1* – single copy overexpression of *YlACO1* in combination with the deletion of *YlYHM2*, Δ*YHM2*Δ*CTP1* – disruption of both genes which code for a mitochondrial citrate transporter *YlCTP1* & *YlYHM2*, Δ*CTP1* – deletion of *YlCTP1*, o*YHM2* – single copy overexpression of *YlYHM2*. Shown are the means of four independent measurements with error bars for standard deviations. Asterisks (*) – statistically significant differences detected with one-tailed t-test relative to the measured activity for the control strain *Y. lipolytica* H222, $p < 0.05$.

3.2.5. Screening of constructed strains for isocitric acid production

The two targets, Ctp1p and Yhm2p, were the only two proteins known to exports significant amounts of CA out of the mitochondria. The working hypothesis therefore was, that the deletion of one or both transport proteins would lead to an observable change in the production pattern of CA and ICA. To test the effect of the genetic alterations on the CA/ICA acid metabolism, the constructed *Y. lipolytica* strains were cultivated under conditions for acid secretion. This was achieved by growing the cells for 5 d in minimal medium with a limited N supply but an excess in C source (Holz et al., 2009; Kruse et al., 2004; Mauersberger et al., 2003).

Figure 41 illustrates the resulting acid producing capabilities of the individual strains. Solely upregulating the *YlACO1* gene already brought a significant rise in the proportion of ICA with it. The ICA:CA ratio rose from 12.5 % (wild type) to 18.4 % with glucose and from 49.3 % to 59.0 % with sunflower seed oil. Also, the total concentration of CA and ICA greatly increased. Strain o*ACO1* produced 9 % more CA and ICA with the hydrophobic substrate than strain H222. With the simple sugar, the increase was almost three-fold (263 %) for both acids combined. The overexpression of the citrate transporter Yhm2p had no effect on product pattern. Surprisingly, the export rate of CA was not augmented. On the contrary, much less CA and ICA were secreted with this genetic modification.

The disruption of the CA transporter Ctp1p had no impact on the ICA:CA product ratio when grown with the hydrophobic substrate. However, the total acid concentration decreased. This decrease was also observable when cultivated with glucose. Only marginal concentrations of CA and ICA were secreted into the surrounding medium. The ICA concentration however was increased compared to CA (ICA:CA = 18.0 %).

The deletion of *YlYHM2* had the strongest effect: with glucose, the total amount of secreted ICA was increased by almost 340 % to 1582 mg l^{-1} compared to the wild type. Simultaneously, CA secretion was diminished to levels of less than 17 %. In the supernatant, 83 % of the organic acids constituted for ICA. After strain o*ACO1*, this constituted for the second highest ICA production but the overall highest elevation in the ICA:CA ratio. Even greater results were attained with sunflower oil as C source. In this case, strain Δ*YHM2* produced the highest total (24.5 g l^{-1} ICA) and relative amount (88.3 %) of ICA.

The attempt of further increase the productivity of this exceptional strain, by additionally overexpressing *YlACO1*, was not successful. The acid production suffered immensely when glucose was fed. Merely base levels of CA and ICA were detected in the supernatant. When cultivated with hydrophobic substrate, again more CA was secreted. However, the ICA:CA ratio shifted back drastically in favour of CA for both C sources: 26.9 % with glucose and 59.4 % with sunflower oil.

ICA & CA production pattern of *Y. lipolytica* strains

ICA & CA concentrations
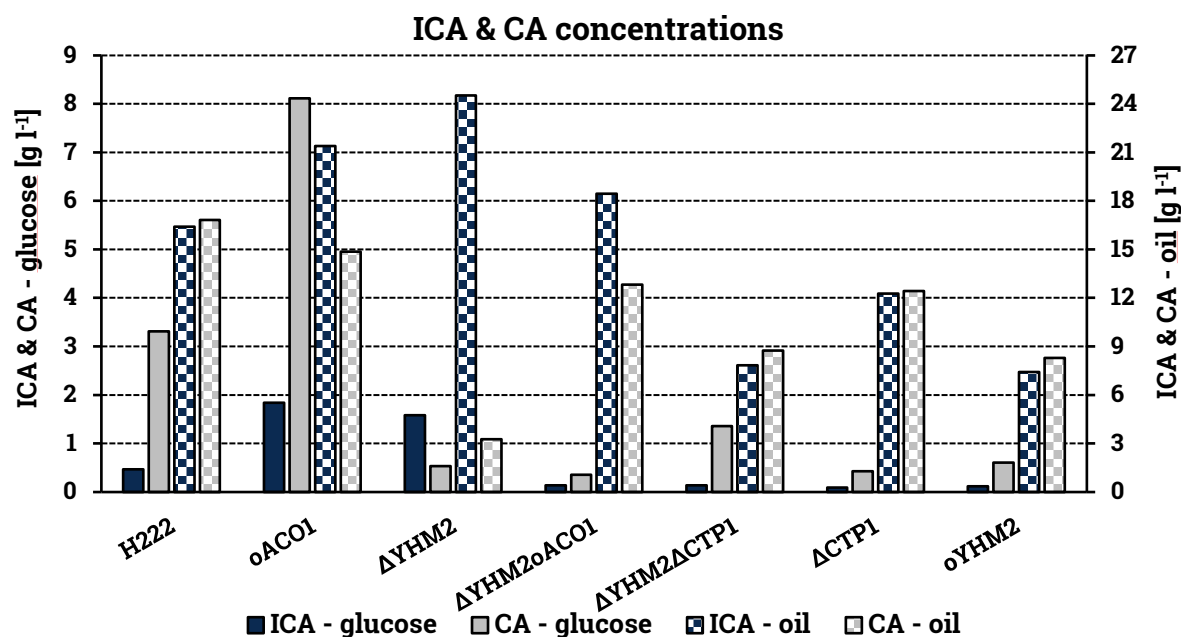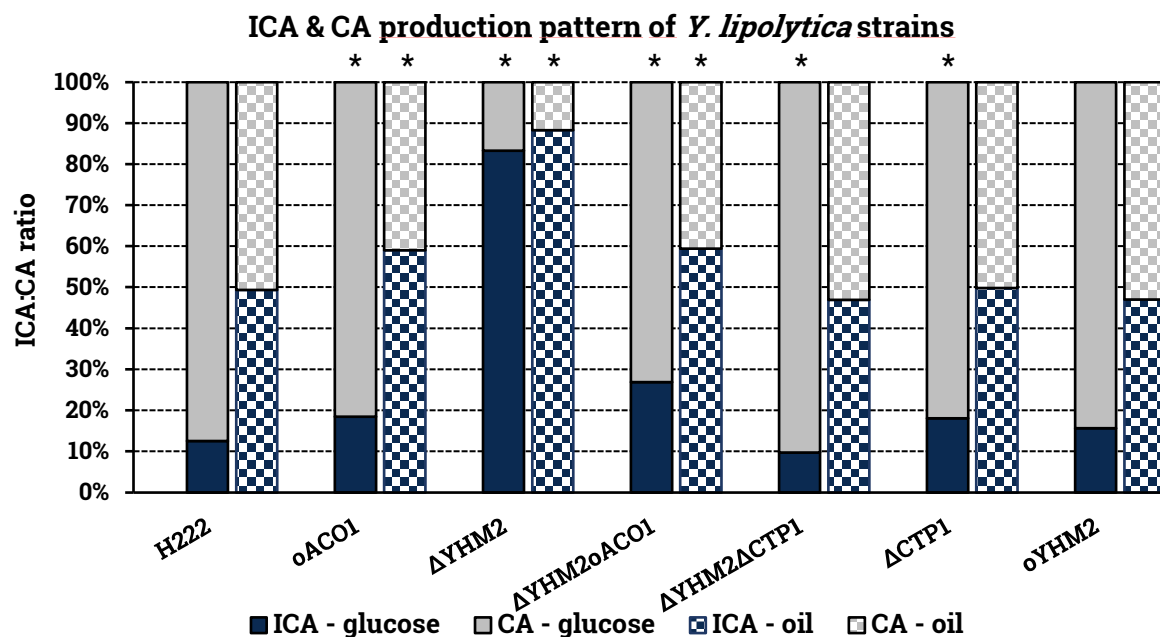
Strain	Characteristics	Sunflower seed oil			Glucose		
		ICA [g l⁻¹]	CA [g l⁻¹]	ICA [%]	ICA [g l⁻¹]	CA [g l⁻¹]	ICA [%]
H222	WT	16.4 ±1.2	16.8 ±0.7	49.3 ±1.4	0.5 ±0.1	3.3 ±0.6	12.5 ±1.8
H222-SW2-1(pIntC-TEF-*ACO1*)	o*ACO1*	21.4 ±2.7	14.9 ±1.5	59.0 ±1.3*	1.8 ±0.5	8.1 ±2.2	18.4 ±0.6*
H222-SW2-1(Δ*YHM2::URA3*)	Δ*YHM2*	24.5 ±1.3	3.3 ±0.5	88.3 ±1.4*	1.6 ±0.9	0.5 ±0.5	83.2 ±12.8*
H222-SW2-1-Δ*YHM2*(pIntC-TEF-*ACO1*)	Δ*YHM2*o*ACO1*	18.4 ±3.0	12.8 ±3.2	59.4 ±2.3*	0.1 ±0.1	0.4 ±0.1	26.9 ±4.4*
H222-SW2-1-Δ*YHM2*(Δ*CTP1::URA3*)	Δ*YHM2*Δ*CTP1*	7.8 ±2.3	8.8 ±2.2	46.9 ±3.0	0.1 ±0.0	1.4 ±0.4	9.7 ±2.3*
H222-SW2-1(Δ*CTP1::URA3*)	Δ*CTP1*	12.3 ±1.6	12.4 ±2.1	49.8 ±1.3	0.1 ±0.0	0.4 ±0.0	18.0 ±1.7*
H222-SW2-1(pIntB-TEF-*YHM2*)	o*YHM2*	7.4 ±2.5	8.3 ±2.6	47.0 ±0.8	0.1 ±0.0	0.6 ±0.1	15.6 ±3.2

Figure 41 Screening of constructed *Y. lipolytica* strains for the production of ICA.
Top: proportions of ICA to CA for the different yeast strains with glucose or sunflower seed oil as carbon source. Bottom: absolute concentrations of secreted ICA and CA, respectively. Shown are the averages for glucose (filled collumns; n ≥ 5) and sunflower seed oil (checkered columns; n ≥ 3). Cells were grown for 5 d at 28 °C, 220 rpm in minimal ICA production medium with 50 g l⁻¹ glucose as C source in 3 ml-well cultures or with 10 % (v/v) sunflowerseed oil in 50 ml-baffled flask cultures. Asterisks (*) − statistically significant differences detected with one-tailed t-test relative to the control strain *Y. lipolytica* H222, p < 0.05.

The *Y. lipolytica* strain with the combined deletion of *YlYHM2* and *YlCTP1* performed very poorly when hydrophobic substrates were available as C source. The product pattern did not change compared to the wild type, but overall much less acid was secreted. The acid production with the simple sugar as substrate however led to an interesting phenomenon. Strain $\Delta YHM2 \Delta CTP1$ formed considerably more CA than the strain in which only the *YlCTP1* gene was disrupted. Since the ICA secretion remained low with this strain, the resulting ICA:CA (9.7 %) was even lower than that of the wild type.

Since little information about the two transport proteins in yeasts is available, the function of Ctp1p and Yhm2p in *Y. lipolytica* was still unclear up until this point. Considering this screening process, it appeared that both expected tricarboxylate carriers, in fact, are responsible for the transport of CA and/or ICA out of the mitochondrion. Deleting one of the coding genes, detrimentally impacted the amount of secreted acids. This observation was notably pronounced when the yeast cells were fed with glucose. When *YlYHM2* was deleted and Ctp1p represented the remaining citrate carrier, mainly ICA was secreted. This indicates that Ctp1p displays a higher affinity for ICA. However, after deleting solely *YlCTP1,* the secretion of CA and ICA collapsed, giving rise to the assumption that Ctp1p represents the main carrier for CA and ICA.

From the standpoint of overproducing ICA, solely strain $\Delta YHM2$ represented a viable candidate for the microbial synthesis of ICA. This yeast strain was able to generate exceedingly high concentrations of ICA in small to medium culture volumes with two different C sources. In addition to that, the concentration of the isomer, CA was nominal.

3.2.6. Isocitrate production under production conditions

During the screening, it appeared evident that *Y. lipolytica* strain $\Delta YHM2$ was the most promising ICA producer. It, therefore, seemed necessary to further elucidate its capabilities of secreting high concentrations of ICA with only marginal CA amounts.

Thus, large volume fed-batch cultivations of strain $\Delta YHM2$ were carried out in a bioreactor under well-defined conditions. The fermentations were conducted in a total volume of 600 ml minimal medium with either 15 % (w/v) glucose or 10 % (v/v) sunflower seed oil as the initial C source. In doing so, the cultivations had in common that during the first 24 h rapid cell multiplication was observable. During this time period approximately 20 g l^{-1} dry biomass was generated. In the same time, almost no ICA nor CA was produced. With the beginning of the 2nd day, after the available nitrogen was depleted and the cell growth slowed down, the synthesis of ICA and CA set in.

Figure 42 illustrates that by fermenting with glucose, a steady, linearly increasing ICA synthesis was achieved. Over the course of 5 d, 22.0 g l^{-1} ICA and merely 1.5 g l^{-1} CA were formed. This amounts to an endpoint ICA:CA ratio of 94 %. By supplying sunflower seed oil as the C source, the productivity rate for ICA was significantly heightened. Per day 26.4 g l^{-1} ICA were secreted into the

medium. At the end of fermentation, a final concentration of 131.9 g l^{-1} ICA was measured. The heightened ICA production came along with also elevated amounts of by-products. More resources were allocated for the formation of biomass (final concentration: 27.2 g l^{-1} DCW) and the synthesis of CA (final concentration: 16.5 g l^{-1} CA). Because of the still elevated CA production, the ICA:CA ratio was lower with sunflower seed oil.

	No itaconate		25 mM itaconate	
C-source	glucose	sunflower oil	glucose	sunflower oil
ICA content [g l^{-1}]	22.0	131.9	21.3	108.2*
CA content [g l^{-1}]	1.5	16.5	0.9	30.5*
ICA:CA ratio (end)	94 %	89 %	96 %*	78 %*
pooled ICA:CA ratio (2.-5. d)	95 %	89 %	97 %*	76 %*
ICA productivity [g l^{-1} d^{-1}]	4.4	26.4	4.3	21.6
DCW [g l^{-1}]	22.6	27.2	29.1*	27.2
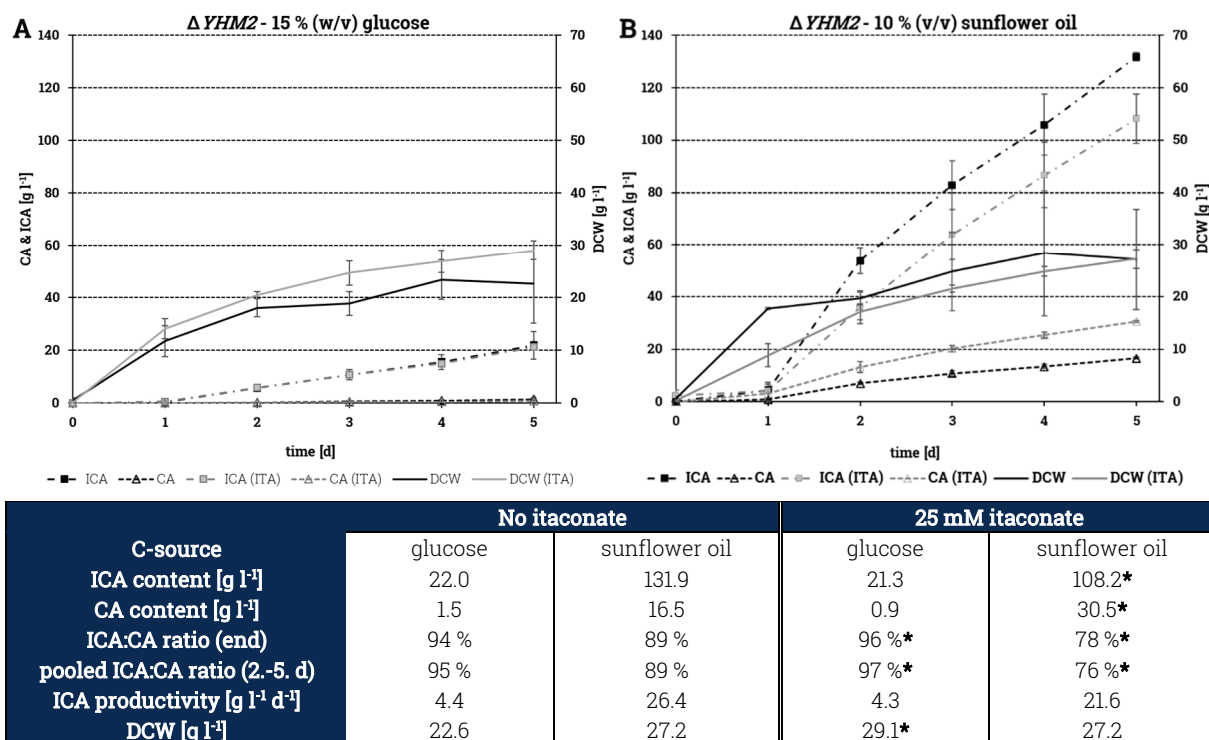
Figure 42 Large-scale cultivation in 600 ml-bioreactor with the ICA producing strain *Y. lipolytica* Δ*YHM2*. The cells were incubated for 5 d at pH 5.5, 28 °C and an oxygen saturation of 55 %. Minimal medium with either 15 % (w/v) glucose (A) or 10 % (v/v) sunflower oil (B) as initial C source was used as substrate. Every 24 h, the amounts of produced isocitrate (ICA) and citrate (CA) were determined as well as the dry cell weight (DCW). Grey lines – cultivation under identical conditions and the initial supplementation of 25 mM itaconic acid (ITA) to the medium. Values are the average of two fermentations with error bars shown for standard deviation. Asterisks (*) – significant influence detected by two-way analysis of variance (ANOVA) with post hoc Holm-Sidak test, P < 0.05.

3.2.6.1. Effect of itaconate on the isocitric acid production

Itaconic acid is also an organic acid. It is known to be a natural inhibitor of the isocitrate lyase (Icl1p), a key enzyme needed in the glyoxylate shunt. Icl1p catalyses an important step in the metabolism of ICA. The enzyme is responsible for the cleavage of ICA into glyoxylate and succinic acid. This metabolic pathway is active in the peroxisomes. The group around Kamzolova (2015, 2016, 2018) demonstrated that the addition of this inhibitory agent to the culture medium of ICA producing *Y. lipolytica* strains, shifted the product ratio in the favour of ICA. It appeared, therefore, logical to investigate the effect of ITA on the ICA production performance of strain Δ*YHM2*. For this purpose, the two above-described fed-batch cultivations were conducted again with the initial supplementation of 25 mM ITA in the medium.

Figure 42 shows (grey lines), that the addition of ITA led to a significant increase in the build-up of biomass when cultivated with glucose. At the end of fermentation 29.1 g l^{-1} DCW were generated

compared to 22.6 g l^{-1} (without ITA). However, the elevated biomass had no significant negative impact on the synthesis of ICA. In total 3 % less ICA were secreted in the presence of the inhibitor, but the concentration of CA was reduced by 40 % to a final concentration of only 0.9 g l^{-1} CA. Thus, an enhanced ICA:CA ratio of at least 96 % was registered.

Inhibiting Icl1p in *Y. lipolytica* strain Δ*YHM2* while feeding the hydrophobic substrate, led to a very distinct consequence. Instead of further increasing the ICA production, the opposite was observed. The final ICA concentration was reduced to 108.2 g l^{-1} while the CA concentration almost doubled (final concentration: 30.5 g l^{-1} CA). As a result, the ICA:CA ratio shifted back exceedingly in favour of CA (ICA:CA: 78 %).

Overall, strain Δ*YHM2* demonstrated exceptional ICA producing capabilities. Up to 131.9 g l^{-1} ICA with a high ICA:CA ratio could be synthesised. With a simple, fermentable sugar as C source, almost exclusively ICA was secreted. Further optimizing the ICA production by the supplementation of ITA and thus the consequential blocking of the glyoxylate shunt was partly beneficial to produce ICA with *Y. lipolytica* Δ*YHM2*. The usefulness of this inhibitor seemed to depend on the underlying metabolic pathway. A significant improvement was achieved when the glycolysis fuelled the tricarboxylate cycle. As a result, a near CA-free supernatant was achieved. The ICA production was adversely affected when metabolites for the TCA originated mainly from β-oxidation of fatty acids. The additional overexpression of *YlACO1* did not prove to be an advantageous strategy at all to improve Δ*YHM2* strain's ICA forming capacity.

4. Discussion

The bio-production of certain organic acids has gained momentum only in the past decade. ITA is one of these versatile platform chemicals that can replace petroleum-based chemicals like acrylic acid (De Guzman, 2009; El-Imam and Du, 2014). At the present time, ITA is still produced with the fungus *A. terreus*. However, due to several drawbacks, like sensitivities towards impurities in the medium and difficult oxygen supply due to its hyphal growth, alternatives to *A. terreus* have been investigated (Klement et al., 2012; Zambanini et al., 2017). In contrast, ICA is an organic acid still produced in fine chemical quantities. With an ever more developing applicability of ICA for pharmaceuticals and nutritional supplements, the demand for it also rises (Aurich et al., 2012; Kamzolova et al., 2018; Moore et al., 2017; Rivera-Angulo and Peña-Ortega, 2014). To this day, no adequate ICA production strains nor fermentation processes have been established.

The scope of this study consisted of the phenotypic and genotypic optimization of two not related yeasts, namely *P. tsukubaensis* and *Y. lipolytica* for the microbial production of ITA and ICA from their common precursor *cis*-aconitate, respectively. Concerning *P. tsukubaensis,* the focus lied on the identification of genes involved in the ITA biosynthesis. Subsequently, a production strain was established through the means of genetic engineering. Then, the ITA production capabilities of the resulting strain were improved by adjusting the fermentation conditions such as the composition of the cultivation medium.

Furthermore, genes encoding CA carrier proteins were identified in the yeast *Y. lipolytica*. The impact of the respective CA transporter on the ICA:CA homeostasis was assessed. After selecting an advantageous ICA overproducing strain, its capacity to secrete ICA under production conditions was examined.

4.1. Identification of minimal medium for *P. tsukubaensis*

In the beginning, the minimal medium composition according to Kawamura et al. (1981, 1982) was used. Because of its complex and varying composition, the containing CSL had to be substituted with an ingredient that offers consistent quality. Two supplements, namely inositol and thiamine hydrochloride, enabled the growth of *P. tsukubaensis* wild type H488 in the minimal medium with glucose as C source. These two substances were critical factors for the optimal growth of strain H488 consistent with the long known fact that thiamine and inositol induce the growth of certain yeast strains (Lochhead and Landerkin, 1942; Williams et al., 1940).

Inositol is needed for the cultivation of *S. cerevisiae* and its related species. Thiamine on the other hand, is only required for some *S. cerevisiae* strains (Spencer et al., 1997). Although, many yeasts show a deficiency for biotin, several *Candida* species are dependent on thiamine instead. In fungi thiamine deficiencies occur commonly, for example in *Hormodendron pedrosoi, Phialophora*

verrucosa & *Sporotrichum schenckii* (Burkholder and Moyer, 1943). It is remarkable, that the two structurally very distinct compounds, thiamine and inositol, which do not share a common metabolic pathway, both enable growth in *P. tsukubaensis* on their own. The underlying mechanisms for that phenomenon are still unclear. However, a similar occurrence has been described for the fungus *Trichophyton faviforme* (Burkholder and Moyer, 1943).

4.2. Nitrogen and phosphate dependency on growth and acid production

It is a well-known phenomenon for certain microorganisms to secrete organic acids under stressful cultivation conditions. Secondary substrate limitation is a stressor and is a general requirement for the unusually high production and accumulation of organic acids by the microorganisms under study. Commonly, N starvation is applied for the microbial production of organic acids. N limitation is used e.g. for the secretion of fumaric acid by *Rhizopus arrhizus*, MA production by *A. flavus* or CA secretion by *Candida / Yarrowia* strains (Barth, 2013; Battat et al., 1991; Goldberg et al., 2006; Kenealy et al., 1986; Mattey, 1992).

For the more closely related yeast species *U. maydis* and *P. antarctica*, it was described that N limitation represents a crucial factor for the enhanced formation of ITA. *P. antarctica* showed an optimal ITA production behaviour with 2 g l^{-1} (NH$_4$)$_2$SO$_4$ where a maximum of 16.7 g l^{-1} ITA was produced under controlled conditions. Further decreasing the N concentration (1 g l^{-1}) lowered the productivity rate but enhanced the yield to some degree (Levinson et al., 2006). *U. maydis* started producing ITA right after the available ammonium in the medium was depleted. With over 20 g l^{-1} ITA, the corn smut caused the yeast to produce the highest amounts of the organic acid when the initial NH$_4$Cl-concentration was limited to 0.8-1.6 g l^{-1}. Further increasing the available N source led to a drop-off in product concentrations (Klement et al., 2012). However, the results of Maassen et al. (2014) painted a slightly different picture. Under pH- and oxygen-controlled conditions, *U. maydis* secreted the most ITA with 4 g l^{-1} NH$_4$Cl.

In other cases, it is reported that P starvation triggers the organic acid production. A link between the synthesis of ITA and a P limitation for example was postulated for *A. terreus* in 1975 by Elnaghy and Megalla. Similar results were published by Rychtera and Wase (1981). KH$_2$PO$_4$ concentrations in the medium as low as 0.1 g l^{-1} have been reported to be most beneficial for ITA production with this fungus (Kuenz, 2008). This phenomenon is described, in that the P limitation is forcing the fungus into the stationary growth phase, which is followed by the induction of ITA production. The reason behind this is that low P levels lead to a decoupling of the glycolysis and the respiration. As a result, the microorganism increases the metabolic flux of glucose through the glycolysis to *cis*-aconitate and into ITA (Haldenwang and Behrens, 1983; Klement and Büchs, 2013; Welter, 2000).

In this study, it was shown that a secondary substrate limitation is also favourable for the ITA production with *P. tsukubaensis*. Correspondingly, high initial concentrations of N and P (10:0.4) did not entail a significant secretion of organic acids. Like the results of Maassen et al. (2014), N concentration equal to or below 5 g l^{-1} did prove to be most beneficial. However, akin to experiments with *A. terreus* low P levels had a more decisive impact on the formation of ITA in *P. tsukubaensis*.

Additionally, the microwell-cultivation (see figure 27) showed that the induction of ITA synthesis is intricately controlled in this yeast. For very low P concentrations, the competing MA was produced. The optimal concentration of P to produce both organic acids was at 0.15 g l^{-1} KH$_2$PO$_4$. Organic acid production dropped off sharply for P concentrations above that value. Interestingly, at KH$_2$PO$_4$ concentrations between 0.05-0.1 g l^{-1} the secretion of MA was lowered by an amount that corresponds to the produced concentration of ITA.

From this data, it can be concluded that the induced ITA pathway was consuming precursors from the TCA cycle and thus slowing down MA production. The TCA cycle activity was potentially highest at 0.15 g l^{-1} KH$_2$PO$_4$ by what the metabolic flux was sufficiently supplying both ITA and MA biosynthesis. However, the detailed underlying control mechanisms for the induction of the acid synthesis, especially, the selective triggering of MA or ITA, are still unknown.

The above-described decoupling of the glycolysis and respiration appears also plausible for *P. tsukubaensis*. The low P levels decrease the adenosine triphosphate (ATP) concentration in the cell. Because of little available P, the oxidative phosphorylation is diminished. To replenish ATP, the substrate-level phosphorylation steps during glycolysis and TCA are enhanced. An increased activity of the TCA also explains increased MA concentration since this organic acid is one of the main intermediates of this pathway. At a certain P level in the cell, the ITA cluster genes are potentially upregulated. This would explain, why solely MA is secreted at very low P concentrations and ITA production is induced with increasing P levels (Haldenwang and Behrens, 1983; Klement and Büchs, 2013).

For the *P. tsukubaensis* wild type strain H488, Bodinus (2011) also described that ITA secretion set in after N and P were exhausted in the medium. Contrary to the present study, Bodinus detected the highest ITA concentration of 3.5 g l^{-1} with only 0.05 g l^{-1} KH$_2$PO$_4$. However, in the medium used by Bodinus, CSL represented an additional P source. Thus, the exact P concentration in the medium was unclear. According to the data of Kalscheur et al. (2008), CSL contains approximately 2 % phosphorus. Therefore, the final P concentration in Bodinus' medium should be well above 0.05 g l^{-1} and closer to 0.15 g l^{-1}. This would substantiate the P optimum identified in the present study.

The assumption of P limitation as the main trigger for ITA production in *A. terreus*, however, has been refuted by now. Neither a limitation in N nor P is needed for the induction of ITA synthesis by this fungus (Hevekerl et al., 2014b, 2014a; Krull et al., 2017; Kuenz and Krull, 2018).

Despite the gained insight into the potential triggering of ITA production by secondary substrate limitation in *P. tsukubaensis*, the overexpression of the *PtRIA1* gene rendered the complete regulatory mechanism redundant. This was an extremely advantageous finding for this study. The ITA synthesis proved to be completely uncoupled from the available P and N concentrations. Furthermore, production of ITA did not follow any growth phases. The organic acid was continuously secreted in high amounts from the beginning of cell growth through stationary phase until the death phase. Cultivations in the bioreactor but also 12-well plate indicated that high biomass resulted in high ITA concentrations. The ITA productivity only reduced when the number of vital cells declined due to cell death. Therefore, the single limiting factor appeared to be solely the cell mass.

4.3. Promoter strength in *P. tsukubaensis*

One important objective of this study was to identify a strong transcriptional regulatory component in *P. tsukubaensis* to ensure a strong and steady gene transcription and thus ITA production. With the help of this information, a suitable promoter sequence for the overexpression of target genes ought to be identified. For this purpose, the *E. coli* *β*-galactosidase protein served as the reporter protein. Five different promoter sequences were examined regarding their transcriptional activity profiles. For one, the HSP70 promoter from *U. maydis* was considered as a benchmark sequence. This promoter was already successfully applied in *P. tsukubaensis* itself and also in the closely related yeast species *P. flocculosa* and *P. antarctica* (Avis et al., 2005, 2008; Bodinus, 2011; Neveu et al., 2007a). Additionally, four novel native promoter sequences were discovered, namely those of *PtActin1*, *PtGAPDH*, *PtHSP70* and the *PtTEF1* genes. These genes were selected because they are well-known housekeeping genes which are described as being highly and constitutively expressed (Gatignol et al., 1990; Holland and Holland, 1979; Kitamoto et al., 1998; Kojic and Holloman, 2000; Matheucci Jr et al., 1995; McDade and Cox, 2001; Müller et al., 1998; Slater and Craig, 1987). The *α*-glucosidase promoter was first taken into consideration, too. However, the *P. tsukubaensis* *α*-glucosidase promoter yielded suboptimal results in *P. flocculosa* compared to the *U. maydis* HSP70-promoter (Avis et al., 2008).

A considerable *β*-galactosidase expression level was achieved with every tested promoter sequence. Striking was the variability among different transformants which contain the same overexpression construct. This variation was similar regardless of the promoter. Variations of this type have been observed in several other promoter studies in the genus of *Pseudozyma* (Avis et al., 2008; Neveu et al., 2007b, 2007a). It is believed that the variability stems from variation in the

copy number and regional effects as a consequence of the genetic location of the insertion loci (Avis et al., 2008; Cheng et al., 2001). The sequencing data of *P. tsukubaensis* strain HR12 underscores this hypothesis. A very strong transcriptional activation of *PtRIA1* was obtained by a two-time integration of the construct in tandem orientation into the genome. On the other hand, the sequencing also showed that parts of the vector were not incorporated into the genome. It is, therefore, possible that in some transformants the promoter sequence was truncated during the integration into the genome. A potentially shortened promoter sequence could lead to the reduced expression levels that were observed in some transformants due to the loss of key transcription factor binding sites.

On a comparative basis, very similar expression profiles were obtained with the various promoters and the different growth media. This is also true for the *U. maydis* HSP70 promoter that served as reference. Previously, it was postulated that *Pseudozyma* species, like other microorganisms, display a high specificity in regard to transcriptional regulatory elements (Godio et al., 2004; Mooibroek et al., 1990; Neveu et al., 2007a; Schillberg et al., 2000). Different heterologous promoter sequences from distant yeast relatives and ascomycetes failed completely to yield protein production in *P. flocculosa*. Even heterologous promoters from more closely related species e.g. GAPDH- & HSP70-promoters from *U. maydis* and *P. tsukubaensis* *α*-glucosidase-promoter showed less activity than comparable native sequences in *P. flocculosa*. The same phenomenon was described for the *P. flocculosa* GAPDH-promoter in *P. antarctica* (Avis et al., 2008; Cheng et al., 2001; Neveu et al., 2007b, 2007a).

Here, the TEF-promoter sequence generally led to low protein expression, but its transcriptional activity proved to be comparatively high in isolated cases. This was also true for pHSP70 and pUmHSP70. Both HSP70 promoters drove similar if not higher *β*-galactosidase expression rates than the other constitutive housekeeping-promoter sequences. For transformants with the pTEF construct, the reason behind this could be differences in the copy number and truncation of the promoter sequence, as already mentioned. One possible explanation for this occurrence with HSP70 promoter sequences are differences in the degree of stress exhibited by the yeast cells. It is known that the HSP70 promoter's function is dependent on the induction by stressors. The group around Avis (2008) showed an up to 6-fold increase in UmHSP70 promoter activity in *P. flocculosa* in the presence of elevated hygromycin concentrations. In this study, the highest *β*-galactosidase activities on average, however, were obtained under the control of the native promoters pActin and pGAPDH. The homologous sequences tested favourably in the native host *P. flocculosa* as well (Neveu et al., 2007b, 2007a). Although, all test conditions considered, pActin showed the highest activities. This is the reason why we recommend use of pActin in future studies with *P. tsukubaensis*.

4.4. Genes involved in the biosynthesis of ITA in *P. tsukubaensis*

In the present study, we were able to demonstrate that the genome of the basidiomycetous yeast *P. tsukubaensis* is highly similar to that of the closely related smut fungus *U. maydis* and other *Ustilaginaceae*. We could not only plot the majority of the *P. tsukubaensis* genome against that of *U. maydis,* but their genome size and GC content resemble each other too (see table 16). Analogous to our findings, the DNA sequence of *P. antarctica* T-34 displays a remarkable degree of synteny to the genome of *U. maydis* (Morita et al., 2014). The nuclear draft genome of *P. antarctica* is 18.0-18.1 Mb large and therefore significantly smaller than that of *P. tsukubaensis*. Its DNA holds a GC content of 60.9 % and contains 6543-6845 automatically predicted protein-coding genes (Morita et al., 2013; Saika et al., 2014). For *P. tsukubaensis* a lower GC content of 52.6 % but more putative ORFs (7017) were predicted. With 20.5 Mb is the genome of *P. tsukubaensis* also larger than that of other related yeasts like *P. aphidis* (17.92 Mb, GC content: 61.2 %; Lorenz et al., 2014) and *P. hubeiensis* (18.44 Mb, GC content: 56.5 %, 7523 putative ORFs; Konishi et al., 2013). An electrophoretic karyotype indicated that the genome of *P. flocculosa* has only a size of 15 Mb and is therefore even smaller (Cheng et al., 2001). The *P. tsukubaensis* NBRC 1940 species sequenced by Geiser et al. (2016c) displayed an even larger genome of 23.8 Mb. The size differences in the genomes exist despite their close phylogenetic relationships and the similar habitats, in that they are phyllosphere yeasts located on the surface of leaves (Boro et al., 2017; Kitamoto et al., 2011; Morita et al., 2010b; Wang et al., 2006). One possible explanation could be, that the yeasts adapt to their specific host plant and this is reflected in their genome size. Another possibility is, that the disparities between genome sizes are due to differences in the number of transposable elements. Activities of transposable elements are very fast and can amplify the transposable copy number up to 20-100 copies (~0.1-1 Mbp) in a single generation (Mohanta and Bae, 2015).

Several different ITA producing organism are known. Most of them are fungi, including the first known ITA producer *A. itaconicus* (Kinoshita, 1932) and the most widely studied species in this context, *A. terreus* (Calam et al., 1939). Several other fungi have been described in more or less detail considering their ITA generating capabilities e.g. *U. maydis* (Haskins et al., 1955), *Candida* sp. (Tabuchi et al., 1981), *Rhodotorula* sp. (Kawamura et al., 1981)*, P. antarctica* (Levinson et al., 2006) and several other members from the *Ustilaginaceae* family (Geiser et al., 2014). Recently, ITA production was also detected in mammalian immune cells (Strelko et al., 2011; Sugimoto et al., 2012).

Although, numerous ITA secreting organisms have been described, the underlying metabolic pathways have only been elucidated for *A. terreus* (Kanamasa et al., 2008; Li et al., 2011), *U. maydis* (Geiser et al., 2016a, 2016b) and mammalian macrophage cells (Michelucci et al., 2013).

The common mechanism for the mentioned producers is structured the following way (see figure 45): Glucose is taken up as the C source for the synthesis of ITA. In the course of glycolysis, the sugar is then broken down into two molecules pyruvic acid. The pyruvic acid either enters the mitochondrion and is supplied to the TCA cycle in the form of acetyl-CoA or it is converted in the cytosol into MA which is transported into the mitochondrion. The anaplerotic intermediate MA enters the TCA cycle where it is re-oxidized into oxaloacetic acid. Subsequently, the oxaloacetic acid and the acetyl-CoA undergo a condensation reaction catalysed by the mitochondrial citrate synthase. The resulting CA is enzymatically dehydrated by the aconitase enzyme into *cis*-aconitic acid, which represents the main precursor of ITA. In *A. terreus*, *cis*-aconitate is then shuttled into the cytosol potentially via an antiport mechanism possibly with an exchange for MA. Responsible for the transport is the protein MttAp (Jaklitsch et al., 1991; Steiger et al., 2013). Until recently, it was unresolved whether MttAp is definitely the carrier of *cis*-aconitate. By the means of metabolic engineering, Steiger et al. (2016) confirmed that the protein controls the export of *cis*-aconitate but not ITA. *cis*-Aconitate is directly decarboxylated in the cytosol into ITA by the enzyme *cis*-aconitate decarboxylase (Bonnarme et al., 1995; Cordes et al., 2015; Klement and Büchs, 2013). In mammalian macrophage cells, the *cis*-aconitic acid is also directly metabolized into ITA. The decarboxylation reaction is catalysed by Irg1p, a homologous protein to Cad1p. In contrast to *A. terreus,* Irg1p is not a cytosolic protein but it is localized inside the mitochondrion where the conversion of *cis*-aconitate to ITA takes place. The ITA is transported out of the mitochondrion into the cytosol or immediately into the phagosome by still unknown mechanisms (Cordes et al., 2015; Michelucci et al., 2013; Strelko et al., 2011).

In 2016, the group of Bölker found that in the smut fungus *U. maydis* the synthesis of ITA deviates from that of *A. terreus* and mammalian macrophages (Geiser et al., 2016b). The basidiomycete fungus does not harbour the enzyme which is capable of directly decarboxylating *cis*-aconitate into ITA (Cad1p/Irg1p). More specifically, *cis*-aconitate is transported from the mitochondrion into the cytosol with the help of Mtt1p which is localized in the mitochondrial membrane (Przybilla, 2014). In the cytosol it must first undergo an isomerization reaction into *trans*-aconitic acid via the enzyme Adi1p. Only this intermediate can be subsequently decarboxylated into ITA by the *trans*-aconitate decarboxylase Tad1p. The completed organic acid is exported into the surrounding medium with the help of the ITA transport protein Itp1p which is located inside the fungal cytoplasmic membrane (Geiser et al., 2016b; Przybilla, 2014). In this study it was possible to show that *P. tsukubaensis* possesses the same genes necessary to generate ITA as does *U. maydis* and that these genes are organized in a very similar cluster. This is also substantiated by the draft genome of *P. tsukubaensis* and other *Ustilaginaceae* published by Geiser et al. (2016c).Due to the fact that *P. tsukubaensis* harbours the respective homologous genes, the same metabolic pathway for the biosynthesis of ITA is very plausible.

In most *Ustilaginaceae,* instead of exporting the ITA, it can be further metabolized into 2-hydroxyparaconate by the P450 monooxygenase Cyp3p. 2-Hydroxyparaconate can then be converted into itatartarate (Geiser et al., 2016a). A homologous gene to *UmCYP3* has been identified in *A. terreus* next to its ITA cluster (Karaffa and Kubicek, 2019). However, this is most likely not the case for *P. tsukubaensis* because it lacks the gene necessary for this particular P450 monooxygenase (present data and Geiser et al., 2016c).

4.4.1. The role of Mtt1p and the effect of *AtCAD1* overexpression

The export of *cis*-aconitate into the cytosol is believed to be a rate limiting step (Jore et al., 2009). The mitochondrial tricarboxylate carrier Mtt1p is described as the responsible *cis*-aconitate transporter during ITA synthesis. Deletion studies carried out by Geiser et al. (2016b) showed that a lack in *UmMTT1* activity did not block ITA synthesis. Implicating, that other mitochondrial transporters are able to substitute the activity through functional redundancy or that other precursors are shuttled into the cytosol and are metabolized there into ITA.

Here, the overexpression of *PtMTT1* in *P. tsukubaensis* led to increases in ITA production. A minor increase not only in ITA but total acid secretion was observed for the predominant part of the transformants with the H488 background. In the M15 strain only a few *PtMTT1*-transformants showed a heightened ITA production, although the effect was much more pronounced compared to the H488 transformants. Similar results have been achieved for other microorganisms. In both *U. maydis* and *U. vetiveriae,* the enhanced transport of the precursor, *cis*-aconitate, by overexpressing the *UmMTT1* gene alone led to 1.5-2.0 fold increase in ITA production (Geiser et al., 2016b; Zambanini et al., 2017).

Furthermore, the naturally ITA-nonproducing fungus *A. niger* can be genetically altered to generate ITA by introducing the *AtCAD1* gene. It was proven by several groups, that the efficiency of the ITA synthesis of these recombinant *A. niger* strains could be further increased by co-overexpressing the heterologous gene *AtMTTA*. Gene *AtMTTA* encodes the *cis*-aconitate shuttling mitochondrial protein from *A. terreus* responsible for the transport of this tricarboxylate. In 2013, Li et al. (2013) co-overexpressed *AtCAD1* with *AtMTTA* in *A. niger.* As a consequence of the co-overexpression, the ITA synthesis was heightened 9-fold compared to the parental strain with only the introduced *AtCAD1* gene. Further improvements in this system were achieved by van der Straat et al. (2014), in that the group overexpressed the codon-optimized genes for *cis*-aconitate decarboxylase (*AtCAD**) and the mitochondrial tricarboxylate transporter (*AtMTTA**) in an oxaloacetate hydrolase and glucose oxidase deficient *A. niger* strain. The additional heterologous overexpression of *AtMTTA** resulted in an over twenty-fold increased secretion of ITA.

As illustrated in the results section, a similar approach in *P. tsukubaensis* led to analogous results. The overexpression of the *AtCAD1* gene itself in *P. tsukubaensis* had a minor positive effect on the wild type. The M15 strain was unaffected by this genetic alteration. However, when *AtCAD1* was co-overexpressed with the *PtMTT1* gene, the ITA production rose substantially. The majority of the resulting transformants produced ITA as the main product. This corroborates the results achieved with *A. niger*.

These findings suggest that a high *cis*-aconitate transport activity is crucial for an enhanced ITA production. According to that, the sole overexpression of *AtCAD1* in the M15 strain was not successful because the heterologous AtCad1p protein was competing with the natural PtAdi1p & PtTad1p proteins (which are potentially upregulated in strain M15) for the limited amount of *cis*-aconitate in the cytosol. The co-overexpression of *AtCAD1* and *PtMTT1* circumvented this bottleneck in strain M15 and allowed for a significant increase in ITA productivity.

A preliminary explanation for the phenomenon of *cis*-aconitate transport being a bottleneck could be due to a competing relationship between the export into the cytosol via Mtt1p and the mitochondrial aconitase enzyme in the TCA cycle. Potentially, the aconitase enzyme possesses a higher affinity for *cis*-aconitate than Mtt1p and, therefore, it is rather metabolized further into ICA than being exported.

It appears natural to assume that the overexpression of the gene encoding the mitochondrial tricarboxylate carrier alone is not sufficient to reliably enhance the ITA synthesis. An increased activity of the proteins responsible for the conversion of *cis*-aconitate into ITA e.g. Adi1p & Tad1p or Cad1p is needed. Nevertheless, the gene for the tricarboxylate carrier is a promising candidate for further genetic engineering approaches when it comes to increased ITA productivity. However, recent research indicates that native transporters are not always the prime choice. An *UmMTT1* deleted *U. maydis* strain was reconstituted with either an upregulated copy of the native *UmMTT1* or the *AtMTTA* gene. The results showed that the transport protein from *A. terreus* is more efficient than the native Mtt1p shuttle protein since the transformant secreted 1.3-fold more ITA (Hosseinpour Tehrani et al., 2019).

4.4.2. Function of Adi1p, Tad1p & Itp1p

In the family of the *Ustilaginaceae* the two enzymes aconitase-Δ-isomerase (Adi1p) and *trans*-aconitate decarboxylase (Tad1p) represent the two key enzymes in the formation process of ITA. Geiser et al. (2016b) demonstrated in *U. maydis,* that a deletion of one of the two genes encoding the metabolic proteins lead to a complete loss in ITA synthesis. Apparently, no other proteins can compensate the lack of activity of these proteins. By BLASTing, no candidate genes could be found in the genome of *P. tsukubaensis* that are suitable to undertake the functions of *PtADI1* or *PtTAD1* in their absence.

During our transformation studies in *P. tsukubaensis*, neither the overexpression of *PtADI1* nor *PtTAD1* had a visible effect on the production of ITA. For one, this illustrates that none of the reactions catalysed by the two proteins represent a rate limiting step. The missing phenotypes are also perfectly reasonable since both proteins are dependent on the activity of at least two other proteins: Naturally, for Adi1p the substrate in the cytosol appears to be lacking because the transporter of *cis*-aconitate into the cytosol represents a significant bottleneck. Even if this rate limiting step - the export of *cis*-aconitate - is bypassed, the overexpression of Adi1p alone is insufficient for an adequate ITA synthesis. Furthermore, it can be detrimental to the cell itself to enhance the transport of *cis*-aconitate and its isomerisation. This is because a low activity of Tad1p is potentially not enough to metabolize the increased concentrations of the resulting *trans*-aconitate. The so generated *trans*-aconitate then can inhibit the aconitase enzyme, thus leading to a halt of the TCA cycle and ultimately to cell death. Without the overexpression of *PtMTT1* and *PtADI1,* there is no available *trans*-aconitate in the cytosol, the overexpressed Tad1p is lacking its substrate and the enzyme is 'running idle'.

The ITA exporter Itp1p, which belongs to the MFS, is located inside the plasma membrane (Przybilla, 2014). The transporter is thought to be the sole transport protein for ITA. Deletion in *U. maydis* however showed that the ITA secretion is not completely blocked by this deletion (Geiser et al., 2016b). There could be two explanations for this. For one, another di- or tricarboxylate transporter substitutes for the lack of protein activity through functional redundancy. A broad substrate specificity was demonstrated for many transporters of the MFS (Taylor, 2017; Yan, 2013). Another explanation is that ITA is excreted as a result of passive diffusion. It has already been observed, that yeasts secrete undissociated organic acids by diffusion (Duro and Serrano, 1981; Salmon, 1987). However, according to the two pK_a values of ITA, it is almost completely dissociated at the intracellular pH 6.5-7.0. Mattey (1992) postulated that citrate^{2-} is excreted by passive diffusion along a gradient of dissociated CA. Under these circumstances, a similar mechanism can be imaginable for diffusion process of ITA as well.

Here, the overexpression of the *PtITP1* gene had almost no effect in the *P. tsukubaensis* H488 wild type strain. Taking the qPCR results into account, this finding is not striking since the expression data indicated that the *PtITP1* transcription is already elevated in the wild type strain. Three transformants with the M15 background displayed a substantial increase in ITA secretion after the overexpression of *PtITP1*. This seems to be an indicator that the random genomic changes in strain M15 lead to an increased ITA biosynthesis rate without the optimal molecular means to export the generated ITA into the yeast's surroundings.

In other organisms, the overexpression of the ITA transport protein led to conflicting conclusions. When overexpressed on its own, no effect has been observed for *U. maydis* (Geiser et al., 2016b). Li

et al. (2013) reported a beneficial outcome for the overexpression of the homologous gene *AtMFSA* in *A. niger* when *AtCAD1* was also overexpressed. This was not the case in the study of van der Straat et al. (2014), even with codon optimized gene sequences. Interestingly, when *AtMFSA** was overexpressed in combination with *AtCAD** and *AtMTTA**, the group around van der Straat et al. (2014) could detect an increase from ca. 5.4 g l⁻¹ to 7.1 g l⁻¹ ITA. However, the overexpression of the unmodified *AtMFSA* gene in *A. niger* in combination with *AtCAD1* and *AtMTTA* did not improve the ITA secretion further (Li et al., 2013). Following this, the literature appears conflicted on the efficacy of the overexpression of the ITA exporter. Even if the overexpression of *PtITP1* and its homologs leads to an improvement, it is solely beneficial when the intracellular concentrations of its substrate – ITA – is already high.

4.4.3. Ria1p - the regulator for itaconic acid

Evidently, the most influential genetic target turned out to be the *UmRIA1* homolog *PtRIA1*. No other genetic modification provided comparable results in this study.

The gene responsible for the regulator protein is located at one end of the ITA cluster next to the *PtMTT1* sequence. Its deduced 393 aa long sequence displays a helix-loop-helix domain at position 86-156 aa. This conserved region is a characteristic DNA-binding motif for one of the largest families of dimerizing transcription factors (Murre et al., 1994).

In *U. maydis*, it was clearly shown that the ITA cluster is controlled by the Ria1 protein. Upon deletion of *UmRIA1* the expression of all genes necessary for ITA synthesis was heavily reduced. Whereas, the overexpression of *UmRIA1* induced the transcription of the ITA biosynthesis genes. This upregulation was accompanied by only a moderate increase in the ITA concentration. The secreted ITA concentration was effectively doubled compared to the wild type strain (Geiser et al., 2016b).

A potential regulator element, *ATEG_09969*, was identified in the genome of *A. terreus* as well. It is also located in direct proximity to the genes encoding the ITA biosynthesis proteins (Li et al., 2011). Contrary to *U. maydis* and *P. tsukubaensis*, the deduced protein of *ATEG_09969* does not belong to the helix-turn-helix transcription factors but the large family of fungal zinc cluster transcription factors (Karaffa and Kubicek, 2019). Its function in *A. terreus* has not been object of active research yet. It is therefore still unclear, whether this regulator protein controls the expression of *AtCAD1, AtMTTA* and *AtMFSA* and if so, in what extent.

In this study, we could demonstrate that all identified ITA cluster genes are regulated by the gene product of *PtRIA1*. The overexpression led to an outstanding upregulation of the complete ITA cluster. Under culture conditions for organic acid production only very low expression levels were observed for the ITA cluster genes in the *P. tsukubaensis* wild type strain H488. Whereas, the transcription rates of the same genes were enhanced 67 to 4766-fold in strain HR12. Contrary to

U. maydis, the overexpression of the regulator *PtRIA*1 in strain HR12 also led to a distinct phenotype where exceedingly high concentrations of ITA are secreted. Under optimized conditions in shaking flasks, the secreted concentration of ITA rose over tenfold from 1.8 g l^{-1} in the wild type to 19.3 g l^{-1} in strain HR12 (see figure 9 and figure 20).

Similar to the overexpression of the other cluster genes, a large variability in the phenotypes of the resulting *PtRIA1*-transformants was observable. During the screening process in the well plate-cultivation, most of the *PtRIA1*-transformants in both the H488 and M15 background produced less to none ITA compared to strain HR12. It is plausible that this is due to differences in the genetic make-up caused by the heterologous integration of the vector. More specifically, it appears likely that only one copy or just a truncated version of the construct got inserted into the genome of the affected *P. tsukubaensis* transformants. Spatial effects of the insert on the chromosome or potentially deleted regions can also be a factor in the performance of those transformants. Interestingly, on average the impact of the *PtRIA1* gene overexpression was similar in both strains. Meaning that the underlying genetic changes in mutant strain M15 do not further enhance ITA synthesis when combined with an upregulated *PtRIA1* gene.

Recently, the group around Geiser (2018) investigated the role of the regulator protein in several members of the *Ustilaginaceae*. They found that the *RIA1* gene sequences are very dissimilar between the investigated species *U. maydis, U. vetiveriae, U. xerochloae, U. cynodontis, Sporisorium iseilematis-ciliati, P. hubeiensis* and *P. tsukubaensis*. Since all tested species harbour the complete genetic means to produce ITA, the overexpression of the respective native *RIA1* sequence induced ITA production. The most universally applicable regulator was the *PtRIA1* sequence. This regulator induced ITA synthesis in 80 % of the cases when expressed heterologously in related species. More importantly, *P. tsukubaensis* was the only species that did not produce 2-hydroxyparaconate or itatartarate at all because the necessary genes (*CYP3, RDO1*) are lacking. Furthermore, Geiser et al. demonstrated that the promoter sequences of the genes regulated by the Ria1p protein share a common conserved putative Ria1p binding domain with a short consensus sequence (CN[T/C]NNNN[G/A]TCACG[C/T]). Although, the promoter sequences of the *RIA1* genes themselves do not contain this consensus sequence. This allows the conclusion that the *RIA1* gene is not controlled by its own protein and cannot enhance its own transcription. The activator for the *RIA1* gene and ultimately the ITA cluster could, therefore, be another yet unknown factor.

Geiser et al. (2018) also quantified the secreted ITA concentration of the constructed transformants. The overexpression of the *PtRIA1* gene in *P. tsukubaensis* NBRC1940 under the control of the strong, constitutive P$_{etef}$ promoter resulted in relatively low ITA production levels compared to the other species of the *Ustilaginaceae* family. The authors, however, tested only one

transformant for each species and did not control for differences in copy number or for the random ectopic integration locus of the inserted regulator.

Here, we could illustrate that the overexpression of *PtRIA1* gene can have heavily varying consequences in the resulting productivity which is potentially influenced by the copy number and the type of integration. Solely 13 out of 21 *P. tsukubaensis* H488 transformants tested positive for ITA secretion. The produced ITA concentration of those 13 transformants ranged from 1.2-31.4 g l^{-1} in 3 ml-well plate cultivations. It is possible that the transformants that did not produce any ITA did not incorporate the complete upregulated *PtRIA1* gene into their genome but only parts of the vector backbone that mediates the resistance for hygromycin B. Strain HR12 evidently integrated the complete pActin-*PtRIA1* construct two times in tandem orientation while also deleting a considerable part of the genome. Other transformants that produced less ITA potentially harbour only one copy of the construct.

Considering the observed variations in ITA production, the region of integration into the genome should also be taken into consideration. The chromatin environment can significantly influence transcriptional activity of newly integrated DNA due to its heterogeneity (Jordan et al., 2001). Other possible factors are genomic rearrangements that occurred while integration of the vector. These structural rearrangements could have positively influenced the ITA biosynthesis in strain HR12 as well. It is also possible that the deletion of the 34 kb long sequence enabled a higher transcription rate or inhibited competing metabolic pathways through still unknown mechanisms. Possibly, also a feedback inhibition mechanism for the ITA biosynthesis could have been circumvented by the deletion. Product inhibition by ITA is a known phenomenon in *A. terreus* and *U. maydis*, especially at concentrations of 20 g l^{-1} and above (Kanamasa et al., 2008; Klement et al., 2012; Yahiro et al., 1995). Such an effect, however, was not observed in the production strain HR12. The yeast produced ITA at a consistent rate.

Approaches to further optimize the system of the upregulated ITA cluster by additionally overexpressing the native *PtACO1* or *PtACO2* gene did not yield additional improvements. This indicates that the intramitochondrial dehydration of CA into *cis*-aconitate does not represent a rate limiting step. On the contrary, too high Aco1p or Aco2p enzyme activities could lead to a competitive condition between the mitochondrial tricarboxylate carrier Mtt1p and the aconitase enzyme that also catalyses the re-hydration of *cis*-aconitate into ICA. Interestingly, co-overexpression of *AtCAD1* and a gene coding for an aconitase in both *A. niger* and *Y. lipolytica* enhanced the synthesis of ITA. The productivities of the constructed strains are still very low with a maximum of 1.4 g l^{-1} and 4.6 g l^{-1} ITA, respectively (Blazeck et al., 2015; Blumhoff et al., 2013). In their study, Blumhoff et al. (2013) also pointed out the importance of the right organelle targeting

of the heterologous genes. Aconitase expressed in the mitochondria was more efficient than in the cytosol.

In conclusion, the known ITA producing organisms generate the wanted organic acid over the course of similar reaction pathways. Nonetheless, there are underlying distinctions between the respective biosynthesis routes, as detailed above. The reasons for the differences in the ITA pathways are most likely adaptations to environmental cues or because of special functions the organic acid serves. *A. terreus* is a soil-borne fungus or can be found on decaying plant material (Thom and Church, 1918). It potentially secretes ITA directly into its surroundings to potentially gain a competitive advantage against other microorganisms. For one thing, this is because of a direct interaction of the organic acid with the surrounding environment: the pH decrease leads to solubilization of soil minerals or it propels acid-catalysed reactions similar to the hydrolysis of holocellulose caused by oxalic acid. Ultimately, a release of nutrient ions is achieved (Green and Highley, 1997; Plassard and Fransson, 2009; Tanaka et al., 1994). On the other hand, the lowering of the surrounding pH by secreting weak organic acids leads to an advantage in a very competitive environment against other microorganisms. The acid inhibits growth of pH sensitive organisms because the undissociated molecules easily diffuse through the plasma membrane into the cytosol where they dissociate and disturb intracellular processes (Dutton and Evans, 1996; Jones, 1998; Lambert and Stratford, 1999).

Mammalian macrophages utilize ITA for defence mechanisms against intruding microorganisms. The synthesised ITA is believed to be directly transported from the mitochondria into the phagosomes, where ITA is needed to block essential metabolic pathways of invading pathogens (Michelucci et al., 2013). This way for example, the key enzyme of the glyoxylate shunt, isocitrate lyase, is inhibited. The glyoxylate shunt is essential for several bacteria like *Salmonella enterica*, *Mycobacterium avium* or *Mycobacterium tuberculosis* when grown on certain C sources (Bentrup et al., 1999; Fang et al., 2005). ITA also blocks supporting metabolic routes like the 2-methylcitrate cycle in *Mycobacterium tuberculosis* (Cordes et al., 2015; Russell et al., 2010).

ITA production in *Ustilaginaceae* via *trans*-aconitate most probably serves purposes akin to that of *A. terreus*. However, the main difference is that it also represents a way to detoxify *trans*-aconitate. Plants like maize and other grasses are known to produce high concentrations of *trans*-aconitate with up to 2.5 % of their DCW as antifeedant (Brauer and Teel, 1981; Burau and Stout, 1965). This intermediate acts by inhibiting essential metabolic pathways. The TCA cycle can be blocked due to *trans*-aconitate by inhibiting the enzymes aconitase and fumarase (Geiser et al., 2016b; Glusker, 1971; Saffran and Prado, 1949). The reaction mechanism catalysed by the *trans*-aconitate decarboxylase can aid the catabolism of this toxic intermediate and hence prevent a

harmful accumulation. Therefore, the generation of ITA via this extra synthesis step appears to be an adaptation to the common habitat of the *Ustilaginaceae*, which are mainly plant leaves (Boro et al., 2017; Kitamoto et al., 2011; Morita et al., 2010b; Wang et al., 2006). This is further substantiated by the fact that the deletion of *ADI1* led to a substantial growth defect of *U. maydis* cells when grown on *trans*-aconitate containing medium (Przybilla, 2014).

4.5. Large volume ITA production with *P. tsukubaensis*

The first large volume fermentation experiments were carried out with the *P. tsukubaensis* strain M15-CAD. This yeast strain was established as a promising ITA overproducing candidate by Bodinus (2011). During experiments in shaking flasks, our study showed that strain M15-CAD can secrete high concentrations of ITA in synthetic minimal medium without the need of complex supplements like CSL. The highest product concentrations of $16.2 \, g \, l^{-1}$ ITA were detected with $2 \, g \, l^{-1} \, NaNO_3$ and $0.1 \, g \, l^{-1} \, KH_2PO_4$ after 5 d of cultivations. Under similar conditions, when cultivated in minimal medium modified according to Kawamura et al. (1981, 1982), the same strain produced approximately $35 \, g \, l^{-1}$ ITA after 5 d of cultivation (Bodinus, 2011). The differences in productivity can be founded on the fact that 0.2 % (v/v) CSL and substantially more glucose ($150 \, g \, l^{-1}$ instead of $50 \, g \, l^{-1}$) were used by Bodinus.

These shaking flask experiments were the basis for large volume bioreactor cultivations under controlled conditions. Here, a maximum ITA secretion of $40.9 \, g \, l^{-1}$ after 8 d with $2 \, g \, l^{-1}$ N source and $0.1 \, g \, l^{-1}$ P source was demonstrated. During this period, the initial $150 \, g \, l^{-1}$ glucose were not consumed completely. Further increasing the N (and P) source had a negative impact on the productivity. This result further illustrates the intricate natural regulatory mechanism for the induction of ITA biosynthesis in *P. tsukubaensis*. Both, the available N and P sources must be limited, and their concentrations must have a specific ratio in order to naturally upregulate ITA production. Bodinus (2011) cultivated strain M15-CAD in a 3.6 l-bioreactor. There, the glucose ($150 \, g \, l^{-1}$) was completely consumed after 10 d. During this time $60.6 \, g \, l^{-1}$ ITA were secreted which corresponds to a productivity rate of $6.1 \, g \, l^{-1} \, d^{1}$ ITA. This productivity rate is still slightly higher than what was achieved earlier ($5.1 \, g \, l^{-1} \, d^{-1}$ ITA). Here, the medium was not supplemented with CSL and in addition a lower oxygen saturation was applied than Bodinus did. A positive impact of the increased O_2 saturation, however, is unlikely. We could demonstrate that by increasing the pO_2 to 90 % the ITA secretion was affected negatively. This was also true for the elevated pH of 7.0 throughout the fermentation.

According to this data, fermentations were carried out with the ITA overproducing *P. tsukubaensis* HR12 strain. The first fermentation was done exactly under the conditions that were deemed best for strain M15-CAD (N: $2 \, g \, l^{-1}$; P: $0.1 \, g \, l^{-1}$; pH: 5.5; pO_2: 55 %; 30 °C; see figure 30 and figure 31). Strain HR12 demonstrated a 2.3-fold increase in ITA productivity compared to M15-CAD.

As was discussed in section 4.2, ITA production with strain HR12 is completely decoupled from any triggers by the available N and P source. Fermentations with increased concentrations of these nutrients reflected that fact. High N & P concentrations led to increases in biomass which entailed enhanced ITA secretion. The highest ITA production of 113.6 g l^{-1} after just 7 d was accomplished during a fed-batch cultivation with a N:P ratio of 8:1. This corresponded to an ITA productivity of 16.2 g l^{-1} d^{-1}. Until recently, the highest achieved ITA concentration in the literature was 90 g l^{-1} ITA with a specific isolated *A. terreus* strain (Kuenz et al., 2012). Shortly thereafter, the ITA producing capability of another screened *A. terreus* strain (DSM 23081) was optimized to secrete up to 146 g l^{-1} after 13 d only under very specific and highly controlled conditions (Hevekerl et al., 2014a). By further adjusting the process conditions for the ITA fermentation with *A. terreus* strain DSM 23081, the overall ITA productivity of 24 g l^{-1} d^{-1} could not be improved but the maximal end-concentration was increased to 160 g l^{-1} ITA. Efforts to upscale this fermentation process with *A. terreus* to a 15 l-bioreactor were successful. However, the productivity suffered greatly. It took 9.7 d to reach a maximal ITA concentration of 150 g l^{-1} (Krull et al., 2017). In addition to that, the process conditions were tightly confined. The P concentration had to be strictly limited because *A. terreus* cells form increasingly large and tight cell aggregates at higher P levels. Cells inside large pellets suffer oxygen deficiency which lowers ITA biosynthesis. However, restricting P drastically limits the cell biomass which also leads to limited ITA production. Also the substrate and the medium for the fermentation often need pre-treatment since trace metal impurities are known to negatively affect organic acid synthesis (Show et al., 2015). Manganese concentrations above 3 µg l^{-1} for example reduce ITA synthesis with *A. terreus* (Karaffa et al., 2015).

In this study several attempts were carried out to improve the already high ITA concentration of 113.6 g l^{-1} ITA with *P. tsukubaensis* strain HR12. From the standpoint of fermentation process handling, slightly decreasing the pH to 4.0 had the positive effect of a reduced accumulation of intracellular storage lipids. This way, the yeast cells stayed inside the culture broth for the whole duration and no biofilm was formed inside the bioreactor. In addition, it made it possible to completely and easily separate the cells from the fermentation broth via centrifugation. In doing so, a relatively high productivity of 10.3 g l^{-1} d^{-1} ITA was maintained. During the fermentation only negligible amounts of the side-products MA and αKG have been produced. The concentrations of those two side-products in the supernatant were considerably lower than for fermentations at pH 5.5. Instead of accumulatively 2 % at the neutral pH, MA and αKG represented together less than 0.5 %. That is to say over 99.5 % of the total organic acid in the supernatant constituted for ITA. It was also striking that these high ITA concentrations were secreted by a relatively low biomass. At the timepoint of decreasing the pH, around 20-25 g l^{-1} DCW were formed. Afterwards, the cells did not grow further but remained in a stationary phase. With the neutral pH 5.5, the cells continued to grow and generated a biomass of 40-50 g l^{-1} DCW. In an attempt to prolong the

exponential growth phase in the acidic environment, the pH was decreased only after the 2nd day. This had the positive effect of leading to a higher initial active biomass. This was reflected in an increased productivity of 11.6 g l^{-1} d^{-1} ITA.

However, further lowering the pH value to 3.5, had a detrimental impact on the yeast cells. Cell growth was slowed down. According to the decreased glucose consumption, the metabolic rate also suffered. Comparable effects have been reported for the oleaginous yeast *Rhodotorula* (*R.*) *glutinis*. During fed-batch fermentation, maximum lipid production of 66 % (w/w biomass) was achieved at pH 4.0. Decreasing the pH to 3.0 drastically lowered the biomass and the lipid content to merely 12 % (w/w biomass) (Johnson et al., 1992). Dias et al. (2016) described similar effects for the lipid and carotenoid accumulation properties of *Rhodosporidium toruloides* (formerly *R. glutinis*). They found maxima in biomass and carotenoid productivities at pH between 4.0-4.5. Further lowering the pH also had a negative effect for this oleaginous yeast. Furthermore, they found that the pH did not affect cell size, internal complexity and membrane polarisation when cells were in the exponential growth phase. However, when stationary growth phase was reached, cell size, internal complexity and cells with polarised membrane increased for lower pH values. Microscopic images taken during this project, however, show that cell size of *P. tsukubaensis* decreased over time at pH 4.0 (see figure 32).

Guiding the metabolic flux towards lipid biosynthesis or away from it through changes in the pH can represent an uncomplicated, straightforward way for process optimization compared to laborious genetic engineering efforts.

For the fermentative production of ITA with *A. terreus,* various strategies are described in the literature regarding the applied pH. A broad range in the initial pH, ranging from 2.0 to 5.9 has been used in different studies (Kuenz and Krull, 2018). A pH below 6 is needed for *A. terreus* to produce any ITA naturally. Although pH values of 3.0 and below postpone germination, thus, also the ITA production (Hevekerl et al., 2014a; Larsen and Eimhjellen, 1955; Mario and Schweiger, 1963). Overall highest concentration of 160 g l^{-1} ITA produced with *A. terreus* has been achieved by keeping the pH constant at 3.4 during production phase (Krull et al., 2017). To this day, no higher concentrations have been described.

For the ITA production with *Ustilaginaceae*, there is few information on the optimal pH. *U. maydis* is generally grown at neutral to somewhat acidic conditions. More specifically, Maassen et al. (2014) did produce relatively high ITA concentrations of 44.5 g l^{-1} with *U. maydis* under a controlled pH of 6.0. The closely related *U. vetiveriae* had to be cultivated at a pH of 6.5 in order to secrete elevated concentrations of ITA (24 g l^{-1}). A pH of 5.5 resulted in a heavily reduced ITA production, whereas further decreasing the pH to 4.0 completely diminished ITA production

(Zambanini et al., 2017). While the *U. maydis* wild type secretes ITA only at a pH between 5 and 7, *U. cynodontis* strains also produce ITA at pH values below 3 (Geiser et al., 2018).

For some CA producing microorganisms like *A. niger*, it is known that CA production increases with rising concentrations of dissolved oxygen (Kubicek et al., 1980). The formation of ITA is strongly dependent on a sufficient oxygen supply. Especially *A. terreus* reacts very sensitive to oxygen limitation. Even short periods of O_2-deficiancy can lead to reduced or halted ITA synthesis (Kuenz and Krull, 2018; Kuenz et al., 2012; Larsen and Eimhjellen, 1955). In an attempt to increase oxidative glucose metabolism and thus increase ITA synthesis, fermentations were carried out with either elevated oxygen saturation or increased temperature. In this study, we found a small improvement in ITA secretion, when the dissolved oxygen concentration was elevated to 70 %. However, this effect was concomitant with an increased glucose consumption, which ultimately lowered the ITA specific yield to 28 % (w/w). This is potentially due to a heightened respiratory activity of the *P. tsukubaensis* cells.

The effect of the temperature on ITA production has not been studied intensively yet. For CA production with *A. niger*, a temperature optimum of 28-30 °C is assumed (Kareem et al., 2010; Karthikeyan and Sivakumar, 2010). The group around Auta (2014), however, demonstrated that CA secretion can be enhanced by increasing the temperature up to 55 °C. For *P. tsukubaensis* HR12, the temperature increase from 30 °C to 32 °C lead to a somewhat lowered ITA production. The glucose consumption rate declined rapidly towards the end of cultivation. In addition to the acidic environment (pH 4.0), the temperature increase to 32 °C potentially represented an additional stress factor and was therefore disadvantageous for the fermentative production of ITA.

4.6. Isocitrate overproduction with *Y. lipolytica*

For the second part of this thesis, the microbial production of another value-added chemical stemming from *cis*-aconitic acid was pursued. Thus, the organic acid ICA got into the focus.

In this study, we were able to identify two main mitochondrial transporters for CA and ICA in *Y. lipolytica*: namely the proteins encoded by *YALI0B10736g* (*YlYHM2*) and *YALI0F26322g* (*YlCTP1*). It was also possible to establish that both proteins are involved in the transport of CA (and ICA) between the mitochondria and the cytosol.

Deletion of *YlYHM2* led to several significant changes in the phenotype of *Y. lipolytica*. Growth was impaired on minimal medium with H_2O_2 compared to the wild type. This is an indicator for a decreased antioxidant function. A reason for this observation could be an imbalance in reducing equivalents (e.g. NADPH).

In *S. cerevisiae,* ScYhm2p is described to play a crucial physiological role in the redox state of cytosolic NADPH by shuttling NADPH reducing equivalents from the mitochondrial matrix to the cytosol. More specifically, CA is transported through the inner mitochondrial membrane by

117

Yhm2p into the cytosol. There, CA is converted via aconitase into ICA which is metabolized into αKG and CO_2 while also generating NADPH. αKG can then be imported into the mitochondrion also by Yhm2p due to its function as an antiporter. Inside the mitochondrion, the backwards reaction can take place and $NADP^+$ is formed (Castegna et al., 2010). This finding is further substantiated by the observation in *C. parapsilosis*, where the expression of *YHM2* is induced by 3-hydroxybenzoate and 4-hydroxybenzoate. Both compounds are metabolized in the NAD(P)H consuming gentisate and 3-oxoadipate pathways, respectively. Thus, Yhm2p potentially contributes to the replenishment of NAD(P)H in these two pathways (Zeman et al., 2016). We, therefore, expect for Yhm2p to have a shuttling role for reducing equivalents (NAD(P)H) as well in *Y. lipolytica*, similar to that of *S. cerevisiae* (see figure 43).
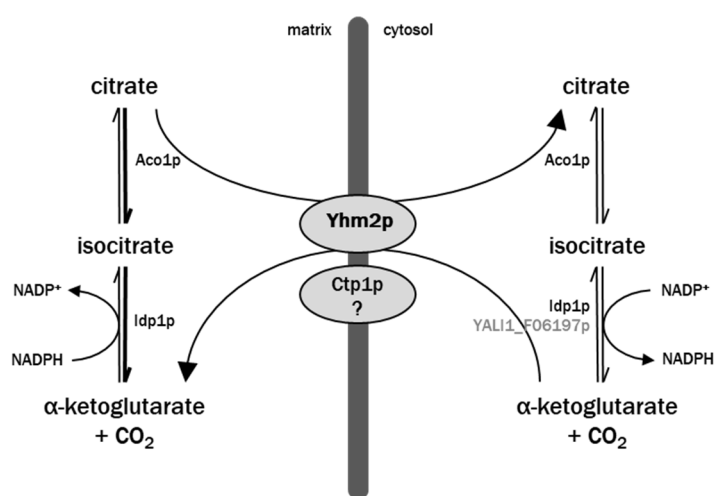

Figure 43 Hypothesized transport of citric acid across the mitochondrial membrane via the citrate carrier Yhm2p in *Y. lipolytica*.
Modified according to Castegna et al. (2010). Citrate is reversibly isomerized into isocitrate by the mitochondrial or cytosolic aconitase (Aco1p). Isocitrate is then converted to α-ketoglutarate and CO_2 by the isocitrate dehydrogenase (Idp1p, or in the cytosol potentially the gene product of *YALI1F06197g*) while also generating NADPH. By the antiport of citrate for α-ketoglutarate, Yhm2p may act as a NADPH redox shuttle between the mitochondria and cytosol. Citrate and isocitrate are also transported via citrate transporting protein, Ctp1p and potentially other members of the mitochondrial carrier family (their transport mechanisms are still subject of current research).

After deleting *YlCTP1,* there was no change in growth observed for all tested C sources. The addition of H_2O_2 had also no negative effect on the growth behaviour. This observation is in accordance with the results of Kaplan et al. (1996), indicating that *YlCTP1* is a non-essential gene in *Y. lipolytica*, too.

However, single copy overexpression of *YlACO1* itself also showed a slightly delayed growth compared to the wild type on medium containing H_2O_2. An elevated amount of active aconitase may sequester a large amount of CA, ICA and *cis*-aconitate in the cell. Inhibiting those metabolites would then negatively affect the TCA cycle and its subsequent reactions e.g. the NADPH generating dehydrogenation of ICA into αKG and CO_2 in the cytosol. Interestingly, the overexpression of *YlACO1* mitigated the growth phenotype of Δ*YHM2*. One possible explanation is, that the CA export is heavily inhibited due to the deleted carrier gene and the natural aconitase

activity is not enough for the excess CA in the mitochondrion which leads to CA accumulation. *YlACO1* overexpression alleviates that by converting more CA into ICA. The generated ICA can then be exported into the cytosol, where it is dehydrogenated into *α*KG while simultaneously generating NADPH. Nevertheless, elevated aconitase activity also leads to the retransformation of ICA into CA in the cytosol, which ultimately results in a reduced ICA:CA ratio. The acid production behaviour of strain Δ*YHM2∘ACO1* substantiates that presumption.

Focusing on acid production, overexpression of aconitase in *Y. lipolytica* significantly reduced CA while elevating the level of ICA. This is a similar result to that of Holz et al. (2009), where multiple copies of *YlACO1* without the control of a constitutive promoter were introduced into *Y. lipolytica*. By doing so, the group accomplished a significant increase in the ICA:CA ratio from 35-49 % to 66-71 % when cultivated with sunflower oil but only a minor shift from 10-12 % to 13-17 % with glucose, glycerol or sucrose.

The knock-out of the transporter Yhm2p potentially rendered the *Y. lipolytica* cells unable to export high amounts of CA from the mitochondrion into the cytosol, from where it is subsequently secreted into the surrounding medium. Therefore, ICA was the main secreted acid. Compared to the *Y. lipolytica* wild type, this corresponds to a drastic change in the ICA:CA ratio from 12 % to 95-97 % under optimized fermentation conditions. This is a strong indicator for the role of Yhm2p as a selective mitochondrial exporter mainly for CA in this oleophilic yeast.

Compared to the highest described ICA:CA ratio of 17 % when cultivated on glucose achieved by Holz et al. (2009), the present ICA:CA ratio of 95 % constitutes for a drastic shift in favour of ICA by a single gene disruption. Similar ratios of ICA and CA were only achieved with a wild type *C. catenulata* (formerly *C. ravautii*) strain and its NG-mutant strain OM-102. Both yeast strains were able to synthesize ICA with only 1-2 % residual CA on glucose (Oogaki et al., 1984). Further strain optimization of *Y. lipolytica* strain Δ*YHM2* with glucose as C source could be realized by increasing glycolytic and TCA cycle activities since our data on aconitase activity suggests a downregulating effect on at least the TCA cycle level.

Contrary to the growth phenotype, it appears that Ctp1p is also an important transport protein needed for the TCA cycle in *Y. lipolytica*. By disrupting the *YlCTP1* gene, CA and ICA production was detrimentally affected when grown with glucose but not so much with sunflower oil. In face of the decreased aconitase activity, it is very plausible that the TCA cycle is downregulated due to an accumulation of both CA and ICA in the mitochondrion. In the white koji fungus *A. luchuensis* mut. *kawachii*, the Ctp1p homolog, CtpA, exhibited also substrate specificity for *cis*-aconitate and MA to some degree (Kadooka et al., 2018). If Ctp1p in *Y. lipolytica* functions similarly, the diminished transport of *cis*-aconitate and MA could play a role in the reduced TCA cycle activity.

CA and ICA production was heavily reduced in strain $\Delta YHM2\Delta CTP1$, in which both mitochondrial carriers are lacking. Surprisingly, this strain showed no reduced growth. Colonies were the same size as the wild type H222 on glucose (with and without H_2O_2), acetate, CA, oxalate and αKG. For *A. kawachii*, the deletion of *CtpA* and *YhmA* (homologous to *YlYHM2*) proved to be lethal (Kadooka et al., 2018). One possible explanation are compensatory mechanisms, where genes e.g. for other mitochondrial transport proteins, are upregulated to ensure the transport of metabolites and avoid build-up of potentially toxic intermediates. This would also explain the higher amounts of secreted acids when grown with glucose compared to strain $\Delta CTP1$. A suitable candidate for such a role is the gene *YALI0D02629g*, which might code for a 2-oxodicarboxylate carrier homologous to ScOdc1p and ScOdc2p. The dicarboxylate carriers ScOdc1p and ScOdc2p are responsible for the transport of 2-oxoadipate and αKG but also small quantities of CA (Palmieri et al., 2001).

There remains the question of where the remaining CA for strain $\Delta YHM2$ on glucose originates from. One explanation is the functional redundancy of other transporters e.g. the 2-oxodicarboxylate carrier, as mentioned above. The residual CA could also be present due to cytosolic aconitase activity (see figure 44). Isoenzymes of the translational product of *YlACO1* are reported to be present in the cytosol of yeasts, where they catalyse for the glyoxylate shunt, despite being prior referred to as an exclusive mitochondrial protein active in the TCA cycle (Regev-Rudzki et al., 2005). The *ScACO1* gene harbours a naturally occurring mitochondrial target sequence but a fraction of the deduced enzyme exerts catalytic activity in the cytosol. (Ben-Menachem et al., 2011, 2018). That way, the abundant ICA can be converted back to CA in the cytosol, because of the natural reaction mechanism for the isomerization of CA to ICA, which is described as a completely reversible reaction catalysed by aconitase (Martius and Leonhardt, 1943). This hypothesis is supported by the acid production behaviour of the *YlYHM2* lacking strain, where *YlACO1* is additionally overexpressed. Cytosolic active aconitase in the transformant most probably catalysed for the back reaction, thus elevating CA levels again.

Figure 44 illustrates that other metabolic pathways cannot be ruled out as sources for cytosolic CA, yet. Although the glyoxylate shunt is a typical target for carbon catabolite repression (Duntze et al., 1969; Ordiz et al., 1996), it is known that key enzymes of it still exert a marginal level of activity. This is based on the observation that the gene of one of its main enzymes, the peroxisomal citrate synthase Cit2p expresses a low activity even on glucose (Kispal et al., 1989; Liao et al., 1991; Rickey and Lewin, 1986). *YALI0E02684g* potentially encodes the peroxisomal citrate synthase, which could convert cytosolic acetyl-CoA into CA even in the presence of high glucose concentrations.
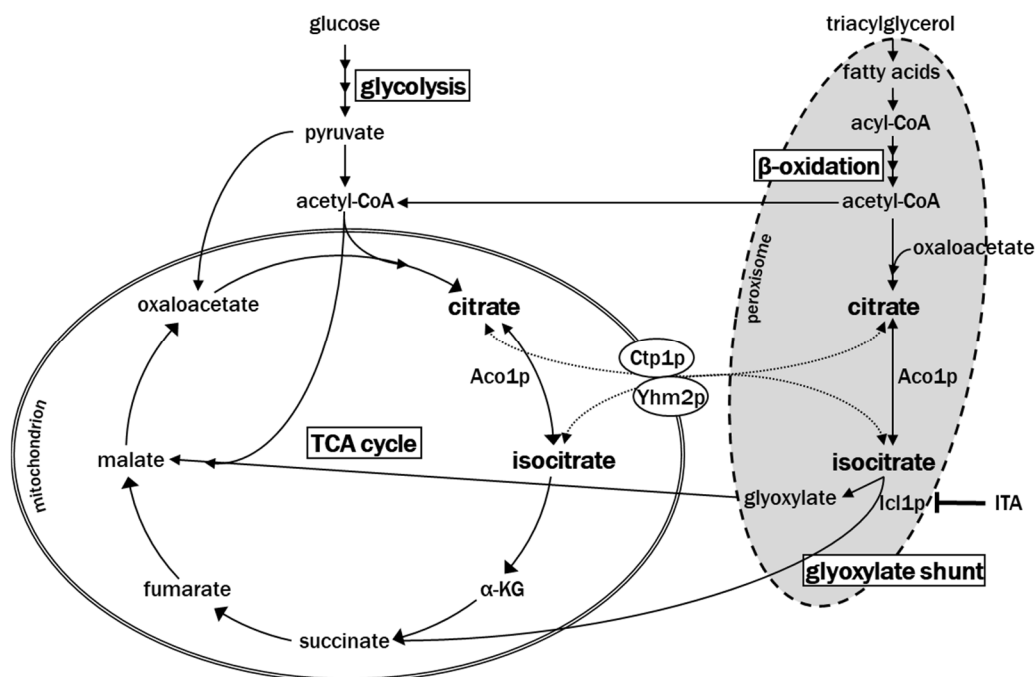
Figure 44 Main pathways involved in the synthesis of citric- and isocitric acid in the oleophilic yeast *Y. lipolytica*.
Fermentable sugars like glucose are broken down during glycolysis. The resulting acetyl-CoA and oxaloacetate fuel the synthesis of citric acid during the tricarboxylic acid (TCA) cycle inside the mitochondrion. Aconitase (Aco1p, or possibly also Aco2p) catalyses the reversible isomerization of citrate into isocitrate. Hydrophobic substrates e.g. vegetable oils are broken down into fatty acids. During the course of *β*-oxidation the activated fatty acids (acyl-CoA) are oxidized in multiple steps into acetyl CoA (and propionyl-CoA in the case of odd chain lengths). This acetyl-CoA can then directly supply the TCA cycle via the metabolites of the glyoxylate shunt. In the glyoxylate shunt, citrate is isomerized into isocitrate by the cytosolic Aco1p. This isocitrate is subsequently cleaved by the isocitrate lyase (Icl1p) into glyoxylate and succinate. The activity of Icl1p can be inhibited by itaconic acid (ITA). Both glyoxylate and succinate are supplied to the TCA cycle. Ctp1p and Yhm2p are citrate and isocitrate shuttling proteins in the inner membrane of the mitochondrion. Their hypothesized transport mechanism is illustrated in a simplified form. *α*KG – *α*-ketoglutarate

As an oleophilic yeast, *Y. lipolytica* strives on hydrophobic substrates like vegetable oils. It has been shown multiple times, that *Y. lipolytica* produces substantial amounts of CA and even ICA on different oils (Förster et al., 2007b; Holz et al., 2009; Kamzolova et al., 2008, 2015, 2016; Venter et al., 2004). The ICA overproducing strain Δ*YHM2* showed a substantial increase in absolute amounts of produced ICA compared to the cultivation with glucose. Proportionately also more CA was synthesized with sunflower seed oil (in total 131.9 g l^{-1} ICA and 16.5 g l^{-1} CA). This result is not surprising, because additional CA generating pathways are active during triacylglycerol/fatty acid degradation. The fatty acids are cleaved from triacylglycerols by lipases and are subsequently broken down into acetyl-CoA during heightened *β*-oxidation activity in the peroxisomes. This acetyl-CoA is then converted into CA by a peroxisomal citrate synthase (potentially YALI0E02684p) in the course of an activated glyoxylate shunt (Eckardt, 2005; Fickers et al., 2003). The ICA production performance of strain Δ*YHM2* is also exceptional with hydrophobic substrates. With a productivity rate of 26.4 g l^{-1} d^{-1} ICA and an ICA:CA ratio of 89 % does the strain outperform existing ICA overproducing *Y. lipolytica* strains on rapeseed oil e.g. strain 704 UV4 A/NG50 - 23.3 g l^{-1} d^{-1} ICA; 81 % ICA or strain VKM Y 2373 - 19.1 g l^{-1} d^{-1} ICA; 76 % ICA (Kamzolova et al., 2013, 2015).

The reason for decreased ICA/CA production when *YlYHM2* is overexpressed is still unclear. A possible explanation is that the transport of CA out of the mitochondrion is increased. Hence, a key metabolite of the TCA cycle is less abundant which slows the total acid production down.

In order to further enhance ICA production in strain Δ*YHM2*, ITA was introduced to the medium. ITA is a natural inhibitor of the isocitrate lyase (Icl1p), a key enzyme in the glyoxylate shunt that catalyses the cleavage of ICA into succinate and glyoxylate (Atomi et al., 1990; McFadden and Purohit, 1977). The addition of ITA further enhanced ICA:CA ratio on glucose significantly from 94 % to 96-97 %. This result is another indicator for a minor activity of proteins in the glyoxylate shunt, despite being inhibited by glucose repression.

The group around Kamzolova (2015, 2016) cultivated a *Y. lipolytica* wild type and an UV/NG mutant strain on canola oil with the addition of ITA. In doing so, the ICA:CA ratio was increased from 2.2:1 (69 %) to 4.5:1 (81 %) with the wild type strain VKM Y 2373 and from 1:1.04 (49 %) to 6:1 (85 %) with the UV/NG strain under optimized conditions while producing 82.7 g l^{-1} and 88.7 g l^{-1} ICA, respectively. Interestingly, during this project when cultivating strain Δ*YHM2* on sunflower oil with ITA, the ICA:CA ratio of 89 % shifted back in the favour of CA to 78 %. At first glance, this observation seems counterintuitive, but it underscores the importance of the CA carrying capabilities of Yhm2p. The import of CA into the mitochondrion is believed to be also facilitated by Yhm2p. During β-oxidation and the glyoxylate cycle an increased amount of CA is produced. The *YHM2* deletion reduces the transport rate of CA into the mitochondrion. Adding to that, the amounts of anaplerotic metabolites, MA and succinate, are heavily reduced due to inhibition of Icl1p. Consequently, ICA cannot fuel its own synthesis via Aco1p in the mitochondrion because its cleavage products from the glyoxylate shunt are diminished. Ultimately, leading to an accumulation of CA in the cytosol. Therefore, it would be advisable not to inhibit Icl1p but dampen the citrate synthase activity to further enhance the ICA ratio of strain Δ*YHM2* on vegetable oils.

5. Conclusion & Prospect

This thesis advocates for the application of oleaginous yeasts in the biotechnological production of organic acids from renewable resources, especially for the production of ITA with *P. tsukubaensis* and ICA with *Y. lipolytica*. The two yeast species are naturally secreting the respective acids. CA but also ITA are already synthesised on a large scale with the help of microorganisms. Biotechnological processes for the biosynthesis of CA and ITA, however, are still dominated by filamentous fungi from the genus *Aspergillus*. *P. tsukubaensis* and *Y. lipolytica* both exhibit several advantages over *Aspergillus* species like fast single cell growth with no need for spores to germinate and fewer sensitivities against contaminations in the medium e.g. heavy metals. These properties make them optimal candidate organisms for the development of alternative, more lucrative biotechnological processes.

The present study focuses on the targeted overproduction of the valuable platform chemicals ITA and ICA with the help of oleaginous yeasts. Here, we were able to identify the genes involved in the biosynthesis of ITA with *P. tsukubaensis*. This information was of great value for subsequent genetic optimization efforts. As it turned out, the investigated yeast possesses the same genes necessary to produce ITA as does the corn smut fungus *U. maydis* MB215. In addition, several promoter sequences that ensure a strong and constitutive expression have been discovered. That way, overexpression studies could be carried out for every gene directly involved in the synthesis of ITA. The generated transformants were screened for their ability to secrete ITA and MA. This screening process was aided by the previous development of a modified culture medium. The medium composition according to Bodinus and Kawamura was adjusted in that it is a completely synthetic medium with no complex components like corn steep liquor. The synthetic medium also made it possible to gain insights into the natural regulation of ITA biosynthesis. *P. tsukubaensis* wild type secretes mainly MA. This MA synthesis is triggered by the depletion of P in the medium. ITA synthesis, on the other hand, is not induced by the complete depletion of P but by high concentrations of N and very low concentrations of the P source (approximately 0.15 g l^{-1} KH_2PO_4).

Despite several overexpression experiments for the various ITA cluster genes leading to nuanced differences in most cases, the efforts to metabolically engineer *P. tsukubaensis* were successful. On their own, the overexpression of the two genes encoding the enzymes *cis*-aconitate-Δ-isomerase (*PtADI1*) and *trans*-aconitate decarboxylase (*PtTAD1*) did not enhance ITA production. With an enhanced activity of either *PtITP1* or *PtMTT1*, the genes encoding important transport proteins in the biosynthesis of ITA, low improvements were possible in the wild type. The effect was significantly greater when other factors were in play as well, like the random genetic changes in strain M15.

The overall highest impact had the overexpression of the regulator gene *PtRIA1*. The prevailing majority of the generated transformants in both the wild type and the mutant strain secreted high amounts of ITA. With this genetic modification, several ITA overproducing transformants have been created. The screening process demonstrated a greatly varying effectiveness of this overexpression between the generated transformants ranging from 1.2 to 31.4 g l^{-1} for wild type transformants and 0.6-33.4 g l^{-1} for M15 transformants, respectively. That way, the here characterized ITA production strain HR12 was created. Gene sequence analysis showed that a double integration of the promoter-gene construct in tandem orientation and possibly the simultaneous deletion of a 34 kb long region were instrumental for the improvement in ITA synthesis. Following experiments demonstrated that strain HR12 is able to utilize several different C sources like glucose, ethanol, acetate, xylose, sucrose, and glycerol. Furthermore, it was revealed that no external trigger was needed for the enhanced biosynthesis of ITA e.g. depletion of a nutrient like N or P because the complete ITA cluster was upregulated by the overexpression of *PtRIA1*. That way, up to 113.6 g l^{-1} ITA was produced within 7 d under controlled conditions. What is more striking is the high specific yield of 42 % (g ITA per g glucose) and the low concentrations of competing by-products like MA or αKG (combined 2.2 g l^{-1}).

As a second objective, the increased secretion of ICA with the oleaginous yeast *Y. lipolytica* was followed since few viable production processes are known besides the resource-intensive chemical synthesis. In the course of our investigations, the new genes *YlCTP1* & *YlYHM2* were identified, which encode putative mitochondrial CA transporting proteins. Deleting each gene individually led to a drastic reduction in aconitase activity in both cases. However, the mode of action of the two transporters appeared to be very distinct from one another. When grown on glucose, the knock-out of *YlCTP1* resulted in a general decrease in total acid secretion. In the case of cultivation with hydrophobic C substrates, strain $\Delta CTP1$ secreted only fewer amounts of organic acids with no discernible changes in the ICA:CA ratio.

By only deleting one target gene, *YlYHM2*, a specific phenotype was achieved, in which the ICA:CA ratio is drastically altered to produce almost exclusively ICA. This is true for both simple sugars and hydrophobic substrates. Strain $\Delta YHM2$ secreted ICA as the main product and in high concentrations of up to 131.9 g l^{-1} with an ICA:CA ratio of 89 % (16.5 g l^{-1} CA). This ratio was raised to 96 % with glucose as C source but the productivity suffered by doing so. To this date, there has been no strain constructed, rationally or by random mutagenesis, with similar ICA producing capabilities. Additional *YlACO1* overexpression negatively affected the ICA production. By inhibiting the enzyme Icl1p with the supplementation of ITA, the ICA yield was further increased significantly with glucose but not with sunflower oil as carbon substrate.

P. tsukubaensis HR12 and *Y. lipolytica* Δ*YHM2* both represent exceptional microbial producers for the respective organic acid, although further improvements are needed in order to compete with established processes and with petrochemical-derived products. From a biotechnological standpoint the main objectives are to heighten product to substrate yield, spacetime yield and the final product concentration. The following sections should illustrate imaginable but also viable strategies to achieve these goals.

Primarily, the possibilities must be exhausted to optimize the direct biosynthesis of the organic acids. In the case of ITA synthesis with the help of *P. tsukubaensis*, heterologous gene or promoter sequences should be taken into consideration. Here, we demonstrated the possibility of a parallel ITA biosynthesis pathway in that *AtCAD1* and *PtMTT1* were overexpressed in combination. Codon optimization of the *AtCAD1* gene to better suit its host organism is one approach to enhance the productivity. In addition, transport proteins must be investigated. This can either be done by protein engineering of the native PtMtt1p and PtItp1p transporters or by identifying suitable heterologous genes from suitable organisms.

A targeted enhancement of *cis*-aconitate shuttling activity into the cytosol and ITA export into the extracellular space can potentially lead to substantial changes in productivity. Promising targets are the *A. terreus* genes encoding the transporters MfsA and MttA. The overexpression of the two genes heightened ITA production in a transgenic *A. niger* strain (Li et al., 2013).

The effect of alternative *RIA1* sequences from the array of ITA secreting *Ustilaginaceae* must be considered as well. As was shown by Geiser et al. (2018), the introduction of *RIA1* sequences from different species had varying consequences on the resulting ITA production. The strongest induction of ITA synthesis was mostly achieved with the help of the *P. tsukubaensis RIA1* gene.

Beyond that there is the possibility to develop a strong synthetic ITA regulating protein by studying how exactly the Ria1 protein functions and how it controls the ITA cluster.

In *Y. lipolytica*, the ICA is a direct product of the TCA cycle. There is no subsequent biosynthesis pathway that must be enhanced. As was shown in our study, transport proteins, especially mitochondrial ones, play a crucial role in the production of ICA as well. A greater focus on these carrier proteins for example by identifying suitable ICA exporters can heavily heighten product formation.

Both ITA and ICA share *cis*-aconitate as a common precursor. Therefore, attempts were carried out to enhance aconitase activity to gain more intramitochondrial *cis*-aconitate and ultimately more of the desired product. A similar approach by Holz et al. (2009) led to an increased ICA production with *Y. lipolytica.* However, additional overexpression of genes encoding native aconitase enzymes had either no effect in the case of *P. tsukubaensis* HR12 or even reversed the

positive effect of the *YlYHM2* deletion in *Y. lipolytica*. This means that the dehydration of CA into *cis*-aconitate is not a bottleneck reaction. Therefore, other genetic targets must be investigated during future projects.

Possible candidates are genes that influence metabolic processes upstream of the *cis*-aconitate formation and thus increase the supply of precursors. In that sense, it is generally important to maintain a high continuous glycolytic activity. However, high CA concentrations in the cytosol can lead to the inhibition of the ATP-dependent phosphofructokinase which ultimately slows down glucose catabolism and subsequently the TCA cycle (Meixner-Monori et al., 1984; Mlakar and Legiša, 2006). Therefore, the modification of the native gene responsible for the phosphofructokinase to eliminate that feedback inhibition could lead to an increased organic acid production.

Another expedient solution would be the introduction of an altered phosphofructokinase gene. It was shown by Tevž et al. (2010) that the introduction of the *pfkA* gene encoding the modified *A. niger* phosphofructokinase resulted in an increased ITA secretion with *A. terreus*. In a separate work, it was demonstrated that the abolishment of pyruvate kinase Pyk1p activity reduces the glycolytic flux (Yu et al., 2018). Therefore, overexpressing the respective homologous gene in *Y. lipolytica* or *P. tsukubaensis* could lead to an increased flow through glycolysis and ultimately higher TCA cycle activity.

A different approach was followed by Hossain et al. (2016) where the overexpression of the putative native cytosolic citrate synthase CitB in an *AtCAD1, AtMTTA* and *AtMFSA* expressing *A. niger* strain diminished side product formation and optimized the production pathway towards ITA. Thus, leading to increased ITA concentrations of up to 26.2 g l^{-1}.

Furthermore, a recent study showed that the glucose uptake in *Kluyveromyces marxianus* is slowed down due to low hexokinase activity (Sakihama et al., 2019). Enhancing hexokinase activity in yeasts with an activated glycolytic and TCA cycle activity, thus, could lead to elevated glucose uptake that would fuel the enhanced organic acid production.

Additionally, ICA and indirectly CA are broken down by the NADH and NADPH dependent isocitrate dehydrogenases (IDHs) during the TCA cycle. The IDH enzyme are activated by high intracellular AMP levels. However, under conditions of N starvation and glucose excess, ammonium is produced from AMP by the adenosine monophosphate deaminase enzyme (Beopoulos et al., 2011). Increasing adenosine monophosphate deaminase activity prevents AMP accumulation and the induction of the IDHs. The practicality of this approach was recently substantiated in *Y. lipolytica* for the overproduction of CA (Yuzbasheva et al., 2019).

The reduction of other competing organic acids is also an essential goal for future studies. In doing so, the flux towards ITA/ICA synthesis would be elevated. An additional advantage would be a less

demanding product recovery. To our advantage, *P. tsukubaensis* ITA overproducing strain HR12 already produces extremely low concentrations of competing organic acids like MA or *α*KG. Luckily, this yeast represents an extremely favourable host organism, because it naturally does not harbour the genes necessary to further metabolize ITA into 2-hydroxyparaconate and itatartarate. However, *Y. lipolytica* ICA producing strain Δ*YHM2* still secretes some amounts of the isoform CA. As was discussed in chapter 4.6, it could be beneficial to diminish Cit2p activity. This would hinder the cell to synthesise CA in the peroxisomes from acetyl-CoA and oxaloacetate.

Contrary to the relatively low levels of organic acid by-products, the accumulation of storage lipids, still represents a considerable destination for the supplied C source. It is known, that both yeast species form large quantities of intracellular lipids, mostly as triacylglycerols and steryl esters. In addition to that, *P. tsukubaensis* also produces intra- and extracellular glycolipids mostly in the form of MEL-B as a storage compound and as a natural biosurfactant (Arutchelvi et al., 2008). Due to their hydrophobic nature, these lipids are cause for increased efforts during sample and culture handling but also during product recovery processes. The reduction of lipid production would have a positive impact on product formation and process handling. Here, the attempts to optimize process conditions by decreasing the pH to 4.0 already had the consequence that significantly less lipids were stored inside *P. tsukubaensis* cells. It is, hence, important to gain insight into the underlying control mechanism and apply this knowledge to effectively bypass lipid formation at conditions with a neutral pH. A potential possibility to reduce lipid synthesis is the inhibition/knock-out of the ATP-citrate lyase. In the cytosol, this enzyme is responsible for the cleavage of CA into acetyl-CoA and oxaloacetate. The resulting acetyl-CoA is then channelled to the lipid biosynthesis (Dourou et al., 2017). Therefore, the knock-out of ATP-citrate lyase would serve two purposes: first by limiting the breakdown of CA as a main precursor for both ITA and ICA and secondly by reducing the formation of storage lipids.

Besides the inhibition of lipids synthesis, another possibility is to enhance lipid degradation. Fatty acids that are stored as lipids inside lipid bodies can potentially be remobilized by upregulating triacylglycerol lipase activity e.g. Tgl3p and Tgl4p in *Y. lipolytica* (Ledesma-Amaro et al., 2016).

These rational genetic modification approaches are extremely valuable, but their implementation is still tied to considerable laborious work. For future metabolic engineering strategies, more suitable genetic tools and techniques are a key aspect. This is especially the case for *P. tsukubaensis*, where only very limited methods are available at the moment because this species has not been a subject for the intense development of genetic tools. With easily configurable and adaptable genetic methods this is, however, starting to change. Recently, the group around Kunitake et al. (2019) described the successful utilization of a RNP-mediated CRISPR/Cas9 system in the closely related basidiomycete *P. antarctica*. The gene targeting was

efficient at two target loci in the genome (*PaPaE* and *PaADE2*). These CRISPR/Cas systems are very promising but other techniques like the golden gate assembly are too. Golden gate systems allow multiple DNA fragments to be cloned and directionally be assembled into a single DNA molecule without leaving behind "scars". An according golden gate system, which is suitable for the overexpression of target genes and which also facilitates CRISPR/Cas mediated gene knock-out, was recently proven efficient for *Y. lipolytica* wild type isolates (Egermeier et al., 2019).

The optimization of the fermentation process is one of the most important strategies besides genetic means, to further improve organic acid production with the two yeasts. The available literature is focused on changes in fermentation conditions including pH and aeration (Yalcin et al., 2012, 2010) and the development of different fermentation strategies like (fed-)batch or continuous fermentations (Liu et al., 2015; Rywińska and Rymowicz, 2011). In the present study, we could demonstrate that the production of ITA with the overproducing strain HR12 can be modulated by changes in pH and aeration, where a slightly acidic pH (4.0-5.5) and a sufficient aeration (pO$_2$: ≥ 55 %) was beneficial for the production. As far as the fermentation scale is concerned, most research work is still carried out on a laboratory scale. It is thus important to investigate the practicability of upscaling these fermentation methods.

At the same time, downstream processes must be developed intensively. Generally, downstream processing involves ultrafiltration and electrodialysis for *in-situ* product recovery of the respective organic acid. Recently, Aurich et al. (2017) developed a novel method to isolate ICA from the fermentation broth by selective adsorption on activated carbon. Thereby, electrodialysis and the removal of water by (vacuum) distillation were no longer necessary.

Since ITA is already produced on an industrial scale, there already exists substantial knowledge on the associated product recovery and purification processes. Industrial degree of purity is achieved by biomass separation (filtration or centrifugation) and subsequent crystallization via multiple evaporation and cooling steps. The current state of the art in recovery and purification for ITA production via bioprocesses was recently reviewed by Magalhães et al. (2017). The development of an efficient process for separating and purifying ITA is challenging due to the high affinity of this hydrophilic solute for aqueous solutions and the complex composition of the fermentation broth. According to the authors, the multitude of applicable ITA recovery processes from the fermentation broth are boiling down to either the use of chemical demanding, reaction-based separations (precipitation, extraction, and adsorption), or the use of energy demanding, physical separation methods (crystallization or membrane separation). For the development of future technologies, there is an increasing emphasis on recovery processes that are directly coupled to the fermentation. This means that no accumulation of ITA occurs, which could dampen the bioconversion by feedback inhibition. Promising technologies are membrane bioreactors,

adsorption, and reactive extractions, since these separation methods do not interfere with the microorganisms.

Lastly, medium compositions must be studied in more detail. Since *Aspergillus* species are known to be sensitive towards heavy metal contaminants, serious effort is directed towards the establishment of more tolerant fungi strains. Here it represents a great advantage, that the yeasts belonging to the *Yarrowia* and *Pseudozyma* genus naturally display a moderate to high tolerance for heavy metals in the medium (Bankar et al., 2018; Vadkertiová and Sláviková, 2006). Hence, the development of alternative media should have an emphasize on other aspects.

One point of interest is the applied C source. Usually, simple sugars are employed as C source in fermentation studies, because of the great efficiency to convert those sugars into value-added bio-chemicals. Their use, on the other hand, competes with the food industry. In order to alleviate this fact and to generate more lucrative applications, alternative substrates have to be investigated. Low cost agro-industrial waste products are promising substrates. For the production of CA with *Y. lipolytica*, C sources such as olive-mill wastewater, raw glycerol from the waste of biodiesel industry and inulin have been proven applicable (Papanikolaou et al., 2008; Rakicka et al., 2016; Rymowicz et al., 2006). Other C sources such as fruit pulps or wood hydrolysates are also feasible.

An overview of all possible points of interest to further optimise the unconventional oleaginous yeasts *P. tsukubaensis* and *Y. lipolytica* for the production of ITA and ICA is shown in figure 45.

In conclusion, two very promising yeast strains have been constructed within the framework of this thesis: *P. tsukubaensis* HR12 and *Y. lipolytica* Δ*YHM2* for the microbial production of ITA and ICA, respectively. In first attempts to improve the efficiency of the fermentation processes, high end concentrations of up to 113.6 g l^{-1} ITA and 131.9 g l^{-1} ICA have been secreted. Our results shall constitute a foundation for future projects and industrial applications to facilitate the potential of these two exceptional yeasts.
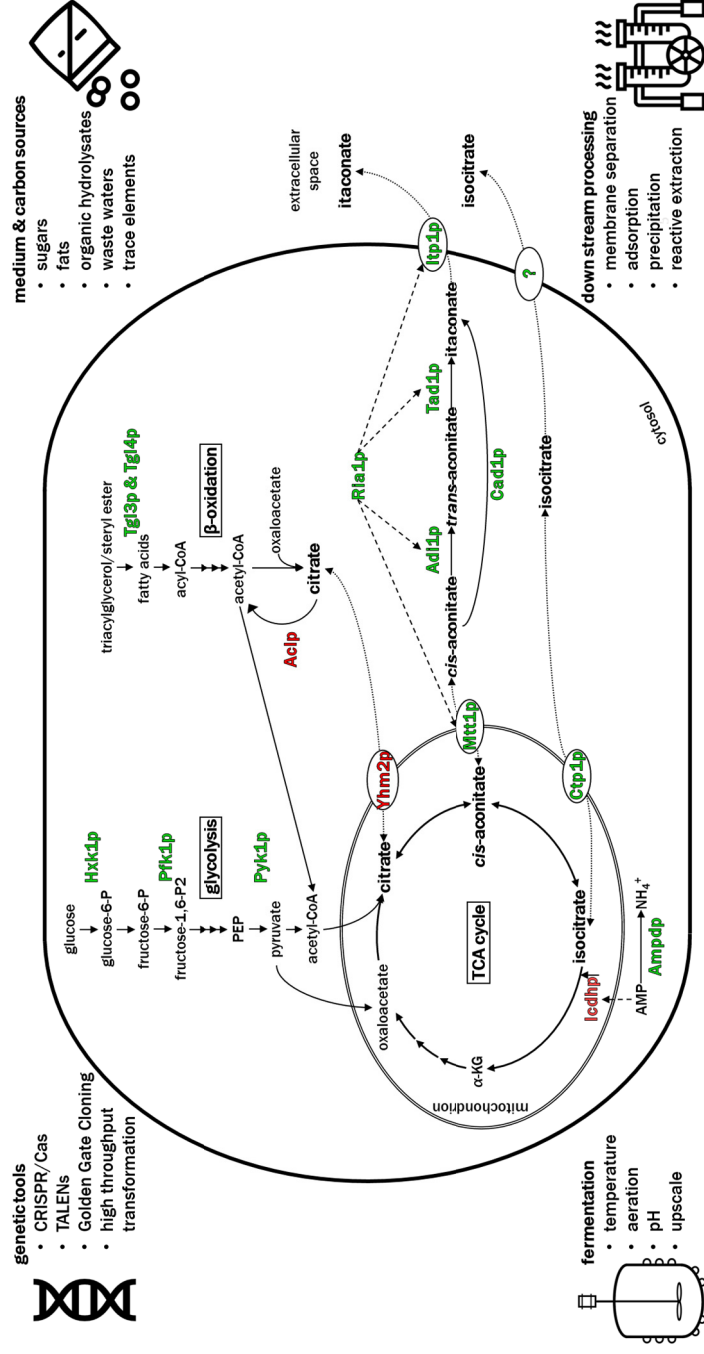
Figure 45 Potential targets to further increase organic acid production with the unconventional yeast species *P. tsukubaensis* and *Y. lipolytica.*

The organic acid *cis*-aconitate is the common precursor for both ITA and ICA. Biosynthesis of *cis*-aconitate can be enhanced by activating glycolysis. Potentially, this is achieved by overexpressing the genes encoding the hexokinase (HxkIp), phosphofructokinase (PfkIp) and pyruvate kinase (PykIp) enzymes. The activated glycolysis provides the necessary acetyl-CoA and oxaloacetate for the TCA cycle. Deletion of the tricarboxylate carrier Yhm2p can prevent the export of CA. The second tricarboxylate shuttling protein in *Y. lipolytica* is CtpIp, which is probably responsible for the transport of ICA into the cytosol. The exact function of CtpIp is still unclear. The generated ICA is broken down by the isocitrate dehydrogenase (Icdhp), which is activated by elevated AMP-levels. This activation can be circumvented by the overexpression of an adenosine monophosphate deaminase (Ampdp) and the resulting break down of AMP into NH₄⁺. In *P. tsukubaensis*, *cis*-aconitate is transported by Mtt1p into the cytosol, where it is isomerised into *trans*-aconitate (Adi1p) and subsequently decarboxylated (Tad1p) into ITA. *cis*-Aconitate can also directly be decarboxylated into ITA by Cad1p. ITA is excreted into the surrounding medium by Itp1p. The transport protein responsible for the secretion of ICA has not been identified yet. The transcription of the genes of Mtt1p, Adi1p, Tad1p, and Itp1p are regulated by Ria1p. For example, protein engineering, codon optimization or homologous genes from suitable organisms could enhance the function of the above-mentioned metabolic proteins and thus the production of ICA and ITA, respectively. Formation of by-products like hydrophobic storage substances can be reduced by knocking-down the ATP-citrate lyse (Acl1p) to dampen lipogenesis. The resulting acetyl-CoA could fuel the TCA cycle. For these metabolic engineering approaches, new genetic tools like genome editing (CRISPR/Cas, TALENs) and multi-gene transformation techniques (Golden Gate Cloning) should be further adapted to suit the unconventional yeasts. Additionally, the fermentation process must be optimized by evaluating alternative, low-cost substrates (e.g. fruit pulp, wood hydrolysates) and by identifying optimal fermentation conditions (pH, temperature, oxygen saturation). It is also imperative to improve the separation and purification technologies to lower costs and establish an overall competitively viable process. Images used from www.flaticon.com

Eidesstattliche Erklärung

I herewith declare that I have produced this work without the prohibited assistance of third parties and without making use of aids other than those specified; notions taken over directly or indirectly from other sources have been identified as such. This work has not previously been presented in identical or similar form to any other German or foreign examination board.

Parts of this work were carried out as subject of a research and development contract with BASF SE. The research project F-000978-531-000-1050491 was concluded with the patent "Microorganisms and the Production of Fine Chemicals" (WO2019233853).

Hiermit versichere ich, dass ich die vorliegende Arbeit ohne unzulässige Hilfe Dritter und ohne Benutzung anderer als der angegebenen Hilfsmittel angefertigt habe; die aus fremden Quellen direkt oder indirekt übernommenen Gedanken sind als solche kenntlich gemacht.

Teile dieser Arbeit entstanden im Rahmen eines Forschungs- und Entwicklungsauftrages mit der BASF SE. Das Forschungsvorhaben F-000978-531-000-1050491 wurde mit dem Patent abgeschlossen " Microorganisms and the Production of Fine Chemicals" (WO2019233853).

Dresden, den

Publications and conference contributions

Publications

Gatter, M., Ottlik, S., **Kövesi, Z.**, Bauer, B., Matthäus, F., & Barth, G. (2016). Three alcohol dehydrogenase genes and one acetyl-CoA synthetase gene are responsible for ethanol utilization in Yarrowia lipolytica. *Fungal genetics and biology*, *95*, 30-38.[8]

Barth, G. (2019). „ Microorganisms and the Production of Fine Chemicals" *Patent*. WO2019233853

Conference contributions

Kövesi Z., Gatter M., Barth G. "Deletion of a Novel Mitochondrial Carrier for Citrate Shifts Acid Production Towards Isocitric Acid in *Yarrowia lipolytica*" Yeast 2017. Prague, CZ. 27.08.-01.09.2017. Poster

Kövesi Z., Gatter M., Barth G. "Substantial Increase of Isocitric Acid-Yield by the Deletion of *YHM2*, a Novel Mitochondrial Carrier for Citrate in the Oleaginous Yeast *Yarrowia lipolytica*". Yeast Genetics Meeting. Stanford, USA. 22.−26.08.2018. Poster

---

[8] The publication was not prepared as a part of this thesis.

Danksagung

Zuallererst möchte ich mich an dieser Stelle bei all den Personen bedanken und ohne deren Unterstützung diese Arbeit niemals möglich gewesen wäre.

Ein besonderer Dank geht ein meinen Doktorvater Herrn Prof. Dr. Gerold Barth für die Möglichkeit, bei ihm dieses interessante Projekt bearbeiten zu dürfen. Natürlich bedanke ich mich hier auch für seine intensive Betreuung während der gesamten Zeit der Zusammenarbeit.

Mein herzlicher Dank geht an meinen Mentor Dr. Michael Gatter dafür, dass er mir Werkzeuge an die Hand geben hat, die nicht nur für diese Arbeit, sondern auch weit darüber hinaus hilfreich sind. Zudem waren seine Vorarbeiten essenziell für dieses Projekt. Danke dir, Micha!

Außerdem gilt mein Dank dem gesamten Institut für Mikrobiologie, insbesondere Herrn Prof. Dr. Thorsten Mascher, für die Bereitstellung der Räumlichkeiten sowie der gesamten Technik, die für diese Arbeit notwendig waren.

Des Weiteren möchte ich mich bei Frau Prof. Dr. Jutta Ludwig-Müller dafür bedanken, dass sie sich die Zeit genommen hat, um das Zweitgutachten zu erstellen.

Bei Dr. Daniela Pinto und Vivien Quitzke möchte ich für ihre anregenden und konstruktiven Gespräche bedanken und für ihre Unterstützung während meiner Zeit am Institut für Mikrobiologie.

Für ihre praktische Mithilfe und die einzigartige Unterhaltung während der Mittagspausen möchte ich mich bei den technischen Assistenten Annett George, Susanne Krause, Silke Hoffmann, Jana Stephan und Silvia Heinze bedanken.

Liebe Stephanie, dir gilt mein größter Dank für deine herzliche Zuwendung, die mir seit Jahren zuteilwird und für deine endlose Geduld, die du während der letzten harten Jahre aufgebracht hast.

Ein besonderer Dank gilt meiner Familie aber auch der Familie Ottlik, die immer für mich da waren und mir konstant Rückhalt gegeben haben.

References

Abe, M., and Tabuchi, T. (1968). Occurrence of biologically active isocitric acid in cultures of yeasts. Agric. Biol. Chem. 32, 392–393.

Adrio, J.L. (2017). Oleaginous yeasts: Promising platforms for the production of oleochemicals and biofuels. Biotechnol. Bioeng. 114, 1915–1920.

Akiyama, S., Suzuki, T., Sumino, Y., Nakao, Y., and Fukuda, H. (1973). Induction and citric acid productivity of fluoroacetate-sensitive mutant strains of Candida lipolytica. Agric. Biol. Chem. 37, 879–884.

Ali, S., Shultz, J.L., and Ikram-ul-Haq (2007). High performance microbiological transformation of L-tyrosine to L-dopa by Yarrowia lipolytica NRRL-143. BMC Biotechnol. 7, 50.

Arutchelvi, J.I., Bhaduri, S., Uppara, P.V., and Doble, M. (2008). Mannosylerythritol lipids: a review. J. Ind. Microbiol. Biotechnol. 35, 1559–1570.

Atomi, H., Ueda, M., Hikida, M., Hishida, T., Teranishi, Y., and Tanaka, A. (1990). Peroxisomal isocitrate lyase of the n-alkane-assimilating yeast Candida tropicalis: gene analysis and characterization. J. Biochem. (Tokyo) 107, 262–266.

Aurich, A., Specht, R., Müller, R.A., Stottmeister, U., Yovkova, V., Otto, C., Holz, M., Barth, G., Heretsch, P., Thomas, F.A., et al. (2012). Microbiologically Produced Carboxylic Acids Used as Building Blocks in Organic Synthesis. In Reprogramming Microbial Metabolic Pathways, (Springer, Dordrecht), pp. 391–423.

Aurich, A., Hofmann, J., Oltrogge, R., Wecks, M., Gläser, R., Blömer, L., Mauersberger, S., Müller, R.A., Sicker, D., and Giannis, A. (2017). Improved Isolation of Microbiologically Produced (2R,3S)-Isocitric Acid by Adsorption on Activated Carbon and Recovery with Methanol.

Aurich, A.D.-I., Barth, G.P.D., Bodinus, C., Kreyss, E., and Specht, R. (2009). A process for the biotechnological production of products.

Auta, H.S., Abidoye, K.T., Tahir, H., Ibrahim, A.D., and Aransiola, S.A. (2014). Citric Acid Production by Aspergillus niger Cultivated on Parkia biglobosa Fruit Pulp. Int. Sch. Res. Not. 2014.

Avis, T.J., Cheng, Y.L., Zhao, Y.Y., Bolduc, S., Neveu, B., Anguenot, R., Labbé, C., Belzile, F., and Bélanger, R.R. (2005). The potential of Pseudozyma yeastlike epiphytes for the production of heterologous recombinant proteins. Appl. Microbiol. Biotechnol. 69, 304–311.

Avis, T.J., Anguenot, R., Neveu, B., Bolduc, S., Zhao, Y., Cheng, Y., Labbé, C., Belzile, F., and Bélanger, R.R. (2008). Usefulness of Heterologous Promoters in the Pseudozyma flocculosa Gene Expression System. Biosci. Biotechnol. Biochem. 0801080715–0801080715.

Azbar, N., Bayram, A., Filibeli, A., Muezzinoglu, A., Sengul, F., and Ozer, A. (2004). A Review of Waste Management Options in Olive Oil Production. Crit. Rev. Environ. Sci. Technol. 34, 209–247.

Bafana, R., and Pandey, R.A. (2018). New approaches for itaconic acid production: bottlenecks and possible remedies. Crit. Rev. Biotechnol. 38, 68–82.

Bandoni, R.J. (1985). On an undescribed, pleomorphic hyphomycete from litter. Bot. J. Linn. Soc. 91, 37–43.

Bankar, A., Zinjarde, S., Shinde, M., Gopalghare, G., and Ravikumar, A. (2018). Heavy metal tolerance in marine strains of Yarrowia lipolytica. Extremophiles 22, 617–628.

Bankar, A.V., Kumar, A.R., and Zinjarde, S.S. (2009a). Environmental and industrial applications of Yarrowia lipolytica. Appl. Microbiol. Biotechnol. 84, 847–865.

Bankar, A.V., Kumar, A.R., and Zinjarde, S.S. (2009b). Removal of chromium (VI) ions from aqueous solution by adsorption onto two marine isolates of Yarrowia lipolytica. J. Hazard. Mater. 170, 487–494.

Barrett, D.G., Merkel, T.J., Luft, J.C., and Yousaf, M.N. (2010a). One-Step Syntheses of Photocurable Polyesters Based on a Renewable Resource. Macromolecules 43, 9660–9667.

Barrett, D.G., Luo, W., and Yousaf, M.N. (2010b). Aliphatic polyester elastomers derived from erythritol and α,ω-diacids. Polym. Chem. 1, 296–302.

Barth, G. (2013). Yarrowia lipolytica: Biotechnological Applications (Springer Science & Business Media).

Barth, G., and Gaillardin, C. (1996). Yarrowia lipolytica. In Nonconventional Yeasts in Biotechnology, (Springer Berlin Heidelberg), pp. 313–388.

References

Barth, G., and Gaillardin, C. (1997). Physiology and genetics of the dimorphic fungus Yarrowia lipolytica. FEMS Microbiol. Rev. 19, 219–237.

Barth, G., and Weber, H. (1985). Improvement of sporulation in the yeast Yarrowia lipolytica. Antonie Van Leeuwenhoek 51, 167–177.

Battat, E., Peleg, Y., Bercovitz, A., Rokem, J.S., and Goldberg, I. (1991). Optimization of L-malic acid production by Aspergillus flavus in a stirred fermentor. Biotechnol. Bioeng. 37, 1108–1116.

Baup, S. (1837). Über eine neue Pyrogen-Citronensäure, und über Benennung der Pyrogen-Säuren überhaupt. Ann. Pharm. 19, 29–38.

Begerow, D., Bauer, R., and Boekhout, T. (2000). Phylogenetic placements of ustilaginomycetous anamorphs as deduced from nuclear LSU rDNA sequences* *Part 174 of the series 'Studies in Heterobasidiomycetes'. Mycol. Res. 104, 53–60.

Bélanger, R.R., and Labbé, C. (2002). Control of powdery mildews without chemicals: prophylactic and biological alternatives for horticultural crops. Powdery Mildews Compr. Treatise 256–267.

Bellou, S., Makri, A., Triantaphyllidou, I.-E., Papanikolaou, S., and Aggelis, G. (2014). Morphological and metabolic shifts of Yarrowia lipolytica induced by alteration of the dissolved oxygen concentration in the growth environment. Microbiology, 160, 807–817.

Ben-Menachem, R., Regev-Rudzki, N., and Pines, O. (2011). The aconitase C-terminal domain is an independent dual targeting element. J. Mol. Biol. 409, 113–123.

Ben-Menachem, R., Wang, K., Marcu, O., Yu, Z., Lim, T.K., Lin, Q., Schueler-Furman, O., and Pines, O. (2018). Yeast aconitase mitochondrial import is modulated by interactions of its C and N terminal domains and Ssa1/2 (Hsp70). Sci. Rep. 8, 5903.

Bentley, R., and Thiessen, C.P. (1957a). Biosynthesis of itaconic acid in Aspergillus terreus. II. Early stages in glucose dissimilation and the role of citrate. J. Biol. Chem. 226, 689–701.

Bentley, R., and Thiessen, C.P. (1957b). Biosynthesis of Itaconic Acid in Aspergillus Terreus I. Tracer Studies with C14-Labeled Substrates. J. Biol. Chem. 226, 673–687.

Bentley, R., and Thiessen, C.P. (1957c). Biosynthesis of itaconic acid in Aspergillus terreus. III. The properties and reaction mechanism of cis-aconitic acid decarboxylase. J. Biol. Chem. 226, 703–720.

Bentrup, K.H.Z., Miczak, A., Swenson, D.L., and Russell, D.G. (1999). Characterization of Activity and Expression of Isocitrate Lyase in Mycobacterium avium and Mycobacterium tuberculosis. J. Bacteriol. 181, 7161–7167.

Beopoulos, A., Cescut, J., Haddouche, R., Uribelarrea, J.-L., Molina-Jouve, C., and Nicaud, J.-M. (2009). Yarrowia lipolytica as a model for bio-oil production. Prog. Lipid Res. 48, 375–387.

Beopoulos, A., Nicaud, J.-M., and Gaillardin, C. (2011). An overview of lipid metabolism in yeasts and its impact on biotechnological processes. Appl. Microbiol. Biotechnol. 90, 1193–1206.

Berg, R.G., and Hetzel, D.S. (1978). Preparation of citraconic anhydride.

Blatt, A.H. (1943). Organic Syntheses (Wiley).

Blazeck, J., Hill, A., Liu, L., Knight, R., Miller, J., Pan, A., Otoupal, P., and Alper, H.S. (2014). Harnessing Yarrowia lipolytica lipogenesis to create a platform for lipid and biofuel production. Nat. Commun. 5, 1–10.

Blazeck, J., Hill, A., Jamoussi, M., Pan, A., Miller, J., and Alper, H.S. (2015). Metabolic engineering of Yarrowia lipolytica for itaconic acid production. Metab. Eng. 32, 66–73.

Blumhoff, M.L., Steiger, M.G., Mattanovich, D., and Sauer, M. (2013). Targeting enzymes to the right compartment: Metabolic engineering for itaconic acid production by Aspergillus niger. Metab. Eng. 19, 26–32.

Bodinus, C. (2011). Phänotypische und genotypische Optimierung der Itaconsäureproduktion mit der Hefe Pseudozyma tsukubaensis. Technische Universität Dresden.

Boeke, J.D., Trueheart, J., Natsoulis, G., and Fink, G.R. (1987). 5-Fluoroorotic acid as a selective agent in yeast molecular genetics. B.-M. in Enzymology, ed. (Academic Press), pp. 164–175.

Boekhout, T. (1995). Pseudozyma Bandoni emend. Boekhout, a Genus for Yeast-like Anamorphs of Ustilaginales. J. Gen. Appl. Microbiol. 41, 359–366.

Boekhout, T. (2011). Chapter 153 - Pseudozyma Bandoni emend. Boekhout (1985) and a comparison with the yeast state of Ustilago maydis (De Candolle) Corda (1842). In The Yeasts (Fifth Edition), C.P. Kurtzman, J.W. Fell, and T. Boekhout, eds. (London: Elsevier), pp. 1857–1868.

References

Bonnarme, P., Gillet, B., Sepulchre, A.M., Role, C., Beloeil, J.C., and Ducrocq, C. (1995). Itaconate biosynthesis in Aspergillus terreus. J. Bacteriol. 177, 3573–3578.

Boro, M.C., Jesus, A.L. de, Souza, J.I. de, Marano, A.V., Pires-Zottarelli, C.L.A., Boro, M.C., Jesus, A.L. de, Souza, J.I. de, Marano, A.V., and Pires-Zottarelli, C.L.A. (2017). Molecular identification of Pseudozyma aphidis (Henninger & Windisch) Boekhout: first record from a Brazilian mangrove swamp. Hoehnea 44, 599–606.

Bradford, M.M. (1976). A rapid and sensitive method for the quantitation of microgram quantities of protein utilizing the principle of protein-dye binding. Anal. Biochem. 72, 248–254.

Brauer, D., and Teel, M.R. (1981). Metabolism of trans-Aconitic Acid in Maize : I. Purification of Two Molecular Forms of Citrate Dehydrase. Plant Physiol. 68, 1406–1408.

Budak, N.H., Aykin, E., Seydim, A.C., Greene, A.K., and Guzel-Seydim, Z.B. (2014). Functional Properties of Vinegar. J. Food Sci. 79, R757–R764.

Bullin, K., Hennig, L., Herold, R., Krautscheid, H., Richter, K., and Sicker, D. (2019). An optimized method for an (2R,3S)-isocitric acid building block. Monatshefte Für Chem. - Chem. Mon. 150, 247–253.

Burau, R., and Stout, P.R. (1965). Trans-Aconitic Acid in Range Grasses in Early Spring. Science 150, 766–767.

Burkholder, P.R., and Moyer, D. (1943). Vitamin deficiencies of fifty yeasts and molds. Bull. Torrey Bot. Club 372–377.

Buxdorf, K., Rahat, I., Gafni, A., and Levy, M. (2013). The Epiphytic Fungus Pseudozyma aphidis Induces Jasmonic Acid- and Salicylic Acid/Nonexpressor of PR1-Independent Local and Systemic Resistance. Plant Physiol. 161, 2014–2022.

Calam, C.T., Oxford, A.E., and Raistrick, H. (1939). Studies in the biochemistry of micro-organisms: Itaconic acid, a metabolic product of a strain of Aspergillus terreus Thom. Biochem. J. 33, 1488–1495.

Cao, X., Wei, L.-J., Lin, J.-Y., and Hua, Q. (2017). Enhancing linalool production by engineering oleaginous yeast Yarrowia lipolytica. Bioresour. Technol. 245, 1641–1644.

Carlsson, M., Habenicht, C., Kam, L.C., Antal, M.J.Jr., Bian, N., Cunningham, R.J., and Jones, M.Jr. (1994). Study of the sequential conversion of citric to itaconic to methacrylic acid in near-critical and supercritical water. Ind. Eng. Chem. Res. 33, 1989–1996.

Carly, F., Steels, S., Telek, S., Vandermies, M., Nicaud, J.-M., and Fickers, P. (2018). Identification and characterization of EYD1, encoding an erythritol dehydrogenase in Yarrowia lipolytica and its application to bioconvert erythritol into erythrulose. Bioresour. Technol. 247, 963–969.

Castegna, A., Scarcia, P., Agrimi, G., Palmieri, L., Rottensteiner, H., Spera, I., Germinario, L., and Palmieri, F. (2010). Identification and Functional Characterization of a Novel Mitochondrial Carrier for Citrate and Oxoglutarate in Saccharomyces cerevisiae. J. Biol. Chem. 285, 17359–17370.

Cavalcante Fai, A.E., Resende Simiqueli, A.P., de Andrade, C.J., Ghiselli, G., and Pastore, G.M. (2015). Optimized production of biosurfactant from Pseudozyma tsukubaensis using cassava wastewater and consecutive production of galactooligosaccharides: An integrated process. Biocatal. Agric. Biotechnol. 4, 535–542.

Cavallo, E., Charreau, H., Cerrutti, P., and Foresti, M.L. (2017). Yarrowia lipolytica: a model yeast for citric acid production. FEMS Yeast Res. 17.

Cheng, Y., Belzile, F., Tanguay, P., Bernier, L., and Bélanger, R. (2001). Establishment of a gene transfer system for Pseudozyma flocculosa, an antagonistic fungus of powdery mildew fungi. Mol. Genet. Genomics 266, 96–102.

Cheng, Y., McNally, D.J., Labbé, C., Voyer, N., Belzile, F., and Bélanger, R.R. (2003). Insertional Mutagenesis of a Fungal Biocontrol Agent Led to Discovery of a Rare Cellobiose Lipid with Antifungal Activity. Appl. Environ. Microbiol. 69, 2595–2602.

Chiusoli, G. (1962). Process for preparing itaconic acid and 2,3-butandienoic acid (to Montecatini, Italy).

Cho, J.H., Ha, S.J., Kao, L.R., Megraw, T.L., and Chae, C.-B. (1998). A Novel DNA-Binding Protein Bound to the Mitochondrial Inner Membrane Restores the Null Mutation of Mitochondrial Histone Abf2p in Saccharomyces cerevisiae. Mol. Cell. Biol. 18, 5712–5723.

Cordes, T., Michelucci, A., and Hiller, K. (2015). Itaconic Acid: The Surprising Role of an Industrial Compound as a Mammalian Antimicrobial Metabolite. Annu. Rev. Nutr. 35, 451–473.

Dai, J., Ma, S., Liu, X., Han, L., Wu, Y., Dai, X., and Zhu, J. (2015). Synthesis of bio-based unsaturated polyester resins and their application in waterborne UV-curable coatings. Prog. Org. Coat. 78, 49–54.

References

Damude, H.G., Gillies, P.J., Macool, D.J., Picataggio, S.K., Pollak, D.W.M., Ragghianti, J.J., Xue, Z., Yadav, N.S., Zhang, H., and Zhu, Q.Q. (2007). High eicosapentaenoic acid producing strains of Yarrowia lipolytica.

Damude, H.G., Gillies, P.J., Macool, D.J., Picataggio, S.K., Pollak, D.M.W., Ragghianti, J.J., Xue, Z., Yadav, N.S., Zhang, H., and Zhu, Q.Q. (2015). High arachidonic acid producing strains of Yarrowia lipolytica.

Darvishi, F. (2012). Microbial Biotechnology in Olive Oil Industry. Olive Oil - Const. Qual. Health Prop. Bioconversions.

De Guzman, D. (2009). What is Itaconic acid. ICIS Green Chem.

De Mot, R., Van Oudenduck, E., and Verachtert, H. (1985). Purification and characterization of an extracellular glucoamylase from the yeast Candida tsukubaensis CBS 6389. Antonie Van Leeuwenhoek 51, 275–287.

De Robertis, A., De Stefano, C., Rigano, C., and Sammartano, S. (1990). Thermodynamic parameters for the protonation of carboxylic acids in aqueous tetraethylammonium iodide solutions. J. Solut. Chem. 19, 569–587.

Delidovich, I., Hausoul, P.J.C., Deng, L., Pfützenreuter, R., Rose, M., and Palkovits, R. (2016). Alternative Monomers Based on Lignocellulose and Their Use for Polymer Production. Chem. Rev. 116, 1540–1599.

Dias, C., Silva, C., Freitas, C., Reis, A., and da Silva, T.L. (2016). Effect of Medium pH on Rhodosporidium toruloides NCYC 921 Carotenoid and Lipid Production Evaluated by Flow Cytometry. Appl. Biochem. Biotechnol. 179, 776–787.

Dourou, M., Mizerakis, P., Papanikolaou, S., and Aggelis, G. (2017). Storage lipid and polysaccharide metabolism in Yarrowia lipolytica and Umbelopsis isabellina. Appl. Microbiol. Biotechnol. 101, 7213–7226.

Dower, W.J., Miller, J.F., and Ragsdale, C.W. (1988). High efficiency transformation of E.coli by high voltage electroporation. Nucleic Acids Res. 16, 6127–6145.

Dudley, B. (2019). BP statistical review of world energy. Lond. UK.

Dulermo, T., and Nicaud, J.-M. (2011). Involvement of the G3P shuttle and β-oxidation pathway in the control of TAG synthesis and lipid accumulation in Yarrowia lipolytica. Metab. Eng. 13, 482–491.

Duntze, W., Neumann, D., Atzpodien, W., Holzer, H., and Gancedo, J.M. (1969). Studies on the Regulation and Localization of the Glyoxylate Cycle Enzymes in Saccharomyces cerevisiae. Eur. J. Biochem. 10, 83–89.

Durant, Y.G. (2009). The development of integrated production of polyitaconic acid from Northeast hardwood biomass. NIFA Proj. 2009-2012 Tech. Rep. Itaconix LLC.

Duro, A.F., and Serrano, R. (1981). Inhibition of succinate production during yeast fermentation by deenergization of the plasma membrane. Curr. Microbiol. 6, 111–113.

Dutton, M.V., and Evans, C.S. (1996). Oxalate production by fungi: its role in pathogenicity and ecology in the soil environment. Can. J. Microbiol. 42, 881–895.

Dwiarti, L., Yamane, K., Yamatani, H., Kahar, P., and Okabe, M. (2002). Purification and characterization of cis-aconitic acid decarboxylase from Aspergillus terreus TN484-M1. J. Biosci. Bioeng. 94, 29–33.

van Dyk, M.S., van Rensburg, E., Rensburg, I.P.B., and Moleleki, N. (1998). Biotransformation of monoterpenoid ketones by yeasts and yeast-like fungi. J. Mol. Catal. B Enzym. 5, 149–154.

Eckardt, N.A. (2005). Peroxisomal Citrate Synthase Provides Exit Route from Fatty Acid Metabolism in Oilseeds. Plant Cell 17, 1863–1865.

Edite Bezerra da Rocha, M., Freire, F. da C.O., Erlan Feitosa Maia, F., Izabel Florindo Guedes, M., and Rondina, D. (2014). Mycotoxins and their effects on human and animal health. Food Control 36, 159–165.

Egermeier, M., Sauer, M., and Marx, H. (2019). Golden Gate-based metabolic engineering strategy for wild-type strains of Yarrowia lipolytica. FEMS Microbiol. Lett. 366.

El-Imam, A.A., and Du, C. (2014). Fermentative Itaconic Acid Production. J. Biodivers. Bioprospecting Dev. 1, 1–8.

Elnaghy, M.A., and Megalla, S.E. (1975). Itaconic-acid production by a local strain of Aspergillus terreus. Eur. J. Appl. Microbiol. Biotechnol. 1, 159–172.

Fan-Chiang, H.-J., and Wrolstad, R.E. (2010). Sugar and nonvolatile acid composition of blackberries. J. AOAC Int. 93, 956–965.

Fang, F.C., Libby, S.J., Castor, M.E., and Fung, A.M. (2005). Isocitrate Lyase (AceA) Is Required for Salmonella Persistence but Not for Acute Lethal Infection in Mice. Infect. Immun. 73, 2547–2549.

References

Ferrara, M.A., Almeida, D.S., Siani, A.C., Lucchetti, L., Lacerda, P.S.B., Freitas, A., Tappin, M.R.R., and Bon, E.P.S. (2014). Bioconversion of R-(+)-limonene to perillic acid by the yeast Yarrowia lipolytica. Braz. J. Microbiol. 44, 1075–1080.

Fickers, P., Nicaud, J.M., Destain, J., and Thonart, P. (2003). Overproduction of lipase by Yarrowia lipolytica mutants. Appl. Microbiol. Biotechnol. 63, 136–142.

Finn, R.D., Clements, J., Arndt, W., Miller, B.L., Wheeler, T.J., Schreiber, F., Bateman, A., and Eddy, S.R. (2015). HMMER web server: 2015 update. Nucleic Acids Res. 43, W30–W38.

Finogenova, T.V., Morgunov, I.G., Kamzolova, S.V., and Chernyavskaya, O.G. (2005). Organic Acid Production by the Yeast Yarrowia lipolytica: A Review of Prospects. Appl. Biochem. Microbiol. 41, 418–425.

Förster, A., Aurich, A., Mauersberger, S., and Barth, G. (2007a). Citric acid production from sucrose using a recombinant strain of the yeast Yarrowia lipolytica. Appl. Microbiol. Biotechnol. 75, 1409–1417.

Förster, A., Jacobs, K., Juretzek, T., Mauersberger, S., and Barth, G. (2007b). Overexpression of the ICL1 gene changes the product ratio of citric acid production by Yarrowia lipolytica. Appl. Microbiol. Biotechnol. 77, 861–869.

Frazzetto, G. (2003). White biotechnology. EMBO Rep. 4, 835–837.

Fukuoka, T., Morita, T., Konishi, M., Imura, T., and Kitamoto, D. (2007). Characterization of new types of mannosylerythritol lipids as biosurfactants produced from soybean oil by a basidiomycetous yeast, Pseudozyma shanxiensis. J. Oleo Sci. 56, 435–442.

Fukuoka, T., Morita, T., Konishi, M., Imura, T., and Kitamoto, D. (2008). A basidiomycetous yeast, Pseudozyma tsukubaensis, efficiently produces a novel glycolipid biosurfactant. The identification of a new diastereomer of mannosylerythritol lipid-B. Carbohydr. Res. 343, 555–560.

Fungaro, M.H.P., Souza Junior, C.L. de, Azevedo, J.L. de, and Pizzirani-Kleiner, A.A. (1994). Recurrent mutation-selection to improve rennet production in Candida tsukubaensis. Rev. Bras. Genet. Braz.

Gardini, F., Suzzi, G., Lombardi, A., Galgano, F., Crudele, M.A., Andrighetto, C., Schirone, M., and Tofalo, R. (2001). A survey of yeasts in traditional sausages of southern Italy. FEMS Yeast Res. 1, 161–167.

Gatignol, A., Dassain, M., and Tiraby, G. (1990). Cloning of Saccharomyces cerevisiae promoters using a probe vector based on phleomycin resistance. Gene 91, 35–41.

Gatter, M. (2015). Biotechnological production of ω-hydroxy fatty acids with the help of metabolically engineered Yarrowia lipolytica strains. Technische Universität Dresden.

Gatter, M., Förster, A., Bär, K., Winter, M., Otto, C., Petzsch, P., Ježková, M., Bahr, K., Pfeiffer, M., Matthäus, F., et al. (2014). A newly identified fatty alcohol oxidase gene is mainly responsible for the oxidation of long-chain ω-hydroxy fatty acids in Yarrowia lipolytica. FEMS Yeast Res. 14, 858–872.

Gatter, M., Ottlik, S., Kövesi, Z., Bauer, B., Matthäus, F., and Barth, G. (2016). Three alcohol dehydrogenase genes and one acetyl-CoA synthetase gene are responsible for ethanol utilization in Yarrowia lipolytica. Fungal Genet. Biol. FG B 95, 30–38.

Geilen, F.M.A., Engendahl, B., Harwardt, A., Marquardt, W., Klankermayer, J., and Leitner, W. (2010). Selective and Flexible Transformation of Biomass-Derived Platform Chemicals by a Multifunctional Catalytic System. Angew. Chem. Int. Ed. 49, 5510–5514.

Geiser, E., Wiebach, V., Wierckx, N., and Blank, L.M. (2014). Prospecting the biodiversity of the fungal family Ustilaginaceae for the production of value-added chemicals. Fungal Biol. Biotechnol. 1, 2.

Geiser, E., Przybilla, S.K., Engel, M., Kleineberg, W., Büttner, L., Sarikaya, E., Hartog, T. den, Klankermayer, J., Leitner, W., Bölker, M., et al. (2016a). Genetic and biochemical insights into the itaconate pathway of Ustilago maydis enable enhanced production. Metab. Eng. 38, 427–435.

Geiser, E., Przybilla, S.K., Friedrich, A., Buckel, W., Wierckx, N., Blank, L.M., and Bölker, M. (2016b). Ustilago maydis produces itaconic acid via the unusual intermediate trans-aconitate. Microb. Biotechnol. 9, 116–126.

Geiser, E., Ludwig, F., Zambanini, T., Wierckx, N., and Blank, L.M. (2016c). Draft Genome Sequences of Itaconate-Producing Ustilaginaceae. Genome Announc. 4, e01291-16.

Geiser, E., Hosseinpour Tehrani, H., Meyer, S., Blank, L.M., and Wierckx, N. (2018). Evolutionary freedom in the regulation of the conserved itaconate cluster by Ria1 in related Ustilaginaceae. Fungal Biol. Biotechnol. 5, 14.

Gillissen, B., Bergemann, J., Sandmann, C., Schroeer, B., Bölker, M., and Kahmann, R. (1992). A two-component regulatory system for self/non-self recognition in Ustilago maydis. Cell 68, 647–657.

References

Glusker, J.P. (1971). 14 Aconitase. In The Enzymes, (Elsevier), pp. 413–439.

Godio, R.P., Fouces, R., Gudiña, E.J., and Martín, J.F. (2004). Agrobacterium tumefaciens-mediated transformation of the antitumor clavaric acid-producing basidiomycete Hypholoma sublateritium. Curr. Genet. 46, 287–294.

Goldberg, I., Rokem, J.S., and Pines, O. (2006). Organic acids: old metabolites, new themes. J. Chem. Technol. Biotechnol. 81, 1601–1611.

Golubev, W.I., Pfeiffer, I., and Golubeva, E.W. (2006). Mycocin production in Pseudozyma tsukubaensis. Mycopathologia 162, 313–316.

Green, F., and Highley, T.L. (1997). Mechanism of brown-rot decay: Paradigm or paradox. Int. Biodeterior. Biodegrad. 39, 113–124.

Groenewald, M., Boekhout, T., Neuvéglise, C., Gaillardin, C., Dijck, P.W.M. van, and Wyss, M. (2014). Yarrowia lipolytica: Safety assessment of an oleaginous yeast with a great industrial potential. Crit. Rev. Microbiol. 40, 187–206.

Guerzoni, M.E., Lanciotti, R., and Marchetti, R. (1993). Survey of the physiological properties of the most frequent yeasts associated with commercial chilled foods. Int. J. Food Microbiol. 17, 329–341.

Guo, B., Chen, Y., Lei, Y., Zhang, L., Zhou, W.Y., Rabie, A.B.M., and Zhao, J. (2011). Biobased Poly(propylene sebacate) as Shape Memory Polymer with Tunable Switching Temperature for Potential Biomedical Applications. Biomacromolecules 12, 1312–1321.

Haldenwang, L., and Behrens, U. (1983). Influence of phosphate concentration on the respiratory activity of Azotobacter vinelandii. Z. Für Allg. Mikrobiol. 23, 491–494.

Harzevili, F. (2014). Biotechnological Applications of the Yeast Yarrowia lipolytica (Cham: Springer International Publishing).

Haskins, R.H., Thorn, J.A., and Boothroyd, B. (1955). Biochemistry of the ustilaginales: xi. metabolic products of Ustilago zeae in submerged culture. Can. J. Microbiol. 1, 749–756.

Heretsch, P., Thomas, F., Aurich, A., Krautscheid, H., Sicker, D., and Giannis, A. (2008). Syntheses with a Chiral Building Block from the Citric Acid Cycle: (2R,3S)-Isocitric Acid by Fermentation of Sunflower Oil. Angew. Chem. Int. Ed. 47, 1958–1960.

Hevekerl, A., Kuenz, A., and Vorlop, K.-D. (2014a). Influence of the pH on the itaconic acid production with Aspergillus terreus. Appl. Microbiol. Biotechnol. 98, 10005–10012.

Hevekerl, A., Kuenz, A., and Vorlop, K.-D. (2014b). Filamentous fungi in microtiter plates—an easy way to optimize itaconic acid production with Aspergillus terreus. Appl. Microbiol. Biotechnol. 98, 6983–6989.

Hewald, S., Josephs, K., and Bölker, M. (2005). Genetic Analysis of Biosurfactant Production in Ustilago maydis. Appl. Environ. Microbiol. 71, 3033–3040.

van der Hoeven, M., Kobayashi, Y., and Diercks, R. (2013). Technology roadmap: Energy and GHG reductions in the chemical industry via catalytic processes. Int. Energy Agency Paris 56.

Holland, J.P., and Holland, M.J. (1979). The primary structure of a glyceraldehyde-3-phosphate dehydrogenase gene from Saccharomyces cerevisiae. J. Biol. Chem. 254, 9839–9845.

Holz, M., Förster, A., Mauersberger, S., and Barth, G. (2009). Aconitase overexpression changes the product ratio of citric acid production by Yarrowia lipolytica. Appl. Microbiol. Biotechnol. 81, 1087–1096.

Hoog, G.S. de (1996). Risk assessment of fungi reported from humans and animals*. Mycoses 39, 407–417.

Hossain, A.H., Li, A., Brickwedde, A., Wilms, L., Caspers, M., Overkamp, K., and Punt, P.J. (2016). Rewiring a secondary metabolite pathway towards itaconic acid production in Aspergillus niger. Microb. Cell Factories 15.

Hosseinpour Tehrani, H., von Helden geb. Geiser, E., Engel, M., Hartmann, S., Hossain, A., Punt, P., Blank, L., and Wierckx, N. (2019). The interplay between transport and metabolism in fungal itaconic acid production. Fungal Genet. Biol. 125.

Husemann, P., and Stoye, J. (2010). r2cat: synteny plots and comparative assembly. Bioinformatics 26, 570–571.

Iacobazzi, V., Lauria, G., and Palmieri, F. (1997). Organization and Sequence of the Human Gene for the Mitochondrial Citrate Transport Protein. DNA Seq. 7, 127–139.

Im, J.H., Yanagishita, H., Ikegami, T., Takeyama, Y., Idemoto, Y., Koura, N., and Kitamoto, D. (2003). Mannosylerythritol lipids, yeast glycolipid biosurfactants, are potential affinity ligand materials for human immunoglobulin G. J. Biomed. Mater. Res. A 65A, 379–385.

References

IPCC (2006). 2006 IPCC guidelines for national greenhouse gas inventories.

Jaklitsch, W.M., Kubicek, C.P., and Scrutton, M.C. (1991). The subcellular organization of itaconate biosynthesis in Aspergillus terreus. Microbiology 137, 533–539.

Jakubowska, J., Metodiewa, D., and Zakowska, Z. (1974). Studies on the metabolic pathway for itatartaric acid formation by Aspergillus terreus. I. Metabolism of glucose and some C5 and C6-carboxylic acids. Acta Microbiol. Pol. B 6, 43–50.

Jeya, M., Lee, K.-M., Tiwari, M.K., Kim, J.-S., Gunasekaran, P., Kim, S.-Y., Kim, I.-W., and Lee, J.-K. (2009). Isolation of a novel high erythritol-producing Pseudozyma tsukubaensis and scale-up of erythritol fermentation to industrial level. Appl. Microbiol. Biotechnol. 83, 225–231.

Johnson, V., Singh, M., Saini, V.S., Sista, V.R., and Yadav, N.K. (1992). Effect of pH on lipid accumulation by an oleaginous yeast: Rhodotorula glutinis IIP-30. World J. Microbiol. Biotechnol. 8, 382–384.

Jones, D.L. (1998). Organic acids in the rhizosphere – a critical review. Plant Soil 205, 25–44.

Jordan, A., Defechereux, P., and Verdin, E. (2001). The site of HIV-1 integration in the human genome determines basal transcriptional activity and response to Tat transactivation. EMBO J. 20, 1726–1738.

Jore, J.P.M., Punt, P.J., and Van Der Werf, M.J. (2009). Production of Itaconic Acid.

Kadooka, C., Izumitsu, K., Onoue, M., Okutsu, K., Yoshizaki, Y., Takamine, K., Goto, M., Tamaki, H., and Futagami, T. (2018). Mitochondrial citrate transporters CtpA and YhmA are involved in lysine biosynthesis in the white koji fungus, Aspergillus luchuensis mut. kawachii. BioRxiv 341370.

Kalscheur, K., Garcia, A., Rosentrater, K., and Wright, C. (2008). Ethanol coproducts for ruminant livestock diets.

Kamzolova, S.V., Finogenova, T.V., and Morgunov, I.G. (2008). Microbiological production of citric and isocitric acids from sunflower oil. Food Technol. Biotechnol. 46, 51–59.

Kamzolova, S.V., Lunina, J.N., and Morgunov, I.G. (2011). Biochemistry of Citric Acid Production from Rapeseed Oil by Yarrowia lipolytica Yeast. J. Am. Oil Chem. Soc. 88, 1965–1976.

Kamzolova, S.V., Vinokurova, N.G., Yusupova, A.I., and Morgunov, I.G. (2012). Succinic acid production from n-alkanes. Eng. Life Sci. 12, 560–566.

Kamzolova, S.V., Dedyukhina, E.G., Samoilenko, V.A., Lunina, J.N., Puntus, I.F., Allayarov, R.L., Chiglintseva, M.N., Mironov, A.A., and Morgunov, I.G. (2013). Isocitric acid production from rapeseed oil by Yarrowia lipolytica yeast. Appl. Microbiol. Biotechnol. 97, 9133–9144.

Kamzolova, S.V., Lunina, Y.N., Allayarov, R.K., Puntus, I.F., Laptev, I.A., Samoilenko, V.A., and Morgunov, I.G. (2015). Biosynthesis of isocitric acid by the yeast Yarrowia lipolytica and its regulation. Appl. Biochem. Microbiol. 51, 249–254.

Kamzolova, S.V., Allayarov, R.K., Lunina, J.N., and Morgunov, I.G. (2016). The effect of oxalic and itaconic acids on threo-Ds-isocitric acid production from rapeseed oil by Yarrowia lipolytica. Bioresour. Technol. 206, 128–133.

Kamzolova, S.V., Shamin, R.V., Stepanova, N.N., Morgunov, G.I., Lunina, J.N., Allayarov, R.K., Samoilenko, V.A., and Morgunov, I.G. (2018). Fermentation Conditions and Media Optimization for Isocitric Acid Production from Ethanol by Yarrowia lipolytica.

Kanamasa, S., Dwiarti, L., Okabe, M., and Park, E.Y. (2008). Cloning and functional characterization of the cis-aconitic acid decarboxylase (CAD) gene from Aspergillus terreus. Appl. Microbiol. Biotechnol. 80, 223–229.

Kane, J.H., Finlay, A.C., and Amann, P.F. (1945). Production of itaconic acid.

Kaplan, R.S., Mayor, J.A., Gremse, D.A., and Wood, D.O. (1995). High Level Expression and Characterization of the Mitochondrial Citrate Transport Protein from the Yeast Saccharomyces cerevisiae. J. Biol. Chem. 270, 4108–4114.

Kaplan, R.S., Mayor, J.A., Kakhniashvili, D., Gremse, D.A., Wood, D.O., and Nelson, D.R. (1996). Deletion of the Nuclear Gene Encoding the Mitochondrial Citrate Transport Protein from Saccharomyces cerevisiae. Biochem. Biophys. Res. Commun. 226, 657–662.

Karaffa, L., and Kubicek, C.P. (2019). Citric acid and itaconic acid accumulation: variations of the same story? Appl. Microbiol. Biotechnol. 103, 2889–2902.

Karaffa, L., Díaz, R., Papp, B., Fekete, E., Sándor, E., and Kubicek, C.P. (2015). A deficiency of manganese ions in the presence of high sugar concentrations is the critical parameter for achieving high yields of itaconic acid by Aspergillus terreus. Appl. Microbiol. Biotechnol. 99, 7937–7944.

References

Kareem, S.O., Akpan, I., and Alebiowu, O.O. (2010). Production of citric acid by Aspergillus niger using pineapple waste. Malays. J. Microbiol. 6, 161–165.

Karthikeyan, A., and Sivakumar, N. (2010). Citric acid production by Koji fermentation using banana peel as a novel substrate. Bioresour. Technol. 101, 5552–5556.

Kawamura, D., Furuhashi, M., Saitou, O., and Matsui, H. (1981). Production of itaconic acid by fermentation.

Kawamura, D., Saito, O., Matsui, H., and Morita, K. (1982). Producing of itaconic acid by yeasts: II Culture conditions of strain No. 668 producing itaconic acid. Shizuoka-Ken Kogyo Shikenjo Hokoku 26, 97–101.

Kawamura, D., Saito, O., Matsui, H., and Morita, K. (1983). Producing of itaconic acid by yeasts: III Culture identification of itaconic acid producing strains. Shizuoka-Ken Kogyo Shikenjo Hokoku 27, 77–88.

Keller, N.P. (2015). Translating biosynthetic gene clusters into fungal armor and weaponry. Nat. Chem. Biol. 11, 671–677.

Kenealy, W., Zaady, E., du Preez, J.C., Stieglitz, B., and Goldberg, I. (1986). Biochemical Aspects of Fumaric Acid Accumulation by Rhizopus arrhizus. Appl. Environ. Microbiol. 52, 128–133.

Khmelnitsky, Y.L., Michels, P.C., Cotterill, I.C., Eissenstat, M., Sunku, V., Veeramaneni, V.R., Cittineni, H., Kotha, G.R., Talasani, S.R., Ramanathan, K.K., et al. (2011). Biocatalytic Resolution of Bis-tetrahydrofuran Alcohol. Org. Process Res. Dev. 15, 279–283.

Kildegaard, K.R., Adiego-Pérez, B., Doménech Belda, D., Khangura, J.K., Holkenbrink, C., and Borodina, I. (2017). Engineering of Yarrowia lipolytica for production of astaxanthin. Synth. Syst. Biotechnol. 2, 287–294.

Kinoshita, K. (1932). Über die Produktion von Itaconsäure und Mannit durch einen neuen Schimmelpilz Aspergillus itaconicus. Acta Phytochim 5, 271–287.

Kinsella, B.T., Hogan, S., Larkin, A., and Cantwell, B.A. (1991). Primary structure and processing of the Candida tsukubaensis alpha-glucosidase. Homology with the rabbit intestinal sucrase-isomaltase complex and human lysosomal alpha-glucosidase. Eur. J. Biochem. 202, 657–664.

Kispal, G., Evans, C.T., Malloy, C., and Srere, P.A. (1989). Metabolic studies on citrate synthase mutants of yeast. A change in phenotype following transformation with an inactive enzyme. J. Biol. Chem. 264, 11204–11210.

Kitamoto, H. (2019). The phylloplane yeast Pseudozyma: a rich potential for biotechnology. FEMS Yeast Res. 19.

Kitamoto, D., Yanagishita, H., Shinbo, T., Nakane, T., Kamisawa, C., and Nakahara, T. (1993). Surface active properties and antimicrobial activities of mannosylerythritol lipids as biosurfactants produced by Candida antarctica. J. Biotechnol. 29, 91–96.

Kitamoto, D., Isoda, H., and Nakahara, T. (2002). Functions and potential applications of glycolipid biosurfactants — from energy-saving materials to gene delivery carriers —. J. Biosci. Bioeng. 94, 187–201.

Kitamoto, D., Morita, T., Fukuoka, T., Konishi, M., and Imura, T. (2009). Self-assembling properties of glycolipid biosurfactants and their potential applications. Curr. Opin. Colloid Interface Sci. 14, 315–328.

Kitamoto, H.K., Shinozaki, Y., Cao, X., Morita, T., Konishi, M., Tago, K., Kajiwara, H., Koitabashi, M., Yoshida, S., Watanabe, T., et al. (2011). Phyllosphere yeasts rapidly break down biodegradable plastics. AMB Express 1, 44.

Kitamoto, N., Matsui, J., Kawai, Y., Kato, A., Yoshino, S., Ohmiya, K., and Tsukagoshi, N. (1998). Utilization of the TEF1-a gene (TEF1) promoter for expression of polygalacturonase genes, pgaA and pgaB, in Aspergillus oryzae. Appl. Microbiol. Biotechnol. 50, 85–92.

Klement, T., and Büchs, J. (2013). Itaconic acid – A biotechnological process in change. Bioresour. Technol. 135, 422–431.

Klement, T., Milker, S., Jäger, G., Grande, P.M., Domínguez de María, P., and Büchs, J. (2012). Biomass pretreatment affects Ustilago maydis in producing itaconic acid. Microb. Cell Factories 11, 43.

Kojic, M., and Holloman, W.K. (2000). Shuttle vectors for genetic manipulations in Ustilago maydis. Can. J. Microbiol. 46, 333–338.

Kondrashova, M.N., Zakharchenko, M.V., Khunderiakova, N.V., Fedotcheva, N.I., Litvinova, E.G., Romanova, O.I., and Guliaev, A.A. (2013). [State of succinate dehydrogenase in the organism--"unbalanced" or hyperactive]. Biofizika 58, 106–116.

Konishi, M., Morita, T., Fukuoka, T., Imura, T., Kakugawa, K., and Kitamoto, D. (2008). Efficient production of mannosylerythritol lipids with high hydrophilicity by Pseudozyma hubeiensis KM-59. Appl. Microbiol. Biotechnol. 78, 37–46.

References

Konishi, M., Hatada, Y., and Horiuchi, J. (2013). Draft Genome Sequence of the Basidiomycetous Yeast-Like Fungus Pseudozyma hubeiensis SY62, Which Produces an Abundant Amount of the Biosurfactant Mannosylerythritol Lipids. Genome Announc 1, e00409-13.

Krebs, H.A., and Johnson, W.A. (1937). The role of citric acid in intermediate metabolism in animal tissues. Enzymologia 4, 148–156.

Kretzschmar, A., Otto, C., Holz, M., Werner, S., Hübner, L., and Barth, G. (2013). Increased homologous integration frequency in Yarrowia lipolytica strains defective in non-homologous end-joining. Curr. Genet. 59, 63–72.

Krull, S., Hevekerl, A., Kuenz, A., and Prüße, U. (2017). Process development of itaconic acid production by a natural wild type strain of Aspergillus terreus to reach industrially relevant final titers. Appl. Microbiol. Biotechnol. 101, 4063–4072.

Kruse, J., Doehlemann, G., Kemen, E., and Thines, M. (2017). Asexual and sexual morphs of Moesziomyces revisited. IMA Fungus 8, 117–129.

Kruse, K., Förster, A., Mauersberger, S., and Barth, G. (2004). Method for the biotechnological production of citric acid by means of a genetically modified yeast Yarrowia lipolytica. World Pat. Appl. WO2004009828.

Kubicek, C.P., Zehentgruber, O., El-Kalak, H., and Röhr, M. (1980). Regulation of citric acid production by oxygen: Effect of dissolved oxygen tension on adenylate levels and respiration in Aspergillus niger. Eur. J. Appl. Microbiol. Biotechnol. 9, 101–115.

Kuenz, A. (2008). Itaconsäureherstellung aus nachwachsenden Rohstoffen als Ersatz für petrochemisch hergestellte Acrylsäure. PhD Thesis.

Kuenz, A., and Krull, S. (2018). Biotechnological production of itaconic acid—things you have to know. Appl. Microbiol. Biotechnol. 102, 3901–3914.

Kuenz, A., Gallenmüller, Y., Willke, T., and Vorlop, K.-D. (2012). Microbial production of itaconic acid: developing a stable platform for high product concentrations. Appl. Microbiol. Biotechnol. 96, 1209–1216.

Kulakovskaya, T.V., Shashkov, A.S., Kulakovskaya, E.V., and Golubev, W.I. (2005). Ustilagic acid secretion by Pseudozyma fusiformata strains. FEMS Yeast Res. 5, 919–923.

Kumar, S., Krishnan, S., Samal, S.K., Mohanty, S., and Nayak, S.K. (2017). Itaconic acid used as a versatile building block for the synthesis of renewable resource-based resins and polyesters for future prospective: a review. Polym. Int. 66, 1349–1363.

Kunitake, E., Tanaka, T., Ueda, H., Endo, A., Yarimizu, T., Katoh, E., and Kitamoto, H. (2019). CRISPR/Cas9-mediated gene replacement in the basidiomycetous yeast Pseudozyma antarctica. Fungal Genet. Biol. 130, 82–90.

Kunthiphun, S., Chokreansukchai, P., Hondee, P., Tanasupawat, S., and Savarajara, A. (2018). Diversity and characterization of cultivable oleaginous yeasts isolated from mangrove forests. World J. Microbiol. Biotechnol. 34, 125.

Kurtzman, C., Fell, J.W., and Boekhout, T. (2011). The Yeasts: A Taxonomic Study (Elsevier).

Kyong, S.H., and Shin, C.S. (2000). Optimized production of L-β-hydroxybutyric acid by a mutant of Yarrowia lipolytica. Biotechnol. Lett. 22, 1105–1110.

Lambert, R.J., and Stratford, M. (1999). Weak-acid preservatives: modelling microbial inhibition and response. J. Appl. Microbiol. 86, 157–164.

Laptev, I.A., Filimonova, N.A., Allayarov, R.K., Kamzolova, S.V., Samoilenko, V.A., Sineoky, S.P., and Morgunov, I.G. (2016). New recombinant strains of the yeast Yarrowia lipolytica with overexpression of the aconitate hydratase gene for the obtainment of isocitric acid from rapeseed oil. Appl. Biochem. Microbiol. 52, 699–704.

Larroude, M., Celinska, E., Back, A., Thomas, S., Nicaud, J.-M., and Ledesma-Amaro, R. (2018). A synthetic biology approach to transform Yarrowia lipolytica into a competitive biotechnological producer of β-carotene. Biotechnol. Bioeng. 115, 464–472.

Larsen, H., and Eimhjellen, K.E. (1955). The mechanism of itaconic acid formation by Aspergillus terreus. 1. The effect of acidity. Biochem. J. 60, 135–139.

Ledesma-Amaro, R., Dulermo, R., Niehus, X., and Nicaud, J.-M. (2016). Combining metabolic engineering and process optimization to improve production and secretion of fatty acids. Metab. Eng. 38.

Lee, G., Lee, S.-H., Kim, K.M., and Ryu, C.-M. (2017). Foliar application of the leaf-colonizing yeast Pseudozyma churashimaensis elicits systemic defense of pepper against bacterial and viral pathogens. Sci. Rep. 7, 39432.

References

Levi, P.G., and Cullen, J.M. (2018). Mapping Global Flows of Chemicals: From Fossil Fuel Feedstocks to Chemical Products. Environ. Sci. Technol. 52, 1725–1734.

Levinson, W.E., Kurtzman, C.P., and Kuo, T.M. (2006). Production of itaconic acid by Pseudozyma antarctica NRRL Y-7808 under nitrogen-limited growth conditions. Enzyme Microb. Technol. 39, 824–827.

Li, A., van Luijk, N., ter Beek, M., Caspers, M., Punt, P., and van der Werf, M. (2011). A clone-based transcriptomics approach for the identification of genes relevant for itaconic acid production in Aspergillus. Fungal Genet. Biol. FG B 48, 602–611.

Li, A., Pfelzer, N., Zuijderwijk, R., Brickwedde, A., van Zeijl, C., and Punt, P. (2013). Reduced by-product formation and modified oxygen availability improve itaconic acid production in Aspergillus niger. Appl. Microbiol. Biotechnol. 97, 3901–3911.

Liao, X.S., Small, W.C., Srere, P.A., and Butow, R.A. (1991). Intramitochondrial functions regulate nonmitochondrial citrate synthase (CIT2) expression in Saccharomyces cerevisiae. Mol. Cell. Biol. 11, 38–46.

Ligon, B.L. (2004). Penicillin: its discovery and early development. Semin. Pediatr. Infect. Dis. 15, 52–57.

Limmer, S. (2008). Beeinflussung der Itaconsäureproduktion in P. tsukubaensis durch Überexpression der heterologen Aconitase aus Y. lipolytica. Diplomarbeit.

Liu, L., Wang, J., Rosenberg, D., Zhao, H., Lengyel, G., and Nadel, D. (2018). Fermented beverage and food storage in 13,000 y-old stone mortars at Raqefet Cave, Israel: Investigating Natufian ritual feasting. J. Archaeol. Sci. Rep. 21, 783–793.

Liu, Q., Ouyang, S.-P., Chung, A., Wu, Q., and Chen, G.-Q. (2007). Microbial production of R-3-hydroxybutyric acid by recombinant E. coli harboring genes of phbA, phbB, and tesB. Appl. Microbiol. Biotechnol. 76, 811–818.

Liu, X., Lv, J., Zhang, T., and Deng, Y. (2015). Citric acid production from hydrolysate of pretreated straw cellulose by Yarrowia lipolytica SWJ-1b using batch and fed-batch cultivation. Prep. Biochem. Biotechnol. 45, 825–835.

Lochhead, A.G., and Landerkin, G.B. (1942). Nutrilite requirements of osmophilic yeasts. J. Bacteriol. 44, 343.

Lorenz, S., Guenther, M., Grumaz, C., Rupp, S., Zibek, S., and Sohn, K. (2014). Genome Sequence of the Basidiomycetous Fungus Pseudozyma aphidis DSM70725, an Efficient Producer of Biosurfactant Mannosylerythritol Lipids. Genome Announc 2, e00053-14.

Luskin, L. (1974). Acid monomers – itaconic acid. Funct. Monomers Their Prep. Polym. Appl. R H Yocum E B Nyquist Eds N. Y. Vol. 2, 465–501.

Maassen, N., Panakova, M., Wierckx, N., Geiser, E., Zimmermann, M., Bölker, M., Klinner, U., and Blank, L.M. (2014). Influence of carbon and nitrogen concentration on itaconic acid production by the smut fungus Ustilago maydis. Eng. Life Sci. 14, 129–134.

Madzak, C. (2018). Engineering Yarrowia lipolytica for Use in Biotechnological Applications: A Review of Major Achievements and Recent Innovations. Mol. Biotechnol. 60, 621–635.

Magalhães, A.I., de Carvalho, J.C., Medina, J.D.C., and Soccol, C.R. (2017). Downstream process development in biotechnological itaconic acid manufacturing. Appl. Microbiol. Biotechnol. 101, 1–12.

Mario, B., and Schweiger, L.B. (1963). Process for the production of itaconic acid.

Markham, K.A., and Alper, H.S. (2018). Synthetic Biology Expands the Industrial Potential of Yarrowia lipolytica. Trends Biotechnol. 36, 1085–1095.

Markham, K.A., Palmer, C.M., Chwatko, M., Wagner, J.M., Murray, C., Vazquez, S., Swaminathan, A., Chakravarty, I., Lynd, N.A., and Alper, H.S. (2018). Rewiring Yarrowia lipolytica toward triacetic acid lactone for materials generation. Proc. Natl. Acad. Sci. 115, 2096–2101.

Martius, C., and Knoop, F. (1937). Physiological breakdown of citric acid. Prelim. Z Physiol Chem 246, 1–11.

Martius, C., and Leonhardt, H. (1943). Über aconitase. Hoppe-Seyler Z. Für Physiol. Chem. 278, 208–212.

Matheucci Jr, E., Henrique-Silva, F., El-Gogary, S., Rossini, C.H.B., Leite, A., Vera, J.E., Urioste, J.C., Crivellaro, O., and El-Dorry, H. (1995). Structure, organization and promoter expression of the actin-encoding gene in Trichoderma reesei. Gene 161, 103–106.

Mattey, M. (1992). The production of organic acids. Crit. Rev. Biotechnol. 12, 87–132.

Matthäus, F., Ketelhot, M., Gatter, M., and Barth, G. (2014). Production of Lycopene in the Non-Carotenoid-Producing Yeast Yarrowia lipolytica. Appl. Environ. Microbiol. 80, 1660–1669.

References

Mauersberger, S., Wang, H.-J., Gaillardin, C., Barth, G., and Nicaud, J.-M. (2001). Insertional Mutagenesis in then-Alkane-Assimilating Yeast Yarrowia lipolytica: Generation of Tagged Mutations in Genes Involved in Hydrophobic Substrate Utilization. J. Bacteriol. 183, 5102–5109.

Mauersberger, S., Kruse, K., and Barth, G. (2003). Induction of Citric Acid/Isocitric Acid and α-Ketoglutaric Acid Production in the Yeast Yarrowia lipolytica. In Non-Conventional Yeasts in Genetics, Biochemistry and Biotechnology, (Springer, Berlin, Heidelberg), pp. 393–400.

Mayor, J.A., Kakhniashvili, D., Gremse, D.A., Campbell, C., Krämer, R., Schroers, A., and Kaplan, R.S. (1997). Bacterial overexpression of putative yeast mitochondrial transport proteins. J. Bioenerg. Biomembr. 29, 541–547.

McDade, H.C., and Cox, G.M. (2001). A new dominant selectable marker for use in Cryptococcus neoformans. Med. Mycol. 39, 151–154.

McFadden, B.A., and Purohit, S. (1977). Itaconate, an isocitrate lyase-directed inhibitor in Pseudomonas indigofera. J. Bacteriol. 131, 136–144.

Medway, A.M., and Sperry, J. (2014). Heterocycle construction using the biomass-derived building block itaconic acid. Green Chem. 16, 2084–2101.

Meixner-Monori, B., Kubicek, C.P., and Röhr, M. (1984). Pyruvate kinase from Aspergillus niger: a regulatory enzyme in glycolysis? Can. J. Microbiol. 30, 16–22.

Michelucci, A., Cordes, T., Ghelfi, J., Pailot, A., Reiling, N., Goldmann, O., Binz, T., Wegner, A., Tallam, A., and Rausell, A. (2013). Immune-responsive gene 1 protein links metabolism to immunity by catalyzing itaconic acid production. Proc. Natl. Acad. Sci. 110, 7820–7825.

Mimee, B., Labbé, C., Pelletier, R., and Bélanger, R.R. (2005). Antifungal Activity of Flocculosin, a Novel Glycolipid Isolated from Pseudozyma flocculosa. Antimicrob. Agents Chemother. 49, 1597–1599.

Mlakar, T., and Legiša, M. (2006). Citrate Inhibition-Resistant Form of 6-Phosphofructo-1-Kinase from Aspergillus niger. Appl. Environ. Microbiol. 72, 4515–4521.

Mohanta, T.K., and Bae, H. (2015). The diversity of fungal genome. Biol. Proced. Online 17.

Molnár, Á.P., Németh, Z., Kolláth, I.S., Fekete, E., Flipphi, M., Ág, N., Soós, Á., Kovács, B., Sándor, E., Kubicek, C.P., et al. (2018). High oxygen tension increases itaconic acid accumulation, glucose consumption, and the expression and activity of alternative oxidase in Aspergillus terreus. Appl. Microbiol. Biotechnol. 102, 8799–8808.

Mooibroek, H., Kuipers, A.G., Sietsma, J.H., Punt, P.J., and Wessels, J.G. (1990). Introduction of hygromycin B resistance into Schizophyllum commune: preferential methylation of donor DNA. Mol. Gen. Genet. MGG 222, 41–48.

Moon, H.-J., Jeya, M., Kim, I.-W., and Lee, J.-K. (2010). Biotechnological production of erythritol and its applications. Appl. Microbiol. Biotechnol. 86, 1017–1025.

Moore, G.L., Stringham, R.W., Teager, D.S., and Yue, T.-Y. (2017). Practical Synthesis of the Bicyclic Darunavir Side Chain: (3R,3aS,6aR)-Hexahydrofuro[2,3-b]furan-3-ol from Monopotassium Isocitrate. Org. Process Res. Dev. 21, 98–106.

Morgunov, I.G., Kamzolova, S.V., Perevoznikova, O.A., Shishkanova, N.V., and Finogenova, T.V. (2004). Pyruvic acid production by a thiamine auxotroph of Yarrowia lipolytica. Process Biochem. 39, 1469–1474.

Morgunov, I.G., Kamzolova, S.V., and Lunina, J.N. (2013). The citric acid production from raw glycerol by Yarrowia lipolytica yeast and its regulation. Appl. Microbiol. Biotechnol. 97, 7387–7397.

Morgunov, I.G., Karpukhina, O.V., Kamzolova, S.V., Samoilenko, V.A., and Inozemtsev, A.N. (2018). Investigation of the effect of biologically active threo-Ds-isocitric acid on oxidative stress in Paramecium caudatum. Prep. Biochem. Biotechnol. 48, 1–5.

Morgunov, I.G., Kamzolova, S.V., Karpukhina, O.V., Bokieva, S.B., and Inozemtsev, A.N. (2019). Biosynthesis of isocitric acid in repeated-batch culture and testing of its stress-protective activity. Appl. Microbiol. Biotechnol. 103, 3549–3558.

Morita, T., Konishi, M., Fukuoka, T., Imura, T., Yamamoto, S., Kitagawa, M., Sogabe, A., and Kitamoto, D. (2008a). Identification of Pseudozyma graminicola CBS 10092 as a producer of glycolipid biosurfactants, mannosylerythritol lipids. J. Oleo Sci. 57, 123–131.

Morita, T., Konishi, M., Fukuoka, T., Imura, T., and Kitamoto, D. (2008b). Production of glycolipid biosurfactants, mannosylerythritol lipids, by Pseudozyma siamensis CBS 9960 and their interfacial properties. J. Biosci. Bioeng. 105, 493–502.

References

Morita, T., Kitagawa, M., Yamamoto, S., Sogabe, A., Imura, T., Fukuoka, T., and Kitamoto, D. (2010a). Glycolipid Biosurfactants, Mannosylerythritol Lipids, Repair the Damaged Hair. J. Oleo Sci. 59, 267–272.

Morita, T., Takashima, M., Fukuoka, T., Konishi, M., Imura, T., and Kitamoto, D. (2010b). Isolation of basidiomycetous yeast Pseudozyma tsukubaensis and production of glycolipid biosurfactant, a diastereomer type of mannosylerythritol lipid-B. Appl. Microbiol. Biotechnol. 88, 679–688.

Morita, T., Koike, H., Koyama, Y., Hagiwara, H., Ito, E., Fukuoka, T., Imura, T., Machida, M., and Kitamoto, D. (2013). Genome Sequence of the Basidiomycetous Yeast Pseudozyma antarctica T-34, a Producer of the Glycolipid Biosurfactants Mannosylerythritol Lipids. Genome Announc 1, e00064-13.

Morita, T., Koike, H., Hagiwara, H., Ito, E., Machida, M., Sato, S., Habe, H., and Kitamoto, D. (2014). Genome and Transcriptome Analysis of the Basidiomycetous Yeast Pseudozyma antarctica Producing Extracellular Glycolipids, Mannosylerythritol Lipids. PLOS ONE 9, e86490.

Morita, T., Fukuoka, T., Imura, T., and Kitamoto, D. (2015). Mannosylerythritol lipids: production and applications. J. Oleo Sci. 64, 133–141.

Müller, S., Sandal, T., Kamp-Hansen, P., and Dalbøge, H. (1998). Comparison of expression systems in the yeasts Saccharomyces cerevisiae, Hansenula polymorpha, Klyveromyces lactis, Schizosaccharomyces pombe and Yarrowia lipolytica. Cloning of two novel promoters from Yarrowia lipolytica. Yeast Chichester Engl. 14, 1267–1283.

Murre, C., Bain, G., van Dijk, M.A., Engel, I., Furnari, B.A., Massari, M.E., Matthews, J.R., Quong, M.W., Rivera, R.R., and Stuiver, M.H. (1994). Structure and function of helix-loop-helix proteins. Biochim. Biophys. Acta BBA - Gene Struct. Expr. 1218, 129–135.

Nelson, G.E.N., Traufler, D.H., Kelley, S.E., and Lockwood, L.B. (1952). Production of Itaconic Acid by Aspergillus terreus in 20-Liter Fermentors. Ind. Eng. Chem. 44, 1166–1168.

Neveu, B., Michaud, M., Belzile, F., and Bélanger, R.R. (2007a). The Pseudozyma flocculosa actin promoter allows the strong expression of a recombinant protein in the Pseudozyma species. Appl. Microbiol. Biotechnol. 74, 1300–1307.

Neveu, B., Belzile, F., and Bélanger, R.R. (2007b). Cloning of the glyceraldehyde-3-phosphate dehydrogenase gene from Pseudozyma flocculosa and functionality of its promoter in two Pseudozyma species. Antonie Van Leeuwenhoek 92, 245–255.

Nicaud, J.-M. (2012). Yarrowia lipolytica. Yeast 29, 409–418.

Nielsen, T.B., Ishii, M., and Kirk, O. (1999). Lipases A and B from the yeast Candida antarctica. In Biotechnological Applications of Cold-Adapted Organisms, R. Margesin, and F. Schinner, eds. (Berlin, Heidelberg: Springer Berlin Heidelberg), pp. 49–61.

Nowakowska-Waszczuk, A. (1973). Utilization of Some Tricarboxylic-acid-cycle Intermediates by Mitochondria and Growing Mycelium of Aspergillus terreus. Microbiology, 79, 19–29.

Nury, H., Dahout-Gonzalez, C., Trézéguet, V., Lauquin, G. j. m., Brandolin, G., and Pebay-Peyroula, E. (2006). Relations Between Structure and Function of the Mitochondrial ADP/ATP Carrier. Annu. Rev. Biochem. 75, 713–741.

OECD, I. (2016). Energy and Air Pollution: World Energy Outlook Special Report 2016.

Okabe, M., Lies, D., Kanamasa, S., and Park, E.Y. (2009). Biotechnological production of itaconic acid and its biosynthesis in Aspergillus terreus. Appl. Microbiol. Biotechnol. 84, 597–606.

Onishi, H. (1972). Candida tsukubaensis sp.n. Antonie Van Leeuwenhoek 38, 365–367.

Oogaki, M., Inoue, M., Kaimaktchiev, A.C., Nakahara, T., and Tabuchi, T. (1984). Production of Isocitric Acid from Glucose by Candida ravautii. Agric. Biol. Chem. 48, 789–795.

Ordiz, I., Herrero, P., Rodicio, R., and Moreno, F. (1996). Glucose-induced inactivation of isocitrate lyase in Saccharomyces cerevisiae is mediated by the cAMP-dependent protein kinase catalytic subunits Tpk 1 and Tpk2. FEBS Lett. 385, 43–46.

Otto, C., Yovkova, V., Aurich, A., Mauersberger, S., and Barth, G. (2012). Variation of the by-product spectrum during α-ketoglutaric acid production from raw glycerol by overexpression of fumarase and pyruvate carboxylase genes in Yarrowia lipolytica. Appl. Microbiol. Biotechnol. 95, 905–917.

Palmieri, F. (1994). Mitochondrial carrier proteins. FEBS Lett. 346, 48–54.

Palmieri, F. (2004). The mitochondrial transporter family (SLC25): physiological and pathological implications. Pflüg. Arch. 447, 689–709.

References

Palmieri, F. (2013). The mitochondrial transporter family SLC25: identification, properties and physiopathology. Mol. Aspects Med. 34, 465–484.

Palmieri, F., and Monné, M. (2016). Discoveries, metabolic roles and diseases of mitochondrial carriers: A review. Biochim. Biophys. Acta 1863, 2362–2378.

Palmieri, F., and Pierri, C.L. (2010). Mitochondrial metabolite transport. Essays Biochem. 47, 37–52.

Palmieri, L., Runswick, M.J., Fiermonte, G., Walker, J.E., and Palmieri, F. (2000). Yeast mitochondrial carriers: bacterial expression, biochemical identification and metabolic significance. J. Bioenerg. Biomembr. 32, 67–77.

Palmieri, L., Agrimi, G., Runswick, M.J., Fearnley, I.M., Palmieri, F., and Walker, J.E. (2001). Identification in Saccharomyces cerevisiae of two isoforms of a novel mitochondrial transporter for 2-oxoadipate and 2-oxoglutarate. J. Biol. Chem. 276, 1916–1922.

Papanikolaou, S., Galiotou-Panayotou, M., Fakas, S., Komaitis, M., and Aggelis, G. (2008). Citric acid production by Yarrowia lipolytica cultivated on olive-mill wastewater-based media. Bioresour. Technol. 99, 2419–2428.

Patty, F. (1963). Industrial Hygiene and Toxicology Vol. II. (New York: John Wiley & Sons Inc.).

Perera, F. (2018). Pollution from Fossil-Fuel Combustion is the Leading Environmental Threat to Global Pediatric Health and Equity: Solutions Exist. Int. J. Environ. Res. Public. Health 15.

Pfeifer, V.F., Vojnovich, C., and Heger, E.N. (1952). Itaconic Acid by Fermentation with Aspergillus terreus. Ind. Eng. Chem. 44, 2975–2980.

Pichler, H., Obenaus, F., and Franz, G. (1967). Über die Bildung von Citraconsäureanhydrid bei der katalytischen Oxydation von Methylaromaten und Isopren, Erdöl und Kohle, Erdgas. Petrochemie 20, 188–192.

Plassard, C., and Fransson, P. (2009). Regulation of low-molecular weight organic acid production in fungi. Fungal Biol. Rev. 23, 30–39.

Przybilla, S.K. (2014). Genetische und biochemische Charakterisierung der Itaconsäure-Biosynthese in Ustilago maydis. PhD Thesis. Philipps-Universität Marburg.

Pucher, G.W., Abrahams, M.D., and Vickery, H.B. (1948). The preparation of optically active isocitric acid from Bryophyllum leaf tissue. J. Biol. Chem. 172, 579–588.

Rabl, A., Benoist, A., Dron, D., Peuportier, B., Spadaro, J.V., and Zoughaib, A. (2007). How to account for CO_2 emissions from biomass in an LCA. Int. J. Life Cycle Assess. 12, 281.

Rakicka, M., Lazar, Z., Rywińska, A., and Rymowicz, W. (2016). Efficient utilization of inulin and glycerol as fermentation substrates in erythritol and citric acid production using Yarrowia lipolytica expressing inulinase. Chem. Pap. 70, 1452–1459.

RÅnby, M., Gojceta, T., Gustafsson, K., Hansson, K.M., and Lindahl, T.L. (1999). Isocitrate as Calcium Ion Activity Buffer in Coagulation Assays. Clin. Chem. 45, 1176–1180.

Ratledge, C. (2004). Fatty acid biosynthesis in microorganisms being used for Single Cell Oil production. Biochimie 86, 807–815.

Regev-Rudzki, N., Karniely, S., Ben-Haim, N.N., and Pines, O. (2005). Yeast Aconitase in Two Locations and Two Metabolic Pathways: Seeing Small Amounts Is Believing. Mol. Biol. Cell 16, 4163–4171.

Rickey, T.M., and Lewin, A.S. (1986). Extramitochondrial citrate synthase activity in bakers' yeast. Mol. Cell. Biol. 6, 488–493.

Ritchie, H., and Roser, M. (2017). Fossil Fuels. Our World Data.

Rivera-Angulo, A.-J., and Peña-Ortega, F. (2014). Isocitrate supplementation promotes breathing generation, gasping, and autoresuscitation in neonatal mice. J. Neurosci. Res. 92, 375–388.

Robert, T., and Friebel, S. (2016). Itaconic acid – a versatile building block for renewable polyesters with enhanced functionality. Green Chem. 18, 2922–2934.

Rodrigues, L., Banat, I.M., Teixeira, J., and Oliveira, R. (2006). Biosurfactants: potential applications in medicine. J. Antimicrob. Chemother. 57, 609–618.

Russell, D.G., VanderVen, B.C., Lee, W., Abramovitch, R.B., Kim, M., Homolka, S., Niemann, S., and Rohde, K.H. (2010). Mycobacterium tuberculosis Wears What It Eats. Cell Host Microbe 8, 68–76.

References

Rychtera, M., and Wase, D.J. (1981). The growth of Aspergillus terreus and the production of itaconic acid in batch and continuous cultures. The influence of pH. J. Chem. Technol. Biotechnol. 31, 509–521.

Rymowicz, W., Rywińska, A., Żarowska, B., and Juszczyk, P. (2006). Citric acid production from raw glycerol by acetate mutants of Yarrowia lipolytica. Chem. Pap. 60, 391–394.

Rywińska, A., and Rymowicz, W. (2010). High-yield production of citric acid by Yarrowia lipolytica on glycerol in repeated-batch bioreactors. J. Ind. Microbiol. Biotechnol. 37, 431–435.

Rywińska, A., and Rymowicz, W. (2011). Continuous production of citric acid from raw glycerol by Yarrowia lipolytica in cell recycle cultivation. Chem. Pap. 65, 119–123.

Saavedra, L., García, A., and Barbas, C. (2000). Development and validation of a capillary electrophoresis method for direct measurement of isocitric, citric, tartaric and malic acids as adulteration markers in orange juice. J. Chromatogr. A 881, 395–401.

Saffran, M., and Prado, J.L. (1949). Inhibition of aconitase by trans-aconitate. J Biol Chem 180, 1301–1309.

Saha, B.C. (2017). Emerging biotechnologies for production of itaconic acid and its applications as a platform chemical. J. Ind. Microbiol. Biotechnol. 44, 303–315.

Saha, B.C., Kennedy, G.J., Qureshi, N., and Bowman, M.J. (2017). Production of itaconic acid from pentose sugars by Aspergillus terreus. Biotechnol. Prog. 33, 1059–1067.

Saha, B.C., Kennedy, G.J., Bowman, M.J., Qureshi, N., and Dunn, R.O. (2019). Factors Affecting Production of Itaconic Acid from Mixed Sugars by Aspergillus terreus. Appl. Biochem. Biotechnol. 187, 449–460.

Saika, A., Koike, H., Hori, T., Fukuoka, T., Sato, S., Habe, H., Kitamoto, D., and Morita, T. (2014). Draft Genome Sequence of the Yeast Pseudozyma antarctica Type Strain JCM10317, a Producer of the Glycolipid Biosurfactants, Mannosylerythritol Lipids. Genome Announc 2, e00878-14.

Saika, A., Koike, H., Fukuoka, T., Yamamoto, S., Kishimoto, T., and Morita, T. (2016). A Gene Cluster for Biosynthesis of Mannosylerythritol Lipids Consisted of 4-O-β-D-Mannopyranosyl-(2R,3S)-Erythritol as the Sugar Moiety in a Basidiomycetous Yeast Pseudozyma tsukubaensis. PLOS ONE 11, e0157858.

Saika, A., Koike, H., Fukuoka, T., and Morita, T. (2018a). Tailor-made mannosylerythritol lipids: current state and perspectives. Appl. Microbiol. Biotechnol. 102, 6877–6884.

Saika, A., Utashima, Y., Koike, H., Yamamoto, S., Kishimoto, T., Fukuoka, T., and Morita, T. (2018b). Biosynthesis of mono-acylated mannosylerythritol lipid in an acyltransferase gene-disrupted mutant of Pseudozyma tsukubaensis. Appl. Microbiol. Biotechnol. 102, 1759–1767.

Saika, A., Utashima, Y., Koike, H., Yamamoto, S., Kishimoto, T., Fukuoka, T., and Morita, T. (2018c). Identification of the gene PtMAT1 encoding acetyltransferase from the diastereomer type of mannosylerythritol lipid-B producer Pseudozyma tsukubaensis. J. Biosci. Bioeng. 126, 676–681.

Sakai, M. (1976). Studies of the Isomerization of Unsaturated Carboxylic Acids. II. The Thermal Rearrangement of Citraconic Acid to Itaconic Acid in Aqueous Solutions. Bull. Chem. Soc. Jpn. 49, 219–223.

Sakihama, Y., Hidese, R., Hasunuma, T., and Kondo, A. (2019). Increased flux in acetyl-CoA synthetic pathway and TCA cycle of Kluyveromyces marxianus under respiratory conditions. Sci. Rep. 9, 5319.

Salmon, J.M. (1987). l-Malic-acid permeation in resting cells of anaerobically grown Saccharomyces cerevisiae. Biochim. Biophys. Acta BBA - Biomembr. 901, 30–34.

Sambrook, J., Fritsch, E.F., and Maniatis, T. (1989). Molecular Cloning :a Laboratory Manual.

Saraste, M., and Walker, J.E. (1982). Internal sequence repeats and the path of polypeptide in mitochondrial ADP/ATP translocase. FEBS Lett. 144, 250–254.

Sauer, M., Porro, D., Mattanovich, D., and Branduardi, P. (2008). Microbial production of organic acids: expanding the markets. Trends Biotechnol. 26, 100–108.

Sayama, A., Kobayashi, K., and Ogoshi, A. (1994). Morphological and physiological comparisons ofHelicobasidium mompa andH. purpureum. Mycoscience 35, 15–20.

Scarcia, P., Palmieri, L., Agrimi, G., Palmieri, F., and Rottensteiner, H. (2017). Three mitochondrial transporters of Saccharomyces cerevisiae are essential for ammonium fixation and lysine biosynthesis in synthetic minimal medium. Mol. Genet. Metab. 122, 54–60.

References

Schillberg, S., Tiburzy, R., and Fischer, R. (2000). Transient transformation of the rust fungus Puccinia graminis f. sp. tritici. Mol. Gen. Genet. MGG 262, 911–915.

Schulz, B., Banuett, F., Dahl, M., Schlesinger, R., Schäfer, W., Martin, T., Herskowitz, I., and Kahmann, R. (1990). The b alleles of U. maydis, whose combinations program pathogenic development, code for polypeptides containing a homeodomain-related motif. Cell 60, 295–306.

Shekhawat, D., Jackson, J.E., and Miller, D.J. (2006). Process model and economic analysis of itaconic acid production from dimethyl succinate and formaldehyde. Bioresour. Technol. 97, 342–347.

Shimi, I.R., and Nour El Dein, M.S. (1962). Biosynthesis of itaconic acid by aspergillus terreus. Arch. Mikrobiol. 44, 181–188.

Shinozaki, Y., Morita, T., Cao, X., Yoshida, S., Koitabashi, M., Watanabe, T., Suzuki, K., Sameshima-Yamashita, Y., Nakajima-Kambe, T., Fujii, T., et al. (2013). Biodegradable plastic-degrading enzyme from Pseudozyma antarctica: cloning, sequencing, and characterization. Appl. Microbiol. Biotechnol. 97, 2951–2959.

Show, P.L., Oladele, K.O., Siew, Q.Y., Zakry, F.A.A., Lan, J.C.-W., and Ling, T.C. (2015). Overview of citric acid production from Aspergillus niger. Front. Life Sci. 8, 271–283.

Singh, M., Rathi, R., Singh, A., Heller, J., Talwar, G.P., and Kopecek, J. (1991). Controlled release of LHRH-DT from bioerodible hydrogel microspheres. Int. J. Pharm. 76, R5–R8.

Sitepu, I.R., Garay, L.A., Sestric, R., Levin, D., Block, D.E., German, J.B., and Boundy-Mills, K.L. (2014). Oleaginous yeasts for biodiesel: Current and future trends in biology and production. Biotechnol. Adv. 32, 1336–1360.

Slater, M.R., and Craig, E.A. (1987). Transcriptional regulation of an hsp70 heat shock gene in the yeast Saccharomyces cerevisiae. Mol. Cell. Biol. 7, 1906–1916.

Smale, S.T. (2010). β-Galactosidase Assay. Cold Spring Harb. Protoc. 2010, pdb.prot5423.

Smets, B.F., Yin, H., and Esteve-Nuñez, A. (2007). TNT biotransformation: when chemistry confronts mineralization. Appl. Microbiol. Biotechnol. 76, 267–277.

Smil, V. (2016). Energy transitions: global and national perspectives (ABC-CLIO).

Soderstrom, T.R. (1962). The Isocitric Acid Content of Crassulacean Plants and a Few Succulent Species from Other Families. Am. J. Bot. 49, 850–855.

Specht, R., Andreas, D.-I.A., Kreyß, E., Gerold, P.D.B., and Bodinus, C. (2014). Verfahren zur biotechnologischen Herstellung von Itaconsäure.

Spencer, J., Spencer, A.R. de, and Laluce, C. (2002). Non-conventional yeasts. Appl. Microbiol. Biotechnol. 58, 147–156.

Spencer, J.F.T., Spencer, D.M., and de Figueroa, L.I.C. (1997). Yeasts as Living Objects: Yeast Nutrition. In Yeasts in Natural and Artificial Habitats, J.F.T. Spencer, and D.M. Spencer, eds. (Berlin, Heidelberg: Springer Berlin Heidelberg), pp. 68–79.

Steiger, M.G., Blumhoff, M.L., Mattanovich, D., and Sauer, M. (2013). Biochemistry of microbial itaconic acid production. Front. Microbiol. 4.

Steiger, M.G., Punt, P.J., Ram, A.F.J., Mattanovich, D., and Sauer, M.G. (2016). Characterizing MttA as a mitochondrial cis-aconitic acid transporter by metabolic engineering. Metab. Eng. 35, 95–104.

Stój, A., and Targoñski, Z. (2006). Use of content analysis of selected organic acids for the detection of berry juice adulterations. Pol. J. Food Nutr. Sci. 15, 41.

Stottmeister, U., Behrens, U., Weissbrodt, E., Barth, G., Franke-Rinker, D., and Schulze, E. (1982). Nutzung von Paraffinen und anderen Nichtkohlenhydrat-Kohlenstoffquellen zur mikrobiellen Citronensäuresynthese. Z. Für Allg. Mikrobiol. 22, 399–424.

van der Straat, L., Vernooij, M., Lammers, M., van den Berg, W., Schonewille, T., Cordewener, J., van der Meer, I., Koops, A., and de Graaff, L.H. (2014). Expression of the Aspergillus terreus itaconic acid biosynthesis cluster in Aspergillus niger. Microb. Cell Factories 13, 11.

Strelko, C.L., Lu, W., Dufort, F.J., Seyfried, T.N., Chiles, T.C., Rabinowitz, J.D., and Roberts, M.F. (2011). Itaconic Acid Is a Mammalian Metabolite Induced during Macrophage Activation. J. Am. Chem. Soc. 133, 16386–16389.

Sugimoto, M., Sakagami, H., Yokote, Y., Onuma, H., Kaneko, M., Mori, M., Sakaguchi, Y., Soga, T., and Tomita, M. (2012). Non-targeted metabolite profiling in activated macrophage secretion. Metabolomics 8, 624–633.

Tabuchi, T., Sugisawa, T., Ishidori, T., Nakahara, T., and Sugiyama, J. (1981). Itaconic Acid Fermentation by a Yeast Belonging to the Genus Candida. Agric. Biol. Chem. 45, 475–479.

References

Takahashi, M., Morita, T., Fukuoka, T., Imura, T., and Kitamoto, D. (2012). Glycolipid Biosurfactants, Mannosylerythritol Lipids, Show Antioxidant and Protective Effects against H_2O_2-Induced Oxidative Stress in Cultured Human Skin Fibroblasts. J. Oleo Sci. 61, 457–464.

Tanaka, N., Akamatsu, Y., Hattori, T., and Shimada, M. (1994). < Preliminary> Effect of Oxalic Acid on the Oxidative Breakdown of Cellulose by the Fenton Reaction.

Tate, B. (1981). Itaconic acid and derivatives. Grayson M Eckroth E Eds Kirk-Othmer Encycl Chem Technol 3 865–873.

Taylor, E.B. (2017). Functional Properties of the Mitochondrial Carrier System. Trends Cell Biol. 27, 633–644.

Tehlivets, O., Scheuringer, K., and Kohlwein, S.D. (2007). Fatty acid synthesis and elongation in yeast. Biochim. Biophys. Acta BBA - Mol. Cell Biol. Lipids 1771, 255–270.

Teleky, B.-E., and Vodnar, D.C. (2019). Biomass-Derived Production of Itaconic Acid as a Building Block in Specialty Polymers. Polymers 11, 1035.

Tevž, G., Benčina, M., and Legiša, M. (2010). Enhancing itaconic acid production by Aspergillus terreus. Appl. Microbiol. Biotechnol. 87, 1657–1664.

Thom, C., and Church, M.B. (1918). Aspergillus fumigatus, A. nidulans, A. terreus N. sp. and their Allies. Am. J. Bot. 5, 84–104.

Tolbert, N.E., and Zill, L.P. (1954). Isolation of Carbon-14-Labeled Sedoheptulose and Other Products from Sedum Spectabile. Plant Physiol. 29, 288–292.

Tomaszewska, L., Rywińska, A., and Gładkowski, W. (2012). Production of erythritol and mannitol by Yarrowia lipolytica yeast in media containing glycerol. J. Ind. Microbiol. Biotechnol. 39, 1333–1343.

Transparency Market Research (2015). Itaconic acid market-global industry analysis, size, share, growth, trends and forecast 2015–2023.

Vadkertiová, R., and Sláviková, E. (2006). Metal tolerance of yeasts isolated from water, soil and plant environments. J. Basic Microbiol. 46, 145–152.

Van Beuzekom, B., and Arundel, A. (2006). OECD Biotechnology statistics-2006.

Vasdinyei, R., and Deák, T. (2003). Characterization of yeast isolates originating from Hungarian dairy products using traditional and molecular identification techniques. Int. J. Food Microbiol. 86, 123–130.

Venter, T., Kock, J.L.F., Botes, P.J., and Smit, M.S. (2004). Acetate enhances citric acid production by Yarrowia lipolytica when grown on sunflower oil. Syst. Appl. Microbiol. 27, 135.

Verma, A.S., Agrahari, S., Rastogi, S., and Singh, A. (2011). Biotechnology in the Realm of History. J. Pharm. Bioallied Sci. 3, 321–323.

Vickery, H.B. (1969). [75] Preparation of monopotassium threo-ds-isocitrate. In Methods in Enzymology, (Academic Press), pp. 601–609.

Walt, J.P. van der, and Arx, J.A. von (1980). The yeast genus Yarrowia gen. nov. Antonie Van Leeuwenhoek 46, 517–521.

Wang, Q.-M., Jia, J.-H., and Bai, F.-Y. (2006). Pseudozyma hubeiensis sp. nov. and Pseudozyma shanxiensis sp. nov., novel ustilaginomycetous anamorphic yeast species from plant leaves. Int. J. Syst. Evol. Microbiol. 56, 289–293.

Wang, Q.-M., Begerow, D., Groenewald, M., Liu, X.-Z., Theelen, B., Bai, F.-Y., and Boekhout, T. (2015). Multigene phylogeny and taxonomic revision of yeasts and related fungi in the Ustilaginomycotina. Stud. Mycol. 81, 55–83.

WEASTRA, s. r. o. (2013). Wp 8.1, determination of market potential for selected platform chemicals: itaconic acid, succinic acid, 2,5-furandicarboxylic acid (Bioconsept).

Welter, K. (2000). Biotechnische Produktion von Itaconsäure aus nachwachsenden Rohstoffen mit immobilisierten Zellen. PhD Thesis. Technische Universität Carolo-Wilhelmina zu Braunschweig.

Werpy, T.A., Holladay, J.E., and White, J.F. (2004). Top Value Added Chemicals From Biomass: I. Results of Screening for Potential Candidates from Sugars and Synthesis Gas. ResearchGate.

Williams, R.J., Eakin, R.E., and Snell, E.E. (1940). The relationship of inositol, thiamin, biotin, pantothenic acid and vitamin B6 to the growth of yeasts. J. Am. Chem. Soc. 62, 1204–1207.

Willke, T., and Vorlop, K.-D. (2001). Biotechnological production of itaconic acid. Appl. Microbiol. Biotechnol. 56, 289–295.

Woodbine, M. (1959). Microbial fat: microorganisms as potential fat producers. Prog Ind Microbiol 179–245.

References

Xu, P., Qiao, K., Ahn, W.S., and Stephanopoulos, G. (2016). Engineering Yarrowia lipolytica as a platform for synthesis of drop-in transportation fuels and oleochemicals. Proc. Natl. Acad. Sci. U. S. A. 113, 10848–10853.

Yahiro, K., Takahama, T., Park, Y.S., and Okabe, M. (1995). Breeding of Aspergillus terreus mutant TN-484 for itaconic acid production with high yield. J. Ferment. Bioeng. 79, 506–508.

Yalcin, S., Tijen Bozdemir, M., and Ozbas, Y. (2012). Effects of initial medium pH and temperature on growth and citric acid production kinetics of a novel domestic Yarrowia lipolytica strain. New Biotechnol. 29, S62.

Yalcin, S.K., Bozdemir, M.T., and Ozbas, Z.Y. (2010). Citric acid production by yeasts: fermentation conditions, process optimization and strain improvement. Curr. Res. Technol. Educ. Top. Appl. Microbiol. Microb. Biotechnol. 9, 1374–1382.

Yamamoto, S., Morita, T., Fukuoka, T., Imura, T., Yanagidani, S., Sogabe, A., Kitamoto, D., and Kitagawa, M. (2012). The Moisturizing Effects of Glycolipid Biosurfactants, Mannosylerythritol Lipids, on Human Skin. J. Oleo Sci. 61, 407–412.

Yan, N. (2013). Structural advances for the major facilitator superfamily (MFS) transporters. Trends Biochem. Sci. 38, 151–159.

Yarrow, D. (1972). Four new combinations in yeasts. Antonie Van Leeuwenhoek 38, 357–360.

Yoshida, S., Koitabashi, M., Nakamura, J., Fukuoka, T., Sakai, H., Abe, M., Kitamoto, D., and Kitamoto, H. (2015). Effects of biosurfactants, mannosylerythritol lipids, on the hydrophobicity of solid surfaces and infection behaviours of plant pathogenic fungi. J. Appl. Microbiol. 119, 215–224.

Yu, T., Zhou, Y.J., Huang, M., Liu, Q., Pereira, R., David, F., and Nielsen, J. (2018). Reprogramming Yeast Metabolism from Alcoholic Fermentation to Lipogenesis. Cell 174, 1549-1558.e14.

Yuzbasheva, E.Y., Agrimi, G., Yuzbashev, T.V., Scarcia, P., Vinogradova, E.B., Palmieri, L., Shutov, A.V., Kosikhina, I.M., Palmieri, F., and Sineoky, S.P. (2019). The mitochondrial citrate carrier in Yarrowia lipolytica: Its identification, characterization and functional significance for the production of citric acid. Metab. Eng. 54, 264–274.

Zambanini, T., Hosseinpour Tehrani, H., Geiser, E., Merker, D., Schleese, S., Krabbe, J., Buescher, J.M., Meurer, G., Wierckx, N., and Blank, L.M. (2017). Efficient itaconic acid production from glycerol with Ustilago vetiveriae TZ1. Biotechnol. Biofuels 10, 131.

Zeman, I., Neboháčová, M., Gérecová, G., Katonová, K., Jánošíková, E., Jakúbková, M., Centárová, I., Dunčková, I., Tomáška, L., Pryszcz, L.P., et al. (2016). Mitochondrial Carriers Link the Catabolism of Hydroxyaromatic Compounds to the Central Metabolism in Candida parapsilosis. G3 Genes Genomes Genet. 6, 4047–4058.

Zhang, Y., Wang, Y., Yao, M., Liu, H., Zhou, X., Xiao, W., and Yuan, Y. (2017). Improved campesterol production in engineered Yarrowia lipolytica strains. Biotechnol. Lett. 39, 1033–1039.

Zhao, M., Lu, X., Zong, H., Li, J., and Zhuge, B. (2018). Itaconic acid production in microorganisms. Biotechnol. Lett. 40, 455–464.

Zhao, X., Murata, T., Ohno, S., Day, N., Song, J., Nomura, N., Nakahara, T., and Yokoyama, K.K. (2001). Protein Kinase Cα Plays a Critical Role in Mannosylerythritol Lipid-induced Differentiation of Melanoma B16 Cells. J. Biol. Chem. 276, 39903–39910.